The role of cytochrome P450 enzymes in the biosynthesis of abietane diterpenes from rosemary and sage

Kumulative Dissertation

zur Erlangung des Doktorgrades der Naturwissenschaften (Dr. rer. nat.)

der

Naturwissenschaftlichen Fakultät I – Biowissenschaften –

der Martin-Luther-Universität

Halle-Wittenberg,

vorgelegt von

Frau Ulschan Bathe

geb. am 01. Februar 1989 in Eisenhüttenstadt

Gutachter:

Prof. Dr. Alain Tissier

Prof. Dr. Jörg Degenhardt

Prof. Dr. Albert Ferrer

Halle (Saale), 12. November 2019

To Nathan and Valerian

List of contents

Summary 1

Zusammenfassung 2

List of figures 3

List of tables 3

List of abbreviations 4

1. Introduction 6

1.1. What is the reason for the interest in Lamiaceae abietane diterpenes? 8

1.1.1. The potential of abietane diterpenes from rosemary and sage species for medicinal and industrial applications 8

1.1.2. The proposed ecological role of Lamiaceae abietane diterpenes 9

1.2. Diterpene biosynthesis *in planta* 10

1.2.1. Production of precursors for diterpene biosynthesis – MEP pathway and geranylgeranyl diphosphate production 10

1.2.2. Diterpene synthases provide the hydrocarbon skeletons and eminently contribute to diterpenoid diversity 13

1.3. Cytochrome P450 enzymes in plant metabolism 16

1.3.1. The function of cytochrome P450 enzymes in plants 16

1.3.2. Cytochrome P450 enzymes as key player in the biosynthesis of plant specialized diterpenes 19

1.4. Tools and expression platforms for elucidation and engineering of diterpene pathways 21

1.4.1. Cytochrome P450 engineering to elucidate, modify and optimize biosynthetic pathways 21

1.4.2. Expression systems for the elucidation of diterpene pathways and their high-value production 23

1.5. Questions addressed in the thesis 24

2. Results 25

2.1. Contribution to the publications 25

2.2. The role of cytochrome P450 enzymes in the carnosic acid biosynthesis from rosemary and sage 26

2.2.1. Aims and summary 26

2.2.2. Publication 27

2.3. CYP76 oxidation network that contributes to the diversity of abietane diterpenes in rosemary and sage 38

2.3.1. Aims and summary 38

2.3.2. Publication 38

2.4. A review about cytochrome P450 enzymes involved in plant specialized diterpene pathways 54

2.4.1. Aims and summary 54

2.4.2. Publication 54

3. Discussion and perspectives 70

3.1. The biosynthesis of abietane diterpenes in Lamiaceae 70

3.1.1. Promiscuous and multifunctional CYP76s 71

3.1.2. C2 oxidases 73

3.1.3. Non-enzymatic oxidations 75

3.1.4. Further chemical decorations 77

3.2. The antioxidative protection cascade of abietane diterpenes *in planta* 78

3.3. Modular cloning developed for yeast enables combinatorial biosynthesis: production of "new-to-nature" diterpenes with potential bioactivity 80

4. References 83

5. Appendix 103

5.1. Supporting information to 2.2.2. 103

5.2. Supporting information to 2.3.2. 143

5.3. Supporting information to 2.4.2. 173

5.4. List of publications 183

Acknowledgements 184

Eidesstattliche Erklärung 185

Curriculum vitae 186

Summary

Abietane diterpenes are a diverse group of specialized metabolites which occur in a wide range of species throughout the plant kingdom. They exhibit various *in vitro* bioactivities that may allow pharmaceutical and industrial utilization, but their biosynthesis is only partially understood. The main aim of the present thesis was to investigate the catalytic role of cytochrome P450 enzymes in the oxidation of abietane diterpenoids from the Lamiaceae.

In the frame of elucidating the oxidative steps *en route* to carnosic acid, the Golden Gate modular cloning technique was used to assemble the biosynthesis of ferruginol in *Saccharomyces cerevisiae* by expressing previously characterized ferruginol synthases (CYP76AH1, CYP76AH4 and CYP76AH22-24). Except for CYP76AH1, all CYP76AHs carried out two instead of one expected hydroxylation, resulting in the production of 11-hydroxy ferruginol. As all investigated CYPs showed high sequence similarity on the protein level, modelling-based reciprocal mutagenesis of three amino acids was found to be sufficient to convert ferruginol synthase to hydroxy ferruginol synthase and *vice versa*. To elucidate the downstream oxidation that yield carnosic acid, gene candidates were selected from an EST sequence database and tested in *S. cerevisiae*. CYP76AK6-8 were shown to possess C20 oxidase activity on 11-hydroxy ferruginol allowing the reconstitution of the biosynthesis of carnosic acid in yeast.

To further explore the enzymatic activities of promiscuous CYP76s in abietane diterpene biosynthesis from Lamiaceae, CYP76AHs and CYP76AK1 from *Rosmarinus officinalis* and *Salvia miltiorrhiza* were characterized in more detail. Expressed alone or in combination they catalyzed the formation of 14 oxidized abietane diterpenoids in yeast, eight of which have never been reported. The presence of all synthesized metabolites in the plants, from which the CYPs originate, validates *S. cerevisiae* as a suitable production platform for plant specialized abietane diterpenoids.

The thesis further gives a comprehensive survey of CYPs related to plant diterpene pathways. A phylogenetic analysis revealed that three CYP clans, namely CYP71, CYP85 and CYP72, contribute to the oxidation of plant diterpenoids known to date, and that within these clans only a few CYP families are involved. Some of them have expanded in plant families such as CYP720B in conifers, CYP726A in Euphorbiaceae and CYP76 in Lamiaceae. The analysis further demonstrated that labdane-related diterpenes are a dominant class. However, no relationship between diterpene structures and involved CYPs could be found. Instead, CYPs from plant diterpenoid metabolism appear barely homogeneous concerning evolutionary origin and biosynthetic function. Future investigations will clarify if other CYP families participate in plant diterpenoid pathways and how they are related to the already known CYPs.

Zusammenfassung

Abietanditerpene bilden eine vielfältige Gruppe von spezialisierten Metaboliten, die in einer Vielzahl von Spezies im gesamten Pflanzenreich auftreten. Sie zeigen diverse *in-vitro*-Bioaktivitäten, die eine pharmazeutische und industrielle Nutzung möglich machen können. Ihre Biosynthese dagegen wird nur teilweise verstanden. Das Hauptziel der vorliegenden Arbeit war es, die katalytische Rolle von Cytochrom-P450-Enzymen in den Stoffwechselwegen von oxidierten Abietanditerpenen aus Lippenblütengewächsen zu untersuchen.

Im Rahmen der Aufklärung der Carnosinsäurebiosynthese wurde die modulare Golden-Gate-Klonierungstechnik dazu verwendet, die Ferruginolbiosynthese durch Expression zuvor charakterisierter Ferruginolsynthasen (CYP76AH1, CYP76AH4 und CYP76AH22-24) in *Saccharomyces cerevisiae* zu modellieren. Mit Ausnahme von CYP76AH1 katalysierten alle untersuchten CYP76AH-Enzyme zwei statt einer erwarteten Hydroxylierung, wodurch 11-Hydroxyferruginol produziert wurde. Da alle untersuchten CYP-Enzyme eine hohe Sequenzidentität auf Proteinebene zeigten, war eine modell-basierte reziproke Mutagenese von drei Aminosäuren ausreichend, um Ferruginol- und Hydroxyferruginolsynthase ineinander umzuwandeln. Um die weitere biosynthetische Oxidation hin zur Carnosinsäure aufzuklären wurden Genkandidaten aus einer EST-Sequenzdatenbank selektiert und in *S. cerevisiae* getestet. Es wurde gezeigt, dass CYP76AK6-8 11-Hydroxyferruginol an Position C20 oxidieren, wodurch die Carnosinsäurebiosynthese in Hefe rekonstruiert werden konnte.

Um die enzymatische Aktivität der CYP76-Enzyme in der Abietanditerpenbiosynthese aus Lippenblütlern besser zu verstehen, wurden CYP76AH-Enzyme und CYP76AK1 aus *Rosmarinus officinalis* und *Salvia miltiorrhiza* genauer charakterisiert. Eine Expression allein oder in Kombination miteinander katalysierte die Bildung von 14 oxidierten Abietanditerpenen in Hefe, von denen acht noch nie beschrieben wurden. Dass alle synthetisierten Metabolite auch in den Pflanzen vorkommen, aus denen die CYP-Enzyme stammen, beweist, dass *S. cerevisiae* ein geeignetes Produktionssystem für spezialisierte Abietanditerpene aus Pflanzen darstellt.

Weiterhin beinhaltet diese Arbeit eine umfassende Übersicht der CYP-Enzyme, die zu pflanzlichen Diterpenstoffwechselwegen beitragen. Eine phylogenetische Analyse ergab, dass nach heutigem Wissensstand drei CYP-Clane, nämlich CYP71, CYP85 und CYP72, pflanzliche Diterpene oxidieren, und dass innerhalb dieser Clane nur wenige CYP-Familien beteiligt sind. Einige von ihnen expandierten in Pflanzenfamilien wie CYP720B in Koniferen, CYP726A in Wolfsmilchgewächsen und CYP76 in Lippenblütengewächsen. Die Analyse zeigte auch, dass Labdanditerpene eine dominante Klasse darstellen. Jedoch konnte keine Beziehung zwischen den Diterpenstrukturen und den beteiligten CYP-Enzymen gefunden werden. Stattdessen erscheinen die CYP-Enzyme aus dem pflanzlichen Diterpenmetabolismus wenig einheitlich in Bezug auf ihren evolutionären Ursprung und ihre biosynthetische Funktion. Zukünftige Untersuchungen werden zeigen, ob weitere CYP-Familien im Diterpenstoffwechsel aus Pflanzen beteiligt sind und in welcher Beziehung sie zu den schon bekannten CYP-Enzymen stehen.

List of figures

Fig. 1.1 Chemical structures of the isoprenoid precursors, isopentenyl diphosphate and dimethylallyl diphosphate, and some diterpenoids of considerable pharmacological and industrial interest. 7
Fig. 1.2 Abietane diterpenoids and tanshinones from Lamiaceae. 9
Fig. 1.3 The proposed mechanism of radical quenching by carnosic acid. 10
Fig. 1.4 Isoprenoid precursor metabolism *in planta* and derived metabolite classes. 11
Fig. 1.5 Biosynthesis of isoprenyl diphosphates. 12
Fig. 1.6 Proposed diterpene synthase activity in Lamiaceae. 15
Fig. 1.7 Biosynthesis of abietane diterpenes in Lamiaceae. 16
Fig. 1.8 Selected reactions catalyzed by cytochrome P450 enzymes. 17
Fig. 1.9 The catalytic mechanism of substrate hydroxylation by cytochrome P450 enzymes. 18
Fig. 1.10 Promiscuity of cytochrome P450 enzymes involved in specialized metabolic pathways. 20
Fig. 1.11 Cytochrome P450 engineering to elucidate, modify and optimize the production of valuable plant specialized metabolites. 22
Fig. 3.1 The contribution of CYP76s and CYP71s to the biosynthesis of abietane diterpenoids from rosemary and sage. 71
Fig. 3.2 Abietane and abietane-like diterpenes with various chemical decorations. 74
Fig. 3.3 Proposed biosynthesis of 2α-hydroxy-*O*-methyl-pisiferic acid from *Salvia pomifera* and *Rosmarinus officinalis*. 75
Fig. 3.4 Non-enzymatic oxidations observed on abietane diterpenoids from Lamiaceae. 76
Fig. 3.5 Proposed localization and function of abietane diterpenes in rosemary and sage species. 80
Fig. 3.6 Combinatorial biosynthesis of diterpenoids using the modular Golden Gate cloning system and libraries of pathway modules. 82

List of tables

Tab. 3.1 Some examples of abietane diterpenoids from rosemary and sage species with oxidations at the given positions. 78

List of abbreviations

A. annua	*Artemisia annua*
A. thaliana	*Arabidopsis thaliana*
CA	carnosic acid
CDP-ME	4-diphosphocytidyl-2-C-methylerythritol
CDP-MEP	4-diphosphocytidyl-2-C-methyl-D-erythritol 2-phosphate
CMK	4-diphosphocytidyl-2-C-methyl-D-erythritol kinase
CMS	2-C-methyl-D-erythritol 4-phosphate cytidylyltransferase
CO	carnosol
CO_2	carbon dioxide
CPR	cytochrome P450 reductase
CPS	copalyl diphosphate synthase
CTP	cytidine triphosphate
CYP	cytochrome P450 monooxygenase
diTPS	diterpene synthase
DMAPP	dimethylallyl diphosphate
DXP	1-deoxy-D-xylulose-5-phosphate
DXR	1-deoxy-D-xylulose-5-phosphate reductoisomerase
DXS	1-deoxy-D-xylulose-5-phosphate synth*ase*
ent-CPP	*ent*-copalyl diphosphate
ER	endoplasmic reticulum
FPP	farnesyl diphosphate
G3P	glyceraldehyde 3-phosphate
GC-MS	gas chromatography-mass spectrometry
GGPP	geranylgeranyl diphosphate
GGPPS	geranylgeranyl diphosphate synthase
GPP	geranyl diphosphate
HDR	hydroxymethylbutenyl 4-diphosphate reductase
HDS	Hydroxymethylbutenyl 4-diphosphate synthase
HFS	hydroxy ferruginol synthase
HMBPP	hydroxymethylbutenyl 4-diphosphat
I. rubescens	*Isodon rubescens*
IDI	IPP:DMAPP isomerase
IPP	isopentenyl diphosphate
KO	kaurene oxidase
KOL	kaurene oxidase-like enzyme
KPP	kolavenyl diphosphate

List of abbreviations

KS	kaurene synthase
KSL	kaurene synthase-like
LPP	labda-13-en-8-ol diphosphate
M. vulgare	*Marrubium vulgare*
MCS	ME-cPP synthase
ME-cPP	2-C-methylerythritol 2,4-cyclodiphosphate
MEP	2-C-methyl-D-erythritol 4-phosphate
MEV	mevalonate
MiS	miltiradiene synthase
MTPSL	microbial terpene synthase-like
N. benthamiana	*Nicotiana benthamiana*
NADPH	nicotinamide adenine dinucleotide phosph*ate*
NMR	Nuclear Magnetic Resonance
NNPP	nerylneryl diphosphate
NPP	neryl diphosphate
P. patens	*Physcomitrella patens*
PP_i	pyrophosphate
PPP	peregrinol diphosphate
R. officinalis	*Rosmarinus officinalis*
ROS	reactive oxygen species
S. cerevisiae	*Saccharomyces cerevisiae*
S. fruticosa	*Salvia fruticosa*
S. miltiorrhiza	*Salvia miltiorrhiza*
S. moellendorffii	*Selaginella moellendorffii*
S. officinalis	*Salvia officinalis*
S. sclarea	*Salvia sclarea*
TPS	terpene synthase
V. agnus-castus	*Vitex agnus-castus*

1. Introduction

Plants produce a wide range of metabolites which secure survival, increase fitness and help counter and adapt to abiotic and biotic stresses. Among them, isoprenoids constitute one of the largest and most diverse natural product classes contributing to both general and specialized metabolism. They are involved in growth and developmental processes, photosynthesis, respiration, signaling processes and pigmentation. Specialized functions include the participation in defense mechanisms against herbivores and pathogens, the contribution to ecological interactions and communication and the attraction of pollinators. All terpenoids are assembled from the universal C-5 isoprene units, isopentenyl diphosphate (IPP) and dimethylallyl diphosphate (DMAPP) (**Fig. 1.1**). Leopold Ružička claimed this principle first in 1953 as the isoprene rule [1]. After the production in the cytosolic mevalonate (MEV) pathway and the plastidial 2-C-methyl-D-erythritol 4-phosphate (MEP) pathway, IPP and DMAPP can be linked in a head-to-tail condensation to form elongated isoprenyl chains. The most common isoprenyl diphosphates, which are synthesized from IPP and DMAPP by isoprenyl diphosphate synthases, are geranyl diphosphate (GPP, C-10), farnesyl diphosphate (FPP, C-15) and geranylgeranyl diphosphate (GGPP, C-20). They serve as the starting point for the biosynthesis of monoterpenes (C-10), sesquiterpenes (C-15), diterpenes (C-20), triterpenes (C-30) and polyterpenes ($C_{n>40}$). A first level of diversity of this metabolite class is established by terpene synthases (TPS), which form the hydrocarbon backbones from the isoprenyl diphosphate precursors. Next, chemical decorations such as oxidation, acetylation, methylation, rearrangements, cleavage and glycosylation expand the chemical variety. Among the terpenes, diterpenoids represent a very diverse group with ~12.000 estimated structures [2]. Based on their structural complexity, isoprenoids that derive from GGPP have diverse ecological functions *in planta* which include hormonal signaling (gibberellins), photosynthesis (plastoquinones, carotenoids and as part of chlorophylls) and defense mechanisms (diterpene resin acids and phytoalexins) [3-7].

Diterpenoids and their derivatives have aroused wide scientific interest during the last decades. The multifarious bioactivities and advantageous properties have been exploited for several applications in medicine and industry. Some of the most prominent pharmaceuticals are Taxol® from *Taxus* species which is used as powerful anticancer drug, and ingenol mebutate from Euphorbiaceae which is applied to treat actinic keratosis (**Fig. 1.1**) [8, 9]. Industrially relevant diterpenoids are e.g. carnosic acid (CA), an abietane diterpene from *Rosmarinus officinalis* which serves as an antioxidant additive in food and cosmetics, and the fragrance precursor sclareol from *Salvia sclarea* (**Fig. 1.1**) [10, 11]. Diterpenoids are also the presumed active ingredients in many medicinal plants from traditional medicine from all over the world. For example, ginkgolides from *Ginkgo biloba* are supposed to have beneficial effects on Alzheimer's disease, and extracts of African Euphorbiaceae, which accumulate macrocyclic diterpenoids, are used to medicate epilepsy, cancer and fungal infections [12, 13]. Additional aspects on the bioactivities of abietane diterpenes are described in chapter 1.1.

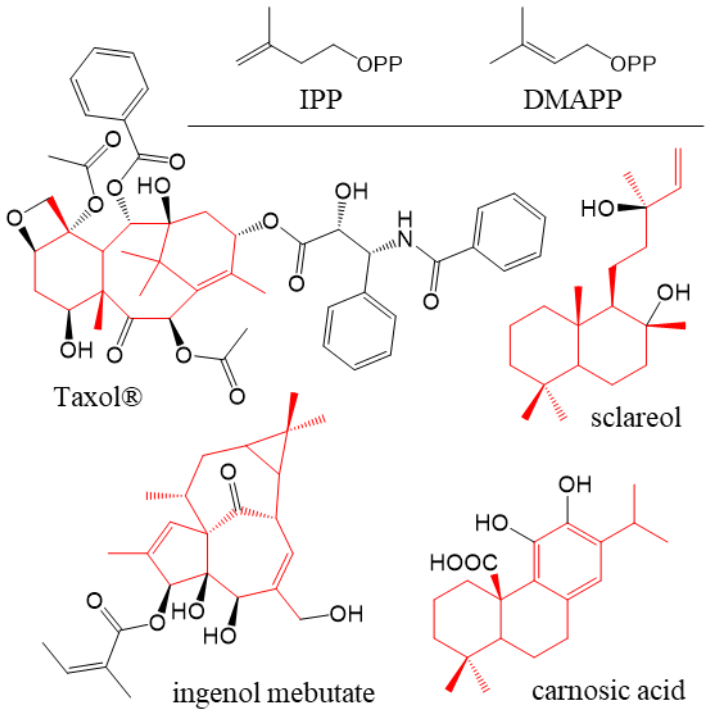

Fig. 1.1 Chemical structures of the isoprenoid precursors, isopentenyl diphosphate and dimethylallyl diphosphate, and some diterpenoids of considerable pharmacological and industrial interest. IPP and DMAPP are the universal precursors of all terpenoids. During their biosynthesis, diterpenoids often undergo complex chemical decorations as exemplified on Taxol®, ingenol mebutate and carnosic acid. The diterpene skeletons are highlighted in red.

In order to use the beneficial properties of diterpenoids for medicinal and industrial applications, high-value productions can be realized by metabolic engineering in appropriate hosts but require detailed knowledge on the biosynthetic pathways. Unfortunately, for most diterpenoids, the biosynthetic genes are not known or have not been well characterized yet. This is a future challenge which can be solved with a combination of metabolite profiling, modern sequencing techniques, biochemical characterization of gene candidates and reconstitution of whole pathways in model organisms such as *Saccharomyces cerevisiae* and plant hosts (e.g. algae or *Nicotiana benthamiana*).

In the following chapters of this introduction, I would like to highlight the importance of Lamiaceae abietane diterpenes with respect to their commercial and physiological relevance. I will further introduce the general biosynthesis of plant diterpenoids and give an overview of the role of cytochrome P450 monooxygenases (CYPs) in plant metabolisms. Finally, some aspects of metabolic engineering for elucidating and modifying diterpenoid biosynthesis will be addressed.

1.1. What is the reason for the interest in Lamiaceae abietane diterpenes?

1.1.1. The potential of abietane diterpenes from rosemary and sage species for medicinal and industrial applications

Traditional medicine has been used for millennia all over the world by indigenous people. For example, the first written evidence of drug preparation from medicinal plants is a 5000-year-old Sumerian clay slab with receipts referring to more than 250 different plants [14]. Such knowledge is traditionally passed from generation to generation, but the beneficial effects of (medicinal) plants and other organisms are also progressively rediscovered for modern drug development. In that respect, Lamiaceae is an important plant family, not only because of its fragrance and taste for culinary uses (*R. officinalis* and *Salvia officinalis*) but also because of the health promoting properties which are applied in traditional medicine e.g. in China (*Salvia miltiorrhiza*), North Africa (*Vitex agnus-castus*) and India (*Coleus forskohlii*) [15-17]. The plant family comprises 236 genera and ~7800 species (http://www.theplantlist.org). *R. officinalis* and *Salvia* species, commonly known as rosemary and sage, respectively, are native to Mediterranean regions, Middle East and Asia, but have been naturalized throughout the world. In traditional medicine, *S. officinalis* was used to treat diarrhea and gout, whereas *S. miltiorrhiza* (Chinese sage, danshen) is still very popular in China to medicate inflammation and vascular diseases [18, 19]. Rosemary was formerly used to treat liver diseases, asthma and rheumatism [16], but nowadays, extracts are used commercially in Europe, China and Japan as antioxidant for food preservation and cosmetics [10]. The most powerful antioxidant compounds in those extracts are CA and carnosol (CO). Like all abietane diterpenoids, they are composed of the tricyclic C-20 abietane skeleton with a characteristic catechol function in the C-ring (**Fig. 1.1** and **Fig. 1.2A**). This moiety is believed to generate the antioxidant activity by the oxidative conversion to the quinone form. In addition, CA can spontaneously oxidize to CO (**Fig. 1.2B**) [20]. Notably, CO has antioxidant activity, too, but to a lower extent than CA [21]. The first isolations of CO and CA date back to 1942 (*Salvia carnosa*) and 1964 (*S. officinalis*), respectively, but the highest abundance of CA has been reported in rosemary [10, 22, 23].

More than 20 Lamiaceae genera have been reported to accumulate labdane-type diterpenes with potential bioactivity [24]. Next to antioxidant properties, abietane diterpenes and related tanshinones, which are exclusively present in *S. miltiorrhiza* (**Fig. 1.2A**), have anticancer, anti-inflammatory, antibacterial, neuroprotective, antifungal, anti-HIV and antimalarial activity [25-33]. Because sage and especially rosemary grow slowly, isolation of active compounds from these species is fairly expensive. Additionally, similar compounds interfere with the purification. The recombinant synthesis in microbial systems offers a cost- and time-saving alternative for high-value production of these compounds. Therefore, elucidation and characterization of biosynthetic genes is an essential need to develop production processes for fermentation in microorganisms.

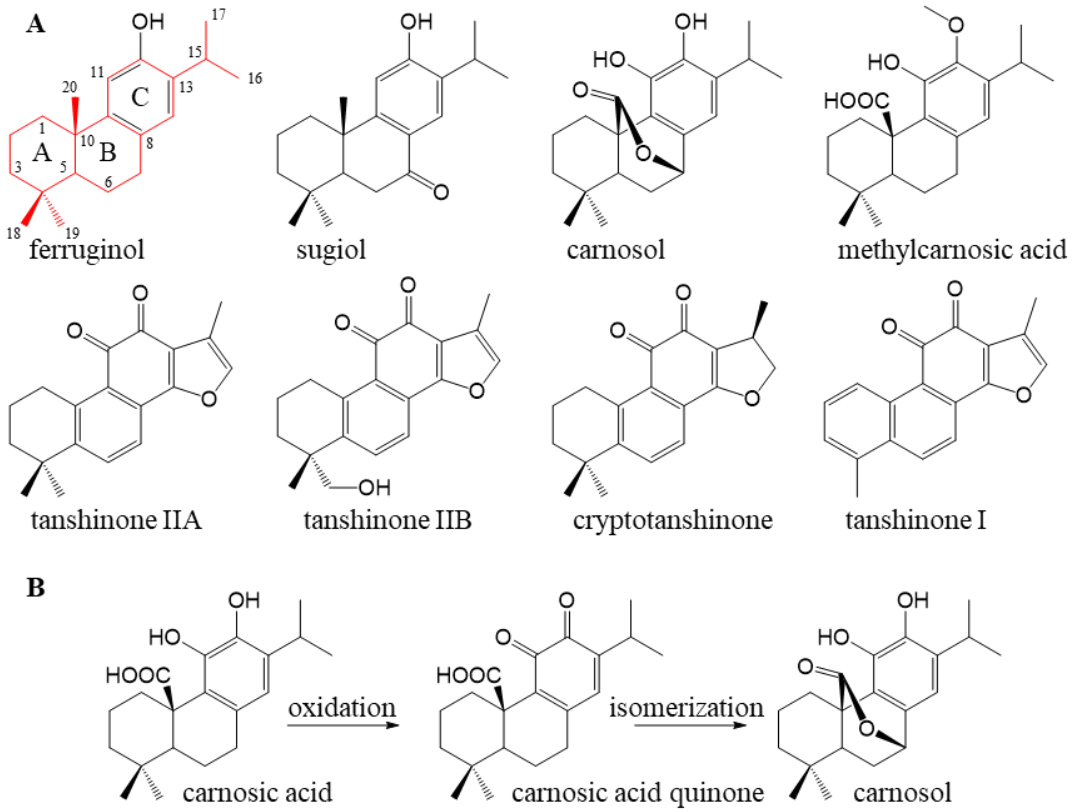

Fig. 1.2 Abietane diterpenoids and tanshinones from Lamiaceae. A, Structures of abietane diterpenes with reported bioactivity and tanshinones present in the genera *Rosmarinus* and *Salvia* are given. The hydrocarbon skeleton that all abietane diterpenes have in common is highlighted in red. B, The antioxidant activity of CA has been hypothesized to lead to CA quinone which can subsequently isomerize to CO. Modified from Masuda et al. (2002) [34].

1.1.2. The proposed ecological role of Lamiaceae abietane diterpenes

Much effort has been invested in understanding the bioactivity of abietane diterpenes as potential targets for drug development and for industrial usage. However, their ecological role *in planta* remains poorly understood. Among the diverse abietane diterpenes, CA is probably one of the best studied metabolite. It is exclusively produced in species of Lamiaceae, although other abietane diterpenoids have been detected in distantly related plant species, e.g. ferruginol and pisiferic acid are present in conifers [10, 35, 36]. CA and related diterpenes occur in both aerial parts and below-ground tissues such as in trichomes on leaves, sepals and petals (CA in rosemary), or in roots (tanshinones in *S. miltiorrhiza*) [10, 37]. The Lamiaceae plants are often localized to regions with high light, low water availability, high temperatures and limited nutrient access. This is true for *R. officinalis* and *Salvia fruticosa* which are native to the Mediterranean basin, and *S. miltiorrhiza* to central and southern China. Indeed, the prevailing climatic conditions influence the metabolite content in rosemary with varying amounts of abietane diterpenes in dependence of seasonal changes and stress conditions [38, 39]. Whereas CA decreased upon darkness, drought/water stress, high temperature and light stress, oxidation-derived products (e.g. CA quinone, CO, rosmanol and isorosmanol) increased [39-41].

Plants constantly produce reactive oxygen species (ROS) in diverse metabolic processes, but the climate conditions of the Mediterranean basin may lead to oxidative stress by increased ROS accumulation [42]. In that context, it is assumed that CA quenches ROS (see **Fig. 1.3** as an example of the proposed scavenging mechanism), and therefore may act as antioxidant in *Rosmarinus* and *Salvia* but also in *Lepechinia*, *Oreganum*, *Ocimum* and *Thymus* [10]. ROS including singlet oxygen, superoxide, hydrogen peroxide and hydroxyl radical are mostly produced in photosynthetic and respiration processes [43]. It is therefore not surprising that CA and derivatives have been detected in chloroplasts of mesophyll cells. Additionally, CA present in plasma membranes, in the Golgi apparatus and in the endoplasmic reticulum (ER) of vascular tissue was hypothesized to stabilize and protect these compartments against oxidative stress [41, 44, 45]. CA biosynthetic genes, however, were shown to be active in trichomes of young rosemary leaves in which the derived metabolites accumulate at high levels [46, 47]. This indicates that CA is synthesized in trichomes and is then transported to mesophyll cells by yet unknown mechanisms.

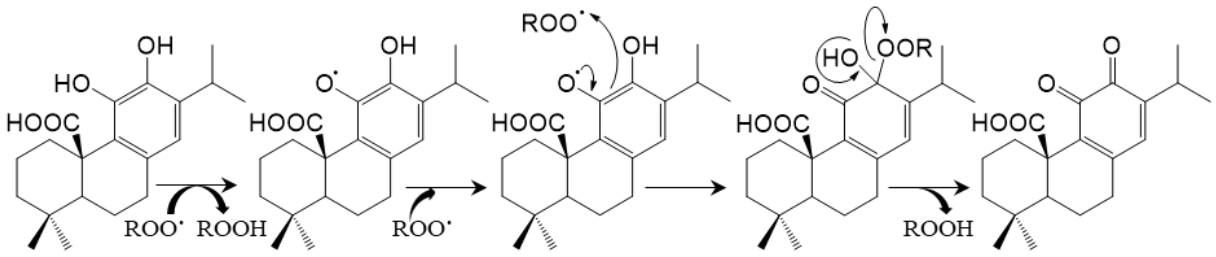

Fig. 1.3 The proposed mechanism of radical quenching by carnosic acid. Reactive oxygen species (ROO˙) abstract hydrogen from CA which is subsequently converted to the quinone form. Modified from Masuda et al. (2001) [48].

1.2. Diterpene biosynthesis *in planta*

1.2.1. Production of precursors for diterpene biosynthesis – MEP pathway and geranylgeranyl diphosphate production

The universal precursors of plant terpenoids, namely IPP and DMAPP, are produced in two separate pathways. Although there is a crosstalk of isoprenoids between these pathways [49], the cytosolic MVA pathway mainly provides isoprenyl diphosphates for the production of sesquiterpenes, triterpenes, brassinosteroids, cytokinins and protein prenylation (**Fig. 1.4**) [50]. IPP and DMAPP that are used for the biosynthesis of monoterpenes, diterpenes, carotenoids, gibberellins, chlorophylls, tocopherols and plastoquinones are produced via the MEP pathway [50]. Its plastidial localization suggests a bacterial origin of which genes most likely have been brought to the cell by the endosymbiosis of cyanobacteria and eukaryotes. However, some MVA and MEP pathway genes are supposed to share common ancestors because they exhibit similar catalytic activities. These include for example condensation (acetoacetyl-CoA thiolase and 1-deoxy-D-xylulose-5-phosphate synthase)

and phosphorylation (mevalonate kinase and 4-(cytidine 5′-diphospho)-2-C-methylerythritol kinase) [51].

The MEP pathway (**Fig. 1.4**) is initiated by 1-deoxy-D-xylulose-5-phosphate synthase (DXS) which condensates pyruvate and glyceraldehyde 3-phosphate (G3P) to 1-deoxy-D-xylulose-5-phosphate (DXP) [52]. This reaction is a rate-limiting step and releases CO_2 [53]. Afterwards, DXP is rearranged and reduced by 1-deoxy-D-xylulose-5-phosphate reductoisomerase (DXR) to MEP, a reaction that requires NADPH [54, 55]. Cytidine triphosphate (CTP) and MEP are then linked by 2-C-methyl-D-erythritol 4-phosphate cytidylyltransferase (CMS), releasing diphosphate (PP_i) [56]. The product 4-diphosphocytidyl-2-C-methylerythritol (CDP-ME) is further phosphorylated by 4-diphosphocytidyl-2-C-methyl-D-erythritol kinase (CMK) to 4-diphosphocytidyl-2-C-methyl-D-erythritol 2-phosphate (CDP-MEP) [57] which is subsequently cyclized by ME-cPP synthase (MCS) to produce 2-C-methylerythritol 2,4-cyclodiphosphate (ME-cPP) [58]. Hydroxymethylbutenyl 4-diphosphate synthase (HDS) catalyzes the ring-opening and reductive dehydration of ME-cPP which results in the formation of hydroxymethylbutenyl 4-diphosphate (HMBPP) [59]. Using NADPH, hydroxymethylbutenyl 4-diphosphate reductase (HDR) finally releases five units IPP and one DMAPP from HMBPP [60]. The 5:1 ratio fits the additional need of IPP in the downstream biosynthesis of isoprenyl diphosphates (**Fig. 1.4**). However, plastidial and cytosolic IPP:DMAPP isomerases (IDI) interconvert the isoprenyl diphosphates into each other to secure sufficient amounts of both DMAPP and IPP [61].

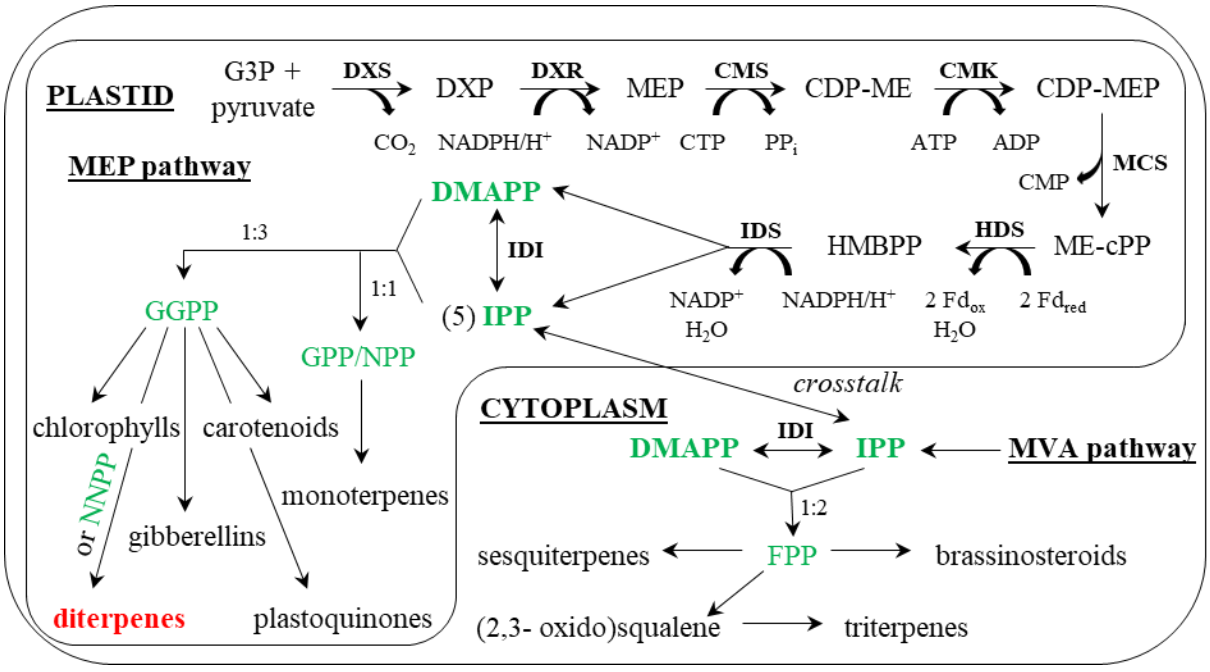

Fig. 1.4 Isoprenoid precursor metabolism *in planta* and derived metabolite classes. The plastidial MEP pathway provides IPP and DMAPP for the downstream production of GPP, neryl diphosphate (NPP), GGPP and nerylneryl diphosphate (NNPP). IPP and DMAPP as biosynthetic precursors of FPP and derived metabolites are produced via the cytosolic MVA pathway. The required ratios of DMAPP:IPP for the biosynthesis of each isoprenyl diphosphate are given on the tracks.

GGPP is a universal metabolite precursor in organisms of all taxa and plays a crucial role in plants as starting molecule for the biosynthesis of a range of essential molecules including the phytol chain of chlorophyll, carotenoids and diterpenoids to which the plant hormones gibberellins belong. Although GGPP production usually occurs in plastids, it can also be produced in the cytosol and in mitochondria for protein prenylation and for the production of polyprenols, respectively [62]. In plants and bacteria, geranylgeranyl diphosphate synthases (GGPPS) of type II, which belong to short chain prenyl diphosphate synthases, successively add three units IPP to one DMAPP with GPP and FPP as intermediates (**Fig. 1.5**) [63, 64]. The chain elongation of the allylic isoprenoid diphosphates (DMAPP, GPP and FPP) with IPP is an electrophilic alkylation of its carbon-carbon double bond. This sequential ionization-condensation-elimination mechanism is also known as the head-to-tail condensation of C-5 isoprene units (IPP and DMAPP) to form GGPP [65]. In that catalysis, most GGPPS act as homodimers [66]. More recently, the stereoisomer nerylneryl diphosphate (NNPP) produced by a *cis*-prenyltransferase was reported to serve as substrate for diterpene biosynthesis, too (**Fig. 1.4** and **Fig. 1.5**) [67, 68].

In plants, one or more GGPPS homologues exist with one of the largest number of genes found in *Arabidopsis thaliana* [5, 69]. Interestingly, only five of the twelve paralogues in *A. thaliana* produce GGPP, whereas five produce geranylfarnesyl diphosphate, one is inactive and another is a pseudogene [62, 70]. As *Physcomitrella patens* has at least three GGPPS paralogues, GGPPS might have duplicated close after diversification from green algae [69]. However, all *trans*-isoprenyl diphosphate synthases most likely derived from a common ancestor which has been hypothesized to be closest in time to archaeal GGPPS [64, 71, 72].

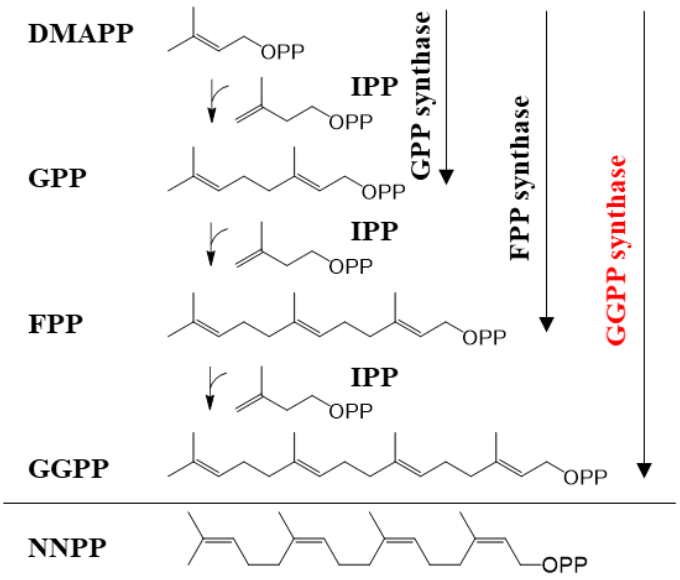

Fig. 1.5 Biosynthesis of isoprenyl diphosphates. IPP is successively added to DMAPP, GPP and FPP to finally form GGPP. The reactions to the corresponding products are catalyzed by the given prenyl diphosphate synthases GPP synthase, FPP synthase and GGPP synthase. The *cis*-stereoisomer of GGPP, NNPP, is given in the bottom. Modified from Vandermoten et al. (2009) [65].

1.2.2. Diterpene synthases provide the hydrocarbon skeletons and eminently contribute to diterpenoid diversity

In the biosynthesis of diterpenoids, diterpene synthases (diTPS) constitute a key branch point as they synthesize the diverse diterpene hydrocarbon scaffolds. The plastidial localized cyclization of the isoprenyl diphosphates GGPP and NNPP results in single or multiple terpene olefins and alcohols which can have linear, macrocyclic, bi- or tricyclic structures. Thereby, diTPS eminently contribute to the diterpene diversity which is further increased by downstream decorating enzymes such as oxygenases and transferases. Based on their catalytic mechanism, three types of diTPS can be distinguished. i) Monofunctional class II diTPS form terpene diphosphates through protonation-induced cyclization of GGPP. ii) Monofunctional class I diTPS ionize GGPP to form a carbocation intermediate that can undergo rearrangements such as cyclization and hydride shifts. The final end product is formed via deprotonation or nucleophile capture. Both, monofunctional class II diTPS and class I diTPS are conserved in embryophytes. iii) Bifunctional class I/II diTPS, which are present in gymnosperms, lycophytes and mosses, combine both catalytic activities of class II and class I enzymes in separated active sites [73]. Plant diTPS are composed of a domain triad, γβα, except for some monofunctional class I diTPS containing only βα domains [74, 75]. Although most diTPS have the domain triad, only bifunctional diTPS catalyze the successive cyclization of GGPP to a diterpene. This is true e.g. for abietadiene synthase from *Abies grandis*, labda-7,13*E*-dien-15-ol synthase from *Selaginella moellendorffii* and *cis*-abienol synthase from *Abies balsamea* [76-78]. The catalytic center of class II diTPS activity is formed by the N-terminal γβ domains harboring a conserved DxDD motif decisive for the protonation-initiated cyclization of GGPP [79]. Some of the possible products are *ent*-copalyl diphosphate (*ent*-CPP), normal CPP and labda-13-en-8-ol diphosphate (LPP) by activity of CPP and LPP synthases, respectively [75, 79]. Monofunctional class I enzymes are e.g. taxadiene synthase from *Taxus* spp., kaurene synthase-like (KSL) enzymes from phytoalexin production in *Oryza sativa* (rice) and kaurene synthases (KS) from the gibberellin biosynthesis [80-82]. Their catalytic activity is accomplished by the C-terminal α domain which facilitates an ionization-initiated cyclization of either isoprenyl diphosphates or class II diTPS products. The conserved DDxxD and NSE/DTE motifs enable the Mg^{2+}-mediated substrate binding [76]. As class I diTPS can allow the carbocation intermediate to undergo cyclization, water attack and other rearrangements, one or multiple products can be formed by class I diTPS activity [73]. In addition, the substrate promiscuity of diTPS is another feature that contribute to the diversity of hydrocarbon skeletons [83-85].

Many diterpene pathways known to date involve monofunctional diTPS such as the highly conserved formation of *ent*-kaurene by *ent*-copalyl diphosphate synthase (*ent*-CPS) and *ent*-KS in embryophytes [86]. However, *P. patens* harbors a bifunctional *ent*-CPS/KS that catalyzes the direct formation of *ent*-kaurene and 16-hydroxy-*ent*-kaurane from GGPP [87]. Such bifunctional KS in primordial plants are likely to constitute the evolutionary origin of monofunctional plant TPS [73]. Most likely, the ancient

bifunctional *ent*-CPS/KS gene was duplicated followed by subfunctionalization and activity loss of one TPS domain or even domain loss [88].

Recently, a new type of TPS has been identified in non-seed plants. Because they are closely related to bacterial TPS, these genes have been named microbial terpene synthase-like (MTPSL) [89]. In contrast to typical plant TPS, they only consist of an α domain, whereby they are much smaller. Moreover, they contain varying aspartate-rich motifs which comprise in most cases the classical DDxxD sequence but can also occur as DDxxxD or DDxxx [89]. So far, 24 MTPSL have been characterized, only two of which have activity on GGPP giving rise to diterpenes [90-92]. It was therefore concluded that MTPSL are rather responsible for the diversity of mono- and sesquiterpenes in those plants [89]. Phylogenetic analysis demonstrated that MTPSL are either related to bacterial or fungal TPS suggesting a different evolutionary origin than the typical plant TPS. Interestingly, MTPSL are widely distributed in non-seed plants (at least in 143 species) but are completely absent in seed plants and green algae [90]. It is likely that they have been integrated by horizontal gene transfer from bacteria and fungi at the time when plants entered terrestrial habitats. Giving a selection benefit they were kept in non-seed plants but probably got lost in seed plants because typical TPS took over their function [89].

DiTPS from gibberellin biosynthesis have the potential to serve as genetic reservoir for the evolution of (specialized) diTPS [79]. Notably, only a single amino acid exchange can alter the product outcome from hormonal towards specialized diterpenoids and *vice versa* [93-95]. The underlying process of gene duplication and neofunctionalization gave rise to the extensive expansion of the TPS gene family during the evolution of embryophytes. This has been analyzed in detail by Chen and colleagues who showed that the ratio of TPS genes to the entire genome increases from 0.002 gene/Mb in ancient *P. patens* to 0.08 gene/Mb in rice, 0.13 gene/Mb in *S. moellendorffii* and 0.3 gene/Mb in *A. thaliana* [73]. At the time of this review, in average, 20 to 150 TPS could be found in genomes of sequenced plants, except *P. patens* which harbors only one functional TPS gene [73]. Modern sequencing techniques which allow a fast and reliable read-out of plant genomes will demonstrate in the future if this range of TPS genes per species can be stretched.

DiTPS activity in Lamiaceae is mostly related to labdanoid diterpenes which derive from GGPP (**Fig. 1.6**). Although the occurrence of 91 diterpene skeletons within the Lamiaceae has been estimated [24], only few genes providing the olefin backbones have been identified yet. In the next section, I will focus on the supply of the hydrocarbon backbones for the abietane diterpene biosynthesis in rosemary (*R. officinalis*) and sage species (e.g. *S. fruticosa*, *Salvia pomifera* and *S. miltiorrhiza*). Additionally, diTPS examples from other labdane-related diterpenes of this plant family will be introduced.

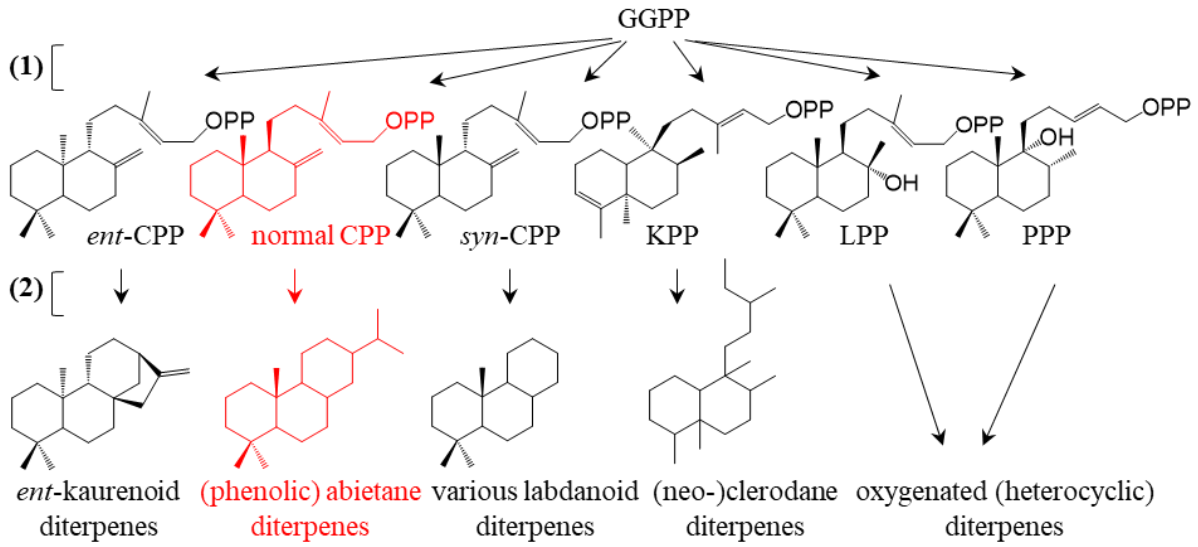

Fig. 1.6 Proposed diterpene synthase activity in Lamiaceae. GGPP is cyclized by class II diTPS (1) to *ent*-CPP, normal CPP, *syn*-CPP, KPP, PPP and LPP. Downstream class I diTPS, CYPs and transferases (2) generate the final diterpenoids which are given here as their characteristic skeleton.

In the biosynthesis of Lamiaceae abietane diterpenes such as CA from rosemary and tanshinones from *S. miltiorrhiza*, CPS catalyzes the bicyclization of GGPP to normal CPP (**Fig. 1.6**). This class II diTPS product is further dephosphorylated and cyclized by a KSL enzyme, called miltiradiene synthase (MiS), to miltiradiene (**Fig. 1.7**) [46, 47, 96, 97]. Like many other class I diTPS from specialized pathways, MiS has an "internal/γ" domain loss [46, 98]. Additionally, it has similarities with KS from gibberellin biosynthesis and has been hypothesized to have evolved from KS before the monocot-eudicot split. Therefore its olefin product can also be found in other Lamiaceae species such as in *C. forskohlii*, *Isodon rubescens* and *Marrubium vulgare* [99-101]. In those plants, miltiradiene, or its aromatic form abietatriene which derives by spontaneous oxidation (**Fig. 1.7**), constitutes one possible precursor of labdanoid diterpenes because of the characteristic tricyclic abietane skeleton (**Fig. 1.6**) [102, 103].

In addition to abietane diterpenes, diTPS in Lamiaceae synthesize several more labdane-related hydrocarbon backbones including halimadanes, clerodanes, pimaranes, kauranes, beyeranes, trachylobanes and icetexanes [104-108]. The biosynthesis remains in most cases unknown, but genes for some industrially relevant diterpenoids have been characterized. For example, oridonin is an *ent*-kaurenoid diterpene with antimicrobial and anticancer activities from *I. rubescens* [109]. The biosynthesis was proposed to run through *ent*-CPP and nezukol which are generated by the diTPS *ent*-CPS and nezukol synthase, respectively [100]. Six additional diTPS from this plant produce miltiradiene, isopimaradiene, *ent*-kaurene and *ent*-atiserene from normal or *ent*-CPP [110]. In addition to *ent*-CPP and normal CPP which are quite common in diterpenoid pathways [79], *syn*-CPP, kolavenyl diphosphate (KPP) and the oxygenated products LPP and peregrinol diphosphate (PPP) are required for the biosynthesis of a number of bioactive diterpenes. Serving as substrates for class I

diTPS enzymes, they give rise to diverse diterpenes (**Fig. 1.6**). For example, viteagnusin D, *syn*-isopimara-7,15-diene, labda-13(16),14-dien-9-ol, vitexifolin A, dehydroabietadiene and 9,13(*R*)-epoxy-labd-14-ene are formed in *V. agnus-castus* from *syn*-CPP and PPP [111]. Sclareol from *S. sclarea*, 13-epoxy-labd-14-ene in *M. vulgare* and manoyl oxide present in *C. forskohlii* derive from phosphorylated terpene alcohols produced by class II diTPS. They are intermediates in the biosynthesis of Ambrox®, antidiabetic marrubiin and forskolin [11, 99, 101, 112]. Furthermore, KPP and (–)-kolavenol are proposed intermediates *en route* to hallucinogenic neo-clerodane salvinorin A from *Salvia divinorum* [95, 113]. In some of the mentioned examples, the involved diTPS exhibit substrate promiscuity which contributes to the diversity of plant specialized diterpenoids.

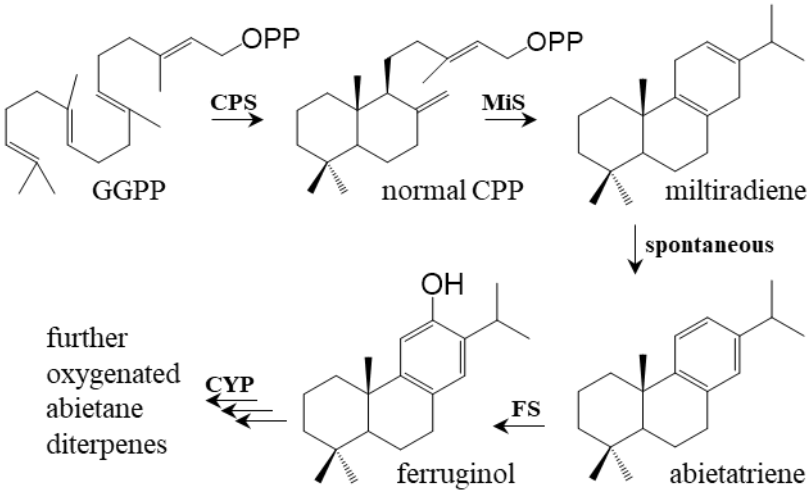

Fig. 1.7 Biosynthesis of abietane diterpenes in Lamiaceae. The biosynthesis of abietane diterpene skeletons in rosemary and sage species require activity of the diTPS CPS and MiS. Whether miltiradiene or abietatriene constitutes the preferred substrate of downstream CYP enzymes (ferruginol synthase (FS) and others) remains unclear.

1.3. Cytochrome P450 enzymes in plant metabolism

1.3.1. The function of cytochrome P450 enzymes in plants

CYPs are heme-dependent monooxygenases from all life kingdoms and constitute the third largest family of plant genes [114, 115]. Most of them are associated to the membrane of the ER via their N-terminus. They participate in detoxification processes and in the biosynthesis of general and specialized metabolites. The most common catalyzed reactions are hydroxylation and further oxygenation in a stereospecific manner. Moreover, also epoxidation, C-C cleavage, C-C coupling, ring rearrangements and desaturation occur in this very diverse enzyme family (**Fig. 1.8**) [116]. CYPs often are promiscuous and/or can produce several products from a single substrate. For example, CYP720B1 from *Pinus taeda* accepts four substrates to produce a total of nine products [117].

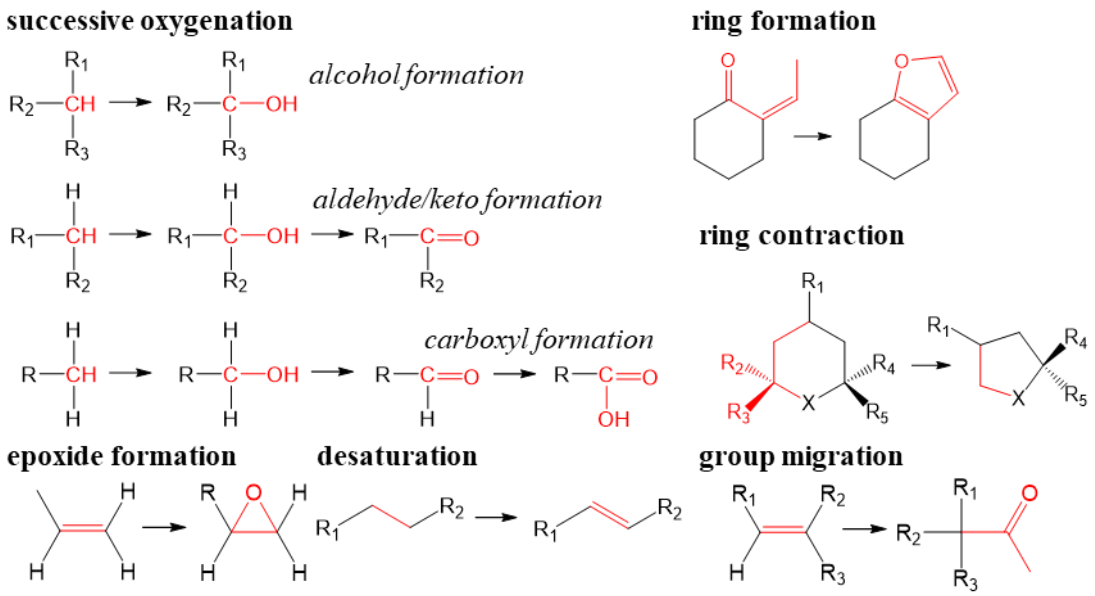

Fig. 1.8 Selected reactions catalyzed by cytochrome P450 enzymes. Modified from Lamb and Waterman (2013) [116].

CYP enzymes belong to clans in which they are classified into families and subfamilies. A CYP clan is a deep gene clade that separates from others on a phylogenetic tree [115]. Within each CYP family members share at least 39 % amino acid identity, and at least 55 % in a subfamily. According to this, CYPs are named for their family, subfamily and isoform number [115, 118]. For example, CYP76AH22 represents isoform 22 in the CYP76AH subfamily that belongs to the CYP76 family.

CYP51, CYP71, CYP72, CYP74, CYP85, CYP86, CYP97, CYP710, CYP711, CYP727 and CYP746 constitute the CYP clans that are present in embryophytes [115]. Among them CYP51 is one of the oldest clans which is involved in sterol biosynthesis [115, 119]. Four of the mentioned clans, namely CYP71, CYP72, CYP85 and CYP86, are multi-family clans and the first three have expanded the most in embryophytes [115]. They are involved in the metabolism of isoprenoids and brassinosteroids (CYP85) as well as in the catabolism of hormones and in the biosynthesis of cytokinins and fatty acids (CYP72) [120-125]. Notably, the CYP71 clan contains more than 50 % of all land plant CYPs with commitment in isoprenoid, alkaloid, fatty acid and hormone metabolism [115].

It is difficult to predict substrate preferences based on CYP clan and family memberships. For example, CYPs from different clans can be involved in the same metabolic pathway as for CYP88D6 and CYP72A154 which contribute to the biosynthesis of triterpene glycyrrhizin from *Glycyrrhiza* plants [126, 127]. On the other hand, members of one CYP clan can act in separate pathways (e.g. CYP71Ds hydroxylate limonene and flavone [128, 129]), or biosynthetic and catabolic CYPs belong to different clans like in the brassinosteroid metabolism [125, 130].

Because CYP sequence identity is sometimes lower than 20 %, a huge metabolic diversity derives [131]. Nevertheless, all plant CYPs share the same overall architecture including a cysteine from the heme-binding domain, the oxygen binding and activating I-helix (AG×D/ET), a proline-rich

membrane hinge and an E-E-R triad formed by the P**E**RF motif and the K-helix (K**E**TL**R**) [118]. The K-helix and the PERF motif are believed to guide the heme pocket and to stabilize the conserved core structure [132]. Additionally, the catalytic center contains a heme with an iron ligand coordinated to the thiolate of the conserved cysteine (**Fig. 1.9**) [118]. Other CYP regions are highly variable and are mainly related to membrane anchoring, substrate binding and recognition [114].

The catalytic mechanism of the most common CYP reaction, namely oxygenation, can be summarized as a transfer of atmospheric oxygen and two electrons from the co-factor NAD(P)H to a non-activated carbon-hydrogen bond of the substrate [116]. In most cases, plants require a cytochrome P450 reductase (CPR), or in some cases cytochrome b_5, for the electron transfer [133, 134]. The detailed catalytic mechanism of substrate hydroxylation by CYPs is shown in **Fig. 1.9** [114, 135]. First, water from the resting state of the enzyme is released upon substrate binding (**Fig. 1.9 I**). Guided by CPR, one electron is transferred from NAD(P)H to the complex (**Fig. 1.9 II**). Afterwards, atmospheric oxygen is bound to the heme to form a superoxide complex (**Fig. 1.9 III**). A second reduction by electron transfer from NAD(P)H activates the oxygen (**Fig. 1.9 IV**) [136]. The two-electron-reduced dioxygen is than protonated which cleaves the O-O bond and releases one oxygen atom as water (**Fig. 1.9 V** and **VI**). Finally, the second oxygen atom with two electrons is inserted into the substrate (**Fig. 1.9 VII**) and replaced by water to restore the resting state of the enzyme (**Fig. 1.9 VIII**).

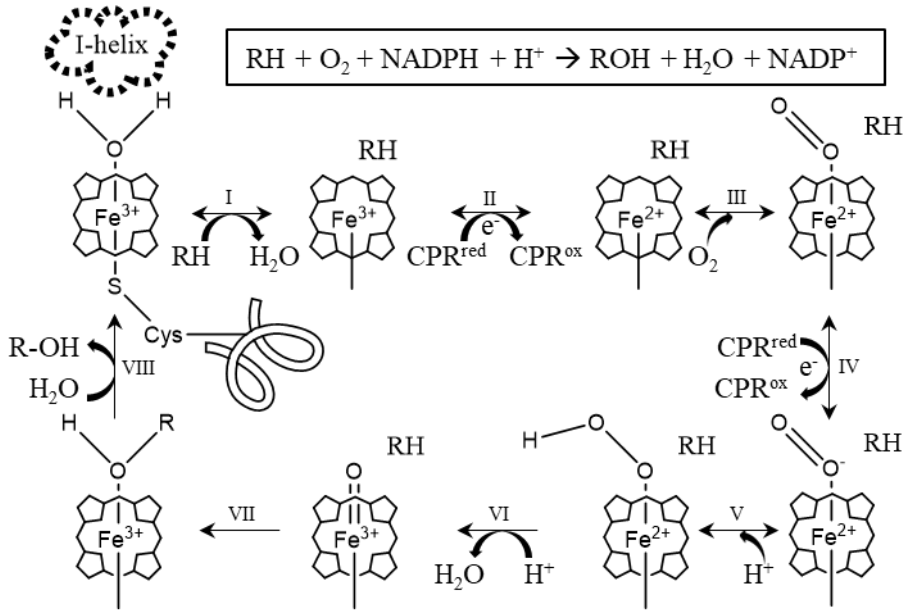

Fig. 1.9 The catalytic mechanism of substrate hydroxylation by cytochrome P450 enzymes. The overall reaction is summarized in the box. In plants, the CPR transfers two electrons (e^-) from NAD(P)H, and itself undergoes oxidation. By abstraction of two protons, one atom of molecular oxygen can be introduced into the substrate (RH) upon release of water. Finally, the hydroxylated substrate is replaced by water to restore the resting state of the CYP. The depiction of the I-helix, which coordinates the oxygen binding and activation, and the heme-binding cysteine were omitted after catalytic step I in order to simplify the scheme. The figure was modified from Werck-Reichhart and Feyereisen (2000) and Guengerich (2007) [114, 135].

1.3.2. Cytochrome P450 enzymes as key player in the biosynthesis of plant specialized diterpenes

Specialized metabolites that are produced by plants are highly diverse and their number has been estimated to exceed 200.000 [137]. Most of them are oxidized, such as 97 % of all known terpenoids [138]. In the biosynthesis, CYPs play a crucial role because they carry out the vast majority of oxidation reactions. Considering the number of compounds plants can produce, the structural diversity reflects the expansion of CYP genes required for their metabolism [137]. It is therefore not surprising that plants contain the largest number of CYP genes compared with other taxonomic groups [114]. The expansion of some plant CYP families led to the appearance of many specialized metabolites but often in a limited number of species or taxa. For example, the biosynthesis of casbene and neocembrene derived diterpenoids involves CYP726As and is limited to the plant family Euphorbiaceae [139]. The clan that expanded the most is CYP71 [115]. In addition to the biosynthesis of other compound classes, it contains CYPs involved in sesquiterpene (e.g. CYP71AV1 from *Artemisia annua* [140]) and diterpene synthesis pathways (e.g. in rice [141]) as well as all CYPs which are related to monoterpenes, apart from one exception (Madagascar periwinkle CYP72A1) [120].

Beside the high number of CYP genes present in plants, the CYP flexibility is an important factor that drives metabolic diversity and evolution *in planta* [142]. It is assumed that enzymes from specialized pathways are more promiscuous than their relatives from general metabolism [143]. The conventional view of enzyme activity as a one substrate-one product mechanism through the key-lock principle (**Fig. 1.10A**) is outdated for most cases because enzymes have been documented to exhibit flexibility in substrate recognition and binding as well as in catalyzed reactions. Three types of CYP flexibility can be distinguished that occur in the biosynthesis of specialized compounds. i) One substrate can be successively converted to a product through one or more stable intermediates, which can, most likely depend on the reaction conditions, dissociate from the active center (**Fig. 1.10B**). ii) Several products can be formed from one substrate. In this case, two sub-types are known: the catalytic flexibility which is characterized by different reaction mechanisms, and the product multiplicity which leads to alternative products through the same reaction (**Fig. 1.10C**). iii) The third type of CYP flexibility is substrate promiscuity and can appear in combination with the successive conversion via stable intermediates (**Fig. 1.10D**) [144]. Such a case is found in the biosynthesis of diterpene resin acids from conifers. CYP720B4 turns eight different labdane-related diterpenes into the corresponding acids via the alcohol and aldehyde intermediates [145]. Remarkably, CYP71D55 from *Hyoscyamus muticus* unites all other mentioned types of CYP promiscuity. In the biosynthesis of the sesquiterpene phytoalexins, CYP71D55 catalyzes the successive oxidation of premnaspirodiene to solavetivone with solavetivol as intermediate. Additionally, it accepts (+)-valencene and 5-epiaristolochene as substrates, the latter being converted to 2β(OH)-epiaristolochene, 1β(OH)-epiaristolochene and 3α(OH)-epiaristolochene [146]. Both CYP720B4 and CYP71D55 are excellent examples of the distinctive plant CYP flexibility.

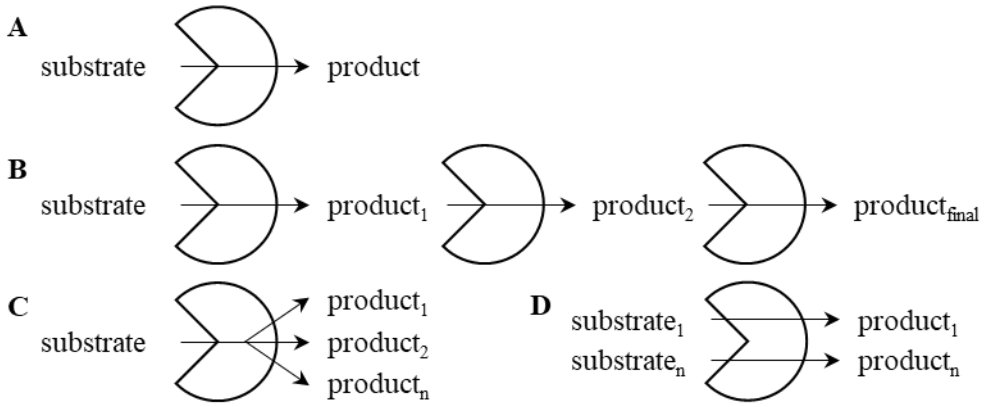

Fig. 1.10 Promiscuity of cytochrome P450 enzymes involved in specialized metabolic pathways. A, Conventional enzyme activity following the principle of one substrate-one product. B, One substrate is successively converted to a final product through one or several stabile intermediates which can dissociate from the active center. C, Multiple products are formed from one substrate either through different catalytic mechanisms (catalytic flexibility) or through the same reactions towards alternative substrates (product multiplicity). D, Substrate promiscuity leads to several products, each derived from a different substrate. This enzyme activity can occur in combination with the successive conversion (B).

CYP genes involved in specialized metabolite biosynthesis are sometimes organized in metabolic gene clusters together with distantly related genes that are involved in the same pathway. The following examples illustrate this. i) *CYP705A5* and *CYP708A2* from thalianol production in *A. thaliana* co-cluster with a BAHD acyltransferase gene and an oxidosqualene cyclase gene. ii) *CYP99As* participating in rice phytoalexin biosynthesis are localized to the same genetic region as diTPS genes and a dehydrogenase gene involved in the same pathway. iii) CYPs from benzoxazinoid biosynthesis in *Zea mays* form a cluster with an indole-glycerolphosphate lyase and a 2-oxoglutarate-dependent dioxygenase [147-150]. Metabolic gene clusters are a common feature of prokaryotes (in this case termed operons), but more plant examples are expected to be identified in the future. If they originate from horizontal gene transfer or more likely derived through gene duplication followed by neo- and sub-functionalization remains to be elucidated [151]. Additionally, CYP genes involved in specialized metabolism have been proposed to have evolved from primary and hormonal pathways. For example, CYP84A1 is a lignin-biosynthetic enzyme and thus can be considered as contributing to general metabolism in vascular plants [152]. Weng and co-workers (2012) identified a paralogue in *A. thaliana* which acts in the biosynthesis of arabidopyrones [153]. The pathway branches off from phenylpropanoid metabolism and gives rise to a set of compounds (arabidopyl alcohol, *iso*-arabidopyl alcohol, arabidopic acid and *iso*-arabidopic acid) with so far unknown function. Other striking examples are the kaurene oxidase-like enzymes (KOL) from rice which are closely related to kaurene oxidase (KO) from gibberellin biosynthesis (71 % amino acid sequence identity with KO2) but contribute to specialized diterpenoid metabolism [154]. More aspects on diterpenoid CYPs regarding evolution and biosynthesis can be found in chapter 2.4.

1.4. Tools and expression platforms for elucidation and engineering of diterpene pathways

1.4.1. Cytochrome P450 engineering to elucidate, modify and optimize biosynthetic pathways

In order to understand or modify the function of plant specialized CYPs, bioinformatics and synthetic biology have supplied helpful tools. They allow rapid gene identification, biosynthetic modification towards desired compounds and pathway optimization regarding substrate flux and product yield (**Fig. 1.11**). If assuming that more biosynthetic genes well be identified e.g. by RNA-Seq methods, the characterization of candidate CYPs is a challenging task. However, modular expression systems provided by modern cloning techniques enable CYPs to be co-expressed with upstream biosynthetic genes in natural or artificial combinations. Particularly, the "Golden Gate" cloning technique allows the modular assembly of several genes into one expression vector [155, 156]. It was already previously used to optimize the production of benzylpenicillin in *S. cerevisiae* and of β-carotene in *Yarrowia lipolytica* [157, 158]. This one-pot method is of particular benefit as it enables the fast coupling of gene modules in a defined order by using Type IIS restriction enzymes which create 4-bp-overhangs. The derived reconstruction of whole pathways in model organisms has been documented frequently and offers a valuable complement to *in vitro* assays and traditional enzyme kinetics [141, 159-163].

After having explored the substrate specificity of a particular CYP, the characterization of the catalytic mechanism remains to be elucidated. This is required to potentially modify the CYP reaction with respect to product ratio, stereospecificity, or the position of oxidation/hydroxylation. In the absence of any CYP crystal structures, researchers perform homology modelling using established 3D structures as templates to identify amino acids that potentially contribute to substrate binding and turnover. The identified residues are then subjected to (site-directed) mutagenesis and afterwards the derived mutant CYPs are biochemically characterized. In some cases, a small number of amino acid exchanges are sufficient to alter a CYP activity. For example, tobacco CYP74D3 and flax CYP74B16 involved in plant oxylipin metabolism are divinyl ether synthases but have been converted into allene oxide synthases by single-point mutations [164]. In other cases, a few more mutations are required to affect the catalytic mechanism. Indeed, a sextuple mutation of *Hypericum* CYP81AA2, which is involved in xanthone biosynthesis, switched the regioselectivity from *ortho* hydroxylation to *para* [165]. Besides controlling the regioselectivity, substrate binding has been investigated using homology modelling and mutagenesis. In CYP73A1 from lignin biosynthesis, modification of specific amino acids led to a reduced interaction between enzyme and substrate [166]. The authors speculated that the amino acid mutations affected the substrate positioning in the active center which was verified by a 50 % decrease in the catalytic activity.

Amino acid mutagenesis is also used to modify CYP activities. With respect to protein engineering, a forward-looking approach has been performed by Ignea and colleagues (2015) who created a library of mutated CYP720B1 in order to characterize the hydroxylation of the substrate but also to generate

new CYP activities. The co-expression of diTPS and (mutated) CYPs in a "plug and play platform" allowed the modular reconstruction of artificial gene combinations to produce diterpenes that are new or difficult to isolate from natural biological sources [85]. Such approaches offer great potential for drug developments (e.g. antibiotics) since multi-drug resistant microbes and cancer cells have never met the artificial metabolites.

Once a metabolic pathway is elucidated and modified towards a desired target compound, the production can be performed in recombinant systems. Notably, gene expression and metabolic flux require optimization to increase product yield. Probably the most prominent example of pathway optimization is the synthesis of artemisinic acid in *S. cerevisiae*. CYP71AV1 from *A. annua* catalyzes three successive oxidations on amorpha-4,11-diene which yield artemisinic acid *en route* to the antimalaria drug artemisinin [140]. Paddon and co-workers (2013) reported about the improved electron transfer to CYP71AV1 via a moderate expression of the NADPH dependent P450 oxidoreductase and via the introduction of *A. annua* cytochrome b_5. Both steps protected the yeast cells against ROS and toxic intermediates, and together with other optimizations achieved a yield increase to 25g/l artemisinic acid [167].

In summary, CYP engineering is a promising field to develop enzyme activities towards compounds that can be used to develop new drugs or other valuable materials. In order to achieve this, time-efficient and cost-saving production systems are required. With the increasing knowledge about biosynthetic genes and the catalytic mechanism of the encoded enzymes, metabolite pathways can be reconstructed using modular cloning techniques and recombinant systems.

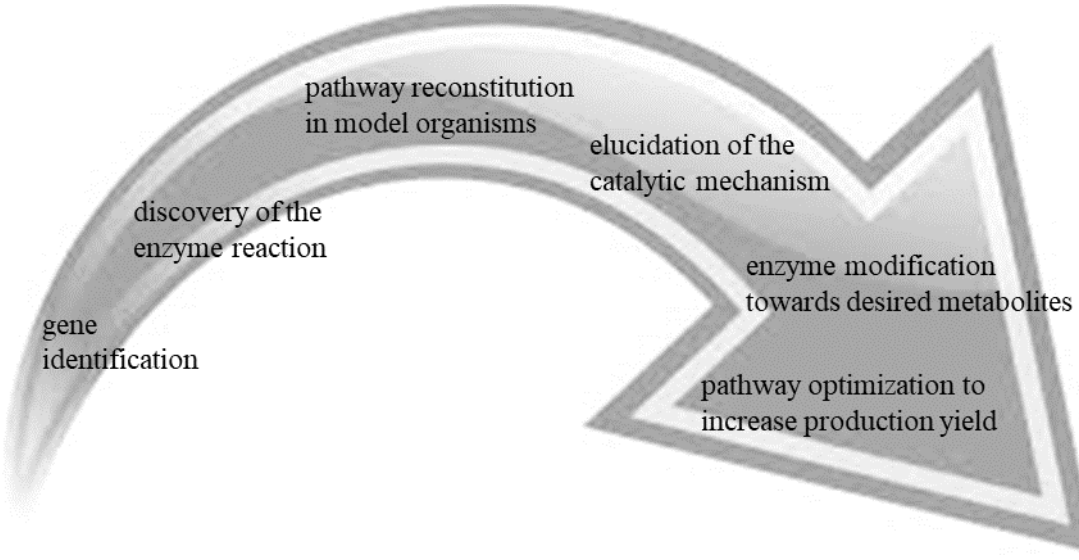

Fig. 1.11 Cytochrome P450 engineering to elucidate, modify and optimize the production of valuable plant specialized metabolites.

1.4.2. Expression systems for the elucidation of diterpene pathways and their high-value production

Plant natural products for pharmaceutical and other industrial applications are often difficult to obtain. They occur in low abundancy, in complex mixtures with similar metabolites which demands extensive purification, and in undomesticated plant species that lack cultivation and geographic availability. In addition, some compounds are exclusively produced seasonally or upon contact with a particular environmental or other elicitor. To benefit from such metabolites anyway, total or semisynthesis have been developed for some industrial relevant compounds such as for (+)-ingenol which is the precursor of the anticancer drug ingenol mebutate [168]. However, chemical synthesis is expensive, time-consuming due to multiple complex reaction steps and polluting [169-171]. Furthermore, the protection of chemical groups needs to be considered as well as the correct stereochemistry which is often difficult to achieve. Plant cell cultures offer a feasible alternative also because consumers rather accept supplements from such sources as opposed to artificial production. In comparison to field grown plants, the accomplished product yields can be sufficient (e.g. 13.5-fold shikonin, 12-fold ubiquinone-10 and 9-fold rosmarinic acid [169]), but the overall production costs are significantly higher [172]. Plant expression platforms come up with advantageous properties which include the same subcellular compartmentation as the native organism which is beneficial for protein localization, availability of similar metabolic building blocks useful for precursor supply and a complex protein expression machinery which performs required folding, glycosylation and assembly. Stable or *Agrobacterium*-mediated expression in *Nicotiana tabacum* and *N. benthamiana* have become standard tools for pathway elucidation and reconstruction [173]. However, large-scale metabolite production for industrial applications can be challenging due to pathway interferences and competitions as exemplified by the artemisinic acid biosynthesis in *N. benthamiana* which led to glycosylated derivatives [174].

Microbial systems (e.g. *Escherichia coli* and *S. cerevisiae*) are popular as expression platforms because they are robust, fast growing, economical, scalable and benefit from a broad repertoire of tools for DNA assembly and host optimization [175]. Furthermore, biosynthetic intermediates do not need to be purified before being used as substrates in the next reaction step. In terms of CYPs, eukaryotic systems are to be preferred, for example *S. cerevisiae*. Baker's yeast became a key model organism for fundamental molecular biology research including the reconstruction of diverse plant specialized pathways that require participation of CYPs (e.g. terpenes, alkaloids and flavonoids [176-180]). This is due to the endomembrane required for CYP localization and the post-translational modification which is similar to plant systems [181]. Moreover, as *S. cerevisiae* has only a few specialized metabolites, interference with the engineered compound biosynthesis is limited. However, a few challenges need to be overcome including toxicity of individual target metabolites as well as substrate supply and metabolic flux.

1.5. Questions addressed in the thesis

The overall aim of this thesis is to provide insights into the role of CYPs from plant diterpene biosynthesis in particular from abietane diterpene pathways in Lamiaceae. In the first part, the elucidation of the CA biosynthesis and its reconstitution in yeast is addressed. For this, CYP candidate genes identified by mining transcriptome data were co-expressed with upstream biosynthetic genes using a modular assembly system for yeast. The formed abietane diterpenes were detected and identified by chromatographic methods and by NMR analysis. To investigate the catalytic mechanism of involved CYPs, candidate amino acids were selected for site-directed mutagenesis using a 3D model, and the activity of derived mutants were examined.

The second part of this thesis explores the complex CYP76 oxidation network that contributes to the diversity of oxidized abietane diterpenes in *R. officinalis* and *S. miltiorrhiza*. Combinatorial synthesis in *S. cerevisiae* was used to co-express diTPS and promiscuous CYP76s, and the derived diterpenoid products were analyzed by tandem mass spectrometry and compared to product profiles *in planta*.

The third part of the present thesis is a comprehensive review of CYPs that were reported to be involved in diterpene biosynthesis in plants. Moreover, the documented enzymes were subjected to phylogenetic analysis to find potential correlations between structural classes of diterpenes and the CYPs that contribute to their biosynthesis as well as to discover evolutionary trends in the distribution of CYPs that play a role in the diterpenoid biosynthesis.

2. Results

2.1. Contribution to the publications

Chapter 2.2.2.: U. Scheler, W. Brandt, A. Porzel, K. Rothe, D. Manzano, D. Božić, D. Papaefthimiou, G. U. Balcke, A. Henning, S. Lohse, S. Marillonnet, A. K. Kanellis, A. Ferrer and A. Tissier (2016) Elucidation of the biosynthesis of carnosic acid and its reconstitution in yeast. *Nature Communications*, **7**: p. 12942

Own contributions:

Experimentation: cloning of yeast compatible constructs and expression; isolation, purification and chromatographic analysis (GC-MS and LC-MS) of diterpenes from rosemary and sage or formed by yeast expression; mutagenesis of CYPs and activity test; *in vitro* enzyme assays; phylogenetic analysis (95 %)

Data analysis: analysis of the above data (95 %)

Writing: design and preparation of figures (70 %); writing of the manuscript (50 %)

Other contributions:

W. Brandt performed and analyzed the modelling experiments, created the modelling figures; A. Porzel performed and analyzed the NMR experiments and created the NMR figures; K. Rothe isolated the TPS genes; D. Manzano designed the qPCR experiments; D. Božić and D. Papaefthimiou isolated *CYP76AH22*, *CYP76AH23*, *CYP76AH24* and the *CYP76AKs*; D. Papaefthimiou performed the qPCR experiments; G. U. Balcke developed the LC-MS method; A. Henning assisted the diterpene isolation for NMR experiments; S. Lohse, A. Tissier and S. Marillonnet designed and developed the Golden Gate modular cloning system for yeast; W. Brandt, A. Porzel and A. Tissier wrote the manuscript.

Chapter 2.3.2.: U. Bathe, A. Frolov, A. Porzel and A. Tissier (2019) CYP76 oxidation network of abietane diterpenes in Lamiaceae reconstituted in yeast. *Journal of Agricultural and Food Chemistry*, In Press

Own contributions:

Experimentation: cloning of yeast compatible constructs and expression; isolation, purification and chromatographic analysis (GC-MS and LC-MS) of diterpenes from rosemary and sage or formed by yeast expression; *in vitro* enzyme assays; phylogenetic analysis (100 %)

Data analysis: analysis of the above data (95 %)

Writing: design and preparation of figures (60 %); writing of the manuscript (50 %)

Other contributions:

A. Frolov performed and analyzed the MS^n experiments, created MS^n figures; A. Porzel performed and analyzed the NMR experiments and created NMR figures; W. Brandt, A. Porzel and A. Tissier wrote the manuscript.

Chapter 2.4.2.: U. Bathe and A. Tissier (2019) Cytochrome P450 enzymes: A driving force of plant diterpene diversity. *Phytochemistry*, **161**: p. 149

Own contributions:

Literature research and experimentation: data collection and phylogenetic analysis (95 %)

Data analysis: analysis of the above data (70 %)

Writing: design and preparation of figures (90 %); writing of the manuscript (50 %)

Other contributions:

A. Tissier analyzed the data; A. Tissier wrote the manuscript.

2.2. The role of cytochrome P450 enzymes in the carnosic acid biosynthesis from rosemary and sage

2.2.1. Aims and summary

CA is an abietane diterpene found in *Rosmarinus* and *Salvia* [182]. Its antioxidant activity *in vitro* provides the basis for applications in the food and cosmetic industry [183]. Although genes that provide the biosynthetic intermediates miltiradiene and ferruginol had been identified, the downstream steps remained unknown when this study started [46, 47]. Hypotheses for the pathway from ferruginol to CA included introduction of one additional hydroxylation on the C-ring and a carboxylation at C-20. CYPs were speculated to be likely candidates for both reactions. First, the biosynthesis of ferruginol was reconstituted in yeast. For that, a GGPPS supplying sufficient amounts of GGPP, appropriate diTPS, a CPR enzyme supporting the CYP activity and formerly reported CYP76AH22-24 which possess FS activity were assembled using the Golden Gate modular cloning system. GC-MS and LC-MS were applied to detect the produced diterpenes. Beside the expected metabolites, another diterpenoid more oxidized than ferruginol was found. NMR analysis revealed the identity of 11-hydroxy ferruginol. Consequently, CYP76AH22-24 have hydroxy ferruginol synthase (HFS) activity.

CYP76AH22-24 display high sequence similarities on the protein level with CYP76AH1, a FS from *S. miltiorrhiza*. Using homology modelling, 3D models of FS and HFS were created to identify amino acids that influence substrate positioning. These were subjected to reciprocal mutagenesis and tested by yeast expression. Finally, amino acids 301, 303 and 479 determined FS or HFS activity.

The biosynthesis of CA was suggested to take place in glandular trichomes of rosemary and sage leaves because CA and related metabolites accumulate in such specialized tissues. Accordingly, the highest transcript abundance of diTPS involved in the pathway were detected in trichomes [46]. This led to the hypothesis that downstream CYPs should be highly expressed in those tissues, too. Using a transcriptome database that was provided by the TERPMED project (http://www.terpmed.eu/), candidate CYPs, which could catalyze the three sequential C20 oxidations to CA, were selected. This led to the identification of CYP76AK6-8, and the whole CA biosynthesis was reconstituted in yeast.

2.2.2. Publication

Elucidation of the biosynthesis of carnosic acid and its reconstitution in yeast

U. Scheler, W. Brandt, A. Porzel, K. Rothe, D. Manzano, D. Božić, D. Papaefthimiou, G. U. Balcke, A. Henning, S. Lohse, S. Marillonnet, A. K. Kanellis, A. Ferrer and A. Tissier

[1]Department of Cell and Metabolic Biology, Leibniz Institute of Plant Biochemistry, Weinberg 3, Halle 06120, Germany.
[2]Department of Bioorganic Chemistry, Leibniz Institute of Plant Biochemistry, Weinberg 3, Halle 06120, Germany.
[3]Program of Plant Metabolism and Metabolic Engineering, Centre for Research in Agricultural Genomics, Campus UAB, 08193 Bellaterra, Spain.
[4]Faculty of Pharmacy, Department of Biochemistry and Molecular Biology, University of Barcelona, 08028 Barcelona, Spain.
[5]Group of Biotechnology of Pharmaceutical Plants, Laboratory of Pharmacognosy, Department of Pharmaceutical Sciences, Aristotle University of Thessaloniki, 54124 Thessaloniki, Greece.
†Present address: Institute for Biological Research 'Siniša Stanković', University of Belgrade, Bul. despota Stefana 142, 11060 Belgrade, Serbia.

Abstract

Rosemary extracts containing the phenolic diterpenes carnosic acid and its derivative carnosol are approved food additives used in an increasingly wide range of products to enhance shelf-life, thanks to their high antioxidant activity. We describe here the elucidation of the complete biosynthetic pathway of carnosic acid and its reconstitution in yeast cells. Cytochrome P450 oxygenases (CYP76AH22-24) from *R. officinalis* and *Salvia fruticosa* already characterized as ferruginol synthases are also able to produce 11-hydroxyferruginol. Modelling-based mutagenesis of three amino acids in the related ferruginol synthase (CYP76AH1) from *S. miltiorrhiza* is sufficient to convert it to a 11-hydroxyferruginol synthase (HFS). The three sequential C20 oxidations for the conversion of 11-hydroxyferruginol to carnosic acid are catalysed by the related CYP76AK6-8. The availability of the genes for the biosynthesis of carnosic acid opens opportunities for the metabolic engineering of phenolic diterpenes, a class of compounds with potent anti-oxidant, anti-inflammatory and anti-tumour activities.

Nature Communications (2016) **7**: p.12942. (DOI: 10.1038/ncomms12942)

2.3. CYP76 oxidation network that contributes to the diversity of abietane diterpenes in rosemary and sage

2.3.1. Aims and summary

Abietane diterpenes occur in rosemary and sage as a complex mix of structurally similar compounds [184, 185]. Besides methylation, oxygenation is the most common chemical decoration on such metabolites and therefore CYPs are believed to be critical for their biosynthesis. Previous studies suggested that the family of CYP76 is particularly important as demonstrated for several abietane diterpenes from *S. miltiorrhiza*, for CA from *R. officinalis* and for forskolin from *C. forskohlii* [17, 97, 103, 186-188]. The involved enzymes were assigned to the subfamilies of CYP76AH, which act first on diTPS products, followed by CYP76AK, which possesses C20 oxidase activity. The majority of CYP76AHs and CYP76AKs were shown to be promiscuous because they usually accept a set of substrates. However, the biosynthetic elucidation focused on individual target metabolites but did not consider the crossover between pathways. Thus, the complex network of oxidized abietane diterpenes in Lamiaceae that is likely generated by the CYP76 promiscuity remains only partially explored. Within this study, CYP76s from *R. officinalis* and *S. miltiorrhiza*, namely FS (CYP76AH1), HFSs (CYP76AH3 and CYP76AH22) and C20 oxidase (CYP76AK1) were carefully examined with respect to unknown products that occur by combinatorial synthesis. To achieve this, the modular Golden Gate assembly system for yeast was used [187]. Remarkably, the activity of this small number of enzymes led to the production of 14 oxidized diterpenes, eight of which had not been reported before. Due to the fact that all produced diterpenes were also detected in the parent plants, *S. cerevisiae* was validated as a useful and efficient expression platform for engineering and production of valuable abietane diterpenes.

2.3.2. Publication

CYP76 oxidation network of abietane diterpenes in Lamiaceae reconstituted in yeast

U. Bathe[1], A. Frolov[2], A. Porzel[2] and A. Tissier[1]

[1]Department of Cell and Metabolic Biology, Leibniz Institute of Plant Biochemistry, Weinberg 3, Halle 06120, Germany.

[2]Department of Bioorganic Chemistry, Leibniz Institute of Plant Biochemistry, Weinberg 3, Halle 06120, Germany.

Abstract

Rosemary and sage species from Lamiaceae contain high amounts of structurally related but diverse abietane diterpenes. A number of substances from this compound family have potential pharmacological activities and are used in the food and cosmetic industry. This has raised interest in their biosynthesis. Investigations in *Rosmarinus officinalis* and some sage species have uncovered two main groups of cytochrome P450 oxygenases that are involved in the oxidation of the precursor abietatriene. CYP76AHs produce ferruginol and 11-hydroxyferruginol, while CYP76AKs catalyze oxidations at the C20 position. Using a modular Golden-Gate-compatible assembly system for yeast expression, these enzymes were systematically tested either alone or in combination. A total of 14 abietane diterpenes could be detected, eight of which have not been reported thus far. We demonstrate here that yeast is a valid system for engineering and reconstituting the abietane diterpene network, allowing for the discovery of novel compounds with potential bioactivity.

Journal of Agricultural and Food Chemistry (2019) In Press. (DOI: 10.1021/acs.jafc.9b00714)

2.4. A review about cytochrome P450 enzymes involved in plant specialized diterpene pathways

2.4.1. Aims and summary

CYPs carry out the vast majority of oxidation reactions in the metabolism of plant specialized diterpenes. These oxidations not only contribute to the diversity of this compound class but also provide anchoring points for further modifications such as methylation, acylation and glycosylation. Although most diterpene pathways remain to be elucidated, reports on CYPs involved in plant diterpene biosynthesis accumulated in recent years. This part of the present thesis gives a comprehensive review of all plant CYPs that are known to be involved in diterpenoid production to date. CYP functions on macrocyclic, linear and labdane-related diterpene skeletons were summarized. Furthermore, a phylogenetic analysis was conducted on the collected enzymes that highlights correlations between diterpene structures and CYPs involved in these pathways. This investigation showed no clear relationship between the three contributing CYP clans (CYP71, CYP85 and CYP72) and the derived metabolite structures. Indeed, plant diterpenoid CYPs are highly diverse in their evolutionary origin and in their biosynthetic activity. However, it could be determined that CYP71 is a dominant CYP clan and that species-specific expansions in some families are a common feature of plant diterpene CYPs.

2.4.2. Publication

Cytochrome P450 enzymes: A driving force of plant diterpene diversity

U. Bathe and A. Tissier

Department of Cell and Metabolic Biology, Leibniz Institute of Plant Biochemistry, Weinberg 3, Halle 06120, Germany.

Abstract

In plant terpene biosynthesis, oxidation of the hydrocarbon backbone produced by terpene synthases is typically carried out by cytochrome P450 oxygenases (CYPs). The modifications introduced by CYPs include hydroxylations, sequential oxidations at one position and ring rearrangements and closures. These reactions significantly expand the structural diversity of terpenoids but also provide anchoring points for further decorations by various transferases. In recent years, there has been a significant increase in reports of CYPs involved in plant terpene pathways. Plant diterpenes represent an important class of metabolites that includes hormones and a number of industrially relevant compounds such as pharmaceutical, aroma or food ingredients. In this review, we provide a comprehensive survey on CYPs reported to be involved in plant diterpene biosynthesis to date. A phylogenetic analysis showed that only few CYP clans are represented in diterpene biosynthesis, namely CYP71, CYP85 and CYP72. Remarkably, few CYP families and subfamilies within those

clans are involved, indicating specific expansion of these clades in plant diterpene biosynthesis. Nonetheless, the evolutionary trajectory of CYPs of specialized diterpene biosynthesis is diverse. Some are recently derived from gibberellin biosynthesis, while others have a more ancient history with recent expansions in specific plant families. Among diterpenoids, labdane-related diterpenoids represent a dominant class. The availability of CYPs from diverse plant species able to catalyze oxidations in specific regions of the labdane-related backbones provides opportunities for combinatorial biosynthesis to produce novel diterpene compounds that can be screened for biological activities of interest.

Phytochemistry (2019) **161**: p. 149. (DOI: 10.1016/j.phytochem.2018.12.003)

3. Discussion and perspectives

The first committed steps of the CA biosynthesis from *R. officinalis* and sage species have been identified up to ferruginol, an intermediate which derives from a single hydroxylation on the diterpene backbone miltiradiene/abietatriene at position C12. However, the biosynthesis downstream of ferruginol, which requires oxidation at two additional positions, remained unclear [46, 47]. Using an EST sequence database, HFSs (CYP76AH22-24) and C20 oxidases (CYP76AK6-8) were identified which carry out the final oxidation steps at C11 and C20, respectively [187]. Co-expression with the upstream biosynthetic genes in *S. cerevisiae* led to the successful reconstitution of the CA biosynthesis in a recombinant system which was confirmed by similar studies [97]. Our results proved that yeast is a suitable platform for the synthesis of plant diterpenoid compounds and provide the fundamental knowledge for a production of CA by fermentation for industrial applications.

The role of CYP76AHs and CYP76AKs in abietane diterpene biosynthesis from Lamiaceae was characterized in more detail and allowed the identification of a complex CYP76 oxidation network in rosemary and sage. Combinatorial expression of only three CYPs, namely FS (SmCYP76AH1), HFS (SmCYP76AH3 or RoCYP76AH22) and C20 oxidase (SmCYP76AK1) in yeast produced in total 14 oxidized abietane diterpenoids, eight of which had not been reported before [189]. The reported enzyme promiscuity of HFS and C20 oxidase can be recognized as a general feature of plant specialized diterpenoid CYPs as many other CYPs involved in those pathways have similar substrate flexibilities. A comprehensive survey and a phylogenetic analysis further provided insights into the structural role of CYPs in plant diterpene pathways known to date which appear to be highly diverse but show that only three CYP clans contribute to the diversity of this compound class [190].

3.1. The biosynthesis of abietane diterpenes in Lamiaceae

The present thesis provides clear evidence that CYP76s play a critical role in abietane diterpene pathways in the Lamiaceae. Enzymes from two CYP subfamilies, namely CYP76AH and CYP76AK possess HFS (CYP76AH3-4, CYP76AH22-24) and C20 oxidase (CYP76AK1, CYP76AK6-8) activity, respectively, and contribute to the biosynthesis of CA and related metabolites from rosemary and sage species. Although previous studies reported on some of the mentioned CYPs, they did not uncover the entire functions [47, 97, 102, 103, 186]. Indeed, the diverse abietane diterpenoid mixtures found in Lamiaceae are generated by three main features. i) CYP71s oxidize at positions C2 and flexible CYP76s at positions C7, C11, C12 and C20. ii) CYP76s are able to perform multiple oxidations at a single C-position. iii) Spontaneous oxidations follow enzyme-catalyzed reactions (**Fig. 3.1**).

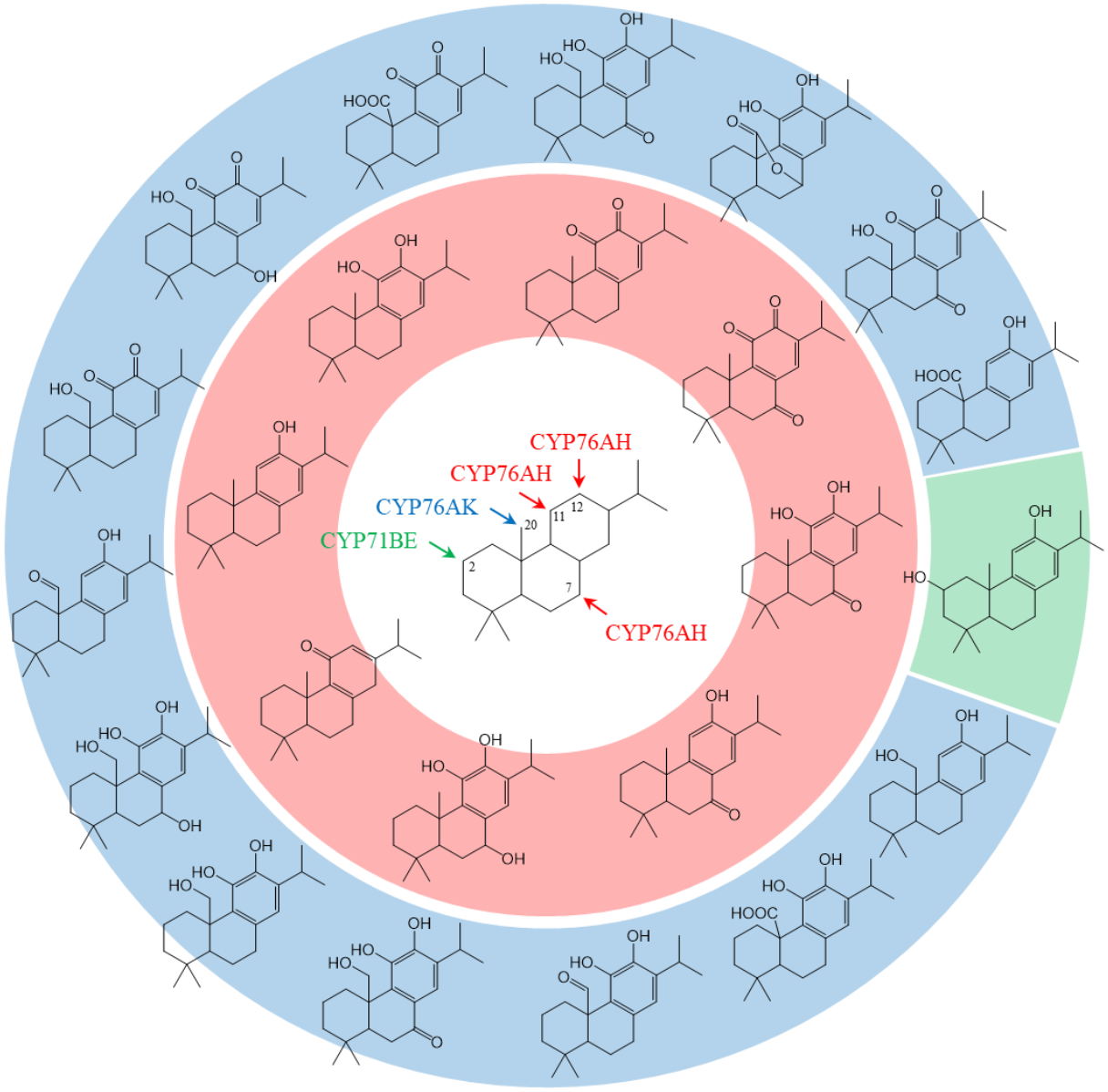

Fig. 3.1 The contribution of CYP76s and CYP71s to the biosynthesis of abietane diterpenoids from rosemary and sage. Products that have been shown to derive from CYP76AH activity (red circle) are decorated at positions C11, C12 and C7. They serve as substrates for CYP76AKs and CYP71BE to get oxidized at positions C20 (blue circle) and C2 (green circle), respectively. In some cases, spontaneous oxidations result in the formation of quinone derivatives or intramolecular ester bonds (e.g. CO) which further increases the diversity of abietane diterpenes in Lamiaceae [47, 97, 102, 103, 186, 187, 189].

3.1.1. Promiscuous and multifunctional CYP76s

So far, the CYP76 family constitutes the dominant catalyzers of abietane diterpene oxidation in Lamiaceae. CYP76 family members are involved in the production of the main constituents from *Rosmarinus* and *Salvia* such as CA but also participate in the biosynthesis of minor products, thus generating a complex mixture of oxidized abietane diterpenoids. This is made possible by the ability of CYP76s to act on diverse substrates and to perform successive oxidations at a single C-position. Interestingly, the involved CYP subfamilies CYP76AH and CYP76AK exhibit different substrate

flexibilities. While CYP76AHs perform (successive) oxidations at positions C7, C11 and C12 which give rise to hydroxyl and keto groups, CYP76AKs are specific to position C20 on which they perform oxidation either to the alcohol product (CYP76AK1) or to the carboxylic acid with the alcohol and the aldehyde forms as intermediates (CYP76AK6-8) (**Fig. 3.1**). The different product outcome of CYP76AK1 and CYP76AK6-8 activity could be due to a reduced substrate binding in CYP76AK1 which prevents the entire oxidation to the final carboxyl group. Which amino acids in CYP76AK enzymes are responsible for the substrate coordination and thus for the formation of the alcohol or the carboxylic acid product remains to be elucidated.

Related enzymes from the CYP76 family were shown to possess catalytic plasticity, too, as illustrated for the biosynthesis of phytoalexins in rice (CYP76Ms) or for *C. forskohlii* diterpenoids (CYP76AHs) [17, 191]. The latter involves CfCYP76AH15 which converts miltiradiene and 13*R*-manoyl oxide – both substrates are native to *C. forskohlii* – to ferruginol and 11-oxo-13*R*-manoyl oxide, respectively [17]. In the same study, the authors supplied RoCYP76AH4, RoCYP76AH22 and SfCYP76AH24 with 13*R*-manoyl oxide, a metabolite that is not present in *R. officinalis* and *S. fruticosa*, and observed formation of 11-oxo-13*R*-manoyl and 11-hydroxy manoyl oxide. Based on these examples, CYPs can be categorized into two groups regarding their substrate flexibility. i) CYPs that accept substrates from other species accomplish "inter-species substrate flexibility" and therefore should actually be termed "promiscuous". ii) CYPs that exclusively exhibit "intra-species substrate flexibility" are rather "multifunctional". In the latter case, one should mention that it cannot be excluded that a CYP accepts any other possible substrate from distant plant species. However, enzyme promiscuity, or named differently, is a poorly understood phenomenon that requires further global investigation across enzyme and species borders to entirely evaluate substrate flexibility in plant specialized pathways.

Next to plant diterpenoid biosynthesis, flexible CYP76s are also involved in other plant specialized pathways such as in sesquiterpene oxidation in sandalwood, in terpene indole alkaloid production and in monoterpene pathways in Brassicaceae [162, 176, 192-194]. For example, *Arabidopsis* CYP76Cs are highly promiscuous because they metabolize several monoterpenols. Interestingly, they also act on phenylurea herbicides, and have, therefore, detoxifying properties [195]. Substrate flexibility has been hypothesized to be more characteristic of enzymes of specialized metabolism in contrast to general metabolism, where enzymes have an overall higher precision [196, 197]. As enzymes are dynamic molecules in solution, this plasticity could occur either due to a flexible substrate binding pocket or due to slightly different conformational states. One or the other leads to relaxed substrate binding, to the recognition of alternative substrates or to the mediation of divergent reaction mechanisms [198]. Additionally, varying reaction conditions such as temperature and pH can alter the original enzyme function, and thus contribute to a deviating product outcome. Certainly, enzyme flexibility can be easily exploited to engineer CYPs towards a desired function by mutation of a small number of amino acids. For example, CYP102A1 (CYPBM3) from *Bacillus megaterium* has been mutated several times to modify its substrate acceptance towards specific molecules such as pesticides and indoles [199,

200]. Many other examples have been documented and provide starting points for industrial applications of (specialized plant) CYPs.

In a publication using data mining, the existence of 91 diterpene skeletons from Lamiaceae was postulated, around 50 of which are abietane-type or labdane-related [201]. Considering possible oxidations and other decorations on the diterpene backbones, thousands of derivatives are theoretically possible. Similarly, conifer diterpene resin acids and rice phytoalexins comprise various labdane-related diterpenoids biosynthesized by flexible CYPs [191, 202]. The high diversity of specialized metabolites implemented by multifunctional enzymes may be considered as an adaption strategy of sessile organisms to help them cope with fluctuating environmental conditions [203]. Promiscuous and multifunctional CYPs that have undergone neo-functionalization upon gene duplication with subsequent (single-) point mutations but also insertions and deletions contribute to the generation of this chemical diversity.

3.1.2. C2 oxidases

Next to oxidations at positions C7, C11, C12 and C20, hydroxylation at C2 is one of the most common chemical decoration found among abietane diterpenoids from rosemary and sage (**Fig. 3.2**). A prominent example is 2α-hydroxy-*O*-methyl-pisiferic acid which is one of the main constituents in *S. pomifera* leaves [97]. Ignea and colleagues demonstrated that its presumed precursor salviol is produced by CYP71BE52 which hydroxylates ferruginol at position C2 (**Fig. 3.3**). The downstream pathway *en route* to 2α-hydroxy-*O*-methyl-pisiferic acid requires additional oxidation at C20 and *O*-methylation at C12. It remains to be elucidated whether the biosynthesis runs through *O*-methyl salviol (**Fig. 3.3A**) or 2α-hydroxy-pisiferic acid (**Fig. 3.3B**), but co-expression analysis of SpCYP71BE52 and SpCYP76AK6 should at least give additional hints in this regard. However, a 12-*O*-methyltransferase, which may also metabolize related abietane diterpenoids such as CA, pisiferic acid, CO and rosmanol, needs to be identified.

Although salviol and 2α-hydroxy-*O*-methyl-pisiferic acid are also present in *R. officinalis*, no homologue to SpCYP71BE52 has been identified from this plant yet. CYP71D381 from *C. forskohlii* was shown to possess C2 oxidase activity by converting 13*R*-manoyl oxide to 2-hydroxy-13*R*-manoyl oxide [17]. SpCYP71BE52 and CfCYP71D381 share only 49 % sequence identity on the protein level, but the introduced C2-hydroxylations have the same α-stereochemistry as for many other known abietane diterpenoids with such decorations (**Fig. 3.2**). Future investigations will demonstrate to which subfamilies other C2 oxidase involved in diterpene oxidation belong and how they are related to CYP71BE52 and CYP71D381.

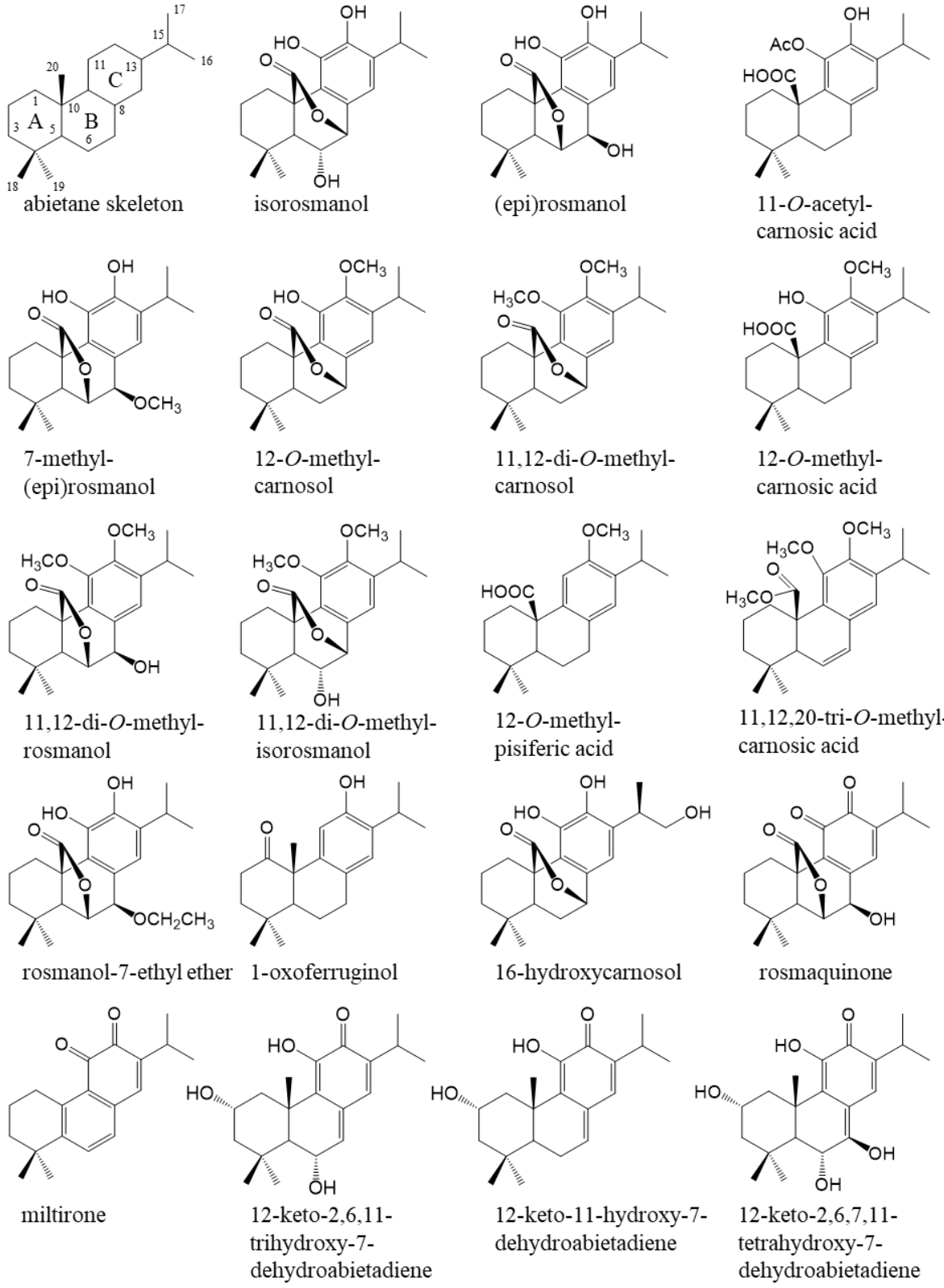

Fig. 3.2 Abietane and abietane-like diterpenes with various chemical decorations. All metabolites were isolated from rosemary and sage species and include decorations such as oxygenation, methylation and acetylation at positions C1, C2, C6, C7, C11, C12, C16 and C20 [10, 97, 204-207]. Isolated compounds with decorations at C8 and other positions have been reported but are not represented here.

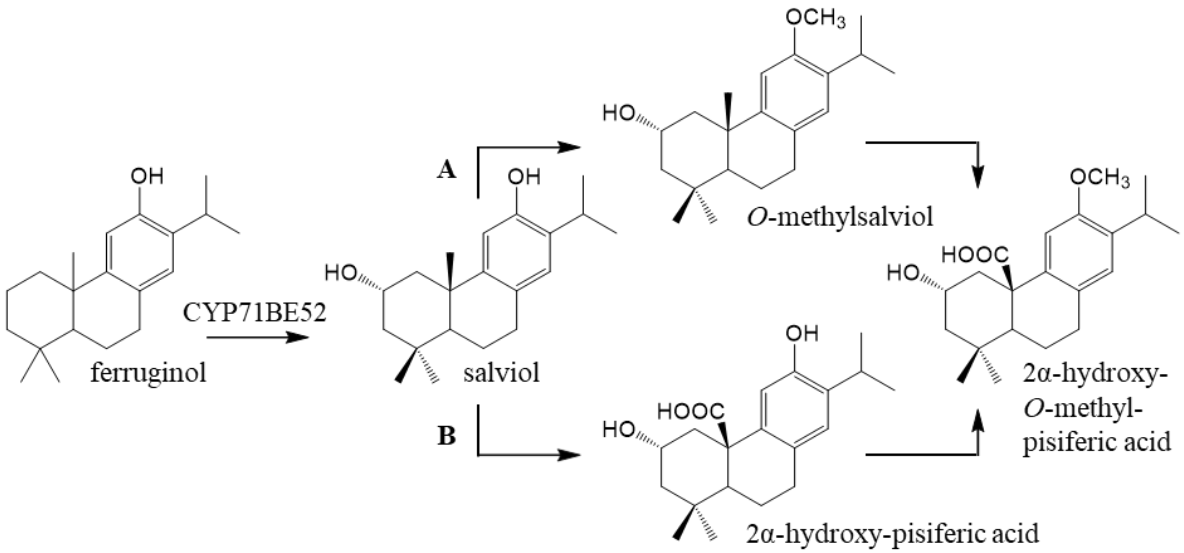

Fig. 3.3 Proposed biosynthesis of 2α-hydroxy-*O*-methyl-pisiferic acid from *Salvia pomifera* and *Rosmarinus officinalis*. SpCYP71BE52 is a C2 oxidase which catalyzes the 2α-hydroxylation of ferruginol [97]. Whether the downstream steps run through *O*-methylsalviol (A) or 2α-hydroxy-pisiferic acid (B) needs to be elucidated.

3.1.3. Non-enzymatic oxidations

Many chemical compounds can undergo autoxidation as they are surrounded by atmospheric oxygen. This reaction is usually caused by the attack of molecular oxygen on prior formed free radical sites. Following the path of initiation, propagation and termination, autoxidation can result in up to 100 hydroperoxide molecules by chain reactions from one initial free radical [208]. Because plants produce diverse ROS in photosynthetic processes and respiration, their biological membranes are continuously in danger of autoxidation. Some abietane diterpenoids are supposed to constitute protection agents thanks to their antioxidant capacity which stops the propagation/chain reaction. To date, three types of non-enzymatic oxidations from abietane diterpenes are known which determine their antioxidant activity. i) Dehydration by spontaneous oxidation yield unsaturated hydrocarbon bonds (**Fig. 3.4A**). For example, miltiradiene and levopimaradiene can aromatize to abietatriene, and ferruginol can oxidize to dehydroferruginol [33, 46, 102, 209]. This type of reaction has the weakest antioxidant power. ii) The catechol moiety of the C-ring can be converted to its quinone form, either as an *o*-quinone derivative (**Fig. 3.4B-1**) (e.g. CA to CA quinone) or as a 12-hydroxy *p*-quinone (**Fig. 3.4B-2**) (e.g. CA to 20-carboxy royleanone) [48]. iii) Oxidative coupling results in the formation of an intramolecular ester (**Fig. 3.4C**). This is the case e.g. for the conversion of CA to CO [210, 211], although this reaction has been suspected to be enzyme catalyzed because HFSs are able to oxidize at position C7 which could be an intermediate step. However, quinone and ester formation can directly follow each other such as for rosmanol which is an oxidation product of CA quinone [34]. It was assumed that the self-regeneration of quinone derivatives to lactone products determines the strong antioxidant activity in rosemary and sage.

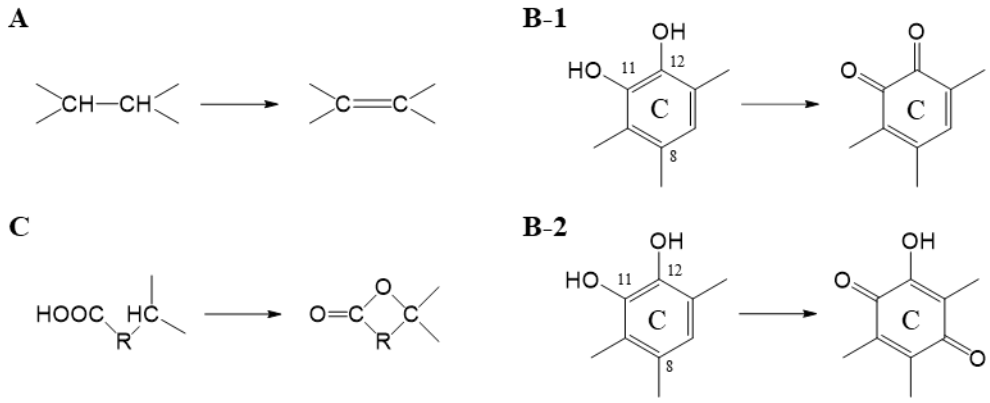

Fig. 3.4 Non-enzymatic oxidations observed on abietane diterpenoids from Lamiaceae. A, Aromatization and other dehydrations of hydrocarbon bonds. B, Quinone formations in the C-ring either to *o*-quinones (B-1) or to hydroxy *p*-quinones (B-2). C, Introduction of intramolecular esters which can follow quinone formation (B).

Within the present thesis it could be shown that the spontaneous oxidation of 11-hydroxy ferruginol to ferruginol quinone occurs very fast. Unfortunately, there are no detailed data available about the speed of quinone formation, but it is assumed that progressing oxidation as well as *O*-methylation stabilizes the structure which decreases the susceptibility to further non-enzymatic oxidation [212]. However, all abietane diterpenoids that contain a catechol moiety can undergo facile spontaneous oxidation and thus have antioxidant activity but with varying intensity.

It is likely that the observed spontaneous oxidations of abietane diterpenes in recombinant systems appear likewise in the native organisms. Nevertheless, it cannot be excluded that there are enzymes which catalyze some of the mentioned reactions. For example, higher amounts of abietatriene than miltiradiene were detected in rosemary and *S. miltiorrhiza* which is the opposite compared with expressions in *E. coli* and *S. cerevisiae* [102, 187]. It was therefore concluded that the aromatization *in planta* is encouraged by enzyme catalysis. Another example includes miltirone (**Fig. 3.2**) which is presumably the product of both enzymatic and non-enzymatic oxidations. The conversion of the catechol moiety in the C-ring to the quinone likely takes place spontaneously (**Fig. 3.4**). However, the double bonds in the B-ring are more likely to be introduced enzymatically, for example by dehydrogenation at specific positions. Here, dehydrogenases are potential candidate enzymes. Other enzyme classes such as 2-oxoglutarate-dependent dioxygenase or short-chain dehydrogenases/ reductases (SDR) could also be involved in the oxidative decoration of abietane diterpenoids from Lamiaceae.

3.1.4. Further chemical decorations

Abietane diterpenes and related compounds can have many chemical modifications which include not only oxygenation but also *O*-methylation, *O*-glycosylation and *O*-acylation (**Fig. 3.2**). In 2008, a remarkable amount of around 180 abietane diterpenoids (tanshinones and rearranged abietanes not included) have been reported only from sage species [213]. According to this survey, oxidations of abietane diterpenes in Lamiaceae can occur at all C-atoms except a few positions (**Tab. 3.1**). These data confirm that oxidizing enzymes play a crucial role in the biosynthesis of abietane diterpenoids. Only CYP76s and CYP71s have been found so far to facilitate some of the various oxidations in Lamiaceae. However, it is likely that CYPs from other families will be identified that can oxidize at positions others than C2, C7, C11, C12 or C20. One possibility is that they are related to CYP families from other plant species that perform oxidations e.g. at C18 (CYP720Bs from conifers) [213]. Future investigations will demonstrate if the involved enzymes, besides CYPs, may share high similarity to catalysts of hormonal pathways such as the gibberellin oxidases.

Following hydroxylations, abietane diterpenes can undergo *O*-alkylation (*O*-methylation and *O*-ethylation) (**Fig. 3.2**). Indeed, metabolites such as 12-*O*-methylcarnosic acid, 11,12-di-*O*-methylisorosmanol and 11,12-di-*O*-methylcarnosol represent major constituents in *Rosmarinus* and *Salvia* [44, 214]. In this thesis, it could be shown that 7-*O*-methyl derivatives of abietane diterpenoids are produced non-specifically in yeast and are also present in the native plants. This raises the question if *O*-methylation of this compound class in Lamiaceae is a product of non-enzymatic reactions or if there are *O*-methyltransferases that are either substrate specific or non-specific. *O*-methyltransferases involved in phenylpropanoid biosynthesis have a high substrate specificity which is determined by only seven amino acids [215]. But CA was converted to methyl derivatives *in vitro* upon exposure to $^1O_2$ and hydroxyl radicals [41]. Consequently, *O*-methylation of abietane diterpenoids in Lamiaceae can also be the result of spontaneous oxidation and could be therefore part of the antioxidant function. However, whether all hydroxylated abietane diterpenoids can undergo facile methylation as part of a spontaneous oxidation reaction, and what the chemical conditions are that support such conversions, need to be investigated.

Further chemical decorations of abietane diterpenes include *O*-glycosylation, *O*-acetylation, peroxidation, dehydration, dimerization, epoxidation, rearrangements as well as modifications on slightly different hydrocarbon backbones such as nor-abietanes, dinor-abietanes and seco-abietanes [185, 204, 216-220]. All these metabolites contribute to the enormous complexity of abietane and abietane-like diterpenoids in rosemary and sage species and increase the diversity of specialized diterpenes *in planta*.

Tab. 3.1 Some examples of abietane diterpenoids from rosemary and sage species with oxidations at the given positions.

Oxidized C position	Metabolite example	Biological source	Reference
1	1-oxo-ferruginol	*Salvia sclarea*	[205]
2	salviol	*Salvia pomifera*	[97]
3	candelabrone	*Salvia candelabrum*	[221]
4	n. d.	-	-
5	5,11,12-trihydroxy-abieta-8,11,13-triene	*Salvia microstegia*	[222]
6	6-hydroxysalvinolone	*Salvia hypargeia*	[223]
7	sugiol	*Salvia miltiorrhiza*	[186]
8	8β-hydroxy-9(11),13-abietadien-12-one	*Salvia pachyphylla*	[206]
9	n. d.	-	-
10	n. d.	-	-
11	carnosic acid	*Rosmarinus officinalis*	[187]
12	ferruginol	*Rosmarinus officinalis*	[187]
13	n. d.	-	-
14	royleanone	*Salvia prionitis*	[224]
15	7-keto-15-hydroxy abietatriene	*Salvia albocaerulea*	[225]
16/17	16-hydroxycarnosol	*Salvia apiana*	[226]
18	18-hydroxy-8,11,13-abietatrien-7-one	*Salvia pomifera*	[227]
19	19-hydroxy-royleanone	*Salvia chinopeplica*	[228]
20	pisiferic acid	*Salvia fruticosa*	[187]

n. d. not detected

3.2. The antioxidative protection cascade of abietane diterpenes *in planta*

Among the different abietane diterpenoids, CA is the most abundant in rosemary plants with concentrations of up to 30 mg per leaf dry weight [229]. Its localization is limited to photosynthetic tissues such as leaves, sepals and petals pointing to its function as antioxidant *in vivo* [38, 210, 230]. Previous studies suggested that the biosynthesis takes place in specialized tissues, namely glandular trichomes [46, 47]. The transcriptome data of *CYP76AH* and *CYP76AK* presented in this thesis confirm that trichomes of young rosemary and sage leaves constitute the production tissue [187]. Trichomes also serve as storage site for CA-related diterpenoids as they accumulate high amounts [46]. Most likely, CA is stored in a cavity on top of the secreting cells until it is transported to other leaf tissues where it gets further modified (**Fig. 3.5**). In agreement with this, the oxidation derivative CO is present exclusively in leaf tissue but not in trichomes [46]. A transport of CA to the parenchyma would require specific transporters which have not been identified yet. However, subcellular localization studies demonstrated that CA is only present in chloroplasts where it is supposed to

protect thylakoid membranes against oxidative stress by scavenging ROS [40, 44, 231]. This non-enzymatic process gives rise to diverse oxidized and *O*-methylated derivatives [44].

Besides CA, other abietane diterpenes undergo facile non-enzymatic oxidation and methylation as proven by this thesis. To date, it is not clear in which leaf tissues or in which compartments these spontaneous conversions take place. The diterpenes could be immediately transformed after their biosynthesis in trichomes. The presence of trace amounts of 12-*O*-methylcarnosic acid in trichomes supports this assumption [46]. On the other hand, they could be transported from trichomes to the parenchyma in order to protect chloroplasts against ROS leading to oxidized and methylated derivatives. To figure this out, subcellular localizations of abietane diterpenoids such as 11-hydroxy ferruginol, 11-hydroxy sugiol or 7,11,20-trihydroxy ferruginol as well as their corresponding quinone and methyl forms are required.

Oxidized and *O*-methylated derivatives of CA which were formed non-enzymatically in chloroplasts do possess further protective activity. For example, CO was shown to have no antioxidant properties against ROS but protected thylakoid membranes probably by inhibition of the lipid peroxidation process [41]. It is possible that other CA-related diterpenes, which are present in chloroplasts such as rosmanol and isorosmanol, have similar functions [44]. But this hypothesis needs further investigation.

As soon as CA gets *O*-methylated, its antioxidant activity is eliminated because of the loss of the catechol moiety. However, its lipid solubility is increased, accounting for the localization of methylated CA derivatives including 11,12-di-*O*-methylrosmanol, 12-*O*-methylcarnosic acid and 11,12-di-*O*-methylisorosmanol in plasma membranes but also in chloroplasts, in the ER and in the Golgi apparatus [44, 214]. To distribute these metabolites throughout the cell, transporters are essential. As membrane components, they are considered to have similar functions to sterols by protecting lipids against peroxidation thanks to their remaining hydroxyl groups [232]. These may interact with the head groups of phospholipids, thereby leading to stabilization of the membrane [10]. In fact, methylcarnosic acid was reported to better protect triglyceride emulsions at 60°C than CA [233].

CA and related abietane diterpenes from rosemary and sage efficiently protect chloroplasts and cell membranes against oxidative stress. This is in line with observations that CA-containing plant species accumulate less tocopherols, common antioxidants *in planta* [234]. Even better, CA possesses stronger antioxidant activity which was proven by chloroplasts that showed lower α-tocopherol oxidation than controls when treated with CA [235]. The efficiency of the antioxidant capacity is further determined by the autoreduction that allow the recovery of CA from quinone and lactone derivatives [34, 236]. In summary, oxidation and *O*-methylation of Lamiaceae abietane diterpenoids established by multifunctional CYPs and non-enzymatic reactions offer an effective antioxidative protection cascade *in planta*. Unfortunately, the function of other chemical decorations such as acetylation and glycosylation remains totally obscure.

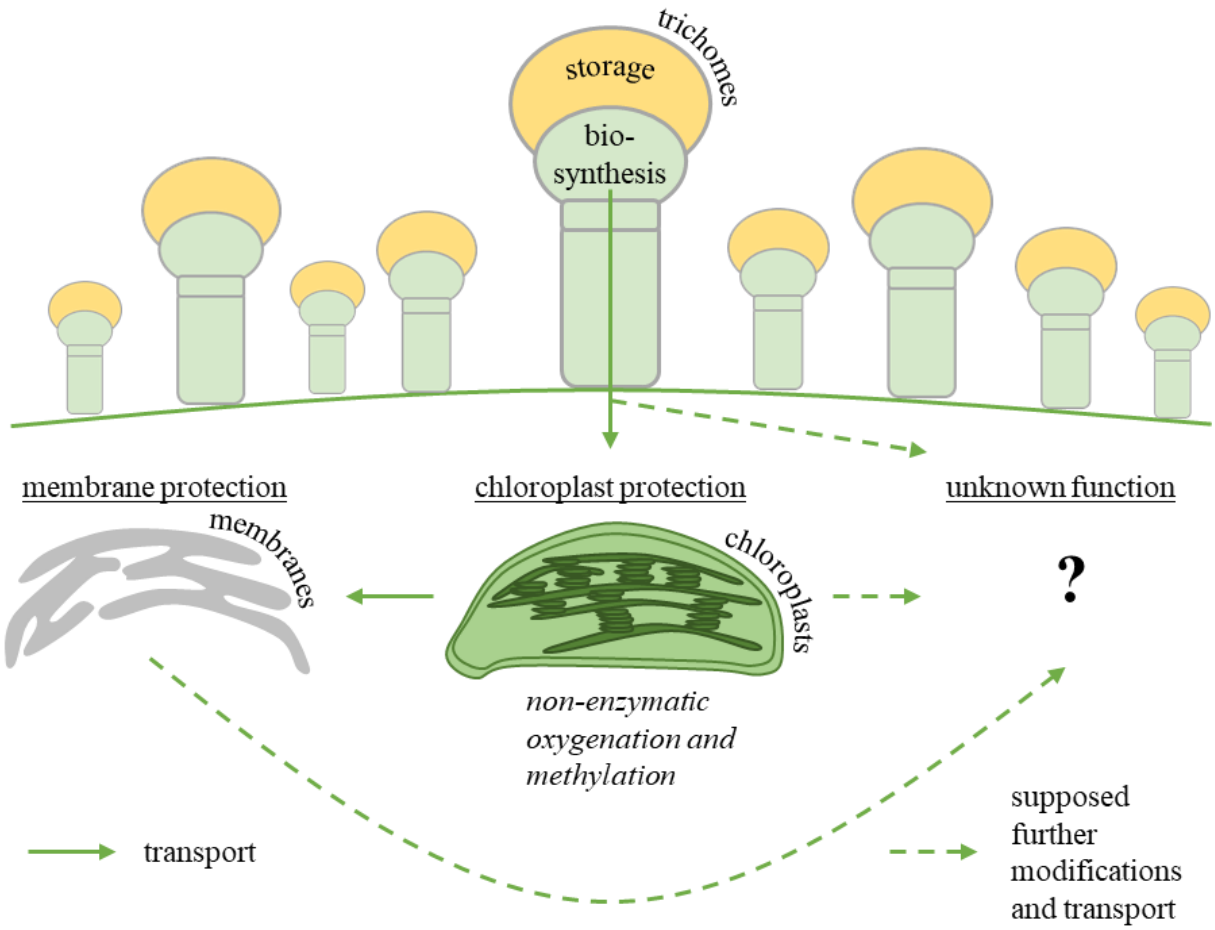

Fig. 3.5 Proposed localization and function of abietane diterpenes in rosemary and sage species. Biosynthetic gene transcripts and the metabolite CA were shown to accumulate in glandular trichomes [46, 47]. Probably, CA is stored in a cavity on top of the secreting trichome cells until it is transported to other leaf tissues. In the vascular tissue, CA is supposed to protect chloroplast against oxidative stress whereby related diterpenes are produced by non-enzymatic oxygenation and methylation. *O*-methylated derivatives rather accumulate in membranes and have stabilizing functions [41, 44, 45]. The transport of CA and related diterpenes require specific transporters.

3.3. Modular cloning developed for yeast enables combinatorial biosynthesis: production of “new-to-nature” diterpenes with potential bioactivity

New drugs are continuously needed because the growing microbial drug tolerance requires the development of antibiotics with novel mechanisms of action. However, since the 1970s only a small number of new antibiotic classes have been approved to the market which could be due to the costly search for natural products with potential bioactivities [237]. Here, artificial compounds based on scaffolds that have proven to be beneficial but with novel structural features could constitute suitable alternatives. Their production by chemical synthesis is, indeed, time-consuming, expensive and often environmentally harmful. The modular nature of biosynthetic pathways offers an elegant strategy to

generate "new-to-nature" metabolites which are truly new or which have not been identified from any species yet. In the case of diterpenoids, this modularity is given by three pathway sections (**Fig. 3.6**). Module 1 includes the cyclization of the precursor GGPP carried out by either class I diTPS, bifunctional diTPS or sequential action of class II and class I diTPS. Afterwards, CYP-mediated decorations (module 2) and further modifications, rearrangements and conjugations (module 3) establish the chemical diversity of diterpenoids. The co-expression of modules from related metabolic pathways of different organisms in a single host creates artificial enzyme combinations and is thus called combinatorial biosynthesis. To do so, substrate flexibility of enzymes to be combined is an essential requirement. This approach has the potential to generate metabolites based on known backbones but with decorations that determine their status as "new-to-nature".

The first attempt of combinatorial biosynthesis on isoprenoids produced four "new-to-nature" carotenoids in *E. coli* by a novel carotene skeleton that was applied to desaturation and cyclization [238]. Another inspiring study was conducted in *N. benthamiana* using eleven class II and nine class I diTPS leading to the synthesis/creation of 41 "new-to-nature" enzyme combinations [159]. With respect to the combinatorial biosynthesis of oxidized diterpenoids, *E. coli* and *N. benthamiana* are not ideal because expression of CYPs in *E. coli* is challenging and transient or stable expression in plant hosts often leads to interactions with the endogenous metabolism. Combinatorial biosynthesis of diterpenoids is therefore better performed in yeast cells which provide the required subcellular compartmentation for sufficient CYP expression as well as limited crossover between the engineered pathway and the host metabolism. Indeed, the results from the present study and reports from the literature proved that *S. cerevisiae* constitutes a promising and sufficient production platform for diverse oxidized metabolites. For example, a forward-looking combinatorial biosynthesis of diterpenes in yeast was performed to biosynthesize diterpenoids that are difficult to obtain from natural sources or that are "new-to-nature" [85]. Combinatorial biosynthesis in yeast is also useful for distantly related metabolite classes as impressively demonstrated by the production of 74 compounds with different backbones, 75 % of which have not been reported before [239].

To realize combinatorial synthesis in yeast, synthetic biology provides useful tools. Within the present thesis, a "Golden Gate" modular cloning vector system developed for yeast was used. In a first level, it allows the assembly of promoter-gene-terminator constructs in a module cassette, and in a second level of several expression cassettes in a single yeast expression vector (**Fig. 3.6**). Applying this to combinatorial biosynthesis of diterpenoids, libraries of diTPS and decorating enzymes, possibly including genes that originated from species beyond plants, could be co-expressed in yeast cells. Diverse "new-to-nature" diterpenoids are expected to be generated. The product spectrum could be expanded by integrating enzymes to the libraries which were randomly mutated in the active center at positions that determine substrate binding and turnover. Production of "new-to-nature" diterpenes by mutated enzymes has recently been demonstrated for a diTPS which yielded 8-hydroxy-*ent*-CPP, a compound that has not been reported to occur in nature [240]. Following biosynthesis and

identification using high-throughput detection methods, novel diterpenoid compounds could be screened for potential bioactivity. Combined with increasing sensitivity and accuracy of analytical tools such as GC-MS and LC-MS they allow to face upcoming challenges in pharmaceutical and industrial applications.

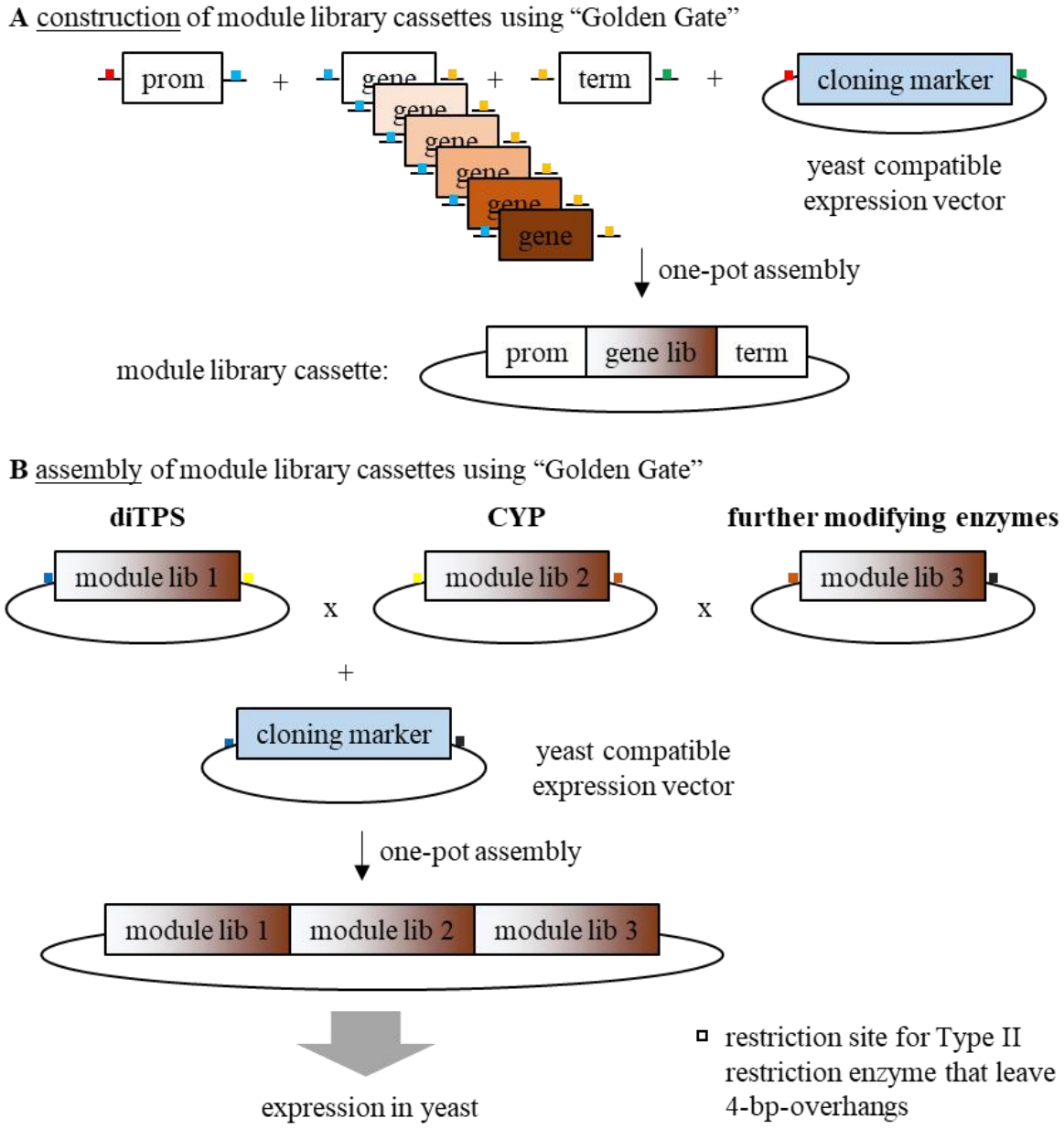

Fig. 3.6 Combinatorial biosynthesis of diterpenoids using the modular Golden Gate cloning system and libraries of pathway modules. A, Libraries of promoter (prom)-gene-terminator (term) combinations are assembled to a module cassette using Type II restriction enzymes. They leave 4-bp-overhangs which match the overhang of the desired neighboring cassette. B, Combinations of module libraries (module lib) containing either diTPS, CYPs or other decorating enzymes are assembled according to A.

4. References

1. **L. Ružička** (1953), The isoprene rule and the biogenesis of terpenic compounds. *Experientia*, **9**(10): p. 357-67.
2. **M. J. Smanski, R. M. Peterson, S. X. Huang, and B. Shen** (2012), Bacterial diterpene synthases: new opportunities for mechanistic enzymology and engineered biosynthesis. *Curr Opin Chem Biol*, **16**(1-2): p. 132-41.
3. **D. Tarkowská and M. Strnad** (2018), Isoprenoid-derived plant signaling molecules: biosynthesis and biological importance. *Planta*, **247**(5): p. 1051-1066.
4. **M. Liu and S. Lu** (2016), Plastoquinone and ubiquinone in plants: Biosynthesis, physiological function and metabolic engineering. *Front Plant Sci*, **7**: p. 1898.
5. **B. M. Lange and M. Ghassemian** (2003), Genome organization in *Arabidopsis thaliana*: a survey for genes involved in isoprenoid and chlorophyll metabolism. *Plant Mol Biol*, **51**(6): p. 925-48.
6. **C. I. Keeling and J. Bohlmann** (2006), Diterpene resin acids in conifers. *Phytochemistry*, **67**(22): p. 2415-23.
7. **A. K. Block, M. M. Vaughan, E. A. Schmelz, and S. A. Christensen** (2018), Biosynthesis and function of terpenoid defense compounds in maize (*Zea mays*). *Planta*.
8. **B. A. Weaver** (2014), How Taxol/paclitaxel kills cancer cells. *Mol Biol Cell*, **25**(18): p. 2677-81.
9. **M. Lebwohl, N. Swanson, L. L. Anderson, A. Melgaard, Z. Xu, and B. Berman** (2012), Ingenol mebutate gel for actinic keratosis. *N Engl J Med*, **366**(11): p. 1010-1019.
10. **S. Birtić, P. Dussort, F. X. Pierre, A. C. Bily, and M. Roller** (2015), Carnosic acid. *Phytochemistry*, **115**: p. 9-19.
11. **A. Caniard, P. Zerbe, S. Legrand, A. Cohade, N. Valot, J. L. Magnard, J. Bohlmann, and L. Legendre** (2012), Discovery and functional characterization of two diterpene synthases for sclareol biosynthesis in *Salvia sclarea* (L.) and their relevance for perfume manufacture. *BMC Plant Biol*, **12**: p. 119.
12. **K. Strømgaard and K. Nakanishi** (2004), Chemistry and biology of terpene trilactones from *Ginkgo biloba*. *Angew Chem Int Ed Engl*, **43**(13): p. 1640-58.
13. **S. C. Chhabra, R. L. Mahunnah, and E. N. Mshiu** (1990), Plants used in traditional medicine in eastern Tanzania. III. Angiosperms (Euphorbiaceae to Menispermaceae). *J Ethnopharmacol*, **28**(3): p. 255-83.
14. **B. B. Petrovska** (2012), Historical review of medicinal plants' usage. *Pharmacogn Rev*, **6**(11): p. 1-5.
15. **Y. Zhang, P. Jiang, M. Ye, S.-H. Kim, C. Jiang, and J. Lü** (2012), Tanshinones: sources, pharmacokinetics and anti-cancer activities. *Int J Mol Sci*, **13**(10): p. 13621-13666.

16. **M. Khoury, D. Stien, V. Eparvier, N. Ouaini, and M. El Beyrouthy** (2016), Report on the medicinal use of eleven Lamiaceae species in Lebanon and rationalization of their antimicrobial potential by examination of the chemical composition and antimicrobial activity of their essential oils. *Evid Based Complement Alternat Med*, **2016**: p. 2547169.

17. **I. Pateraki, J. Andersen-Ranberg, N. B. Jensen, S. G. Wubshet, A. M. Heskes, V. Forman, B. Hallström, B. Hamberger, M. S. Motawia, C. E. Olsen, D. Staerk, J. Hansen, B. L. Møller, and B. Hamberger** (2017), Total biosynthesis of the cyclic AMP booster forskolin from *Coleus forskohlii*. *eLife*, **6**: p. e23001.

18. **A. Ghorbani and M. Esmaeilizadeh** (2017), Pharmacological properties of *Salvia officinalis* and its components. *J Tradit Complement Med*, **7**(4): p. 433-440.

19. **S. Ma, D. Zhang, H. Lou, L. Sun, and J. Ji** (2016), Evaluation of the anti-inflammatory activities of tanshinones isolated from *Salvia miltiorrhiza* var. alba roots in THP-1 macrophages. *J Ethnopharmacol*, **188**: p. 193-9.

20. **T. Satoh, K. Kosaka, K. Itoh, A. Kobayashi, M. Yamamoto, Y. Shimojo, C. Kitajima, J. Cui, J. Kamins, S.-i. Okamoto, M. Izumi, T. Shirasawa, and S. A. Lipton** (2008), Carnosic acid, a catechol-type electrophilic compound, protects neurons both *in vitro* and *in vivo* through activation of the Keap1/Nrf2 pathway via S-alkylation of targeted cysteines on Keap1. *J Neurochem*, **104**(4): p. 1116-1131.

21. **E. N. Frankel, S.-W. Huang, R. Aeschbach, and E. Prior** (1996), Antioxidant activity of a rosemary extract and its constituents, carnosic acid, carnosol, and rosmarinic acid, in bulk oil and oil-in-water emulsion. *J Agric Food Chem*, **44**(1): p. 131-135.

22. **A. I. White and G. L. Jenkins** (1942), *Salvia Carnosa* (Dougl.). I—A Phytochemical Study. *J Am Pharm Assoc*, **31**(2): p. 33-37.

23. **H. Linde** (1964), Ein neues Diterpen aus *Salvia officinalis* L. und eine Notiz zur Konstitution von Pikrosalvin. *HCA*, **47**(5): p. 1234-1239.

24. **S. A. Vestri Alvarenga, J. Pierre Gastmans, G. do Vale Rodrigues, P. Roberto H. Moreno, and V. de Paulo Emerenciano** (2001), A computer-assisted approach for chemotaxonomic studies — diterpenes in Lamiaceae. *Phytochemistry*, **56**(6): p. 583-595.

25. **M. A. González** (2014), Synthetic derivatives of aromatic abietane diterpenoids and their biological activities. *Eur J Med Chem*, **87**: p. 834-42.

26. **M. R. de Oliveira** (2016), The dietary components carnosic ccid and carnosol as neuroprotective agents: a mechanistic view. *Mol Neurobiol*, **53**(9): p. 6155-6168.

27. **J. J. Johnson** (2011), Carnosol: a promising anti-cancer and anti-inflammatory agent. *Cancer Lett*, **305**(1): p. 1-7.

28. **V. Exarchou, L. Kanetis, Z. Charalambous, S. Apers, L. Pieters, V. Gekas, and V. Goulas** (2015), HPLC-SPE-NMR characterization of major metabolites in *Salvia fruticosa*

Mill. extract with antifungal potential: relevance of carnosic acid, carnosol, and hispidulin. *J Agric Food Chem*, **63**(2): p. 457-63.

29. **D. Poeckel, C. Greiner, M. Verhoff, O. Rau, L. Tausch, C. Hörnig, D. Steinhilber, M. Schubert-Zsilavecz, and O. Werz** (2008), Carnosic acid and carnosol potently inhibit human 5-lipoxygenase and suppress pro-inflammatory responses of stimulated human polymorphonuclear leukocytes. *Biochem Pharmacol*, **76**(1): p. 91-7.
30. **J. Bufalo, C. L. Cantrell, M. R. Jacob, K. K. Schrader, B. L. Tekwani, T. S. Kustova, A. Ali, and C. S. Boaro** (2016), Antimicrobial and antileishmanial activities of diterpenoids isolated from the roots of *Salvia deserta*. *Planta Med*, **82**(1-2): p. 131-7.
31. **S. Jieensinue, H. Zhu, G. Li, K. Dong, M. Liang, and Y. Li** (2018), Tanshinone IIA reduces SW837 colorectal cancer cell viability via the promotion of mitochondrial fission by activating JNK-Mff signaling pathways. *BMC Cell Biol*, **19**(1): p. 21.
32. **G. W. Fan, X. M. Gao, H. Wang, Y. Zhu, J. Zhang, L. M. Hu, Y. F. Su, L. Y. Kang, and B. L. Zhang** (2009), The anti-inflammatory activities of Tanshinone IIA, an active component of TCM, are mediated by estrogen receptor activation and inhibition of iNOS. *J Steroid Biochem Mol Biol*, **113**(3-5): p. 275-80.
33. **H. Saijo, H. Kofujita, K. Takahashi, and T. Ashitani** (2015), Antioxidant activity and mechanism of the abietane-type diterpene ferruginol. *Nat Prod Res*, **29**(18): p. 1739-43.
34. **T. Masuda, Y. Inaba, T. Maekawa, Y. Takeda, H. Tamura, and H. Yamaguchi** (2002), Recovery mechanism of the antioxidant activity from carnosic acid quinone, an oxidized sage and rosemary antioxidant. *J Agric Food Chem*, **50**(21): p. 5863-9.
35. **M. Tada, T. Ohkanda, and J. Kurabe** (2010), Syntheses of carnosic acid and carnosol, anti-oxidants in Rosemary, from pisiferic acid, the major constituent of Sawara. *Chem Pharm Bull (Tokyo)*, **58**(1): p. 27-9.
36. **S. I. Alqasoumi and M. S. Abdel-Kader** (2012), Terpenoids from *Juniperus procera* with hepatoprotective activity. *Pak J Pharm Sci*, **25**(2): p. 315-22.
37. **M. Yang, A. Liu, S. Guan, J. Sun, M. Xu, and D. Guo** (2006), Characterization of tanshinones in the roots of *Salvia miltiorrhiza* (Dan-shen) by high-performance liquid chromatography with electrospray ionization tandem mass spectrometry. *Rapid Commun Mass Spectrom*, **20**(8): p. 1266-80.
38. **J. C. Luis and C. B. Johnson** (2005), Seasonal variations of rosmarinic and carnosic acids in rosemary extracts. Analysis of their *in vitro* antiradical activity. *Span J Agric Res*, **3**(1): p. 106-112.
39. **S. Munné-Bosch and L. Alegre** (2000), Changes in carotenoids, tocopherols and diterpenes during drought and recovery, and the biological significance of chlorophyll loss in *Rosmarinus officinalis* plants. *Planta*, **210**(6): p. 925-31.

40. **S. Munné-Bosch, K. Schwarz, and L. Alegre** (1999), Enhanced formation of α-tocopherol and highly oxidized abietane diterpenes in water-stressed rosemary plants. *Plant Physiol*, **121**(3): p. 1047-1052.

41. **M. Loussouarn, A. Krieger-Liszkay, L. Svilar, A. Bily, S. Birtić, and M. Havaux** (2017), Carnosic acid and carnosol, two major antioxidants of rosemary, act through different mechanisms. *Plant Physiol*, **175**(3): p. 1381-1394.

42. **B. C. Tripathy and R. Oelmüller** (2012), Reactive oxygen species generation and signaling in plants. *Plant Signal Behav*, **7**(12): p. 1621-1633.

43. **R. Mittler** (2017), ROS are good. *Trends Plant Sci*, **22**(1): p. 11-19.

44. **S. Munné-Bosch and L. Alegre** (2001), Subcellular compartmentation of the diterpene carnosic acid and its derivatives in the leaves of rosemary. *Plant Physiol*, **125**(2): p. 1094-102.

45. **S. Munné-Bosch, K. Schwarz, and L. Alegre** (1999), Response of abietane diterpenes to stress in *Rosmarinus officinalis* L.: new insights into the function of diterpenes in plants. *Free Radic Res*, **31 Suppl**: p. S107-12.

46. **K. Brückner, D. Božić, D. Manzano, D. Papaefthimiou, I. Pateraki, U. Scheler, A. Ferrer, R. C. de Vos, A. K. Kanellis, and A. Tissier** (2014), Characterization of two genes for the biosynthesis of abietane-type diterpenes in rosemary (*Rosmarinus officinalis*) glandular trichomes. *Phytochemistry*, **101**: p. 52-64.

47. **D. Božić, D. Papaefthimiou, K. Brückner, R. C. de Vos, C. A. Tsoleridis, D. Katsarou, A. Papanikolaou, I. Pateraki, F. M. Chatzopoulou, E. Dimitriadou, S. Kostas, D. Manzano, U. Scheler, A. Ferrer, A. Tissier, A. M. Makris, S. C. Kampranis, and A. K. Kanellis** (2015), Towards elucidating carnosic acid biosynthesis in Lamiaceae: functional characterization of the three first steps of the pathway in *Salvia fruticosa* and *Rosmarinus officinalis*. *PLoS One*, **10**(5): p. e0124106.

48. **T. Masuda, Y. Inaba, and Y. Takeda** (2001), Antioxidant mechanism of carnosic acid: structural identification of two oxidation products. *J Agric Food Chem*, **49**(11): p. 5560-5.

49. **O. Laule, A. Furholz, H. S. Chang, T. Zhu, X. Wang, P. B. Heifetz, W. Gruissem, and M. Lange** (2003), Crosstalk between cytosolic and plastidial pathways of isoprenoid biosynthesis in *Arabidopsis thaliana*. *Proc Natl Acad Sci U S A*, **100**(11): p. 6866-71.

50. **M. Rodríguez-Concepción and A. Boronat** (2002), Elucidation of the methylerythritol phosphate pathway for isoprenoid biosynthesis in bacteria and plastids. A metabolic milestone achieved through genomics. *Plant Physiol*, **130**(3): p. 1079-89.

51. **B. M. Lange, T. Rujan, W. Martin, and R. Croteau** (2000), Isoprenoid biosynthesis: the evolution of two ancient and distinct pathways across genomes. *Proc Natl Acad Sci U S A*, **97**(24): p. 13172-7.

52. **G. A. Sprenger, U. Schorken, T. Wiegert, S. Grolle, A. A. de Graaf, S. V. Taylor, T. P. Begley, S. Bringer-Meyer, and H. Sahm** (1997), Identification of a thiamin-dependent

synthase in *Escherichia coli* required for the formation of the 1-deoxy-D-xylulose 5-phosphate precursor to isoprenoids, thiamin, and pyridoxol. *Proc Natl Acad Sci U S A*, **94**(24): p. 12857-62.

53. **J. M. Estévez, A. Cantero, A. Reindl, S. Reichler, and P. León** (2001), 1-Deoxy-D-xylulose-5-phosphate synthase, a limiting enzyme for plastidic isoprenoid biosynthesis in plants. *J Biol Chem*, **276**(25): p. 22901-9.
54. **T. Kuzuyama, S. Takahashi, H. Watanabe, and H. Seto** (1998), Direct formation of 2-C-methyl-d-erythritol 4-phosphate from 1-deoxy-d-xylulose 5-phosphate by 1-deoxy-d-xylulose 5-phosphate reductoisomerase, a new enzyme in the non-mevalonate pathway to isopentenyl diphosphate. *Tetrahedron Lett*, **39**(25): p. 4509-4512.
55. **S. Takahashi, T. Kuzuyama, H. Watanabe, and H. Seto** (1998), A 1-deoxy-D-xylulose 5-phosphate reductoisomerase catalyzing the formation of 2-C-methyl-D-erythritol 4-phosphate in an alternative nonmevalonate pathway for terpenoid biosynthesis. *Proc Natl Acad Sci U S A*, **95**(17): p. 9879-84.
56. **F. Rohdich, J. Wungsintaweekul, M. Fellermeier, S. Sagner, S. Herz, K. Kis, W. Eisenreich, A. Bacher, and M. H. Zenk** (1999), Cytidine 5'-triphosphate-dependent biosynthesis of isoprenoids: YgbP protein of *Escherichia coli* catalyzes the formation of 4-diphosphocytidyl-2-C-methylerythritol. *Proc Natl Acad Sci U S A*, **96**(21): p. 11758-63.
57. **H. Lüttgen, F. Rohdich, S. Herz, J. Wungsintaweekul, S. Hecht, C. A. Schuhr, M. Fellermeier, S. Sagner, M. H. Zenk, A. Bacher, and W. Eisenreich** (2000), Biosynthesis of terpenoids: YchB protein of *Escherichia coli* phosphorylates the 2-hydroxy group of 4-diphosphocytidyl-2C-methyl-D-erythritol. *Proc Natl Acad Sci U S A*, **97**(3): p. 1062-7.
58. **S. Herz, J. Wungsintaweekul, C. A. Schuhr, S. Hecht, H. Luttgen, S. Sagner, M. Fellermeier, W. Eisenreich, M. H. Zenk, A. Bacher, and F. Rohdich** (2000), Biosynthesis of terpenoids: YgbB protein converts 4-diphosphocytidyl-2C-methyl-D-erythritol 2-phosphate to 2C-methyl-D-erythritol 2,4-cyclodiphosphate. *Proc Natl Acad Sci U S A*, **97**(6): p. 2486-90.
59. **M. Seemann, N. Campos, M. Rodríguez-Concepción, J.-F. Hoeffler, C. Grosdemange-Billiard, A. Boronat, and M. Rohmer** (2002), Isoprenoid biosynthesis via the methylerythritol phosphate pathway: accumulation of 2-C-methyl-d-erythritol 2,4-cyclodiphosphate in a gcpE deficient mutant of *Escherichia coli*. *Tetrahedron Lett*, **43**(5): p. 775-778.
60. **F. Rohdich, S. Hecht, K. Gärtner, P. Adam, C. Krieger, S. Amslinger, D. Arigoni, A. Bacher, and W. Eisenreich** (2002), Studies on the nonmevalonate terpene biosynthetic pathway: metabolic role of IspH (LytB) protein. *Proc Natl Acad Sci U S A*, **99**(3): p. 1158-63.
61. **F. M. Hahn, A. P. Hurlburt, and C. D. Poulter** (1999), *Escherichia coli* open reading frame 696 is idi, a nonessential gene encoding isopentenyl diphosphate isomerase. *J Bacteriol*, **181**(15): p. 4499-504.

62. **G. Beck, D. Coman, E. Herren, M. A. Ruiz-Sola, M. Rodríguez-Concepción, W. Gruissem, and E. Vranová** (2013), Characterization of the GGPP synthase gene family in *Arabidopsis thaliana*. *Plant Mol Biol*, **82**(4-5): p. 393-416.

63. **M. A. Ruiz-Sola, M. V. Barja, D. Manzano, B. Llorente, B. Schipper, J. Beekwilder, and M. Rodríguez-Concepción** (2016), A single *Arabidopsis* gene encodes two differentially targeted geranylgeranyl diphosphate synthase isoforms. *Plant Physiol*, **172**(3): p. 1393-1402.

64. **K. Wang and S. Ohnuma** (1999), Chain-length determination mechanism of isoprenyl diphosphate synthases and implications for molecular evolution. *Trends Biochem Sci*, **24**(11): p. 445-51.

65. **S. Vandermoten, E. Haubruge, and M. Cusson** (2009), New insights into short-chain prenyltransferases: structural features, evolutionary history and potential for selective inhibition. *Cell Mol Life Sci*, **66**(23): p. 3685-95.

66. **K. Ogura and T. Koyama** (1998), Enzymatic aspects of isoprenoid chain elongation. *Chem Rev*, **98**(4): p. 1263-1276.

67. **T. A. Akhtar, Y. Matsuba, I. Schauvinhold, G. Yu, H. A. Lees, S. E. Klein, and E. Pichersky** (2013), The tomato *cis*-prenyltransferase gene family. *Plant J*, **73**(4): p. 640-52.

68. **Y. Matsuba, J. Zi, A. D. Jones, R. J. Peters, and E. Pichersky** (2015), Biosynthesis of the diterpenoid lycosantalonol via nerylneryl diphosphate in *Solanum lycopersicum*. *PLoS One*, **10**(3): p. e0119302.

69. **D. Coman, A. Altenhoff, S. Zoller, W. Gruissem, and E. Vranova** (2014), Distinct evolutionary strategies in the GGPPS family from plants. *Front Plant Sci*, **5**: p. 230.

70. **R. Nagel, C. Bernholz, E. Vranova, J. Kosuth, N. Bergau, S. Ludwig, L. Wessjohann, J. Gershenzon, A. Tissier, and A. Schmidt** (2015), *Arabidopsis thaliana* isoprenyl diphosphate synthases produce the C_{25} intermediate geranylfarnesyl diphosphate. *Plant J*, **84**(5): p. 847-59.

71. **H. Hemmi, M. Noike, T. Nakayama, and T. Nishino** (2003), An alternative mechanism of product chain-length determination in type III geranylgeranyl diphosphate synthase. *Eur J Biochem*, **270**(10): p. 2186-94.

72. **A. Chen, P. A. Kroon, and C. D. Poulter** (1994), Isoprenyl diphosphate synthases: protein sequence comparisons, a phylogenetic tree, and predictions of secondary structure. *Protein Sci*, **3**(4): p. 600-7.

73. **F. Chen, D. Tholl, J. Bohlmann, and E. Pichersky** (2011), The family of terpene synthases in plants: a mid-size family of genes for specialized metabolism that is highly diversified throughout the kingdom. *Plant J*, **66**(1): p. 212-29.

74. **R. Cao, Y. Zhang, F. M. Mann, C. Huang, D. Mukkamala, M. P. Hudock, M. E. Mead, S. Prisic, K. Wang, F. Y. Lin, T. K. Chang, R. J. Peters, and E. Oldfield** (2010), Diterpene cyclases and the nature of the isoprene fold. *Proteins*, **78**(11): p. 2417-32.

75. **P. Zerbe and J. Bohlmann** (2015), Plant diterpene synthases: exploring modularity and metabolic diversity for bioengineering. *Trends Biotechnol*, **33**(7): p. 419-28.

76. **R. J. Peters, J. E. Flory, R. Jetter, M. M. Ravn, H. J. Lee, R. M. Coates, and R. B. Croteau** (2000), Abietadiene synthase from grand fir (*Abies grandis*): characterization and mechanism of action of the "pseudomature" recombinant enzyme. *Biochemistry*, **39**(50): p. 15592-602.

77. **S. Mafu, M. L. Hillwig, and R. J. Peters** (2011), A novel labda-7,13e-dien-15-ol-producing bifunctional diterpene synthase from *Selaginella moellendorffii*. *Chembiochem*, **12**(13): p. 1984-7.

78. **P. Zerbe, A. Chiang, M. Yuen, B. Hamberger, B. Hamberger, J. A. Draper, R. Britton, and J. Bohlmann** (2012), Bifunctional *cis*-abienol synthase from *Abies balsamea* discovered by transcriptome sequencing and its implications for diterpenoid fragrance production. *J Biol Chem*, **287**(15): p. 12121-31.

79. **R. J. Peters** (2010), Two rings in them all: the labdane-related diterpenoids. *Nat Prod Rep*, **27**(11): p. 1521-30.

80. **X. Lin, M. Hezari, A. E. Koepp, H. G. Floss, and R. Croteau** (1996), Mechanism of taxadiene synthase, a diterpene cyclase that catalyzes the first step of taxol biosynthesis in Pacific yew. *Biochemistry*, **35**(9): p. 2968-77.

81. **R. J. Peters** (2006), Uncovering the complex metabolic network underlying diterpenoid phytoalexin biosynthesis in rice and other cereal crop plants. *Phytochemistry*, **67**(21): p. 2307-17.

82. **P. Hedden and S. G. Thomas** (2012), Gibberellin biosynthesis and its regulation. *Biochem J*, **444**(1): p. 11-25.

83. **D. Morrone, M. L. Hillwig, M. E. Mead, L. Lowry, D. B. Fulton, and R. J. Peters** (2011), Evident and latent plasticity across the rice diterpene synthase family with potential implications for the evolution of diterpenoid metabolism in the cereals. *Biochem J*, **435**(3): p. 589-95.

84. **M. Jia, K. C. Potter, and R. J. Peters** (2016), Extreme promiscuity of a bacterial and a plant diterpene synthase enables combinatorial biosynthesis. *Metab Eng*, **37**: p. 24-34.

85. **C. Ignea, E. Ioannou, P. Georgantea, S. Loupassaki, F. A. Trikka, A. K. Kanellis, A. M. Makris, V. Roussis, and S. C. Kampranis** (2015), Reconstructing the chemical diversity of labdane-type diterpene biosynthesis in yeast. *Metab Eng*, **28**: p. 91-103.

86. **S. Yamaguchi** (2008), Gibberellin metabolism and its regulation. *Annu Rev Plant Biol*, **59**: p. 225-51.

87. **K. Hayashi, H. Kawaide, M. Notomi, Y. Sakigi, A. Matsuo, and H. Nozaki** (2006), Identification and functional analysis of bifunctional *ent*-kaurene synthase from the moss *Physcomitrella patens*. *FEBS Lett*, **580**(26): p. 6175-81.

88. **C. I. Keeling, H. K. Dullat, M. Yuen, S. G. Ralph, S. Jancsik, and J. Bohlmann** (2010), Identification and functional characterization of monofunctional *ent*-copalyl diphosphate and *ent*-kaurene synthases in white spruce reveal different patterns for diterpene synthase evolution for primary and secondary metabolism in gymnosperms. *Plant Physiol*, **152**(3): p. 1197-208.

89. **Q. Jia, T. G. Kollner, J. Gershenzon, and F. Chen** (2018), MTPSLs: New Terpene Synthases in Nonseed Plants. *Trends Plant Sci*, **23**(2): p. 121-128.

90. **Q. Jia, G. Li, T. G. Kollner, J. Fu, X. Chen, W. Xiong, B. J. Crandall-Stotler, J. L. Bowman, D. J. Weston, Y. Zhang, L. Chen, Y. Xie, F. W. Li, C. J. Rothfels, A. Larsson, S. W. Graham, D. W. Stevenson, G. K. Wong, J. Gershenzon, and F. Chen** (2016), Microbial-type terpene synthase genes occur widely in nonseed land plants, but not in seed plants. *Proc Natl Acad Sci U S A*, **113**(43): p. 12328-12333.

91. **G. Li, T. G. Köllner, Y. Yin, Y. Jiang, H. Chen, Y. Xu, J. Gershenzon, E. Pichersky, and F. Chen** (2012), Nonseed plant *Selaginella moellendorffii* has both seed plant and microbial types of terpene synthases. *Proc Natl Acad Sci U S A*, **109**(36): p. 14711-14715.

92. **S. Kumar, C. Kempinski, X. Zhuang, A. Norris, S. Mafu, J. Zi, S. A. Bell, S. E. Nybo, S. E. Kinison, Z. Jiang, S. Goklany, K. B. Linscott, X. Chen, Q. Jia, S. D. Brown, J. L. Bowman, P. C. Babbitt, R. J. Peters, F. Chen, and J. Chappell** (2016), Molecular diversity of terpene synthases in the liverwort *Marchantia polymorpha*. *Plant Cell*, **28**(10): p. 2632-2650.

93. **M. Xu, P. R. Wilderman, and R. J. Peters** (2007), Following evolution's lead to a single residue switch for diterpene synthase product outcome. *Proc Natl Acad Sci U S A*, **104**(18): p. 7397-401.

94. **S. Irmisch, A. T. Müller, L. Schmidt, J. Günther, J. Gershenzon, and T. G. Köllner** (2015), One amino acid makes the difference: the formation of *ent*-kaurene and 16α-hydroxy-*ent*-kaurane by diterpene synthases in poplar. *BMC Plant Biol*, **15**: p. 262.

95. **X. Chen, A. Berim, F. E. Dayan, and D. R. Gang** (2017), A (-)-kolavenyl diphosphate synthase catalyzes the first step of salvinorin A biosynthesis in *Salvia divinorum*. *J Exp Bot*, **68**(5): p. 1109-1122.

96. **W. Gao, M. L. Hillwig, L. Huang, G. Cui, X. Wang, J. Kong, B. Yang, and R. J. Peters** (2009), A functional genomics approach to tanshinone biosynthesis provides stereochemical insights. *Org Lett*, **11**(22): p. 5170-3.

97. **C. Ignea, A. Athanasakoglou, E. Ioannou, P. Georgantea, F. A. Trikka, S. Loupassaki, V. Roussis, A. M. Makris, and S. C. Kampranis** (2016), Carnosic acid biosynthesis elucidated by a synthetic biology platform. *Proc Natl Acad Sci U S A*, **113**(13): p. 3681-6.

98. **M. L. Hillwig, M. Xu, T. Toyomasu, M. S. Tiernan, G. Wei, G. Cui, L. Huang, and R. J. Peters** (2011), Domain loss has independently occurred multiple times in plant terpene synthase evolution. *Plant J*, **68**(6): p. 1051-1060.

99. **I. Pateraki, J. Andersen-Ranberg, B. Hamberger, A. M. Heskes, H. J. Martens, P. Zerbe, S. S. Bach, B. L. Møller, J. Bohlmann, and B. Hamberger** (2014), Manoyl oxide (13*R*), the biosynthetic precursor of forskolin, is synthesized in specialized root cork cells in *Coleus forskohlii*. *Plant Physiol*, **164**(3): p. 1222-36.

100. **K. A. Pelot, D. M. Hagelthorn, J. B. Addison, and P. Zerbe** (2017), Biosynthesis of the oxygenated diterpene nezukol in the medicinal plant *Isodon rubescens* is catalyzed by a pair of diterpene synthases. *PLoS One*, **12**(4): p. e0176507.

101. **P. Zerbe, A. Chiang, H. Dullat, M. O'Neil-Johnson, C. Starks, B. Hamberger, and J. Bohlmann** (2014), Diterpene synthases of the biosynthetic system of medicinally active diterpenoids in *Marrubium vulgare*. *Plant J*, **79**(6): p. 914-27.

102. **J. Zi and R. J. Peters** (2013), Characterization of CYP76AH4 clarifies phenolic diterpenoid biosynthesis in the Lamiaceae. *Org Biomol Chem*, **11**(44): p. 7650-2.

103. **J. Guo, Y. J. Zhou, M. L. Hillwig, Y. Shen, L. Yang, Y. Wang, X. Zhang, W. Liu, R. J. Peters, X. Chen, Z. K. Zhao, and L. Huang** (2013), CYP76AH1 catalyzes turnover of miltiradiene in tanshinones biosynthesis and enables heterologous production of ferruginol in yeasts. *Proc Natl Acad Sci U S A*, **110**(29): p. 12108-13.

104. **W. Q. Wang, Y. P. Yin, L. Jun, and L. J. Xuan** (2018), Halimane-type diterpenoids from *Vitex rotundifolia* and their anti-hyperlipidemia activities. *Phytochemistry*, **146**: p. 56-62.

105. **G. Topçu, A. C. Gören, T. Kiliç, Y. K. Yildiz, and G. Tümen** (2002), Diterpenes from *Sideritis trojana*. *Nat Prod Lett*, **16**(1): p. 33-7.

106. **J. Wellsow, R. J. Grayer, N. C. Veitch, T. Kokubun, R. Lelli, G. C. Kite, and M. S. Simmonds** (2006), Insect-antifeedant and antibacterial activity of diterpenoids from species of Plectranthus. *Phytochemistry*, **67**(16): p. 1818-25.

107. **B. M. Fraga, R. Guillermo, M. G. Hernández, T. Mestres, and J. M. Arteaga** (1991), Diterpenes from *Sideritis canariensis*. *Phytochemistry*, **30**(10): p. 3361-3364.

108. **B. Esquivel, C. Bustos-Brito, M. Sánchez-Castellanos, A. Nieto-Camacho, T. Ramírez-Apan, P. Joseph-Nathan, and L. Quijano** (2017), Structure, absolute configuration, and antiproliferative activity of abietane and icetexane diterpenoids from *Salvia ballotiflora*. *Molecules (Basel, Switzerland)*, **22**(10): p. 1690.

109. **J. Xu, E. A. Wold, Y. Ding, Q. Shen, and J. Zhou** (2018), Therapeutic potential of oridonin and its analogs: From anticancer and antiinflammation to neuroprotection. *Molecules*, **23**(2).

110. **B. Jin, G. Cui, J. Guo, J. Tang, L. Duan, H. Lin, Y. Shen, T. Chen, H. Zhang, and L. Huang** (2017), Functional diversification of kaurene synthase-like genes in *Isodon rubescens*. *Plant Physiol*, **174**(2): p. 943-955.

111. **A. M. Heskes, T. C. M. Sundram, B. A. Boughton, N. B. Jensen, N. L. Hansen, C. Crocoll, F. Cozzi, S. Rasmussen, B. Hamberger, B. Hamberger, D. Staerk, B. L. Møller, and I. Pateraki** (2018), Biosynthesis of bioactive diterpenoids in the medicinal plant *Vitex agnus-castus*. *Plant J*, **93**(5): p. 943-958.

112. **N. Günnewich, Y. Higashi, X. Feng, K. B. Choi, J. Schmidt, and T. M. Kutchan** (2013), A diterpene synthase from the clary sage *Salvia sclarea* catalyzes the cyclization of geranylgeranyl diphosphate to (8*R*)-hydroxy-copalyl diphosphate. *Phytochemistry*, **91**: p. 93-9.

113. **K. A. Pelot, R. Mitchell, M. Kwon, D. M. Hagelthorn, J. F. Wardman, A. Chiang, J. Bohlmann, D. K. Ro, and P. Zerbe** (2017), Biosynthesis of the psychotropic plant diterpene salvinorin A: Discovery and characterization of the *Salvia divinorum* clerodienyl diphosphate synthase. *Plant J*, **89**(5): p. 885-897.

114. **D. Werck-Reichhart and R. Feyereisen** (2000), Cytochromes P450: a success story. *Genome Biol*, **1**(6): p. Reviews3003.

115. **D. Nelson and D. Werck-Reichhart** (2011), A P450-centric view of plant evolution. *Plant J*, **66**(1): p. 194-211.

116. **D. C. Lamb and M. R. Waterman** (2013), Unusual properties of the cytochrome P450 superfamily. *Philos Trans R Soc Lond B Biol Sci*, **368**(1612): p. 20120434-20120434.

117. **D.-K. Ro, G.-I. Arimura, S. Y. W. Lau, E. Piers, and J. Bohlmann** (2005), *Loblolly pine* abietadienol/abietadienal oxidase PtAO (CYP720B1) is a multifunctional, multisubstrate cytochrome P450 monooxygenase. *Proc Natl Acad Sci U S A*, **102**(22): p. 8060-8065.

118. **S. Bak, F. Beisson, G. Bishop, B. Hamberger, R. Höfer, S. Paquette, and D. Werck-Reichhart** (2011), Cytochromes p450. *The Arabidopsis Book*, **9**: p. e0144-e0144.

119. **G. I. Lepesheva and M. R. Waterman** (2007), Sterol 14α-demethylase cytochrome P450 (CYP51), a P450 in all biological kingdoms. *Biochimica et biophysica acta*, **1770**(3): p. 467-477.

120. **B. Hamberger and S. Bak** (2013), Plant P450s as versatile drivers for evolution of species-specific chemical diversity. *Philos Trans R Soc Lond B Biol Sci*, **368**(1612): p. 20120426.

121. **S. Ghosh** (2017), Triterpene structural diversification by plant cytochrome P450 enzymes. *Front Plant Sci*, **8**: p. 1886-1886.

122. **K. Takei, T. Yamaya, and H. Sakakibara** (2004), *Arabidopsis* CYP735A1 and CYP735A2 encode cytokinin hydroxylases that catalyze the biosynthesis of *trans*-Zeatin. *J Biol Chem*, **279**(40): p. 41866-72.

123. **S. Kandel, M. Morant, I. Benveniste, E. Blee, D. Werck-Reichhart, and F. Pinot** (2005), Cloning, functional expression, and characterization of CYP709C1, the first sub-terminal hydroxylase of long chain fatty acid in plants. Induction by chemicals and methyl jasmonate. *J Biol Chem*, **280**(43): p. 35881-9.

124. **H. Magome, T. Nomura, A. Hanada, N. Takeda-Kamiya, T. Ohnishi, Y. Shinma, T. Katsumata, H. Kawaide, Y. Kamiya, and S. Yamaguchi** (2013), CYP714B1 and CYP714B2 encode gibberellin 13-oxidases that reduce gibberellin activity in rice. *Proc Natl Acad Sci U S A*, **110**(5): p. 1947-52.

125. **T. Sakamoto, A. Kawabe, A. Tokida-Segawa, B. Shimizu, S. Takatsuto, Y. Shimada, S. Fujioka, and M. Mizutani** (2011), Rice CYP734As function as multisubstrate and multifunctional enzymes in brassinosteroid catabolism. *Plant J*, **67**(1): p. 1-12.

126. **H. Seki, K. Ohyama, S. Sawai, M. Mizutani, T. Ohnishi, H. Sudo, T. Akashi, T. Aoki, K. Saito, and T. Muranaka** (2008), Licorice β-amyrin 11-oxidase, a cytochrome P450 with a key role in the biosynthesis of the triterpene sweetener glycyrrhizin. *Proc Natl Acad Sci U S A*, **105**(37): p. 14204-9.

127. **H. Seki, S. Sawai, K. Ohyama, M. Mizutani, T. Ohnishi, H. Sudo, E. O. Fukushima, T. Akashi, T. Aoki, K. Saito, and T. Muranaka** (2011), Triterpene functional genomics in licorice for identification of CYP72A154 involved in the biosynthesis of glycyrrhizin. *Plant Cell*, **23**(11): p. 4112-23.

128. **C. Haudenschild, M. Schalk, F. Karp, and R. Croteau** (2000), Functional expression of regiospecific cytochrome P450 limonene hydroxylases from mint (*Mentha spp.*) in *Escherichia coli* and *Saccharomyces cerevisiae*. *Arch Biochem Biophys*, **379**(1): p. 127-36.

129. **A. O. Latunde-Dada, F. Cabello-Hurtado, N. Czittrich, L. Didierjean, C. Schopfer, N. Hertkorn, D. Werck-Reichhart, and J. Ebel** (2001), Flavonoid 6-hydroxylase from soybean (*Glycine max* L.), a novel plant P-450 monooxygenase. *J Biol Chem*, **276**(3): p. 1688-95.

130. **N. Verhoef, T. Yokota, K. Shibata, G.-J. de Boer, T. Gerats, M. Vandenbussche, R. Koes, and E. Souer** (2013), Brassinosteroid biosynthesis and signalling in *Petunia hybrida*. *J Exp Bot*, **64**(8): p. 2435-2448.

131. **S. E. Graham and J. A. Peterson** (1999), How similar are P450s and what can their differences teach us? *Arch Biochem Biophys*, **369**(1): p. 24-9.

132. **C. A. Hasemann, R. G. Kurumbail, S. S. Boddupalli, J. A. Peterson, and J. Deisenhofer** (1995), Structure and function of cytochromes P450: a comparative analysis of three crystal structures. *Structure*, **3**(1): p. 41-62.

133. **K. Jensen and B. L. Møller** (2010), Plant NADPH-cytochrome P450 oxidoreductases. *Phytochemistry*, **71**(2-3): p. 132-41.

134. **N. de Vetten, J. ter Horst, H. P. van Schaik, A. de Boer, J. Mol, and R. Koes** (1999), A cytochrome b_5 is required for full activity of flavonoid 3', 5'-hydroxylase, a cytochrome P450 involved in the formation of blue flower colors. *Proc Natl Acad Sci U S A*, **96**(2): p. 778-783.

135. **F. P. Guengerich** (2007), Mechanisms of cytochrome P450 substrate oxidation: MiniReview. *J Biochem Mol Toxicol*, **21**(4): p. 163-8.

136. **D. Hamdane, H. Zhang, and P. Hollenberg** (2008), Oxygen activation by cytochrome P450 monooxygenase. *Photosynth Res*, **98**(1-3): p. 657-666.

137. A. Tissier, J. Ziegler, and T. Vogt, *Specialized plant metabolites: diversity and biosynthesis*, in *Ecological Biochemistry*. 2014. p. 15-37.

138. **H. Renault, J. E. Bassard, B. Hamberger, and D. Werck-Reichhart** (2014), Cytochrome P450-mediated metabolic engineering: current progress and future challenges. *Curr Opin Plant Biol*, **19**: p. 27-34.

139. **A. J. King, G. D. Brown, A. D. Gilday, T. R. Larson, and I. A. Graham** (2014), Production of bioactive diterpenoids in the euphorbiaceae depends on evolutionarily conserved gene clusters. *Plant Cell*, **26**(8): p. 3286-98.

140. **K. H. Teoh, D. R. Polichuk, D. W. Reed, G. Nowak, and P. S. Covello** (2006), *Artemisia annua* L. (Asteraceae) trichome-specific cDNAs reveal CYP71AV1, a cytochrome P450 with a key role in the biosynthesis of the antimalarial sesquiterpene lactone artemisinin. *FEBS Lett*, **580**(5): p. 1411-6.

141. **Y. Wu, M. L. Hillwig, Q. Wang, and R. J. Peters** (2011), Parsing a multifunctional biosynthetic gene cluster from rice: Biochemical characterization of CYP71Z6 & 7. *FEBS letters*, **585**(21): p. 3446-3451.

142. **G. D. Moghe and R. L. Last** (2015), Something old, something new: Conserved enzymes and the evolution of novelty in plant specialized metabolism. *Plant Physiol*, **169**(3): p. 1512-1523.

143. **J. K. Weng and J. P. Noel** (2012), The remarkable pliability and promiscuity of specialized metabolism. *Cold Spring Harb Symp Quant Biol*, **77**: p. 309-20.

144. **P. Gatti-Lafranconi and F. Hollfelder** (2013), Flexibility and reactivity in promiscuous enzymes. *Chembiochem*, **14**(3): p. 285-92.

145. **B. Hamberger, T. Ohnishi, B. Hamberger, A. Séguin, and J. Bohlmann** (2011), Evolution of diterpene metabolism: *Sitka spruce* CYP720B4 catalyzes multiple oxidations in resin acid biosynthesis of conifer defense against insects. *Plant Physiol*, **157**(4): p. 1677-1695.

146. **S. Takahashi, Y.-S. Yeo, Y. Zhao, P. E. O'Maille, B. T. Greenhagen, J. P. Noel, R. M. Coates, and J. Chappell** (2007), Functional characterization of premnaspirodiene oxygenase, a cytochrome P450 catalyzing regio- and stereo-specific hydroxylations of diverse sesquiterpene substrates. *J Biol Chem*, **282**(43): p. 31744-31754.

147. **B. Field and A. E. Osbourn** (2008), Metabolic diversification--independent assembly of operon-like gene clusters in different plants. *Science*, **320**(5875): p. 543-7.

148. **K. Shimura, A. Okada, K. Okada, Y. Jikumaru, K. W. Ko, T. Toyomasu, T. Sassa, M. Hasegawa, O. Kodama, N. Shibuya, J. Koga, H. Nojiri, and H. Yamane** (2007), Identification of a biosynthetic gene cluster in rice for momilactones. *J Biol Chem*, **282**(47): p. 34013-8.

149. **S. Swaminathan, D. Morrone, Q. Wang, D. B. Fulton, and R. J. Peters** (2009), CYP76M7 is an *ent*-cassadiene C11α-hydroxylase defining a second multifunctional diterpenoid biosynthetic gene cluster in rice. *Plant Cell*, **21**(10): p. 3315-25.

150. **M. Frey, K. Schullehner, R. Dick, A. Fiesselmann, and A. Gierl** (2009), Benzoxazinoid biosynthesis, a model for evolution of secondary metabolic pathways in plants. *Phytochemistry*, **70**(15-16): p. 1645-51.

151. **S. Boycheva, L. Daviet, J. L. Wolfender, and T. B. Fitzpatrick** (2014), The rise of operon-like gene clusters in plants. *Trends Plant Sci*, **19**(7): p. 447-59.

152. **J. M. Humphreys, M. R. Hemm, and C. Chapple** (1999), New routes for lignin biosynthesis defined by biochemical characterization of recombinant ferulate 5-hydroxylase, a multifunctional cytochrome P450-dependent monooxygenase. *Proc Natl Acad Sci U S A*, **96**(18): p. 10045-10050.

153. **J. K. Weng, Y. Li, H. Mo, and C. Chapple** (2012), Assembly of an evolutionarily new pathway for α-pyrone biosynthesis in *Arabidopsis*. *Science*, **337**(6097): p. 960-4.

154. **Q. Wang, M. L. Hillwig, Y. Wu, and R. J. Peters** (2012), CYP701A8: a rice *ent*-kaurene oxidase paralog diverted to more specialized diterpenoid metabolism. *Plant Physiol*, **158**(3): p. 1418-1425.

155. **C. Engler and S. Marillonnet** (2014), Golden Gate cloning. *Methods Mol Biol*, **1116**: p. 119-31.

156. **S. Werner, C. Engler, E. Weber, R. Gruetzner, and S. Marillonnet** (2012), Fast track assembly of multigene constructs using Golden Gate cloning and the MoClo system. *Bioeng Bugs*, **3**(1): p. 38-43.

157. **A. R. Awan, B. A. Blount, D. J. Bell, W. M. Shaw, J. C. H. Ho, R. M. McKiernan, and T. Ellis** (2017), Biosynthesis of the antibiotic nonribosomal peptide penicillin in baker's yeast. *Nat Commun*, **8**: p. 15202.

158. **M. Larroude, E. Celinska, A. Back, S. Thomas, J. M. Nicaud, and R. Ledesma-Amaro** (2018), A synthetic biology approach to transform *Yarrowia lipolytica* into a competitive biotechnological producer of β-carotene. *Biotechnol Bioeng*, **115**(2): p. 464-472.

159. **J. Andersen-Ranberg, K. T. Kongstad, M. T. Nielsen, N. B. Jensen, I. Pateraki, S. S. Bach, B. Hamberger, P. Zerbe, D. Staerk, J. Bohlmann, B. L. Møller, and B. Hamberger** (2016), Expanding the landscape of diterpene structural diversity through stereochemically controlled combinatorial biosynthesis. *Angew Chem Int Ed Engl*, **55**(6): p. 2142-6.

160. **Y. J. Zhou, W. Gao, Q. Rong, G. Jin, H. Chu, W. Liu, W. Yang, Z. Zhu, G. Li, G. Zhu, L. Huang, and Z. K. Zhao** (2012), Modular pathway engineering of diterpenoid synthases and the mevalonic acid pathway for miltiradiene production. *J Am Chem Soc*, **134**(6): p. 3234-41.

161. **A. Cyr, P. R. Wilderman, M. Determan, and R. J. Peters** (2007), A modular approach for facile biosynthesis of labdane-related diterpenes. *J Am Chem Soc* **129**(21): p. 6684-6685.

162. **K. Miettinen, L. Dong, N. Navrot, T. Schneider, V. Burlat, J. Pollier, L. Woittiez, S. van der Krol, R. Lugan, T. Ilc, R. Verpoorte, K. M. Oksman-Caldentey, E. Martinoia, H. Bouwmeester, A. Goossens, J. Memelink, and D. Werck-Reichhart** (2014), The seco-iridoid pathway from *Catharanthus roseus*. *Nat Commun*, **5**: p. 3606.

163. **C. Crocoll, N. Mirza, M. Reichelt, J. Gershenzon, and B. A. Halkier** (2016), Optimization of engineered production of the glucoraphanin precursor dihomomethionine in *Nicotiana benthamiana*. *Front Bioeng Biotechnol*, **4**: p. 14.

164. **Y. Y. Toporkova, V. S. Ermilova, S. S. Gorina, L. S. Mukhtarova, E. V. Osipova, Y. V. Gogolev, and A. N. Grechkin** (2013), Structure-function relationship in the CYP74 family: conversion of divinyl ether synthases into allene oxide synthases by site-directed mutagenesis. *FEBS Lett*, **587**(16): p. 2552-8.

165. **I. El-Awaad, M. Bocola, T. Beuerle, B. Liu, and L. Beerhues** (2016), Bifunctional CYP81AA proteins catalyse identical hydroxylations but alternative regioselective phenol couplings in plant xanthone biosynthesis. *Nat Commun*, **7**: p. 11472.

166. **G. A. Schoch, R. Attias, M. Le Ret, and D. Werck-Reichhart** (2003), Key substrate recognition residues in the active site of a plant cytochrome P450, CYP73A1. Homology guided site-directed mutagenesis. *Eur J Biochem*, **270**(18): p. 3684-95.

167. **C. J. Paddon, P. J. Westfall, D. J. Pitera, K. Benjamin, K. Fisher, D. McPhee, M. D. Leavell, A. Tai, A. Main, D. Eng, D. R. Polichuk, K. H. Teoh, D. W. Reed, T. Treynor, J. Lenihan, M. Fleck, S. Bajad, G. Dang, D. Dengrove, D. Diola, G. Dorin, K. W. Ellens, S. Fickes, J. Galazzo, S. P. Gaucher, T. Geistlinger, R. Henry, M. Hepp, T. Horning, T. Iqbal, H. Jiang, L. Kizer, B. Lieu, D. Melis, N. Moss, R. Regentin, S. Secrest, H. Tsuruta, R. Vazquez, L. F. Westblade, L. Xu, M. Yu, Y. Zhang, L. Zhao, J. Lievense, P. S. Covello, J. D. Keasling, K. K. Reiling, N. S. Renninger, and J. D. Newman** (2013), High-level semi-synthetic production of the potent antimalarial artemisinin. *Nature*, **496**(7446): p. 528-32.

168. **L. Jorgensen, S. J. McKerrall, C. A. Kuttruff, F. Ungeheuer, J. Felding, and P. S. Baran** (2013), 14-step synthesis of (+)-ingenol from (+)-3-carene. *Science*, **341**(6148): p. 878-82.

169. **I. Smetanska** (2008), Production of secondary metabolites using plant cell cultures. *Adv Biochem Eng Biotechnol*, **111**: p. 187-228.

170. **T. Nomura, S. Ogita, and Y. Kato** (2018), Rational metabolic-flow switching for the production of exogenous secondary metabolites in bamboo suspension cells. *Sci Rep*, **8**(1): p. 13203-13203.

171. **X. Liu, W. Ding, and H. Jiang** (2017), Engineering microbial cell factories for the production of plant natural products: from design principles to industrial-scale production. *Microb Cell Fact*, **16**(1): p. 125-125.

172. **S. A. Wilson and S. C. Roberts** (2012), Recent advances towards development and commercialization of plant cell culture processes for the synthesis of biomolecules. *Plant Biotechnol J*, **10**(3): p. 249-68.

173. **E. C. Tatsis and S. E. O'Connor** (2016), New developments in engineering plant metabolic pathways. *Curr Opin Biotechnol*, **42**: p. 126-132.

174. **T. W. van Herpen, K. Cankar, M. Nogueira, D. Bosch, H. J. Bouwmeester, and J. Beekwilder** (2010), *Nicotiana benthamiana* as a production platform for artemisinin precursors. *PLoS One*, **5**(12): p. e14222.

175. **J. D. Keasling** (2012), Synthetic biology and the development of tools for metabolic engineering. *Metab Eng*, **14**(3): p. 189-95.

176. **M. L. Diaz-Chavez, J. Moniodis, L. L. Madilao, S. Jancsik, C. I. Keeling, E. L. Barbour, E. L. Ghisalberti, J. A. Plummer, C. G. Jones, and J. Bohlmann** (2013), Biosynthesis of sandalwood oil: *Santalum album* CYP76F cytochromes P450 produce santalols and bergamotol. *PLoS One*, **8**(9): p. e75053.

177. **D. Liu, X. Huang, W. Jing, X. An, Q. Zhang, H. Zhang, J. Zhou, Y. Zhang, and Y. Guo** (2018), Identification and functional analysis of two P450 enzymes of *Gossypium hirsutum* involved in DMNT and TMTT biosynthesis. *Plant Biotechnol J*, **16**(2): p. 581-590.

178. **I. J. Trenchard and C. D. Smolke** (2015), Engineering strategies for the fermentative production of plant alkaloids in yeast. *Metab Eng*, **30**: p. 96-104.

179. **K. M. Hawkins and C. D. Smolke** (2008), Production of benzylisoquinoline alkaloids in *Saccharomyces cerevisiae*. *Nat Chem Biol*, **4**(9): p. 564-573.

180. **A. Rodriguez, T. Strucko, S. G. Stahlhut, M. Kristensen, D. K. Svenssen, J. Forster, J. Nielsen, and I. Borodina** (2017), Metabolic engineering of yeast for fermentative production of flavonoids. *Bioresour Technol*, **245**(Pt B): p. 1645-1654.

181. **M. R. Eckart and C. M. Bussineau** (1996), Quality and authenticity of heterologous proteins synthesized in yeast. *Curr Opin Biotechnol*, **7**(5): p. 525-30.

182. **M.-E. Cuvelier, H. Richard, and C. Berset** (1996), Antioxidative activity and phenolic composition of pilot-plant and commercial extracts of sage and rosemary. *J Am Oil Chem Soc*, **73**(5): p. 645.

183. **J. Xie, P. Van Alstyne, A. Uhlir, and X. Yang** (2017), A review on rosemary as a natural antioxidation solution. *Eur J Lipid Sci Technol*, **119**(6): p. 1600439.

184. **S. Habtemariam** (2016), The therapeutic potential of rosemary (*Rosmarinus officinalis*) diterpenes for Alzheimer's disease. *Evid Based Complement Alternat Med*, **2016**: p. 2680409.

185. **A. Kabouche and Z. Kabouche** (2008), Bioactive diterpenoids of *Salvia* species. *Stud Nat Prod Chem*, **35**: p. 753-833.

186. **J. Guo, X. Ma, Y. Cai, Y. Ma, Z. Zhan, Y. J. Zhou, W. Liu, M. Guan, J. Yang, G. Cui, L. Kang, L. Yang, Y. Shen, J. Tang, H. Lin, X. Ma, B. Jin, Z. Liu, R. J. Peters, Z. K. Zhao, and L. Huang** (2016), Cytochrome P450 promiscuity leads to a bifurcating biosynthetic pathway for tanshinones. *New Phytol*, **210**(2): p. 525-34.

187. **U. Scheler, W. Brandt, A. Porzel, K. Rothe, D. Manzano, D. Božić, D. Papaefthimiou, G. U. Balcke, A. Henning, S. Lohse, S. Marillonnet, A. K. Kanellis, A. Ferrer, and A. Tissier** (2016), Elucidation of the biosynthesis of carnosic acid and its reconstitution in yeast. *Nat Commun*, **7**: p. 12942.

188. **C. Ignea, A. Athanasakoglou, A. Andreadelli, M. Apostolaki, M. Iakovides, E. G. Stephanou, A. M. Makris, and S. C. Kampranis** (2017), Overcoming the plasticity of plant specialized metabolism for selective diterpene production in yeast. *Sci Rep*, **7**(1): p. 8855.

189. **U. Bathe, A. Frolov, A. Porzel, and A. Tissier** (2019), CYP76 oxidation network of abietane diterpenes in Lamiaceae reconstituted in yeast. *J Agric Food Chem*.

190. **U. Bathe and A. Tissier** (2019), Cytochrome P450 enzymes: A driving force of plant diterpene diversity. *Phytochemistry*, **161**: p. 149-162.

191. **Q. Wang, M. L. Hillwig, K. Okada, K. Yamazaki, Y. Wu, S. Swaminathan, H. Yamane, and R. J. Peters** (2012), Characterization of CYP76M5-8 indicates metabolic plasticity within a plant biosynthetic gene cluster. *J Biol Chem*, **287**(9): p. 6159-6168.

192. **R. Höfer, L. Dong, F. André, J. F. Ginglinger, R. Lugan, C. Gavira, S. Grec, G. Lang, J. Memelink, S. Van der Krol, H. Bouwmeester, and D. Werck-Reichhart** (2013), Geraniol hydroxylase and hydroxygeraniol oxidase activities of the CYP76 family of cytochrome P450 enzymes and potential for engineering the early steps of the (seco)iridoid pathway. *Metab Eng*, **20**: p. 221-32.

193. **G. Collu, N. Unver, A. M. Peltenburg-Looman, R. van der Heijden, R. Verpoorte, and J. Memelink** (2001), Geraniol 10-hydroxylase, a cytochrome P450 enzyme involved in terpenoid indole alkaloid biosynthesis. *FEBS Lett*, **508**(2): p. 215-20.

194. **V. Salim, B. Wiens, S. Masada-Atsumi, F. Yu, and V. De Luca** (2014), 7-deoxyloganetic acid synthase catalyzes a key 3 step oxidation to form 7-deoxyloganetic acid in *Catharanthus roseus* iridoid biosynthesis. *Phytochemistry*, **101**: p. 23-31.

195. **R. Höfer, B. Boachon, H. Renault, C. Gavira, L. Miesch, J. Iglesias, J. F. Ginglinger, L. Allouche, M. Miesch, S. Grec, R. Larbat, and D. Werck-Reichhart** (2014), Dual function of the cytochrome P450 CYP76 family from *Arabidopsis thaliana* in the metabolism of monoterpenols and phenylurea herbicides. *Plant Physiol*, **166**(3): p. 1149-61.

196. **A. Bar-Even, E. Noor, Y. Savir, W. Liebermeister, D. Davidi, D. S. Tawfik, and R. Milo** (2011), The moderately efficient enzyme: evolutionary and physicochemical trends shaping enzyme parameters. *Biochemistry*, **50**(21): p. 4402-10.

197. **B. J. Leong and R. L. Last** (2017), Promiscuity, impersonation and accommodation: evolution of plant specialized metabolism. *Curr Opin Struct Biol*, **47**: p. 105-112.

198. **G. G. Hammes** (2002), Multiple conformational changes in enzyme catalysis. *Biochemistry*, **41**(26): p. 8221-8228.

199. **L. Sanchez-Sanchez, R. Roman, and R. Vazquez-Duhalt** (2012), Pesticide transformation by a variant of CYPBM3 with improved peroxygenase activity. *Pest Biochem Physiol*, **102**(2): p. 169-174.

200. **H. M. Li, L. H. Mei, V. B. Urlacher, and R. D. Schmid** (2008), Cytochrome P450 BM-3 evolved by random and saturation mutagenesis as an effective indole-hydroxylating catalyst. *Appl Biochem Biotechnol*, **144**(1): p. 27-36.

201. **S. A. Vestri Alvarenga, J. Pierre Gastmans, G. do Vale Rodrigues, P. R. Moreno, and V. de Paulo Emerenciano** (2001), A computer-assisted approach for chemotaxonomic studies--diterpenes in Lamiaceae. *Phytochemistry*, **56**(6): p. 583-95.

202. **C. I. Keeling, S. Weisshaar, R. P. C. Lin, and J. Bohlmann** (2008), Functional plasticity of paralogous diterpene synthases involved in conifer defense. *Proc Natl Acad Sci U S A*, **105**(3): p. 1085-1090.

203. **T. Sikosek, H. S. Chan, and E. Bornberg-Bauer** (2012), Escape from adaptive conflict follows from weak functional trade-offs and mutational robustness. *Proc Natl Acad Sci U S A*, **109**(37): p. 14888-93.

204. **A. G. González, T. Abad, I. A. Jiménez, A. G. Ravelo, J. G. Luis Zahira Aguiar, L. San Andrés, M. Plasencia, J. R. Herrera, and L. Moujir** (1989), A first study of antibacterial activity of diterpenes isolated from some *Salvia* species (Lamiaceae). *Biochem Syst Ecol*, **17**(4): p. 293-296.

205. **M. Vaccaro, N. Malafronte, M. Alfieri, N. De Tommasi, and A. Leone** (2014), Enhanced biosynthesis of bioactive abietane diterpenes by overexpressing AtDXS or AtDXR genes in *Salvia sclarea* hairy roots. *Plant Cell Tissue Organ Cult*, **119**(1): p. 65-77.

206. **I. C. Guerrero, L. S. Andres, L. G. Leon, R. P. Machin, J. M. Padron, J. G. Luis, and J. Delgadillo** (2006), Abietane diterpenoids from *Salvia pachyphylla* and *S. clevelandii* with cytotoxic activity against human cancer cell lines. *J Nat Prod*, **69**(12): p. 1803-5.

207. **Z. Xu and J. Song** (2017), The 2-oxoglutarate-dependent dioxygenase superfamily participates in tanshinone production in *Salvia miltiorrhiza. J Exp Bot*, **68**(9): p. 2299-2308.

208. **M. G. Simic** (1981), Free radical mechanisms in autoxidation processes. *J Chem Educ*, **58**(2): p. 125.

209. **K. Brückner and A. Tissier** (2013), High-level diterpene production by transient expression in *Nicotiana benthamiana*. *Plant Methods*, **9**(1): p. 46.

210. **O. I. Aruoma, B. Halliwell, R. Aeschbach, and J. Loligers** (1992), Antioxidant and pro-oxidant properties of active rosemary constituents: carnosol and carnosic acid. *Xenobiotica*, **22**(2): p. 257-68.

211. **H. H. Zeng, P. F. Tu, K. Zhou, H. Wang, B. H. Wang, and J. F. Lu** (2001), Antioxidant properties of phenolic diterpenes from *Rosmarinus officinalis*. *Acta Pharmacol Sin*, **22**(12): p. 1094-8.

212. **G. Nieto, G. Ros, and J. Castillo** (2018), Antioxidant and antimicrobial properties of rosemary (*Rosmarinus officinalis*, L.): A review. *Medicines (Basel, Switzerland)*, **5**(3): p. 98.

213. **K. Geisler, N. B. Jensen, M. M. Yuen, L. Madilao, and J. Bohlmann** (2016), Modularity of conifer diterpene resin acid biosynthesis: P450 enzymes of different CYP720B clades use alternative substrates and converge on the same products. *Plant Physiol*, **171**(1): p. 152-64.

214. **J. G. Luis, W. Quiñones, T. A. Grillo, and M. P. Kishi** (1994), Diterpenes from the aerial part of *Salvia columbariae*. *Phytochemistry*, **35**(5): p. 1373-1374.

215. **J. Wang and E. Pichersky** (1999), Identification of specific residues involved in substrate discrimination in two plant *O*-methyltransferases. *Arch Biochem Biophys*, **368**(1): p. 172-180.

216. **Y. Zhang, T. A. Adelakun, L. Qu, X. Li, J. Li, L. Han, and T. Wang** (2014), New terpenoid glycosides obtained from *Rosmarinus officinalis* L. aerial parts. *Fitoterapia*, **99**: p. 78-85.

217. **P. Mena, M. Cirlini, M. Tassotti, K. A. Herrlinger, C. Dall'Asta, and D. Del Rio** (2016), Phytochemical profiling of flavonoids, phenolic acids, terpenoids, and volatile fraction of a rosemary (*Rosmarinus officinalis* L.) extract. *Molecules*, **21**(11).

218. **J. Escudero, L. Perez, R. M. Rabanal, and S. Valverde** (1983), Diterpenoids from *Salvia oxyodon* and *Salvia lavandulifolia*. *Phytochemistry*, **22**(2): p. 585-587.

219. **A. Ulubelen, G. Topçu, H.-B. Chai, and J. M. Pezzuto** (1999), Cytotoxic activity of diterpenoids isolated from *Salvia hypargeia*. *Pharm Biol*, **37**(2): p. 148-151.

220. **G. Topçu and A. Ulubelen** (1996), Abietane and rearranged abietane diterpenes from *Salvia montbretii*. *J Nat Prod*, **59**(8): p. 734-737.

221. **S. Cañigueral, J. Iglesias, F. Sánchez-Ferrando, and A. Virgili** (1988), Candelabrone, a new abietane diterpene from the leaves of *Salvia candelabrum*. *Phytochemistry*, **27**(1): p. 221-224.

222. **A. Ulubelen and G. Topcu** (1991), Abietane diterpenoids from *Salvia microstegia*. *Phytochemistry*, **30**(6): p. 2085-2086.

223. **G. Topçu, Z. Turkmen, J. K. Schilling, D. G. I. Kingston, J. M. Pezzuto, and A. Ulubelen** (2008), Cytotoxic activity of some anatolian *Salvia*. Extracts and isolated abietane diterpenoids. *Pharm Biol*, **46**(3): p. 180-184.

224. **L. Z. Lin, X. M. Wang, X. L. Huang, Y. Huang, and B. J. Yang** (1988), Diterpenoids from *Salvia prionitis. Planta Med*, **54**(5): p. 443-5.

225. **R. Pereda-Miranda, L. Hernandez, and R. Lopez** (1992), A novel antimicrobial abietane-type diterpene from *Salvia albocaerulea. Planta Med*, **58**(2): p. 223-4.

226. **S. V. S. Radhakrishnan, T. Hayes, and S. A. Ross** (2016), Phytochemical and biological investigation of *Salvia apiana. Planta Med*, **82**(05): p. PC75.

227. **A. Ulubelen and G. Topcu** (1992), Abietane diterpenoids from *Salvia pomifera. Phytochemistry*, **31**(11): p. 3949-3951.

228. **J. M. Amaro-Luis, J. R. Herrera, and J. G. Luis** (1998), Abietane diterpenoids from *Salvia chinopeplica. Phytochemistry*, **47**(5): p. 895-897.

229. **P. J. Hidalgo, J. L. Ubera, M. T. Tena, and M. Valcárcel** (1998), Determination of the carnosic acid content in wild and cultivated *Rosmarinus officinalis. J Agric Food Chem*, **46**(7): p. 2624-2627.

230. **M. J. del Baño, J. Lorente, J. Castillo, O. Benavente-García, J. A. del Río, A. Ortuño, K.-W. Quirin, and D. Gerard** (2003), Phenolic diterpenes, flavones, and rosmarinic acid distribution during the development of leaves, flowers, stems, and roots of *Rosmarinus officinalis*. Antioxidant Activity. *J Agric Food Chem*, **51**(15): p. 4247-4253.

231. **H. Haraguchi, T. Saito, N. Okamura, and A. Yagi** (1995), Inhibition of lipid peroxidation and superoxide generation by diterpenoids from *Rosmarinus officinalis. Planta Med*, **61**(4): p. 333-6.

232. **E. J. Dufourc** (2008), Sterols and membrane dynamics. *J Chem Biol*, **1**(1-4): p. 63-77.

233. **S.-W. Huang, E. N. Frankel, K. Schwarz, R. Aeschbach, and J. B. German** (1996), Antioxidant activity of carnosic acid and methyl carnosate in bulk oils and oil-in-water emulsions. *J Agric Food Chem*, **44**(10): p. 2951-2956.

234. **M. E. Abreu, M. Müller, L. Alegre, and S. Munné-Bosch** (2008), Phenolic diterpene and α-tocopherol contents in leaf extracts of 60 *Salvia* species. *J Sci Food Agric*, **88**(15): p. 2648-2653.

235. **S. Munne-Bosch and L. Alegre** (2003), Drought-induced changes in the redox state of α-tocopherol, ascorbate, and the diterpene carnosic acid in chloroplasts of Labiatae species differing in carnosic acid contents. *Plant Physiol*, **131**(4): p. 1816-25.

236. **T. Masuda, T. Kirikihira, and Y. Takeda** (2005), Recovery of antioxidant activity from carnosol quinone: antioxidants obtained from a water-promoted conversion of carnosol quinone. *J Agric Food Chem*, **53**(17): p. 6831-4.

237. **M. S. Butler and A. D. Buss** (2006), Natural products-the future scaffolds for novel antibiotics? *Biochem Pharmacol*, **71**(7): p. 919-29.

238. **D. Umeno and F. H. Arnold** (2003), A C_{35} carotenoid biosynthetic pathway. *Appl Environ Microbiol*, **69**(6): p. 3573-9.

239. **J. Klein, J. R. Heal, W. D. Hamilton, T. Boussemghoune, T. O. Tange, F. Delegrange, G. Jaeschke, A. Hatsch, and J. Heim** (2014), Yeast synthetic biology platform generates novel chemical structures as scaffolds for drug discovery. *ACS Synth Biol*, **3**(5): p. 314-23.

240. **K. Potter, J. Criswell, J. Zi, A. Stubbs, and R. J. Peters** (2014), Novel product chemistry from mechanistic analysis of *ent*-copalyl diphosphate synthases from plant hormone biosynthesis. *Angew Chem Int Ed Engl*, **53**(28): p. 7198-202.

241. **M. Yamanishi, Y. Ito, R. Kintaka, C. Imamura, S. Katahira, A. Ikeuchi, H. Moriya, and T. Matsuyama** (2013), A genome-wide activity assessment of terminator regions in *Saccharomyces cerevisiae* provides a "terminatome" toolbox. *ACS Synth Biol*, **2**(6): p. 337-47.

242. **K. S. Zaret and F. Sherman** (1982), DNA sequence required for efficient transcription termination in yeast. *Cell*, **28**(3): p. 563-73.

243. **M. Mizutani and D. Ohta** (1998), Two isoforms of NADPH:cytochrome P450 reductase in *Arabidopsis thaliana*. Gene structure, heterologous expression in insect cells, and differential regulation. *Plant Physiol*, **116**(1): p. 357-67.

5. Appendix

5.1. Supporting information to 2.2.2.

Supplementary Figures

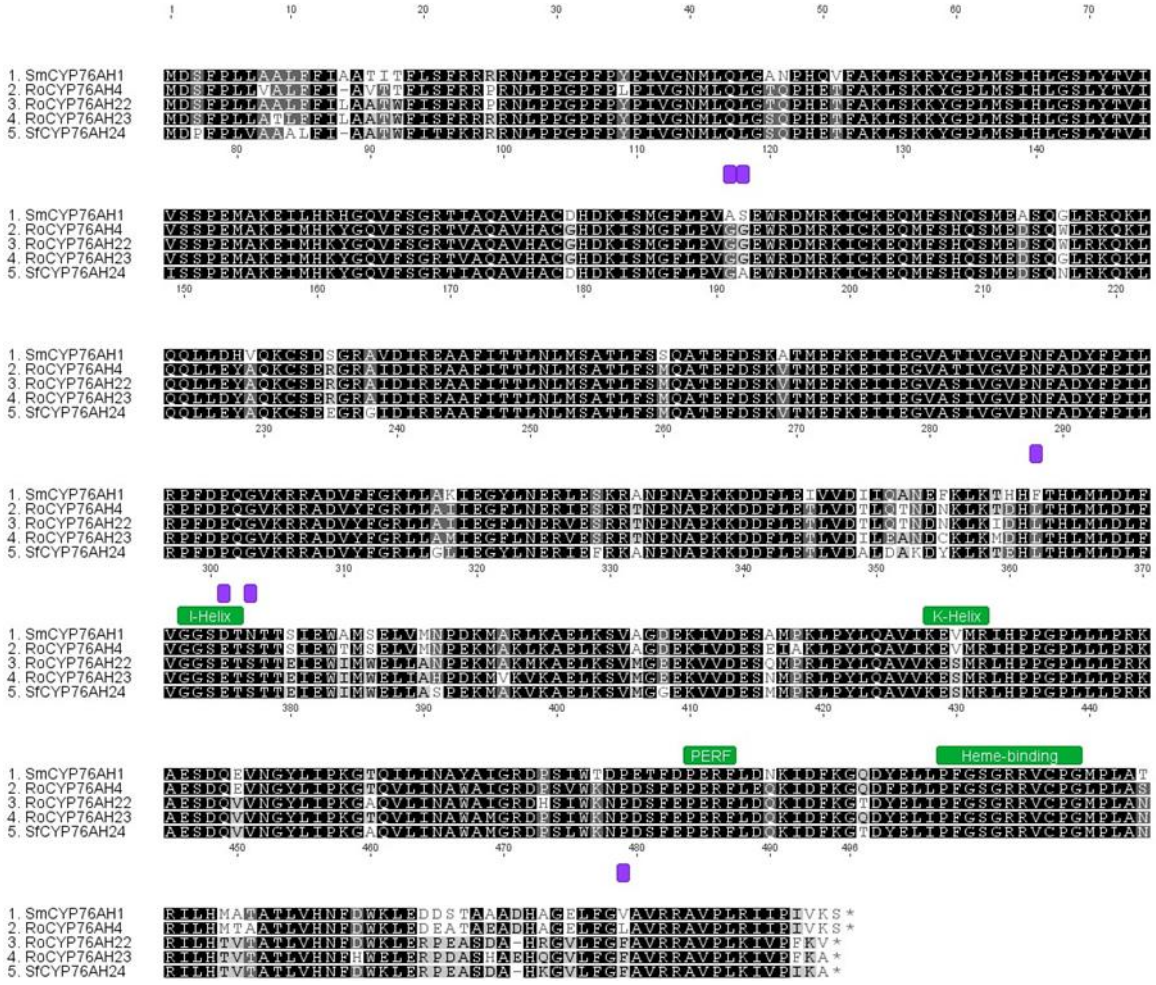

Suppl. Fig. 1 Multiple amino acid sequence alignment of the FS and HFSs. Protein sequences of CYP76AH1 (*S. miltiorrhiza*), CYP76AH24 (SfFS) (*S. fruticosa*), CYP76AH4 and CYP76AH22-23 (RoFS1 and RoFS2) (*R. officinalis*) are given. Conserved CYP domains (green) and amino acids which were mutagenized (purple) are highlighted.

Suppl. Fig. 2 Multiple amino acid sequence alignment of the C20Oxs. CYP76AK6 (*S. fruticosa*) and CYP76AK7-8 (*R. officinalis*) are shown with highlighted conserved CYP domains (green).

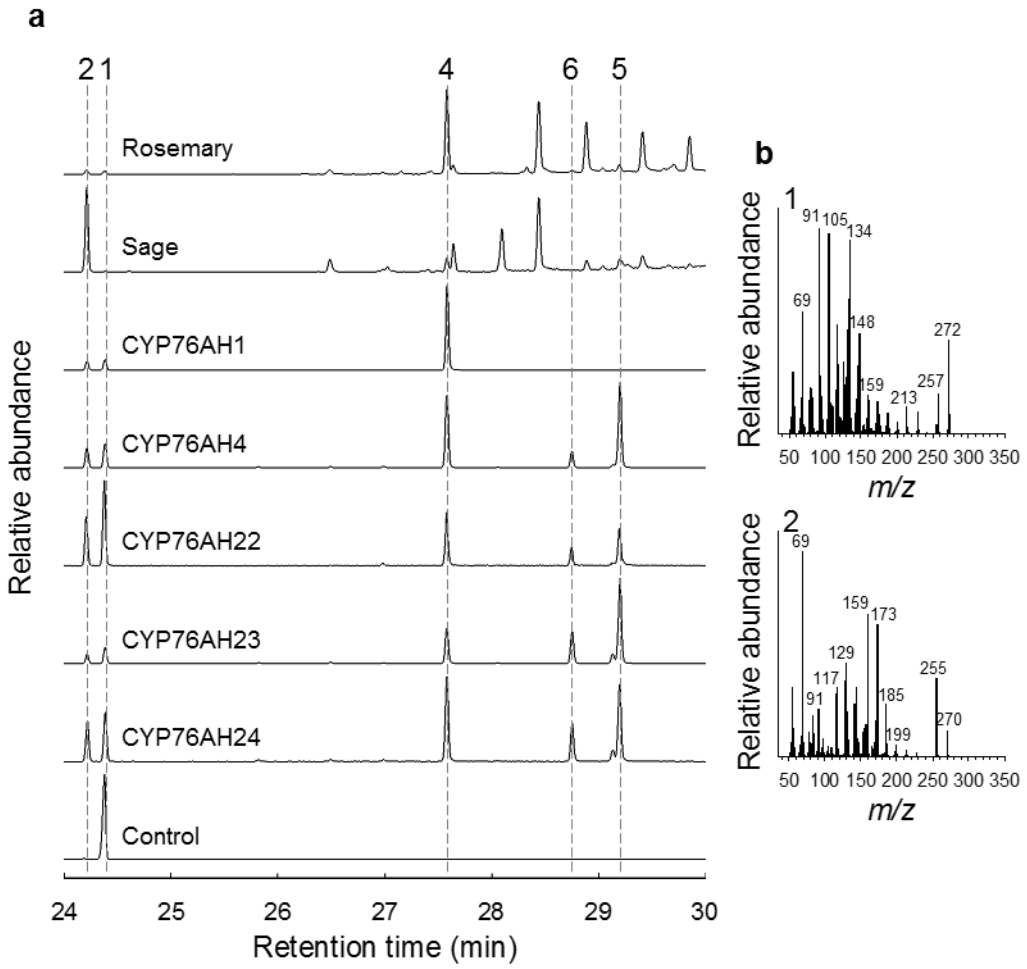

Suppl. Fig. 3 GC-MS analysis of yeast expressing FS and HFS. (**a**) *R. officinalis* and *S. fruticosa* leaf surface extracts, and extracts of yeast strains co-expressing GGPPS, CPS, MiS, ATR1 and indicated CYPs (selected *m/z* signals: 270, 272, 286, 300, 302). Miltiradiene (**1**), abietatriene (**2**), ferruginol (**4**), 11-hydroxyferruginol (**5**) and hydroxyferruginol quinone (**6**). (**b**) EI mass spectra of abietatriene (**1**) and miltiradiene (**2**).

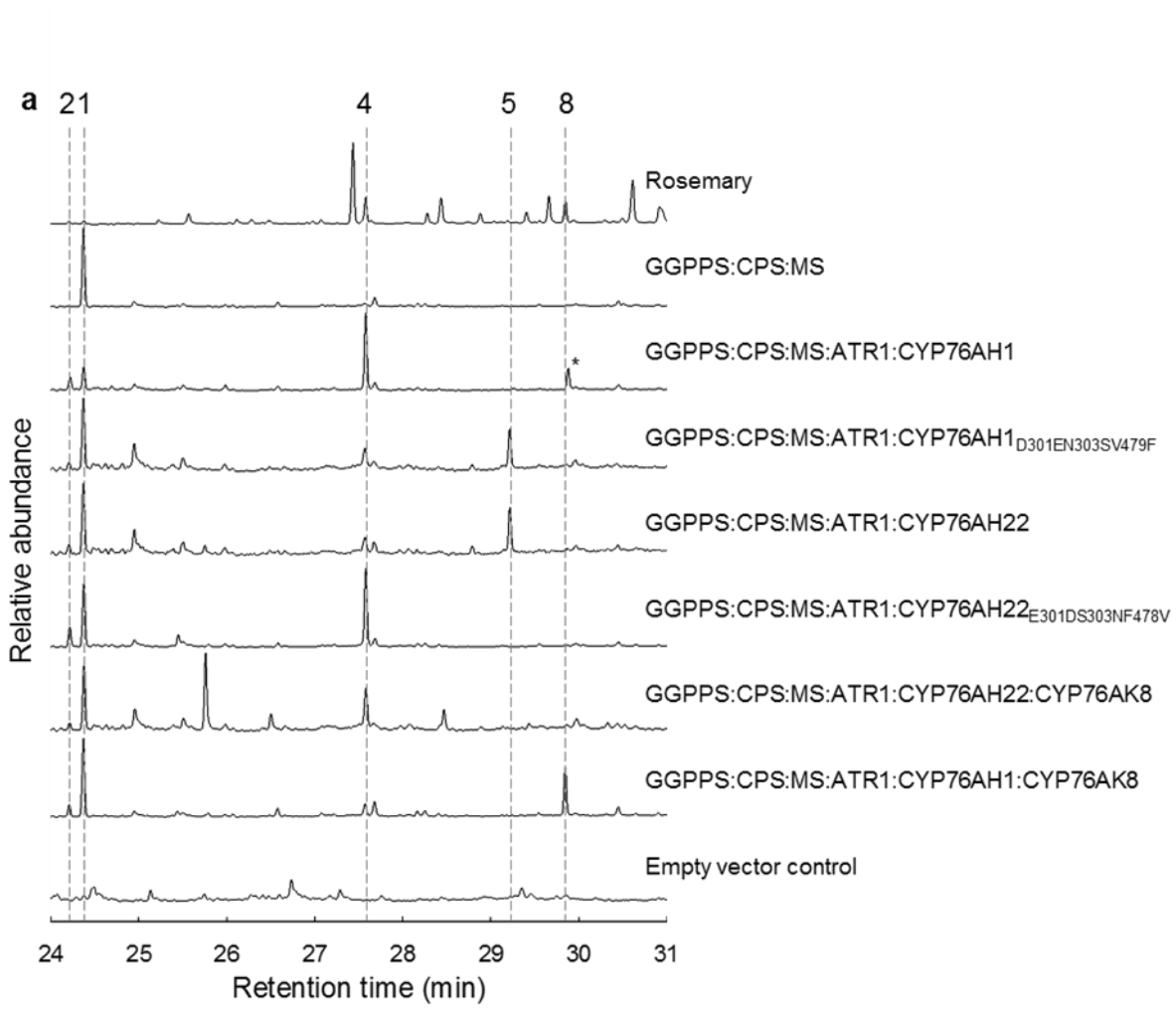
a
2
1
4
5
8
Rosemary
GGPPS:CPS:MS
GGPPS:CPS:MS:ATR1:CYP76AH1
*
GGPPS:CPS:MS:ATR1:CYP76AH1D301EN303SV479F
GGPPS:CPS:MS:ATR1:CYP76AH22
GGPPS:CPS:MS:ATR1:CYP76AH22E301DS303NF478V
GGPPS:CPS:MS:ATR1:CYP76AH22:CYP76AK8
GGPPS:CPS:MS:ATR1:CYP76AH1:CYP76AK8
Empty vector control
Relative abundance
24
25
26
27
28
29
30
31
Retention time (min)

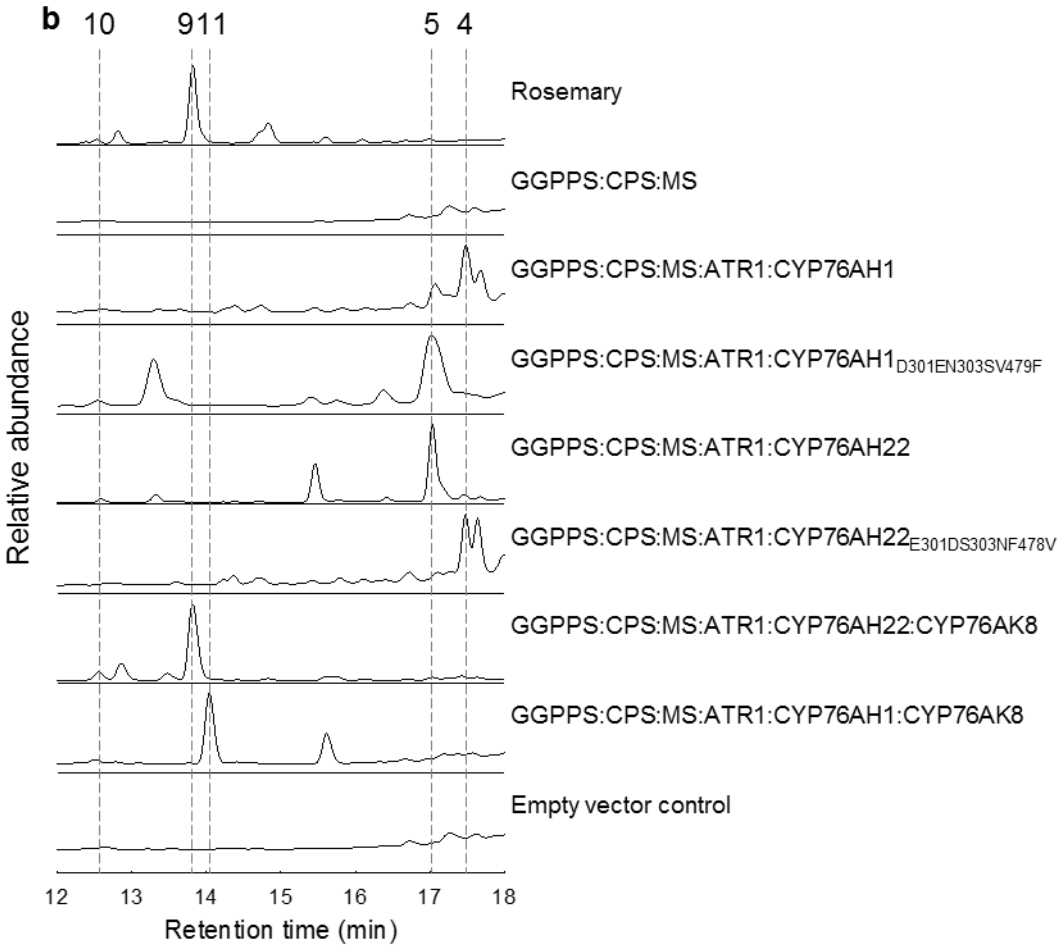

Suppl. Fig. 4 Total ion chromatograms of engineered yeast expressing the indicated enzymes and rosemary leaf surface extracts. (**a**) GC-MS analysis. Miltiradiene (**1**), abietatriene (**2**), ferruginol (**4**), 11-hydroxyferruginol (**5**) and pisiferal (**8**). (**b**) LC-MS analysis. CA (**9**), CO (**10**) and PA (**11**). *Originates from yeast.

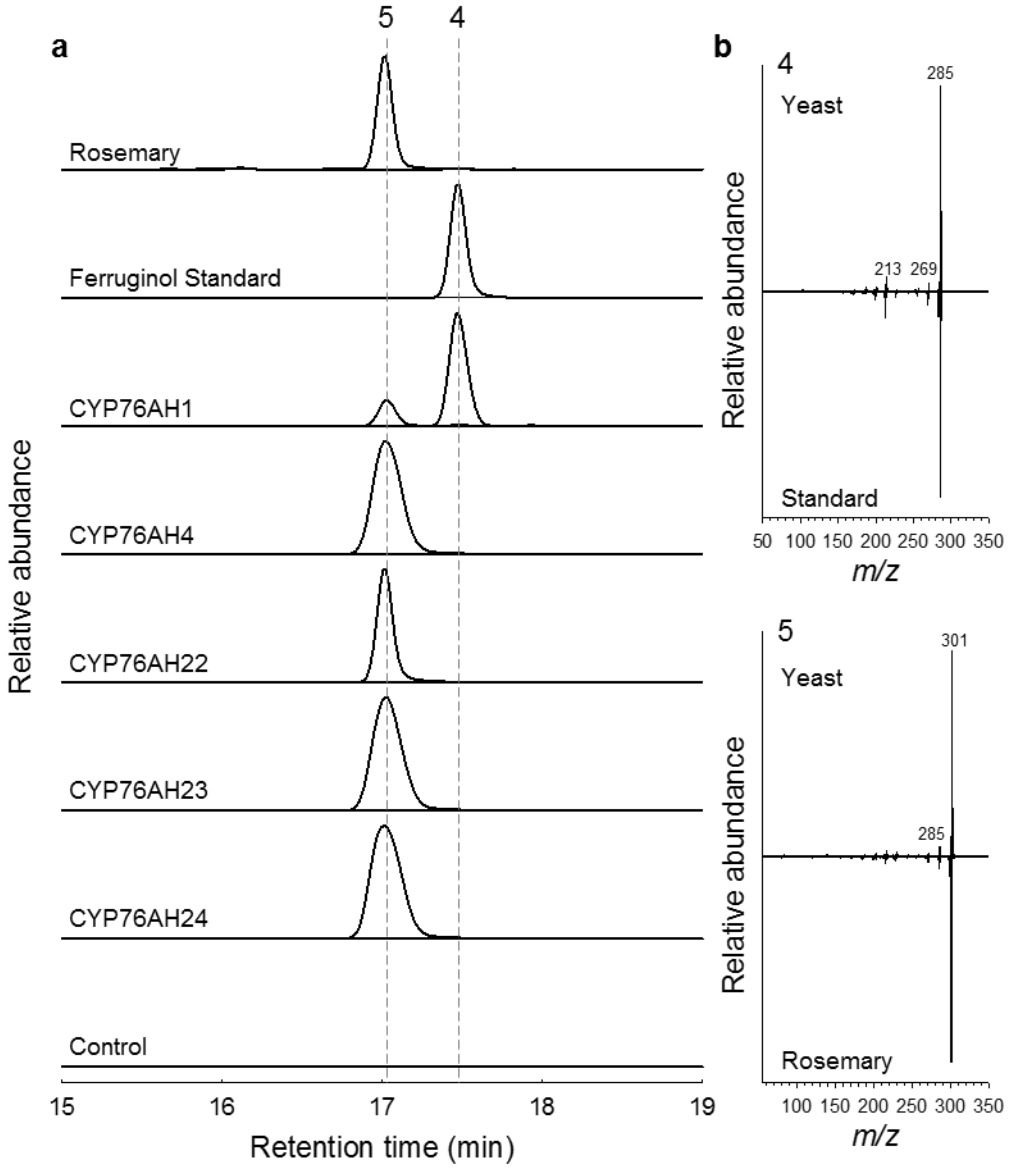

Suppl. Fig. 5 LC-MS analysis of yeast expressing FS and HFS. (**a**) Total ion chromatogram of leaf surface extracts from rosemary and sage, and of extracts from yeast co-expressing GGPPS, CPS, MiS, ATR1 and indicated CYPs. Ferruginol (**4**) and 11-hydroxyferruginol (5). (Selected *m/z* signals: 285.221, 301.217) (**b**) ESI mass spectra of ferruginol (**4**) 11-hydroxyferruginol (**5**) from yeast and rosemary.

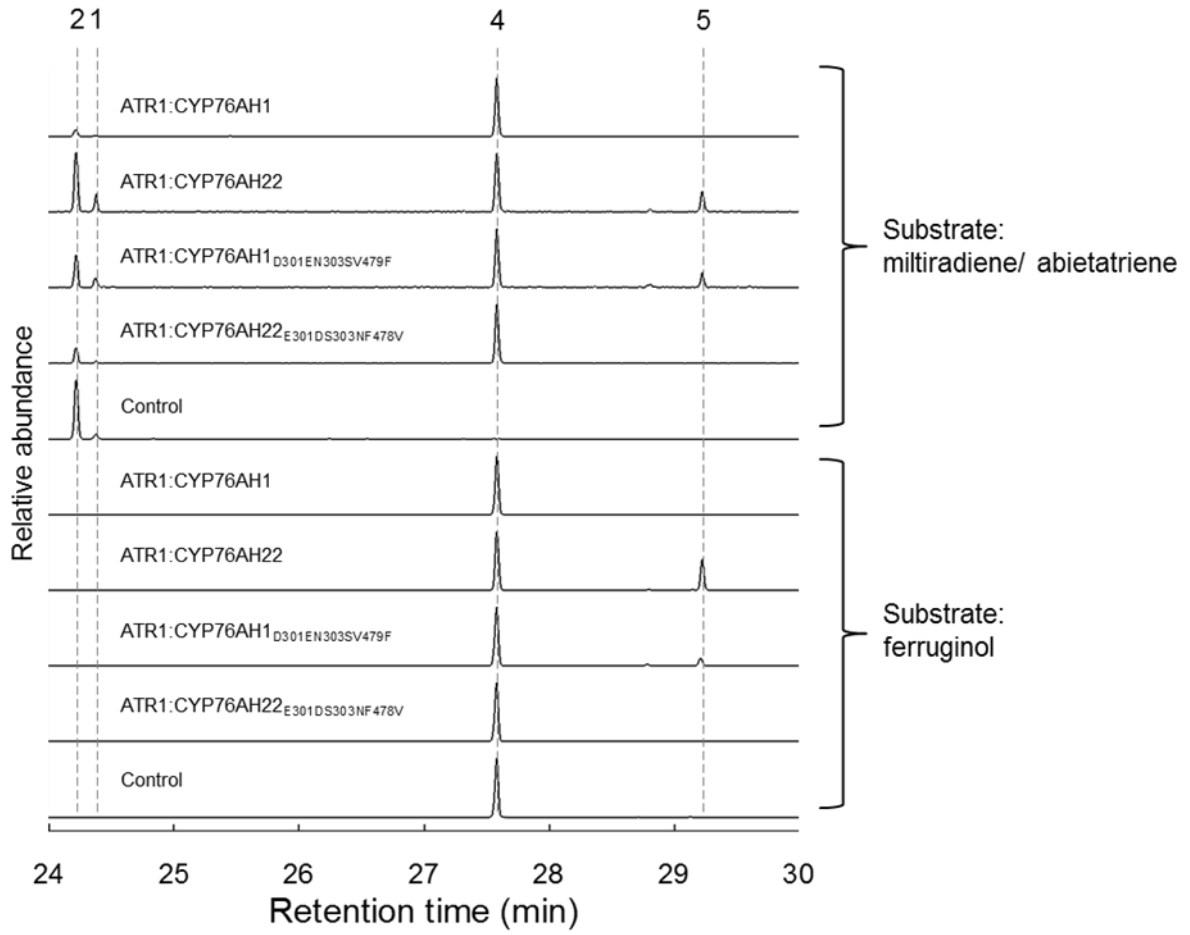

Suppl. Fig. 6 GC-MS analysis (selected *m/z* signals: 270, 272, 286, 302) of *in vitro* enzyme assays from microsomal preparations. Indicated enzymes were incubated with the given substrates. Miltiradiene (**1**), abietatriene (**2**), ferruginol (**4**) and 11-hydroxyferruginol (**5**).

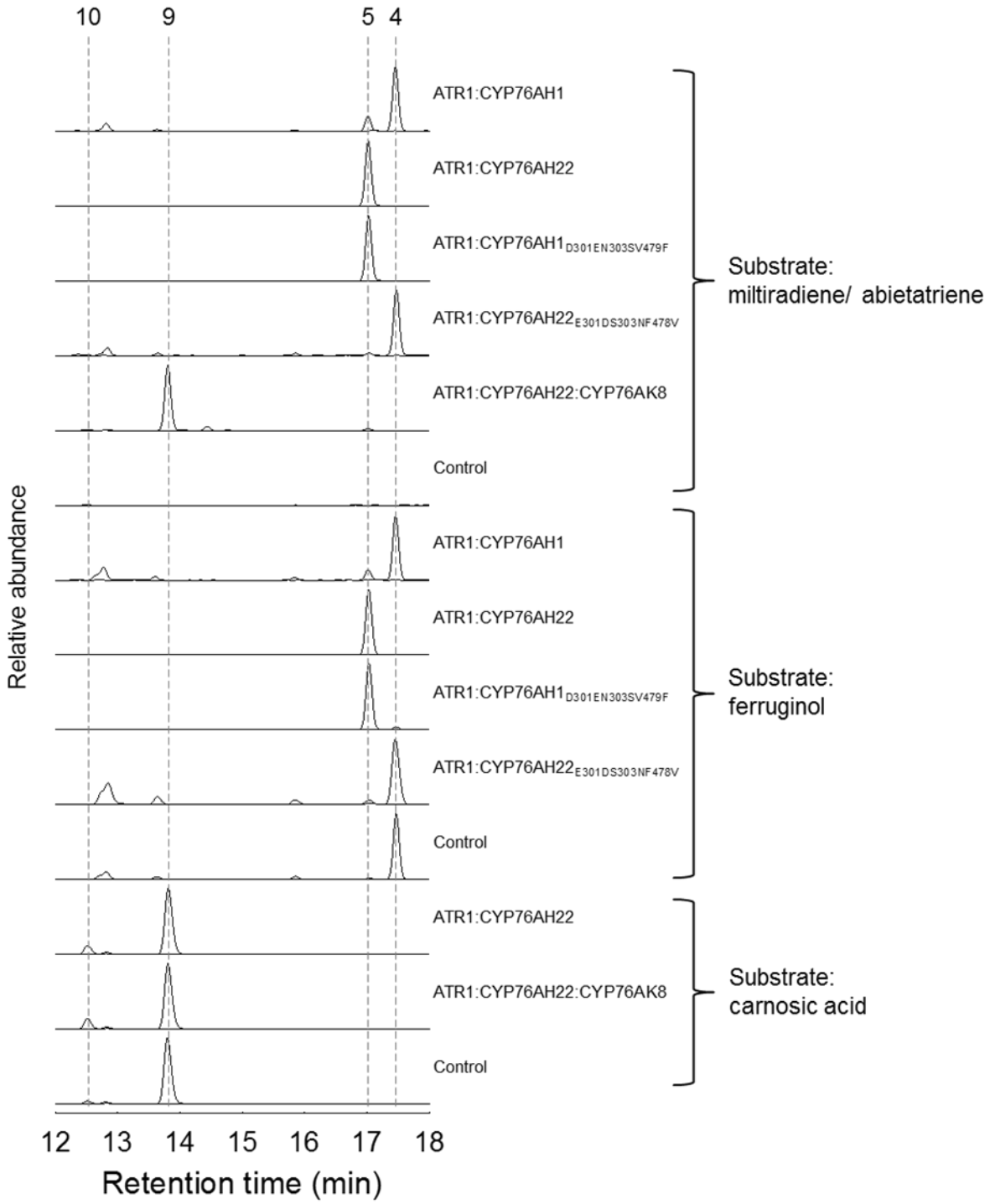

Suppl. Fig. 7 LC-MS analysis (selected *m/z* signals in the negative mode: 285.221, 301.217, 331.191, 329.175) of *in vitro* enzyme assays from microsomal preparations of indicated enzymes. The assays with the given enzymes were incubated with different substrates. Ferruginol (**4**), 11-hydroxyferruginol (**5**), CA (**9**) and CO (**10**). Note: Ferruginol is poorly detected by LC-MS, while 11-hydroxyferruginol is poorly detected by GC-MS.

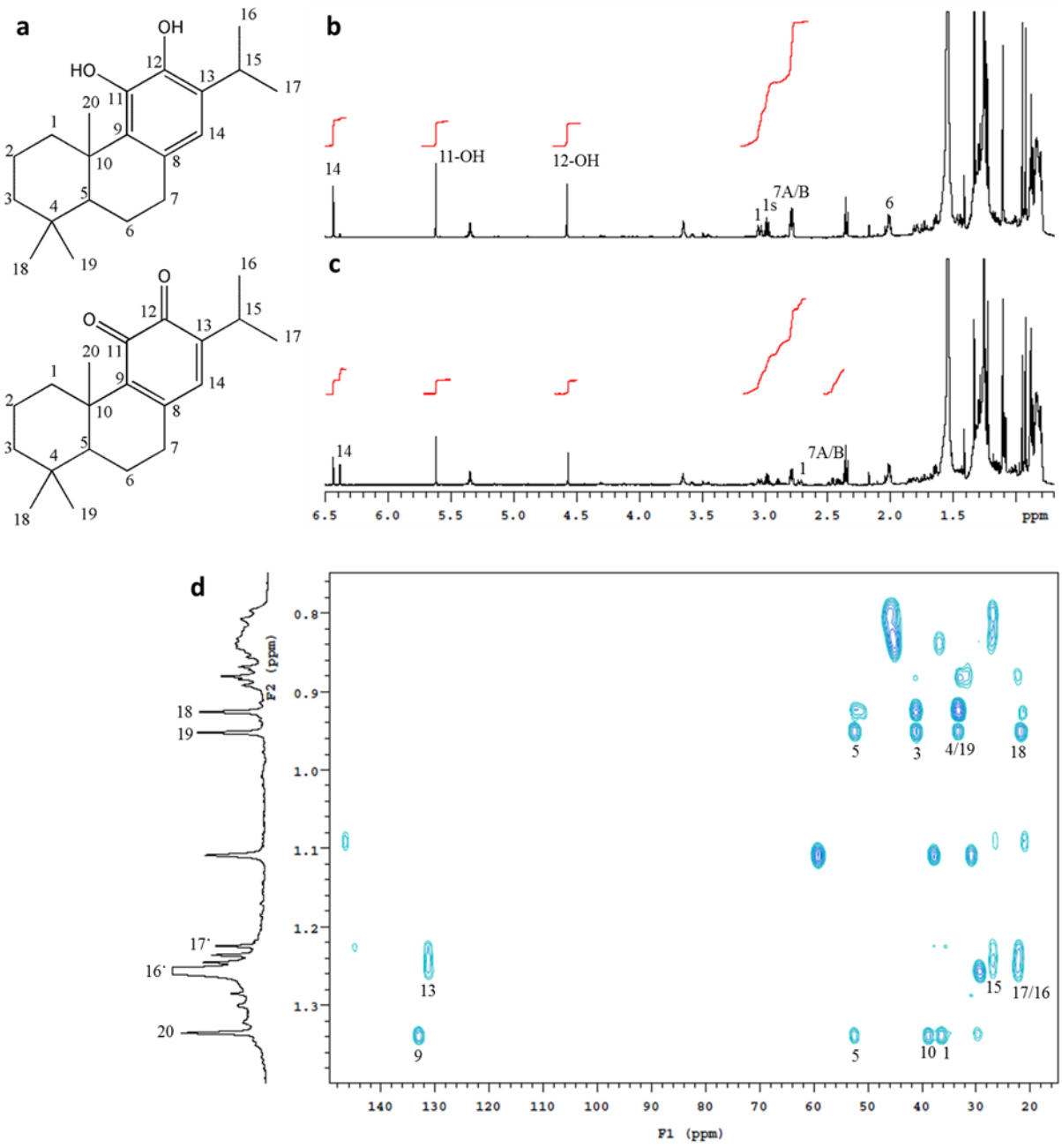
a
b
c
d
OH
HO
O
11-OH
12-OH
7A/B
14
6
ppm
F2 (ppm)
F1 (ppm)
18
19
17'
16'
20
13
9
5
3
4/19
15
17/16
10
1

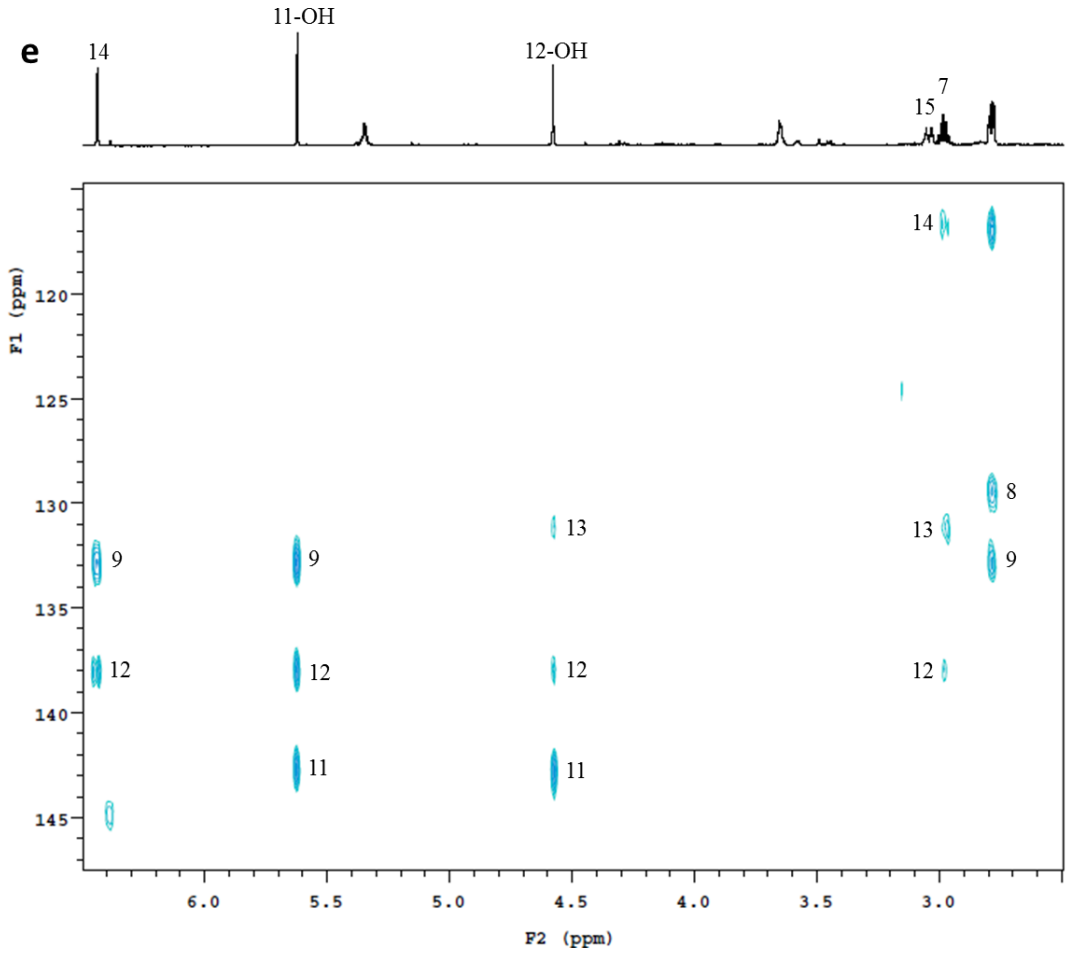
e
11-OH
14
12-OH
7
15
F1 (ppm)
F2 (ppm)
14
8
13
9
12
11

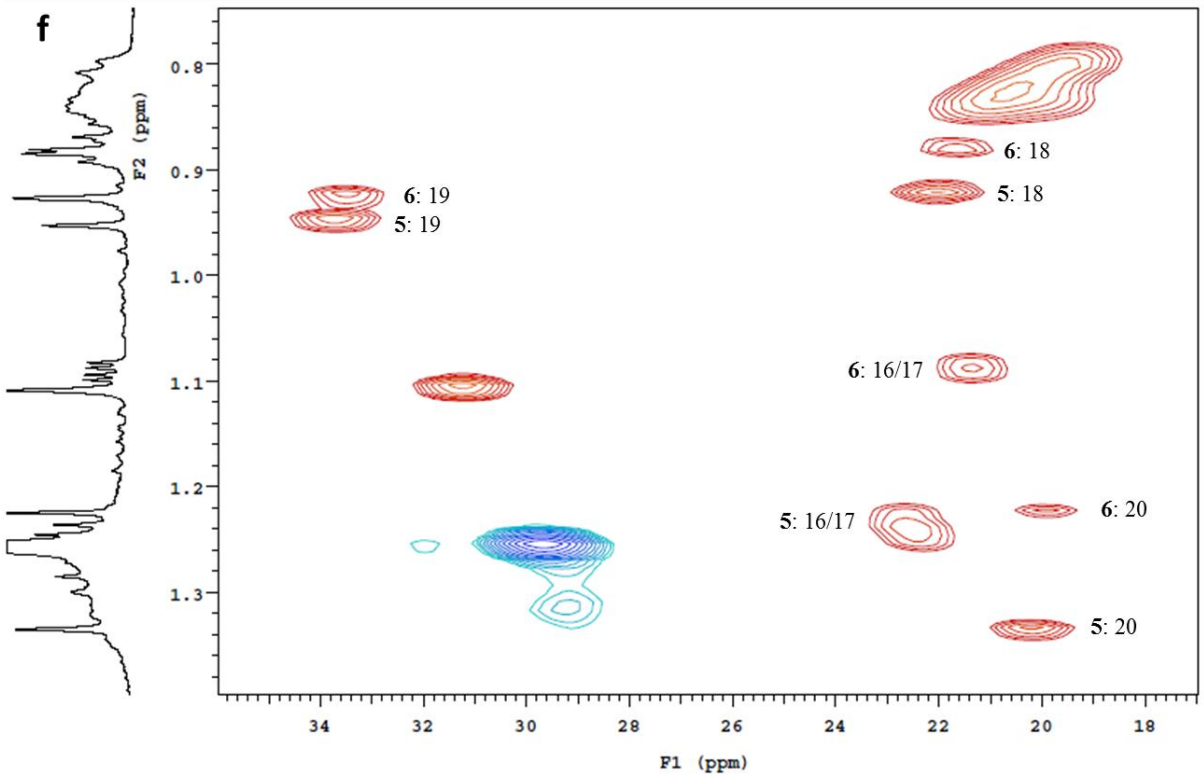
f
F2 (ppm)
F1 (ppm)
6: 18
5: 18
6: 19
5: 19
6: 16/17
5: 16/17
6: 20
5: 20

Suppl. Fig. 8 NMR analysis of 11-hydroxyferruginol. (**a**) Structures of 11-hydroxyferruginol and hydroxyferruginol quinone with labeled carbon atoms. (**b**) ^{1}H NMR spectrum of 11-hydroxyferruginol immediately after dissolving in $CDCl_3$. (**c**) ^{1}H NMR spectrum of 11-hydroxyferruginol 24 h after dissolving in $CDCl_3$ showing signals of 11-hydroxyferruginol and hydroxyferruginol quinone. (**d**) Labeled: HMB correlations via $^{2}J_{CH}$ and $^{3}J_{CH}$ of methyl group proton signals of 11-hydroxyferruginol. Vertical trace: ^{1}H 1D NMR spectrum. (**e**) Low-field part of the HMBC spectrum of 11-hydroxyferruginol. Horizontal trace: ^{1}H 1D NMR spectrum. (**f**) Methyl group region of the HSQC spectrum of 11-hydroxyferruginol (**5**) after partial conversion to hydroxyferruginol quinone (**6**). Vertical trace: ^{1}H 1D NMR spectrum.

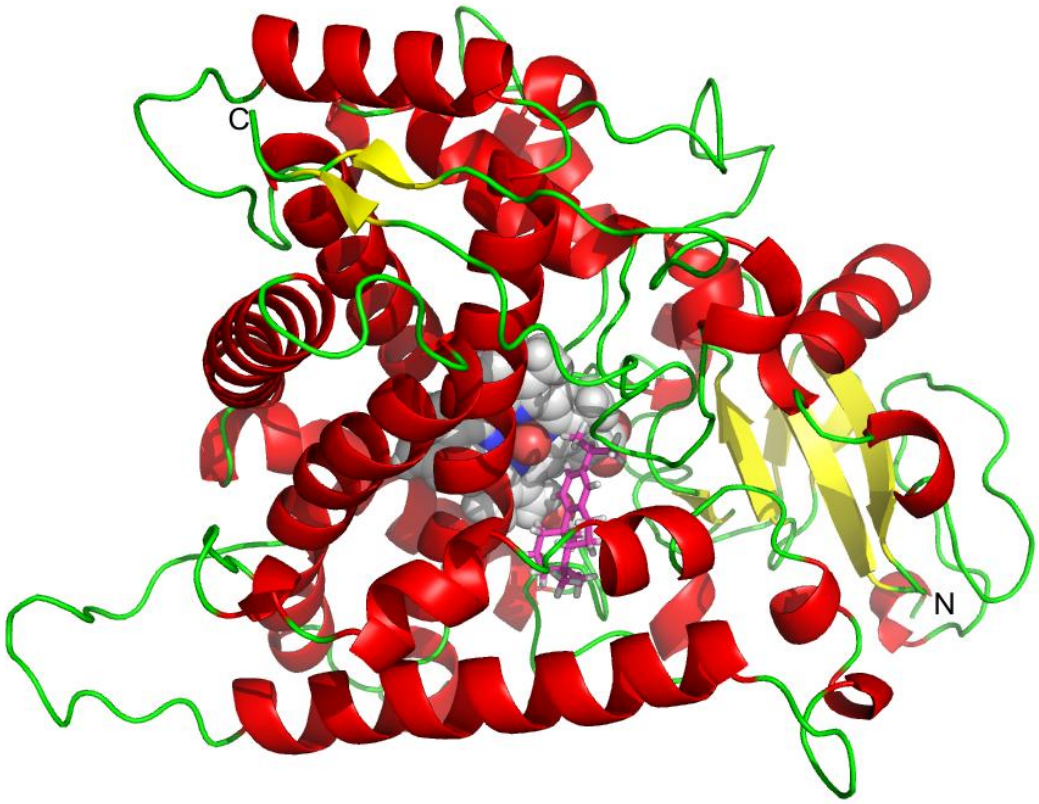

Suppl. Fig. 9 3D-model of CYP76AH1 as representative of all other FS and HFSs. The heme (space fill representation with orange colored iron ion) and the substrate (magenta carbon atoms) are located in the center.

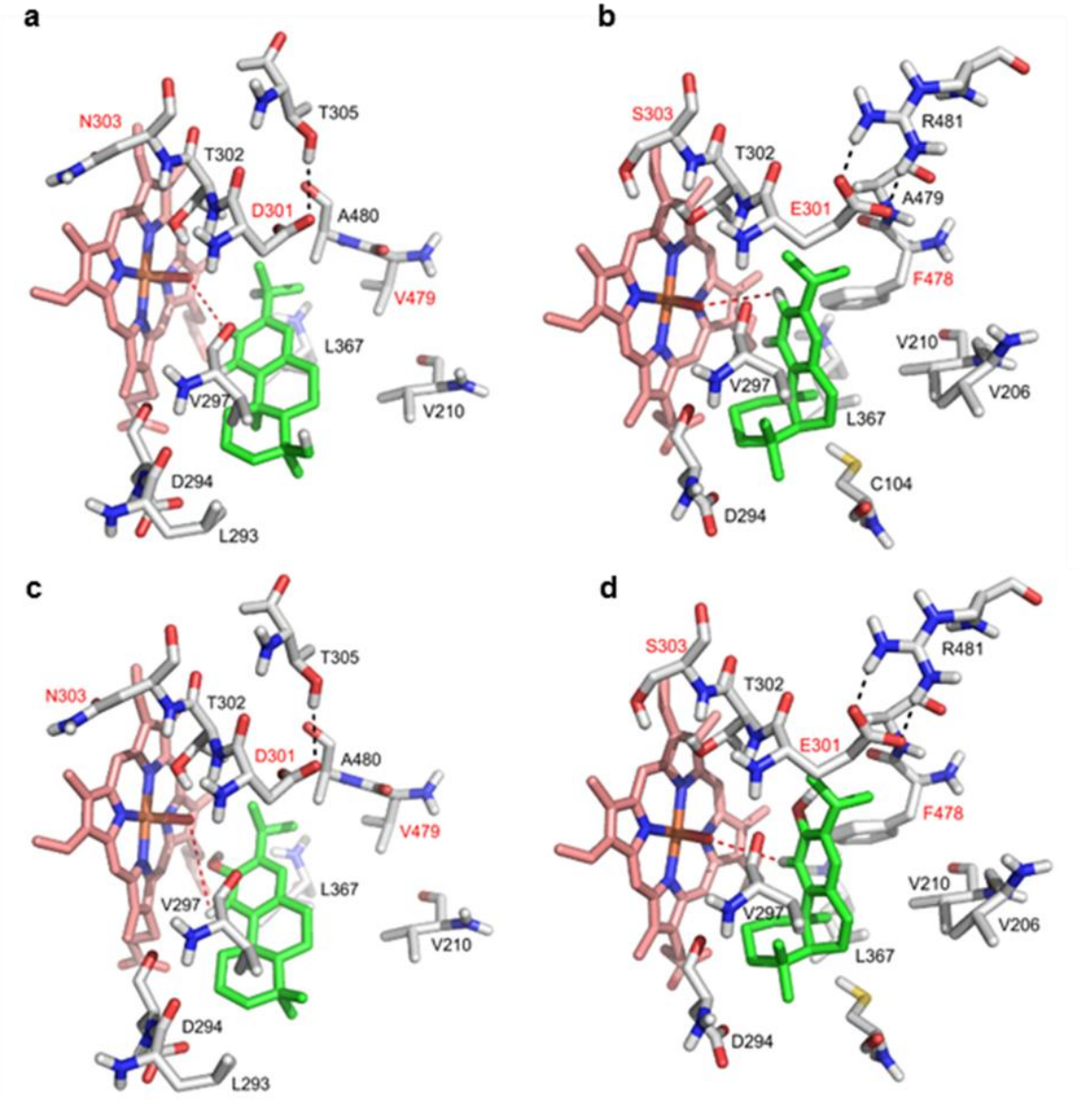

Suppl. Fig. 10 3D-model of the active sites of CYP76AH1 and CYP76AH22 with bound substrate (green carbon atoms) and heme (orange carbon atoms). Red labelled amino acid residues influence the product specificity which was proven by site directed mutagenesis. In the active center of the enzymes the substrate is mainly recognized by hydrophobic amino acid residues (V297, L367, V210 and V479 or F478, respectively). Active sites of (**a**) CYP76AH1 and (**b**) of CYP76AH22 with bound abietatriene. The hydrogen atom of the aromatic ring system of the substrate is abstracted by the reactive oxygen atom bound to the iron ion. They are in closest proximity (3.6 Å in CYP76AH1 and 3.4 Å in CYP76AH22, red dashed line) which supports the oxidation reaction. (**c**) Active site of CYP76AH1 with bound ferruginol. The substrate cannot be efficiently oxidized because its distance to the reactive oxygen atom is 4.6 Å and therefore too far to support oxidation at C12 (red dashed line). In contrast, the substitution of V479 in CYP76AH1 by the more bulky F478 in CYP76AH22 leads to a slightly different docking arrangement of ferruginol (**d**). Therefore, the hydrogen atom at C12 can be abstracted by the reactive oxygen atom which is in a distance of 3.1 Å.

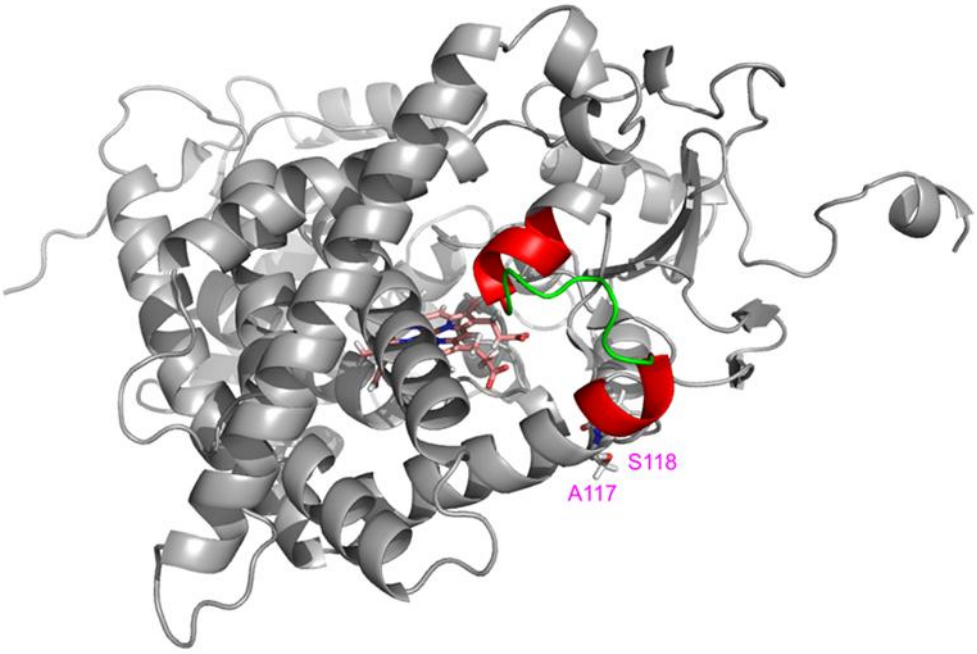

Suppl. Fig. 11 3D-model of CYP76AH1 with bound heme in the center. Labelled amino acids A117 and S118 are distinct from those in HFS. They may influence the secondary structure in the colored region and restrict access to the active site cleft.

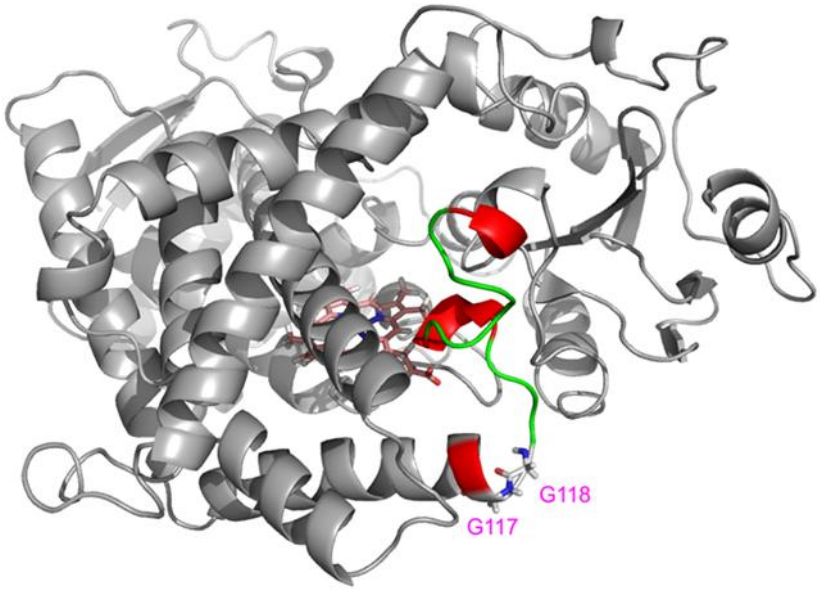

Suppl. Fig. 12 3D-model of CYP76AH22 with bound heme in the center. Labelled amino acids G117 and G118 disturb the α-helix present in CYP76AH1 and influence the secondary structure in the highlighted region.

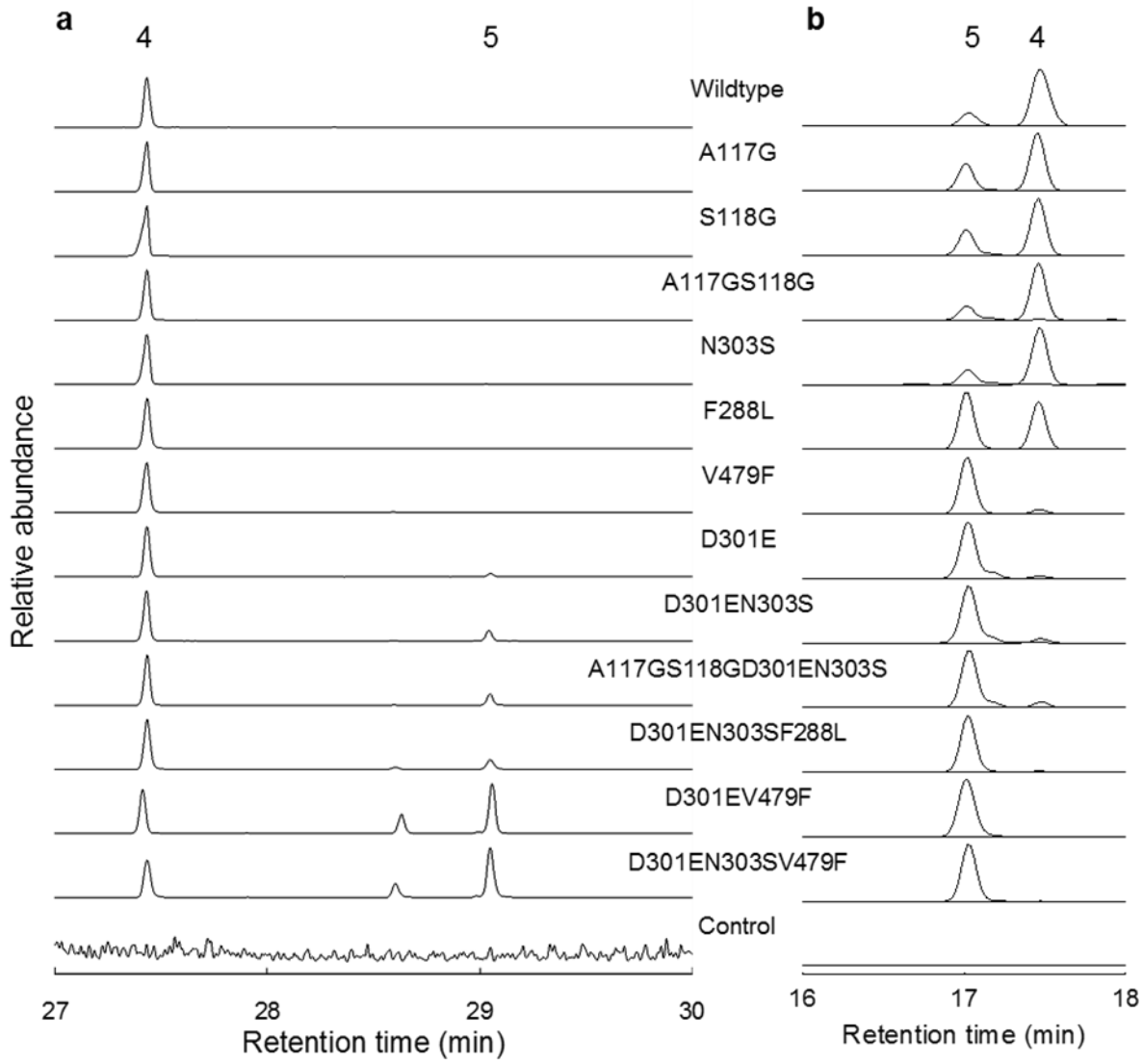

Suppl. Fig. 13 Chromatographic analysis of extracts from yeast strains expressing wild type and mutagenized CYP76AH1. They were co-expressed in yeast with GGPPS, CPS, MiS and ATR1. Part of the chromatograms showing elution of ferruginol (**4**) and 11-hydroxyferruginol (**5**) from (**a**) GC-MS (selected *m/z* signals: 286, 300, 302) and (**b**) LC-MS analysis (selected *m/z* signals in the negative mode: 285.221, 301.217) are given.

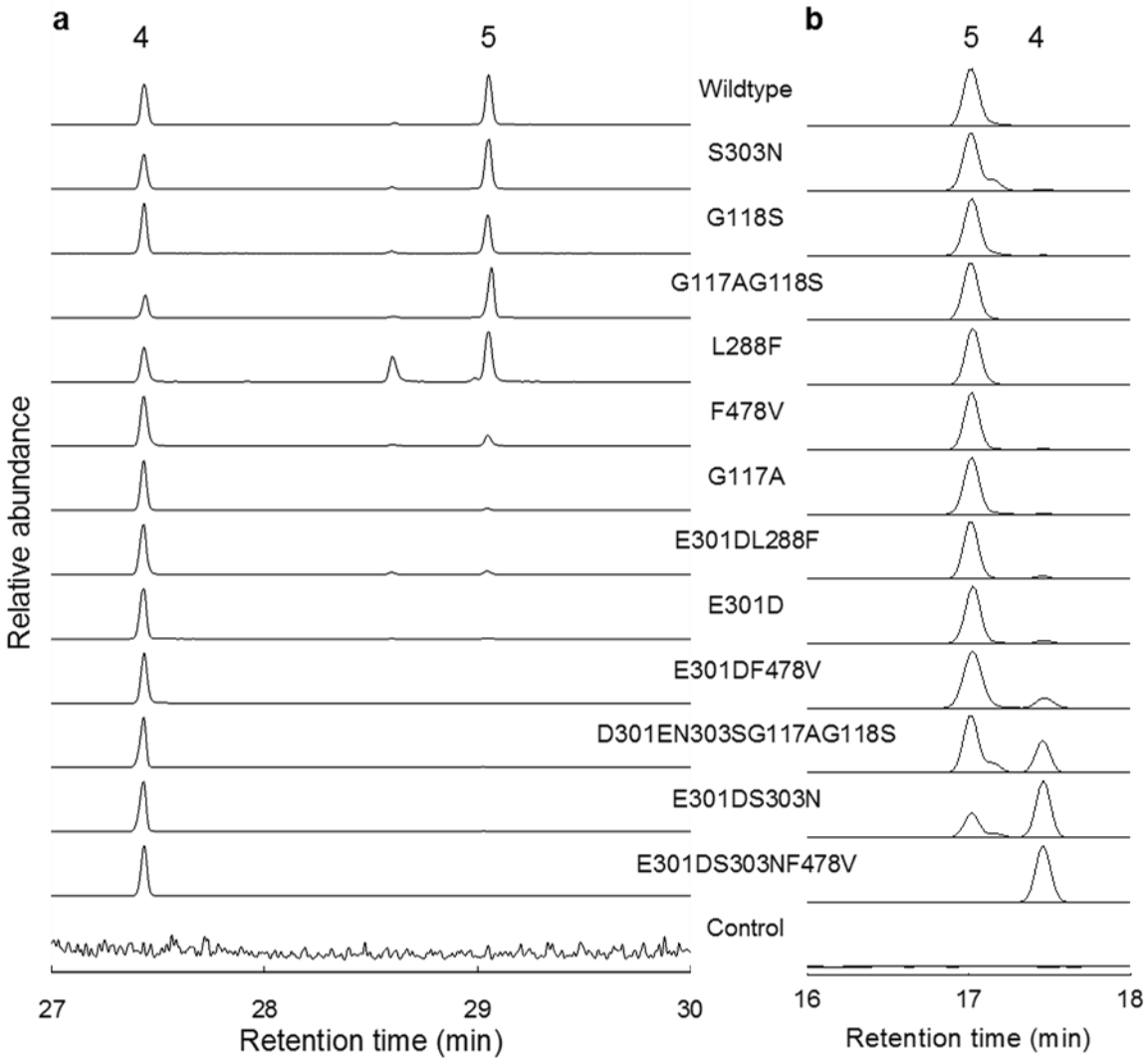

Suppl. Fig. 14 Chromatographic analysis of extracts from yeast strains expressing wild type and mutagenized CYP76AH22. They were co-expressed in yeast with GGPPS, CPS, MiS and ATR1. Part of the chromatograms showing elution of ferruginol (**4**) and 11-hydroxyferruginol (**5**) from (**a**) GC-MS (selected *m/z* signals: 286, 300, 302) and (**b**) LC-MS analysis (selected *m/z* signals in the negative mode: 285.221, 301.217) are given.

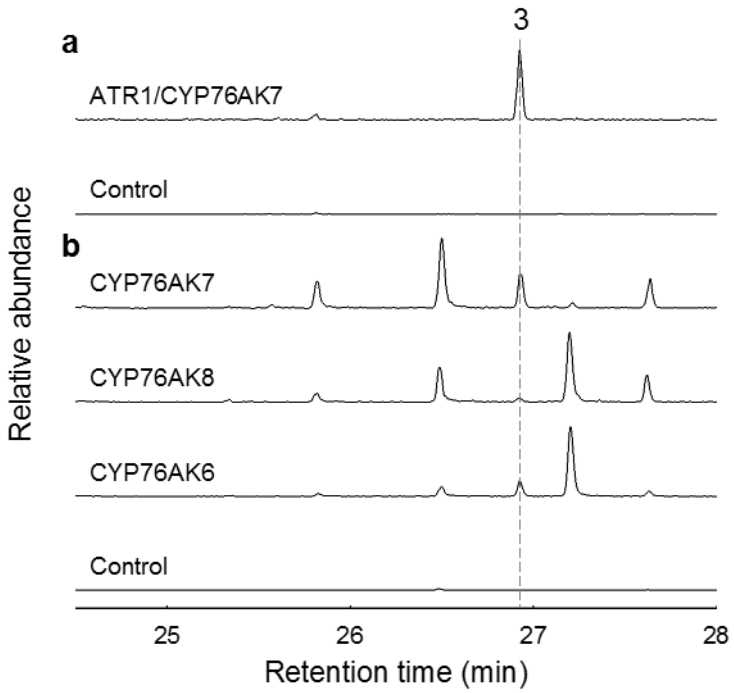

Suppl. Fig. 15 GC-MS analysis of C20Ox expression in yeast and *N. benthamiana* producing miltiradiene/abietatriene. Part of the GC-MS chromatogram containing miltiradien-20-al (**3**) is shown (selected *m/z* signal: 257). (**a**) Transient co-expression of CPS, MiS and indicated enzymes in *N. benthamiana*. (**b**) Co-expression of GGPPS, CPS, MiS, ATR1 and indicated CYPs in yeast.

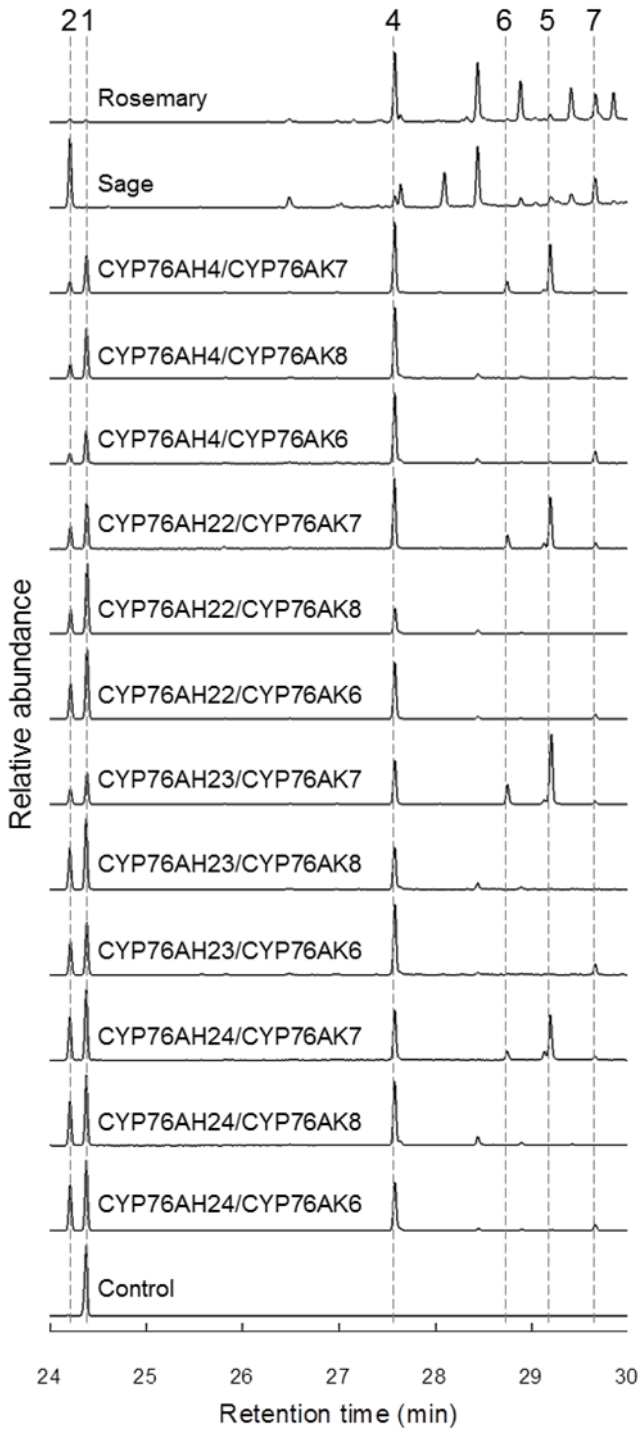

Suppl. Fig. 16 GC-MS analysis of yeast strains co-expressing GGPPS, CPS, MiS, ATR1 and indicated CYPs. (Selected *m/z* signals: 270,272, 286, 300, 302, 316). Miltiradiene (**1**), abietatriene (**2**), ferruginol (**4**), 11-hydroxyferruginol (**5**), hydroxyferruginol quinone (**6**) and carnosaldehyde (**7**).

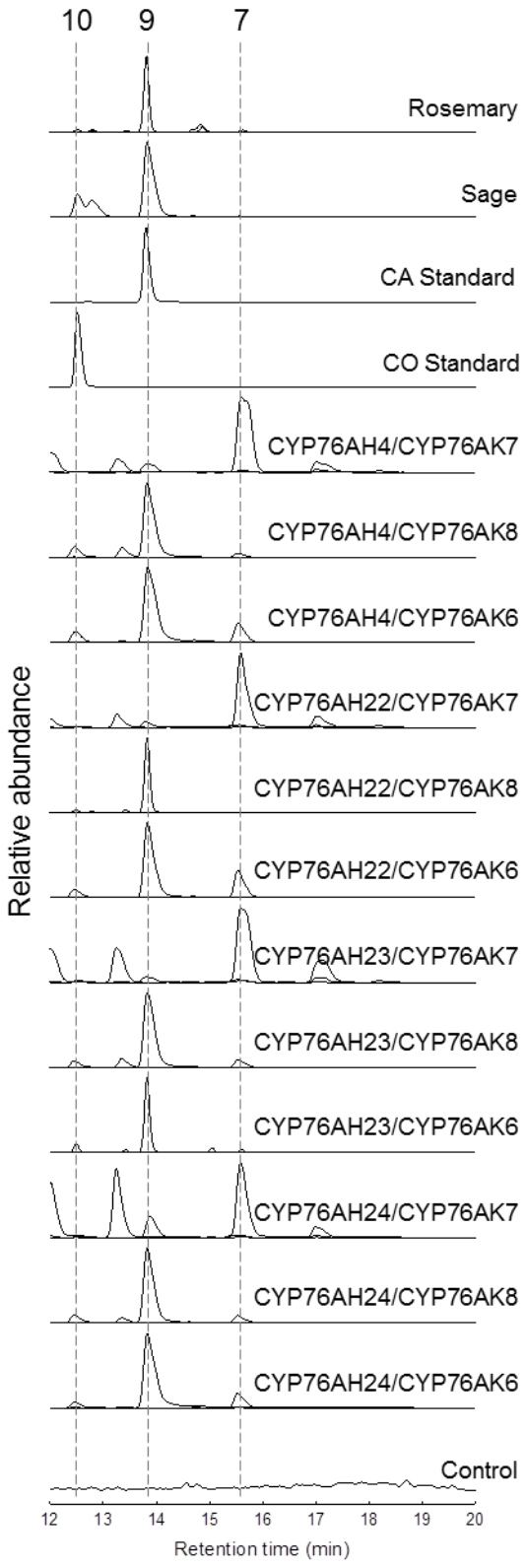

Suppl. Fig. 17 LC-MS analysis of extracts obtained from rosemary and sage leaves, authentic standards and yeast strains expressing GGPPS, CPS, MiS, ATR1 and indicated CYPs. (Selected *m/z* signals in the negative mode: 315.196, 331.191, 329.175). Carnosaldehyde (**7**), CA (**9**) and CO (**10**).

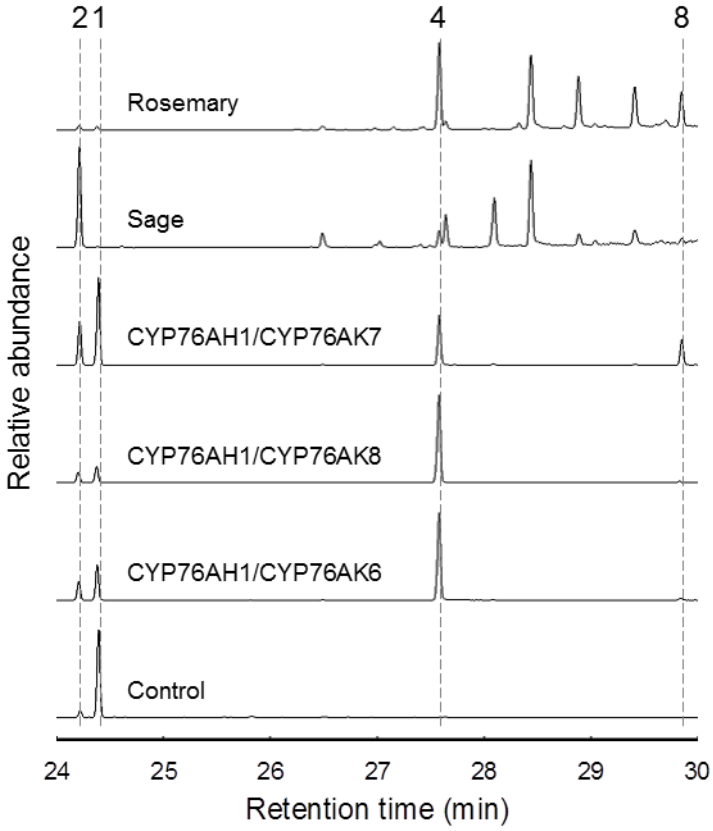

Suppl. Fig. 18 Part of the GC-MS chromatogram of extracts of rosemary and sage as well as of yeast strains co-expressing GGPPS, CPS, MiS, ATR1 and indicated CYPs. (Selected *m/z* signals: 270, 272, 286, 300). Miltiradiene (**1**), abietatriene (**2**), ferruginol (**4**) and pisiferal (**8**).

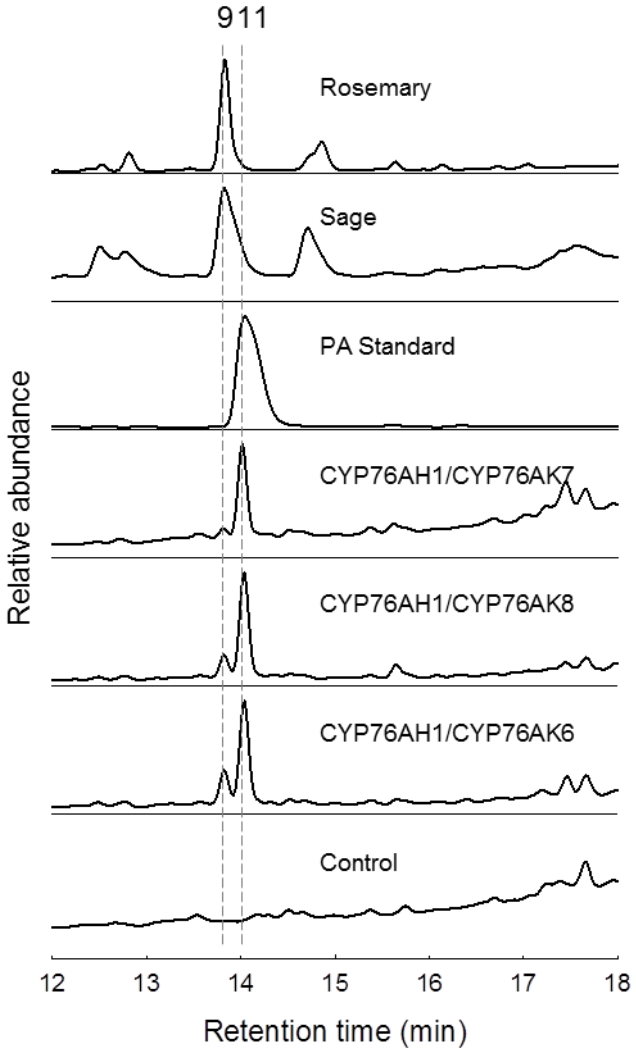

Suppl. Fig. 19 LC-MS total ion chromatogram of extracts from rosemary, sage and from yeast strains co-expressing GGPPS, CPS, MiS, ATR1 and indicated CYPs. CA (**9**) and PA (**11**).

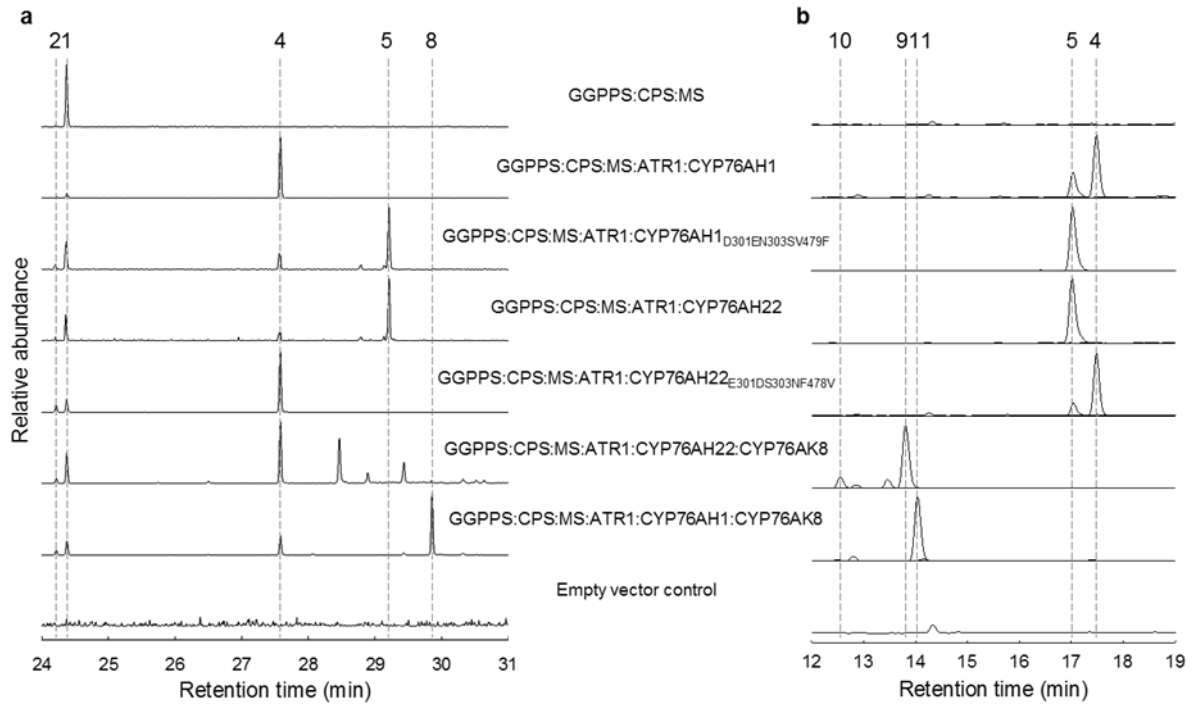

Suppl. Fig. 20 Chromatographic analysis of engineered yeast strains which were used for absolute NMR quantification. (**a**) GC-MS analysis of indicated strains (selected *m/z* signals: 270, 272, 286, 300, 302, 316). (**b**) LC-MS analysis of yeast strains expressing the indicated enzymes (selected *m/z* signals in the negative mode: 285.221, 301.217, 315.196, 331.191, 329.175). Miltiradiene (**1**), abietatriene (**2**), ferruginol (**4**), 11-hydroxyferruginol (**5**), pisiferal (**8**), CA (**9**), CO (**10**) and PA (**11**).

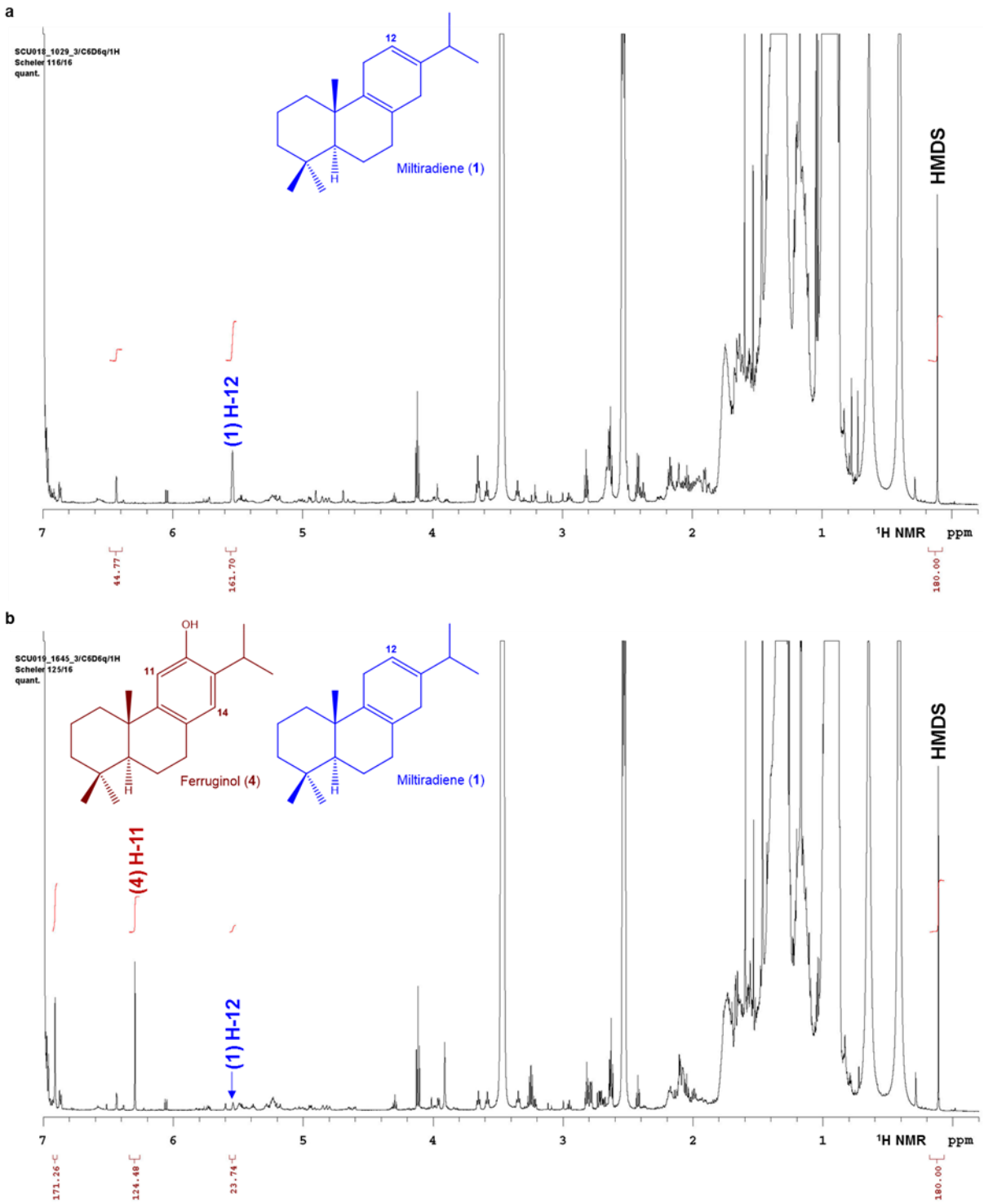
a
SCU018_1029_3/C6D6q/1H
Scheler 116/16
quant.
12
Miltiradiene (1)
HMDS
(1) H-12
7
6
5
4
3
2
1
¹H NMR ppm
44.77
161.70
180.00
b
SCU019_1645_3/C6D6q/1H
Scheler 125/16
quant.
OH
11
14
Ferruginol (4)
12
Miltiradiene (1)
HMDS
(4) H-11
(1) H-12
7
6
5
4
3
2
1
¹H NMR ppm
171.26
124.48
23.74
180.00

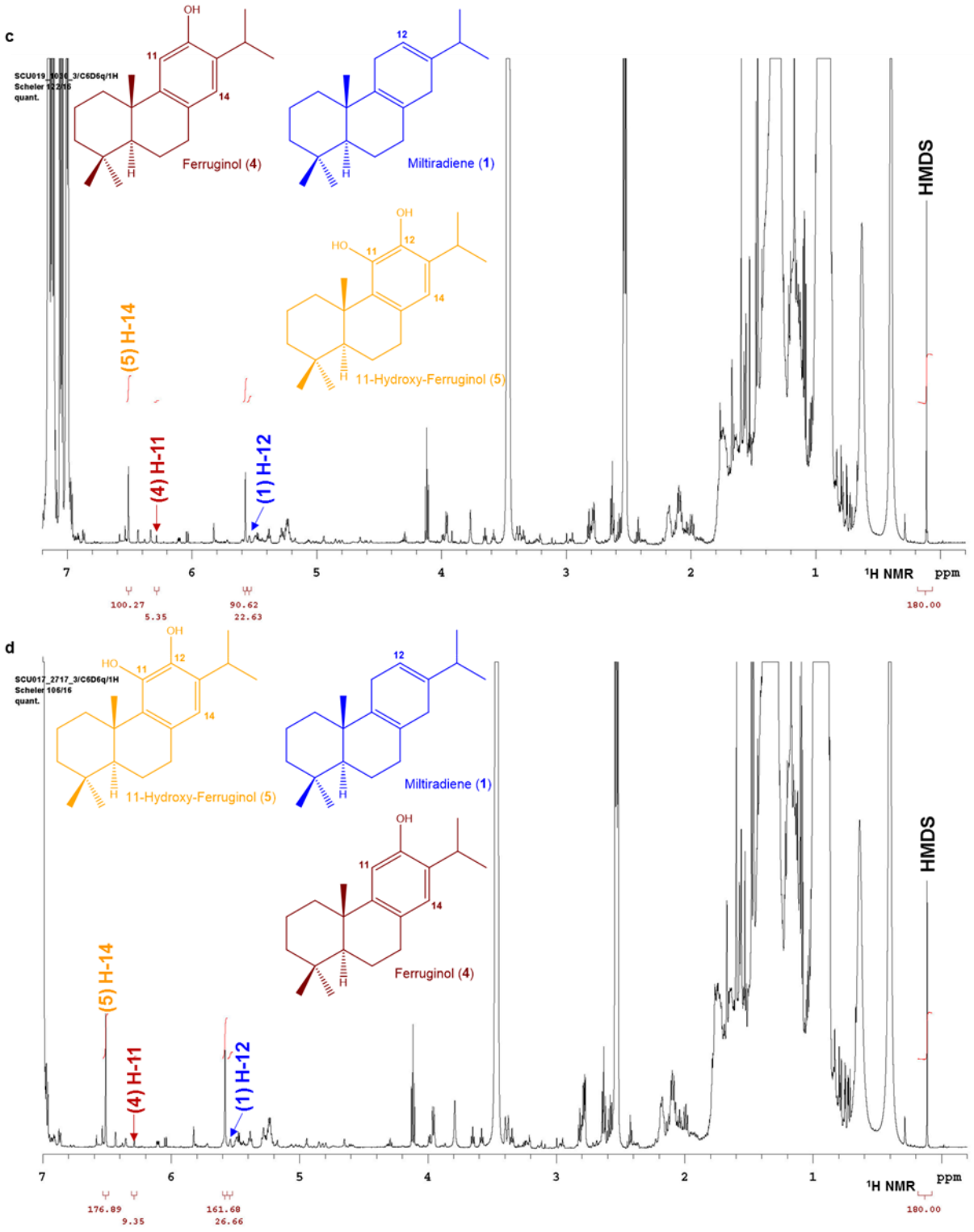
c
Ferruginol (4)
Miltiradiene (1)
11-Hydroxy-Ferruginol (5)
(5) H-14
(4) H-11
(1) H-12
HMDS
¹H NMR ppm
d
11-Hydroxy-Ferruginol (5)
Miltiradiene (1)
Ferruginol (4)
(5) H-14
(4) H-11
(1) H-12
HMDS
¹H NMR ppm

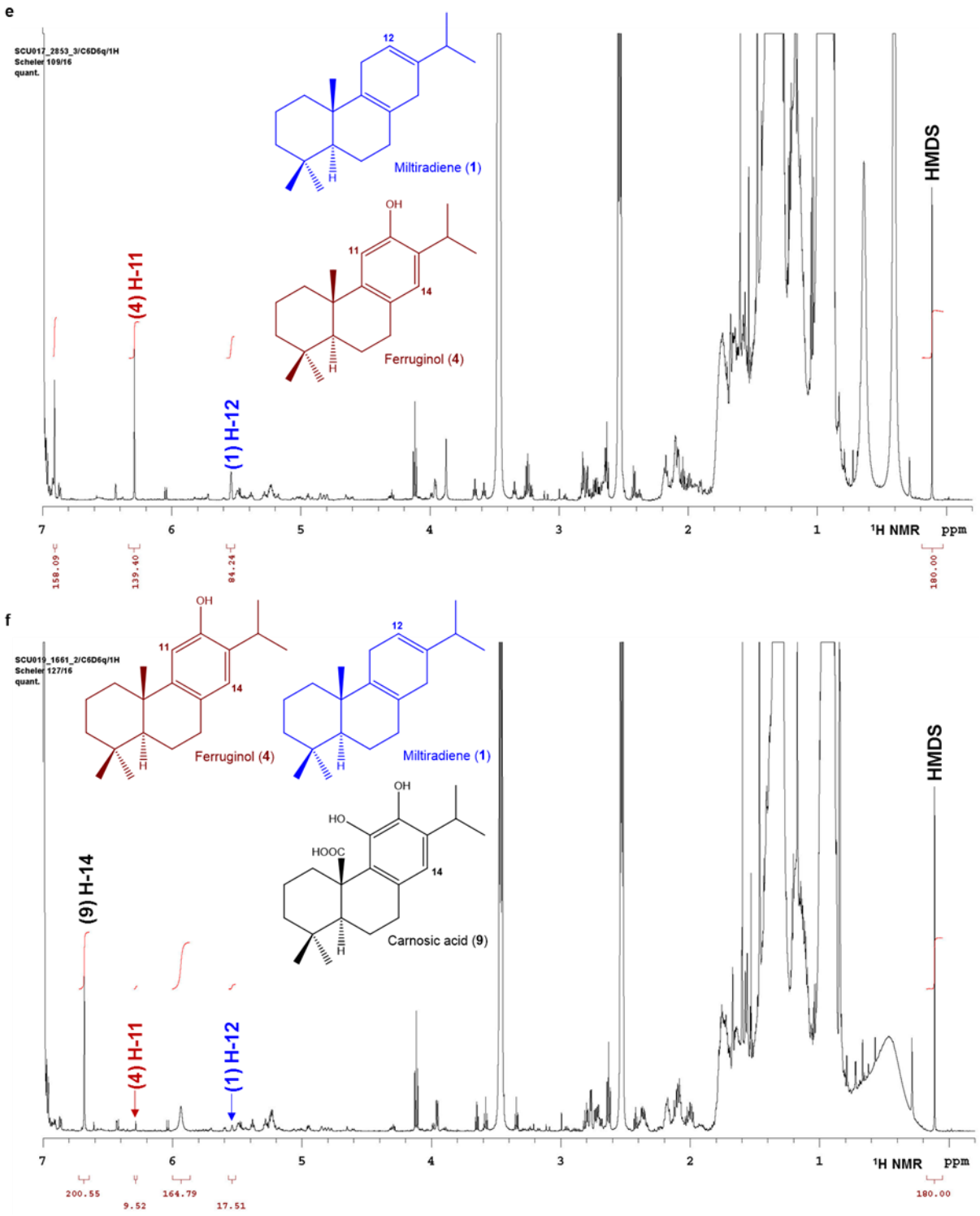
e
SCU017_2853_3/C6D6q/1H
Scheler 109/16
quant.
12
Miltiradiene (1)
OH
11
14
Ferruginol (4)
(4) H-11
(1) H-12
HMDS
7
6
5
4
3
2
1
¹H NMR ppm
158.09
139.40
84.24
180.00
f
SCU019_1661_2/C6D6q/1H
Scheler 127/16
quant.
OH
11
14
Ferruginol (4)
12
Miltiradiene (1)
OH
HO
HOOC
14
Carnosic acid (9)
(9) H-14
(4) H-11
(1) H-12
HMDS
7
6
5
4
3
2
1
¹H NMR ppm
200.55
9.52
164.79
17.51
180.00

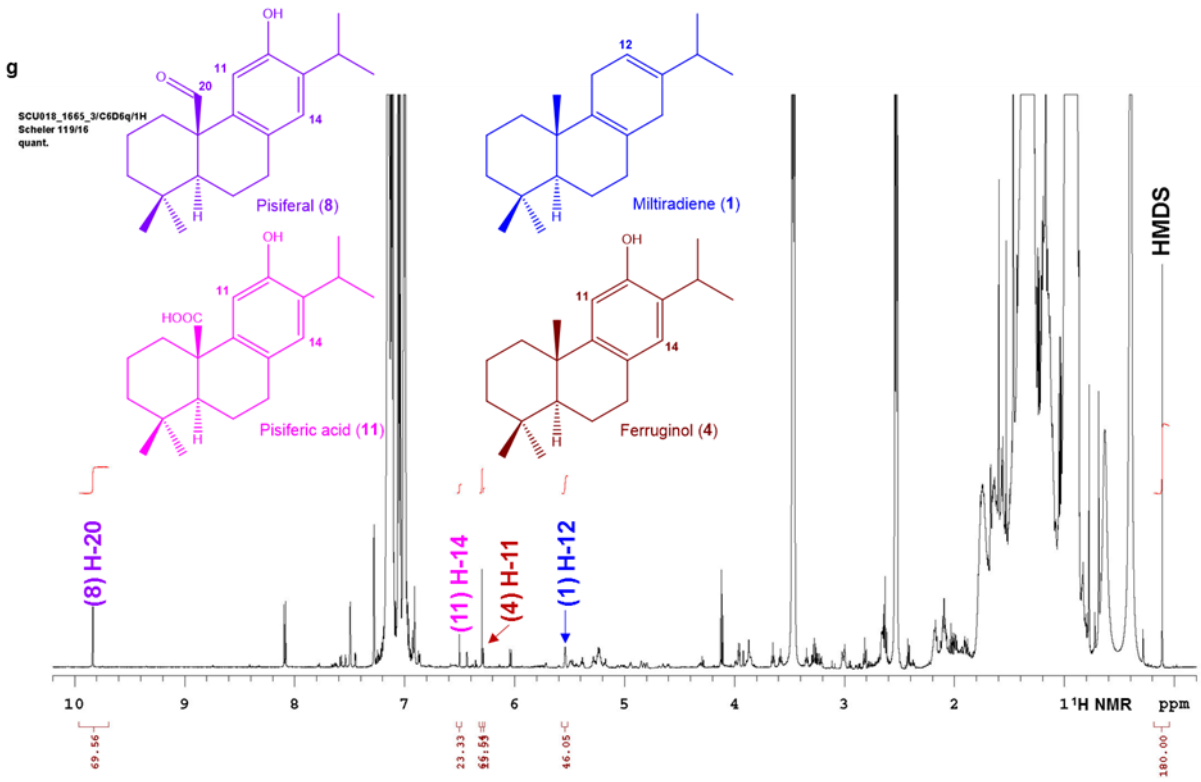

Suppl. Fig. 21 ^{1}H NMR spectra of engineered yeast for quantification. The strains expressed the enzymes GGPPS, CPS, MiS (**a**) together with ATR1 and CYP76AH1 (**b**), CYP76AH22 (**c**), CYP76AH1$_{D301EN303SV479F}$ (**d**), CYP76AH22$_{E301DS303NF478V}$ (**e**), CYP76AH22 and CYP76AK8 (**f**), or CYP76AH1 and CYP76AK8 (**g**). Product specific signals, which were used for quantification, are highlighted. The corresponding integrals including the peak areas are given. As internal standard hexamethyldisiloxane (HMDS) was used for quantification.

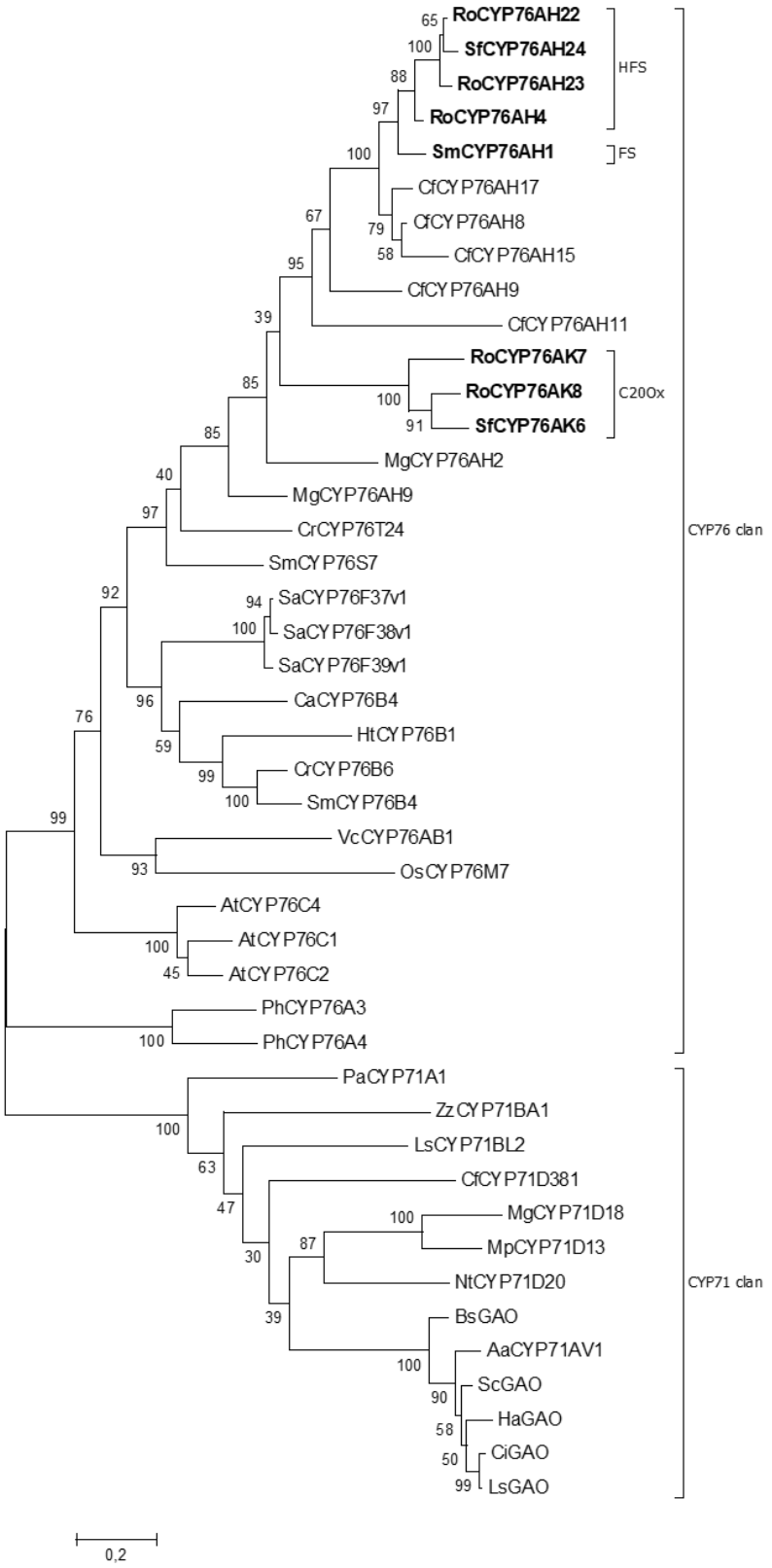

Suppl. Fig. 22 Phylogenetic analysis of CYPs involved in the biosynthesis of CA and PA. The maximum likelihood tree was generated using MEGA (version 6) from protein sequence alignment and illustrates the relationship of CYP enzymes of the PD biosynthesis to other proteins from the CYP76 and CYP71 clan. Bootstrap values (1000 repeats) are indicated for each branch of the tree.

Supplementary Tables

Suppl. Tab. 1 Primers used for cloning, introduction of single point mutations and quantitative real-time PCR.

Gene	Application	Primer ID	Sequence
CYP76AH22	Cloning	RoFS1_for1	TTTGAAGACAAAATGGATTCTTTTCCTCTT
		RoFS1_rev1	TTTGAAGACAGACTTGCCCGTATTTGTG
		RoFS1_for2	TTTGAAGACGCAAGTCTTTTCCGGCAG
		RoFS1_rev2	TTTGAAGACTCCATGCTCTGATGCGAGA
		RoFS1_for3	TTTGAAGACAGCATGGAAGATAGCCAGT
		RoFS1_rev3	TTTGAAGACTTCAACTTGTTGTCGTTCGT
		RoFS1_for4	TTTGAAGACAAGTTGAAGATCGATCACCT
	Introduction of single point mutation	RoFS1E301D_for	GTTTGTTGGAGGATCTGACACAAGCACGACAGAGATCG
		RoFS1E301D_rev	CGATCTCTGTCGTGCTTGTGTCAGATCCTCCAACAAAC
		RoFS1E301DS303N_for	GTTTGTTGGAGGATCTGACACAAACACGACAGAGATCGAG
		RoFS1E301DS303N_rev	CTCGATCTCTGTCGTGTTTGTGTCAGATCCTCCAACAAAC
		RoFS1G117A_for	GGTTCCTCCCCGTGGCGGGCGAGTGGCGCG
		RoFS1G117A_rev	CGCGCCACTCGCCCGCCACGGGGAGGAACC
		RoFS1G117AG118S_for	GGTTCCTCCCCGTGGCGAGCGAGTGGCGCG
		RoFS1G117AG118S_rev	CGCGCCACTCGCTCGCCACGGGGAGGAACC

		RoFS1G118S_for	CCTCCCCGTGGGGAGCGAGTGGCGCG
		RoFS1G118S_rev	CGCGCCACTCGCTCCCCACGGGGAGG
		RoFS1S303N_for	GGAGGATCTGAAACAAACACGACAGAGATCGAGTGG
		RoFS1S303N_rev	CCACTCGATCTCTGTCGTGTTTGTTTCAGATCCTCC
		AH22F478V_for	GGTGTGTTGTTTGGCGTTGCGGTGCGGAGGG
		AH22F478V_rev	CCCTCCGCACCGCAACGCCAAACAACACACC
		AH22L288F_for	GTTGAAGATCGATCACTTCACACATCTCATGCTGG
		AH22L288F_rev	CCAGCATGAGATGTGTGAAGTGATCGATCTTCAAC
CYP76AH23	Cloning	RoFS1_for1	TTTGAAGACAAAATGGATTCTTTTCCTCTT
		RoFS2_rev1	TTTGAAGACTTGCCCGTATTTGTGCATGA
		RoFS2_for2	TTTGAAGACACGGGCAAGTATTCTCCG
		RoFS2_rev2	TTTGAAGACTCCATGCTCTGATGCGAG
		RoFS2_for3	TTTGAAGACAGCATGGAAGATAGTCAGG
		RoFS2_rev3	TTTGAAGACTCAACTTACAGTCGTTGG
		RoFS2_for4	TTTGAAGACTAAGTTGAAGATGGATCACC
		RoFS2_rev4	TTTGAAGACAAAAGCTTATGCCTTAAAGGG

CYP76AH4	Cloning	CYP76AH4_for 1neu	TTTGAAGACAAAATGGATTCCTTTCCT CTTCTCGTTGCTCTCTTCTTCATCGCT GTGACAACTTTCCTT
		CYP76AH4_for 2	TTTGAAGACTACGGGCAAGTATTCTC CGG
		CYP76AH4_for 3	TTTGAAGACGCATGGAAGATAGCCAG TGG
		CYP76AH4_for 4	TTTGAAGACAAGTTGAAAACCGATCA CCT
		CYP76AH4_rev 1	TTTGAAGACTGCCCGTATTTGTGCATG ATT
		CYP76AH4_rev 2	TTTGAAGACTTCCATGCTCTGATGCGA GA
		CYP76AH4_rev 3	TTTGAAGACTTCAACTTGTTGTCGTTC GT
		CYP76AH4_rev 4_2	TTTGAAGACAAAAGCTCAAGACTTAA CTATTGGGA
CYP76AH1	Introduction of single point mutation	CYP76AH1D30 1E_f	CGTGGGAGGATCGGAAACGAACACG ACCTCG
		CYP76AH1D30 1E_r	CGAGGTCGTGTTCGTTTCCGATCCTCC CACG
		CYP76AH1A11 7G_for	GGTTCCTCCCCGTGGGCAGCGAGTGG CGCG
		CYP76AH1A11 7G_rev	CGCGCCACTCGCTGCCCACGGGGAGG AACC
		CYP76AH1A11 7GS118G_for	GGTTCCTCCCCGTGGGCGGCGAGTGG CGCGACATGC
		CYP76AH1A11 7GS118G_rev	GCATGTCGCGCCACTCGCCGCCCACG GGGAGGAACC
		CYP76AH1D30 1EN303S_for	CGTGGGAGGATCGGAAACGAGCACG ACCTCGATCG
		CYP76AH1D30 1EN303S_rev	CGATCGAGGTCGTGCTCGTTTCCGATC CTCCCACG
		CYP76AH1N30 3S_for	GGAGGATCGGACACGAGCACGACCTC GATCG

		CYP76AH1N303S_rev	CGATCGAGGTCGTGCTCGTGTCCGATCCTCC
		CYP76AH1S118G_for	GGTTCCTCCCCGTGGCCGGCGAGTGGCGCG
		CYP76AH1S118G_rev	CGCGCCACTCGCCGGCCACGGGGAGGAACC
		AH1F288L_for	GTTGAAAACGCATCACTTAACCCATCTCATGCTGG
		AH1F288L_rev	CCAGCATGAGATGGGTTAAGTGATGCGTTTTCAAC
		AH1V479F_for	GCGAGTTGTTTGGGTTTGCCGTGCGCAGGGC
		AH1V479F_rev	GCCCTGCGCACGGCAAACCCAAACAACTCGC
CYP76AK7	Amplification from cDNA	Ro34450-fw	CACCATGGATGCTTTTGTTGTTTTCTCCCTG
		Ro34450-rv	TCAAACCTTGATGGGTTTAGCCCTAAGTG
	Golden Gate Cloning	CYP34450 For1	TTTGAAGACAAAATGGATGCTTTTGTTGTTTTCTC
		CYP34450 Rev1	TTTGAAGACCGGAGTTGTAAGATGTTGCC
		CYP34450 For2	TTTGAAGACCAACTCCGCGGTGACCCCCAC
		CYP34450 Rev2	TTTGAAGACGAGGTCGGTCATGGTGGTGAA
		CYP34450 For3	TTTGAAGACCCGACCTCGTTTTCTCGAC
		CYP34450 Rev3	TTTGAAGACAAAAGCTCAAACCTTGATGGGTTTAGC
	qPCR analysis	Roff34450-For1256	ACGCAGATAAATGGCTATACAATCC
		Roff34450-Rev1535	ATTCAGCCCCTCCTTCAAGTTCC
CYP76AK8	Amplification from cDNA	Ro33941-fw	CACCATGCAATTGTTCATTATTCTATCCCTAG

		Ro33941-rv	TCAAACCTTGATGGGAACAGCCCTTAG
	Golden Gate Cloning	CYP33941_For1	TTTGAAGACAAAATGCAATTGTTCATTATTCTATCCCTAG
		CYP33941_Rev1	TTTGAAGACTCTCGGCCAAGTTGTAAGATG
		CYP33941_For2	TTTGAAGACGGCCGAGATCCCCACAAG
		CYP33941_Rev2	TTTGAAGACGGCGACGAAACCACCACG
		CYP33941_For3	TTTGAAGACTCGTCGCCGGAAATGGCGAG
		CYP33941_Rev3	TTTGAAGACAAAAGCTCAAACCTTGATGGGAACAGC
	qPCR analysis	Roff33941-For1791	TGGATAGCGAGATTGATTTTGGAG
		Roff33941-Rev1967	TCTGGAGTTGTTTGGATTCTGCC
CYP76AK6	Amplification from cDNA	0850-fw	CACCATGCAAGTTCTCATCCTTCTTTCTCT
		0850-rev	TCAAACTTTGATGGGAATAGCTCTTAG
	Golden Gate Cloning	SfruCYP850 For1	TTTGAAGACAAAATGCAAGTTCTCATCCTTCTTTCTCTGGCC
		SfruCYP850 Rev1	TTTGAAGACGCACTGCGATCGGAGCGCACGGCGTCGAAAAG
		SfruCYP850 For2	TTTGAAGACCGCAGTGCAAATACTTGGCCACGGCGAGGTTTCTA
		SfruCYP850 Rev2	TTTGAAGACAAAAGCTCAAACTTTGATGGGAATAGCTCTTAGG
	qPCR analysis	For811-Sfru850/2	AGCTCGAAACACGGCGACTTACC
		Rev1067-Sfru850/2	ATTCTTCGATGATGCTTTTGTCTCC

Salvia fruticosa eIF-4a	qPCR - reference gene	For-eIF-4A-Sfru	TTGTTGCCATTGACATCTTCACTT
		Rev-eIF-4A-Sfru	CTCTCCCATGGCTGACATAACACT
Rosmarinus officinalis eIF-4a	qPCR - reference gene	Roff21732/35elf4a-For221	ACGAGATGGGAATAAAGGAGGAG
		Roff21732/35elf4a-Rev546	ATCCTCACCCACACTTTTGCCTC
pGal_syn1	Primer extension PCR	pGal_syn1_1_for	TTTGAAGACAAGGAGATTACTATCCCGGATTAGAA
		pGal_syn1_1_rev	TTTGAAGACACCATTTGTTTTTTTTTTATGACGTTAAGCT
pGal_syn3	Primer extension PCR	pGal_syn1_3_for	TTTGAAGACAAGGAGAGAGTGTGGTCGGATTAGAA
		pGal_syn1_3_rev	TTTGAAGACACCATTTGTTTTTTTTTTATGATGTTAATGT
pGal_syn4	Primer extension PCR	pGal_syn1_4_for	TTTGAAGACAAGGAGTTGTGTTGTTCGGATTAGAAG
		pGal_syn1_4_rev	TTTGAAGACACCATTTGTTTTTTTTCTTTGACGTTAAGCT
pGal_syn5	Primer extension PCR	pGal_syn1_5_for	TTTGAAGACAAGGAGGGCTTAGCGTCGGATTAGAAG
		pGal_syn1_5_rev	TTTGAAGACACCATTTTTTTTTTTTTTATGATGTTAAGGT
pGal_syn6	Primer extension PCR	pGal_syn1_6_for	TTTGAAGACAAGGAGTTAGAAGGCGCGGATTAG
		pGal_syn1_6_rev	TTTGAAGACACCATTTGTTTTTTTTTCTTGACGTTAATGT
pGal_syn7	Primer extension PCR	pGal_syn1_7_for	TTTGAAGACAAGGAGTGGTTGTGGTCGGATTAGAA
		pGal_syn1_7_rev	TTTGAAGACACCATTTTTTTTTTCTCTTTGATGTTAACGT

Suppl. Tab. 2 Sequences of synthetic galactose inducible promoters and assignment to their assembled genes and terminators.

Promoter		Gene	Terminator	
Name	**Sequence**		**Name**	**Source**
pGal_syn1	ATTACTATCCCGGATTAGAAGCCGCCGCACGGGCGACAGCCCTCCGAAACGCGCCGCACTGCTCCGAACAATGGTTCTCGTGCTGTTGCTGACACCGGCGGTCTTTCGTCCGTGCCTTCGACGTGAGACTTCAACTATATAAATGCAAAAACTGTATAAAAACTTTAACTAATACTTTCAACATTTTCGGTTTGTATTGCTCCTCATTCACATCTTATTCAATTATCATCAAAAAATTGTTAATATACCTCTATAGCTTAACGTCATAAAAAAAAAACA	*GGPPS*	tASP3-1	[241]
pGal_syn3	AGAGTGTGGTCGGATTAGAAGCCGCCGCACGGGCGACAGCCCTCCGACCCGCGCCGCACTGCTCCGAACAATAGGGGTTGAGAAAGCCGGCCCACCGGCGGTCTTTCGTCCGGCCAAGTTCCACTTGTCCGGTCTATATAAATGCAAAAACTGCATATAAACTTTAACTAATACTTTCAACAATTTCGGTTTGTATTGCTCCTCATTCTCATCTTATTAAAGTATCATCAAGAAATTGTTAATATACCTCTATACATTAACATCATAAAAAAAAAACA	*MS*	tSAG1	[241]
pGal_syn4	TTGTGTTGTTCGGATTAGAAGCCGCCGACCGGGCGACAGCCCTCCGACTCGCGCCGCACTGCTCCGAACAATCTGGAGATGCACTTGTGGCCCACCGGCGGTCTTTCGTCCGTGCGGCCTGTTGCGTAGCAGAGCTATATAAATGCAAAAACTGCATATCCACTATAACTAATACTTTCAACAATTTGGTGTTGTATTGCTTTTCATTCTAATGTTATTCAAGTATCATCAAGAAATTGTTAATATACCTCTATAGCTTAACGTCAAAGAAAAAAAACA	*ATR1*	tALY2	[241]
pGal_syn5	GGCTTAGCGTCGGATTAGAAGCCGCCGTACGGGCGACAGCCCTCCGAACCGCGCCGCACTGCTCCGAACAATCTGCGCCAAAAAGGGCGT	*$C_{20}Ox$*	tCYC1	[242]

	GGCACCGGCGGTCTTTCGTCCGTGCCTTCCT TTGTAGATTAAGTCTATATAAATGCAAAAA CTGCATAACCACTATAACTAATACTTTCAAC AATTTCGGGTTGTATTACTCTTTATTCTCAT CTTATAAAAGTATCAACAAGAAATAGTTAA TATACCTCTATACCTTAACATCATAAAAAA AAAAAA			
pGal_ syn6	TTAGAAGGCGCGGATTAGAAGCCGCCGCGC GGGCGACAGCCCTCCGACGCGCGCCGCACT GCTCCGAACAATTCTATTAGACGCTCAGTT ATCACCGGCGGTCTTTCGTCCGTGCAGGAT GGAGTAAATGTAGACTATATAAATGCAAAA ACTGTATAACAACTTTAACTAATACTTTCAA CAATTTCGTGTTGTATTGCTTCTCATTCTCA CGTTATTAAAGTATCATCAAAAAATAGTTA ATATACCTCTATACATTAACGTCAAGAAAA AAAAACA	*(H)FS*	tPGK1	[241]
pGal_ syn7	TGGTTGTGGTCGGATTAGAAGCCGCCGTAC GGGCGACAGCCCTCCGATTCGCGCCGCACT GCTCCGAACAATTAGGTCGAGTTGGGTCCG GTCACCGGCGGTCTTTCGTCCGTGCTCCGAC ACTGGACTCTCCACTATATAAATGCAAAAA CTGTATATCAACAATAACTAATACTTTCAAC ATTTTCGGTTTGTATTGCTCCTCATTCAAAT CTAATTAAAGTATCATCAAGAAATTGTTAA TATACCTCTATACGTTAACATCAAAGAGAA AAAAAA	*CPS*	tDIT1	[241]

Suppl. Tab. 3 Constructs and corresponding yeast strains.

Strain	Transformed gene combination	Source
INVS*c*1	*GGPPS:CPS:MiS* (control)	[46]
	GGPPS:CPS:MiS:ATR1:CYP76AH1	[46, 103, 243]
	GGPPS:CPS:MiS:ATR1:CYP76AH22	[46, 47, 243]
	GGPPS:CPS:MiS:ATR1:CYP76AH23	[46, 47, 243]
	GGPPS:CPS:MiS:ATR1:CYP76AH4	[46, 102, 243]
	GGPPS:CPS:MiS:ATR1:CYP76AH24	[46, 47, 243]
	GGPPS:CPS:MiS:ATR1:CYP76AH22:CYP76AK6	[46, 47, 243]
	GGPPS:CPS:MiS:ATR1:CYP76AH23:CYP76AK6	[46, 47, 243]
	GGPPS:CPS:MiS:ATR1:CYP76AH24:CYP76AK6	[46, 47, 243]
	GGPPS:CPS:MiS:ATR1:CYP76AH4:CYP76AK6	[46, 102, 243]
	GGPPS:CPS:MiS:ATR1:CYP76AH1:CYP76AK6	[46, 103, 243]
	GGPPS:CPS:MiS:ATR1:CYP76AH22:CYP76AK7	[46, 47, 243]
	GGPPS:CPS:MiS:ATR1:CYP76AH23:CYP76AK7	[46, 47, 243]
	GGPPS:CPS:MiS:ATR1:CYP76AH24:CYP76AK7	[46, 47, 243]
	GGPPS:CPS:MiS:ATR1:CYP76AH4:CYP76AK7	[46, 102, 243]
	GGPPS:CPS:MiS:ATR1:CYP76AH1:CYP76AK7	[46, 103, 243]
	GGPPS:CPS:MiS:ATR1:CYP76AH22:CYP76AK8	[46, 47, 243]
	GGPPS:CPS:MiS:ATR1:CYP76AH23:CYP76AK8	[46, 47, 243]
	GGPPS:CPS:MiS:ATR1:CYP76AH24:CYP76AK8	[46, 47, 243]
	GGPPS:CPS:MiS:ATR1:CYP76AH4:CYP76AK8	[46, 102, 243]
	GGPPS:CPS:MiS:ATR1:CYP76AH1:CYP76AK8	[46, 103, 243]

CYP76AH22, CYP76AH23 and CYP76AH24 were formerly known as RoFS1, RoFS2 and SfFS, respectively.

Suppl. Tab. 4 NMR data of 11-hydroxyferruginol and hydroxyferruginol quinone. (^{13}C: δ [ppm], ^{1}H: δ [ppm] m (J [Hz]) ($CDCl_3$) obtained from a Agilent VNMRS 600, $CDCl_3$, ^{1}H @ 599.829 MHz (^{1}H; ^{1}H,^{13}C HSQC; ^{1}H,^{13}C HMBC), reference: ^{1}H: TMS int. = 0 ppm; concentration: ca. 0.2 mmol/L. Carbon positions refer to Suppl. Fig. 8a.

	11-Hydroxyferruginol			**Hydroxyferruginol quinone**	
Pos.	**^{13}C[a]**	**^{1}H**	**HMBC (H to C)**	**^{13}C[a]**	**^{1}H**
1	36.8	3.043 dt-like (13.3/3.5)/ 1.33[a]		1	36.8
2	n.d.	n.d.		n.d.	n.d.
3	41.4	1.46[a]/1.23[a]		n.d.	n.d.
4	33.7	---		n.d.	---
5	52.9	1.31[a]		51.5.	n.d.
6	n.d.	n.d.		n.d.	n.d.
7	32.4	2.79[a]/2.79[a]	5, 8, 9, 14	33.8 (?)	2.474 ddd (20.6/6.1/1.1)/
8	129.6	---		n.d.	---
9	133.0	---		144.9	---
10	39.2	---		38.0	---
11	142.9	---		n.d.	---
12	138.1	---		n.d.	---
13	131.4	---		n.d.	---
14	117.2	6.437 s	7, 9, 12, 15,	137.8	6.384 s
15	27.1	2.983 sp (6.9)	12, 13, 14, 16, 17	26.9	2.897 sp (7.1)
16[b]	22.4	1.250 d (6.9)	13, 15, 17	21.5	1.093 d (7.0)
17[b]	22.7	1.230 d (6.9)	13, 15, 16	21.5	1.087 d (7.0)
18	21.9	0.926 s	3, 4, 5, 19	21.7	0.884 s
19	33.7	0.952 s	3, 4, 5, 19	33.5	0.926 s
20	20.2	1.335 s	1, 5, 9, 10	20.0	1.224 s
11-OH	---	5.622 s	9, 11, 12	---	---
12-OH	---	4.577 s	11, 12, 13	---	---

[a] chemical shifts of HSQC or HMBC correlation peaks; [b] may be interchanged; n.d. not detected; s singlet; d doublet; t triplet; sp septet; ddd doublet of doublet of doublet.

Suppl. Tab. 5 NMR data of miltiradien-20-al. (^{13}C: δ [ppm], ^{1}H: δ [ppm] m (J [Hz]) ($CDCl_3$) obtained from a Agilent VNMRS 600, C_6D_{12}, ^{1}H @ 599.829 MHz (^{1}H; ^{1}H,^{13}C HSQC; ^{1}H,^{13}C HMBC), reference: ^{1}H: TMS int. = 0 ppm. Carbon positions refer to Suppl. Fig. 8a.

Miltiradien-20-al			
Pos.	**^{13}C[a]**	**^{1}H**	**HMBC (H to C)**
1	30.3	2.49[a] [β] / 0.78[a] [α]	
2	19.7	1.555 tt-like (13.7/3.6) [β] / 1.42[a] [α]	
3	42.3	1.37[a] [β] / 1.17 [α]	
4	34.0	---	
5	52.0	1.1.506 dd (13.1/2.8)	4, 6, 10, 18, 19, 20
6	18.0	2.06[a] [β] / 1.86[a] [α]	5, 7, 10 5, 7, 8, 10
7	32.0	2.17[a] [α] /2.09[a] [β]	
8	132.8	---	
9	123.6	---	
10	53.6	---	
11	25.5	2.43[a] / 2.24[a]	
12	116.7	5.343 m	11, 14, 15
13	138.8	---	
14	34.8	2.60a / 2.47a	8, 9, 12, 13 8, 9, 12, 13
15	34.8	2.13[a]	12, 13, 14, 16, 17
16	21.1	0.998[b] d (6.9)	13, 15, 17
17	21.1	0.994[b] d (6.9)	13, 15, 16
18	20.6	0.789 s	3, 4, 5, 19
19	31.6	0.920 s	3, 4, 5, 18
20	194.8	9.599 br d (1.8) [$^{1}J_{CH}$ = 181 Hz]	1, 10

[a] chemical shifts of HSQC or HMBC correlation peaks; [b] may be interchanged; s singlet; d doublet; t triplet; [ ] additional information.

Suppl. Tab. 6 NMR data of carnosaldehyde. (^{13}C: δ [ppm], ^{1}H: δ [ppm] m (J [Hz]) ($CDCl_3$) obtained from a Agilent VNMRS 600, $CDCl_3$, ^{1}H @ 599.829 MHz (^{1}H; ^{1}H,^{13}C HSQC; ^{1}H,^{13}C HMBC), reference: ^{1}H: TMS int. = 0 ppm. Carbon positions refer to Suppl. Fig. 8a.

Carnosaldehyde			
Pos.	**^{13}C[a]**	**^{1}H**	**HMBC (H to C)**
1	30.5	3.249 dt-like (13.5/4.2) [β] /1.15[a] [α]	
2	19.7	1.58[a] [α] / 1.54[a] [β]	
3	41.3	1.49[a] [β] /1.330 td-like (13.2/4.8) [α]	
4	34.2	---	
5	52.9	1.62[a]	20
6	18.8	2.029 br d (12.7) [α] /1.863 m [β]	
7	31.5	2.866 dd-like (8.5/3.5) [2H]	5, 6, 8, 9, 14
8	129.9	---	
9	116.2	---	
10	n.d.	---	
11	143.4	---	
12	142.3	---	
13	134.5	---	
14	119.4	6.599 s	7, 9, 12, 15,
15	27.0	3.234 sp (6.9)	12, 13, 14, 16, 17
16	22.2	1.209 d (7.0)	13, 15, 17
17	22.2	1.209 d (7.0)	13, 15, 16
18	21.5	0.903 s	3, 4, 5, 19
19	31.9	1.039 s	3, 4, 5, 18
20	203.5	9.901 s [$^{1}J_{CH}$ = 175 Hz]	1, 5
11-OH	---	7.129 s	11, 12
12-OH	---	5.786 s	11, 12, 13

[a] chemical shifts of HSQC or HMBC correlation peaks; n.d. not detected; s singlet,; d doublet; t triplet; sp septet; [ ] additional information.

Suppl. Tab. 7 Protein sequences used for phylogenetic analysis with their corresponding accession numbers.

Protein	**Species**	**Accession number**
AaCYP71AV1	*Artemisia annua*	BAM68808
AtCYP76C1	*Arabidopsis thaliana*	AT2G45560
AtCYP76C2	*Arabidopsis thaliana*	AT2G45570
AtCYP76C4	*Arabidopsis thaliana*	AT2G45550
BsGAO	*Barnadesia spinosa*	GU256647
CaCYP76B4	*Camptotheca acuminata*	AES93118
CfCYP71D381	*Coleus forskohlii*	Patent WO/2015/113569
CfCYP76AH11	*Coleus forskohlii*	Patent WO/2015/113569
CfCYP76AH15	*Coleus forskohlii*	Patent WO/2015/113569
CfCYP76AH17	*Coleus forskohlii*	Patent WO/2015/113569
CfCYP76AH8	*Coleus forskohlii*	Patent WO/2015/113569
CfCYP76AH9	*Coleus forskohlii*	Patent WO/2015/113569
CiGAO	*Cichorium intybus*	GU256644
CrCYP76B6	*Catharanthus roseus*	AJ251269
CrCYP76T24[a]	*Catharanthus roseus*	KF302075
HaGAO	*Helianthus annuus*	GU256646
HtCYP76B1	*Helianthus tuberosus*	Y09920
LsCYP71BL2	*Lactuca sativa*	F8S1I0
LsGAO	*Lactuca sativa*	GU198171
MgCYP71D18	*Mentha x gracilis*	Q6WKZ1
MgCYP76AH2[a]	*Mimulus guttatus*	1.1978 (http://drnelson.uthsc.edu/CytochromeP450.html)
MgCYP76AH9[a]	*Mimulus guttatus*	14.23151 (http://drnelson.uthsc.edu/CytochromeP450.html)
MpCYP71D13	*Mentha x piperita*	Q9XHE7
NtCYP71D20	*Nicotiana tabacum*	Q94FM7
OsCYP76M7	*Oryza sativa*	AK105913
PaCYP71A1	*Persea americana*	AAA32913
PhCYP76A3	*Petunia x hybrida*	BAC53891
PhCYP76A4	*Petunia x hybrida*	AB016061
RoCYP76AH22	*Rosmarinus officinalis*	KP091843
RoCYP76AH23	*Rosmarinus officinalis*	KP091844
RoCYP76AH4	*Rosmarinus officinalis*	DOI: 10.1039/c000000x/
RoCYP76AK7	*Rosmarinus officinalis*	In submission to GenBank

RoCYP76AK8	*Rosmarinus officinalis*	In submission to GenBank
SaCYP76F37v1	*Santalum album*	KC533717
SaCYP76F38v1	*Santalum album*	KC533715
SaCYP76F39v1	*Santalum album*	KC533716
ScGAO	*Saussurea costus*	GU256645
SfCYP76AH24	*Salvia fruticosa*	KP091842
SfCYP76AK6	*Salvia fruticosa*	In submission to GenBank
SmCYP76AH1	*Salvia miltiorrhiza*	AGN04215
SmCYP76B4	*Swertia mussotii*	D1MI46
SmCYP76S7[a]	*Salvia miltiorrhiza*	KP337691
VcCYP76AB1	*Vanda coerulea*	ACC59773
ZzCYP71BA1	*Zingiber zerumbet*	BAJ39893

[a] not characterized yet

5.2. Supporting information to 2.3.2.

Supplementary Figures

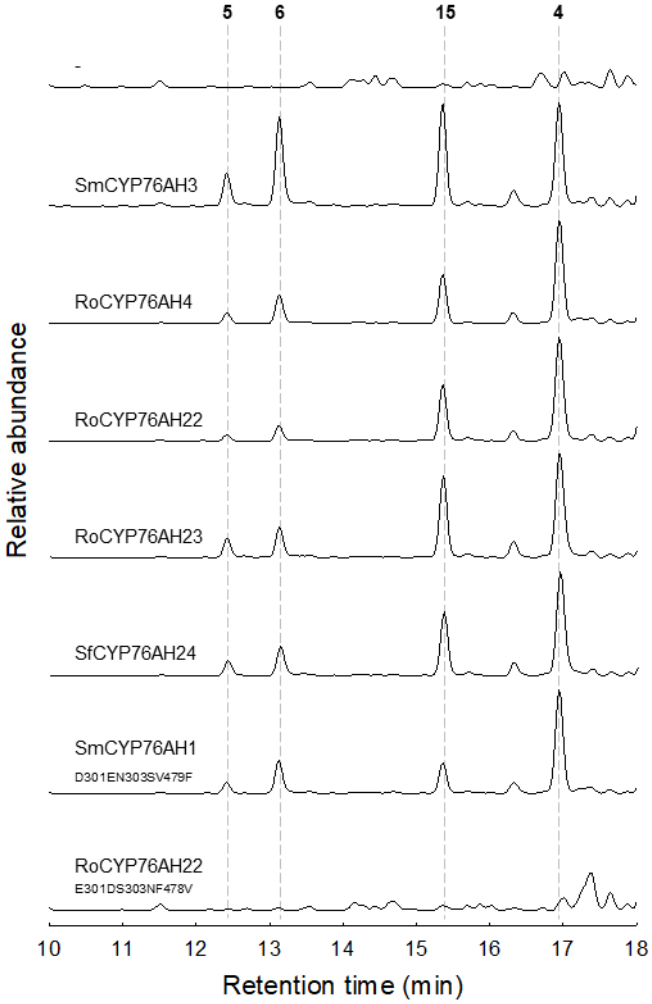

Figure S1: Total ion chromatogram of LC-MS analysis obtained from hexane extracts of yeast strains expressing the CM and the indicated CYPs. 11-Hydroxy ferruginol (**4**), 7,11-dihydroxy ferruginol (**5**), 11-hydroxy sugiol (**6**) and 7-methoxy-11-hydroxy ferruginol (**15**).

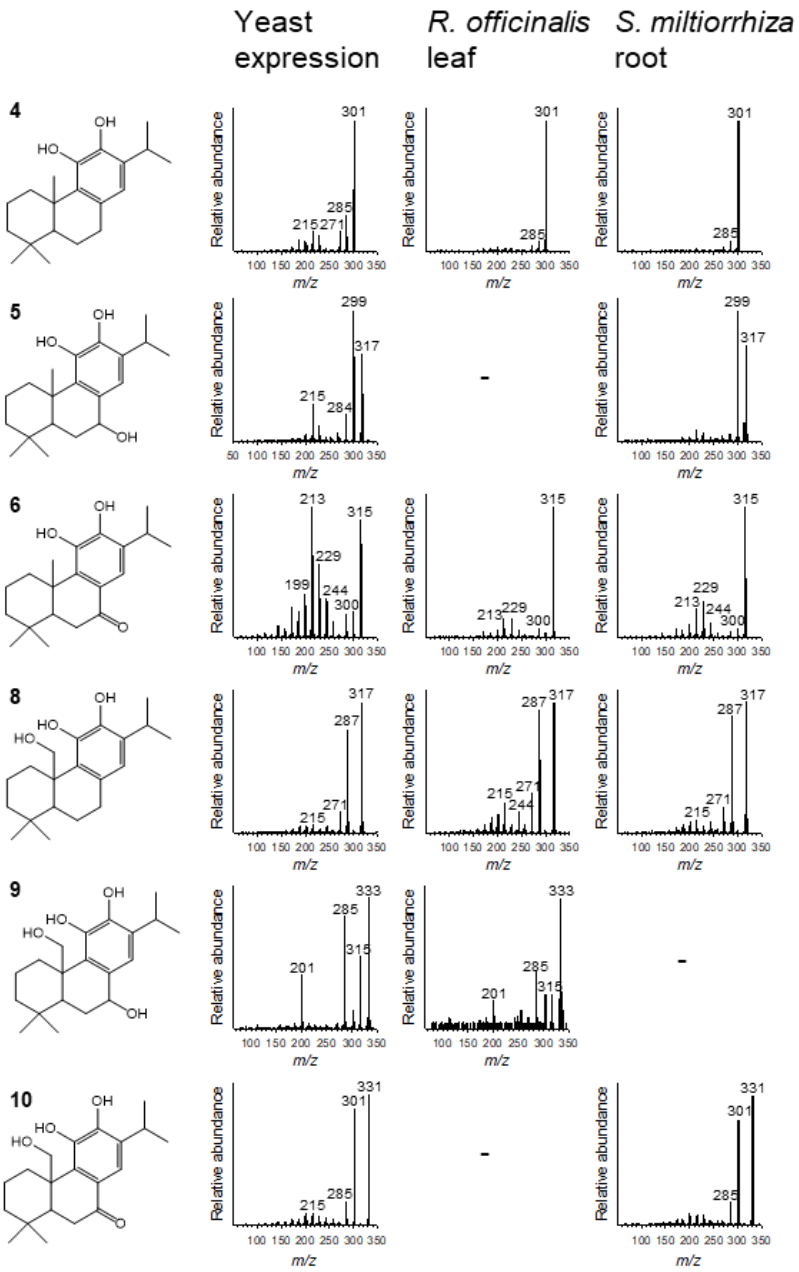
Yeast expression
R. officinalis leaf
S. miltiorrhiza root
4
5
6
8
9
10
Relative abundance
m/z
-

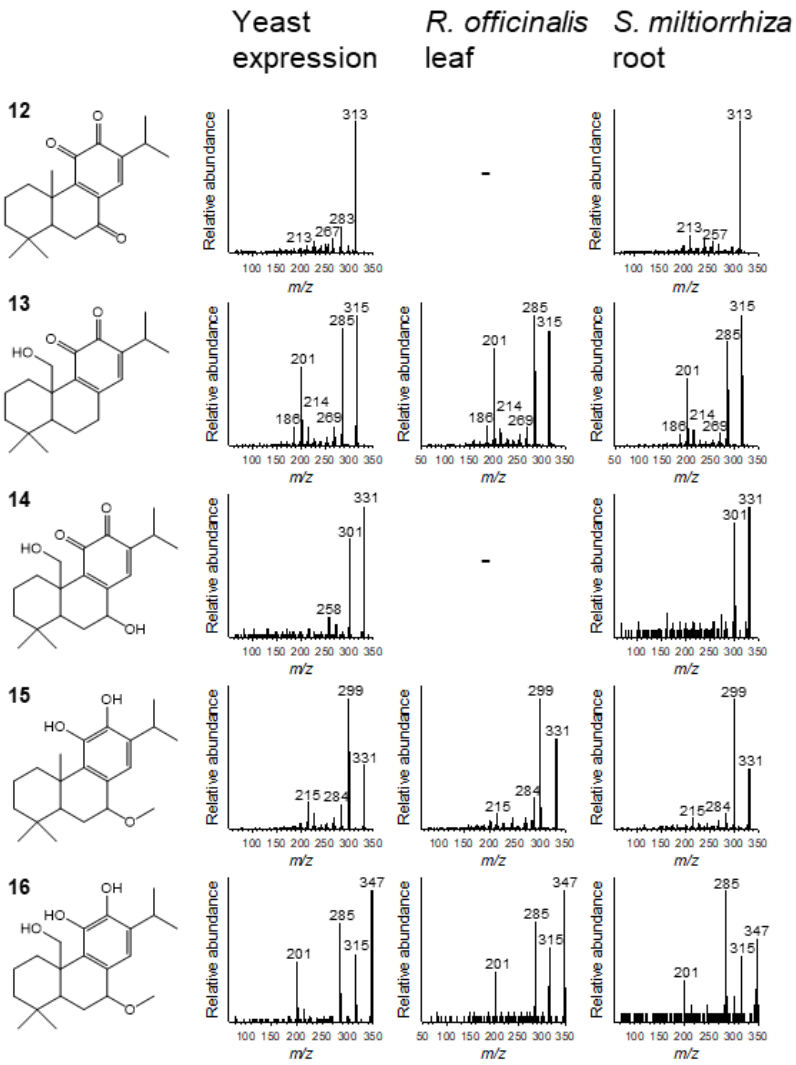

Figure S2: ESI mass spectra of ADs extracted from rosemary leaves, *S. miltiorrhiza* roots or yeast strains expressing the appropriate enzymes. The corresponding structures are given in the left panel. In some cases, the compounds could not be detected in either rosemary or sage (represented by dashes). 11-Hydroxy ferruginol (**4**), 7,11-dihydroxy ferruginol (**5**), 11-hydroxy sugiol (**6**), pisiferol (**7**), 11,20-dihydroxy ferruginol (**8**), 7,11,20-trihydroxy ferruginol (**9**), 11,20-dihydroxy sugiol (**10**), abietaquinone (**11**), 7-keto abietaquinone (**12**), 20-hydroxy abietaquinone (**13**), 7,20-dihydroxy abietaquinone (**14**), 7-methoxy-11-hydroxy ferruginol (**15**) and 7-methoxy-11,20-dihydroxy ferruginol (**16**).

7,11-dihydroxy ferruginol (**5**)

MS^2 of *m/z* 317.2

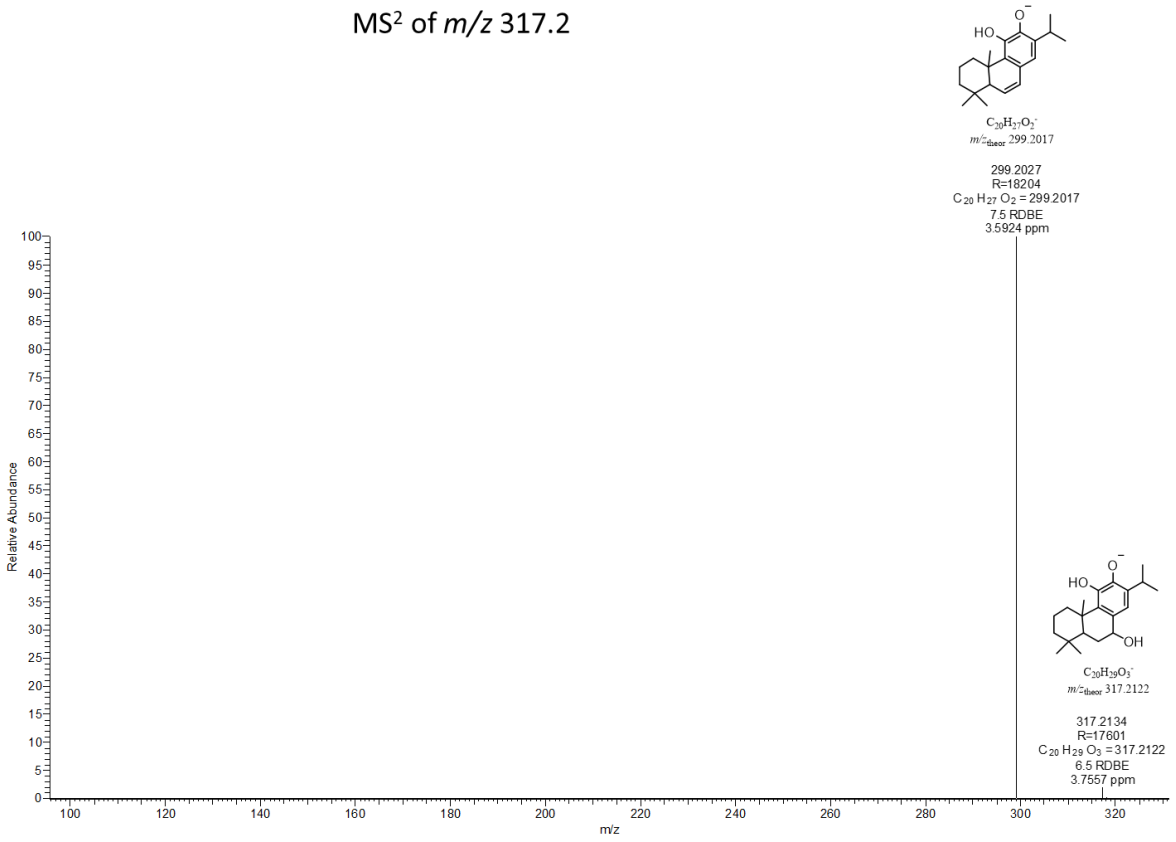

7,11-dihydroxy ferruginol (**5**)

MS^3 of *m/z* 317.2 → 299.2

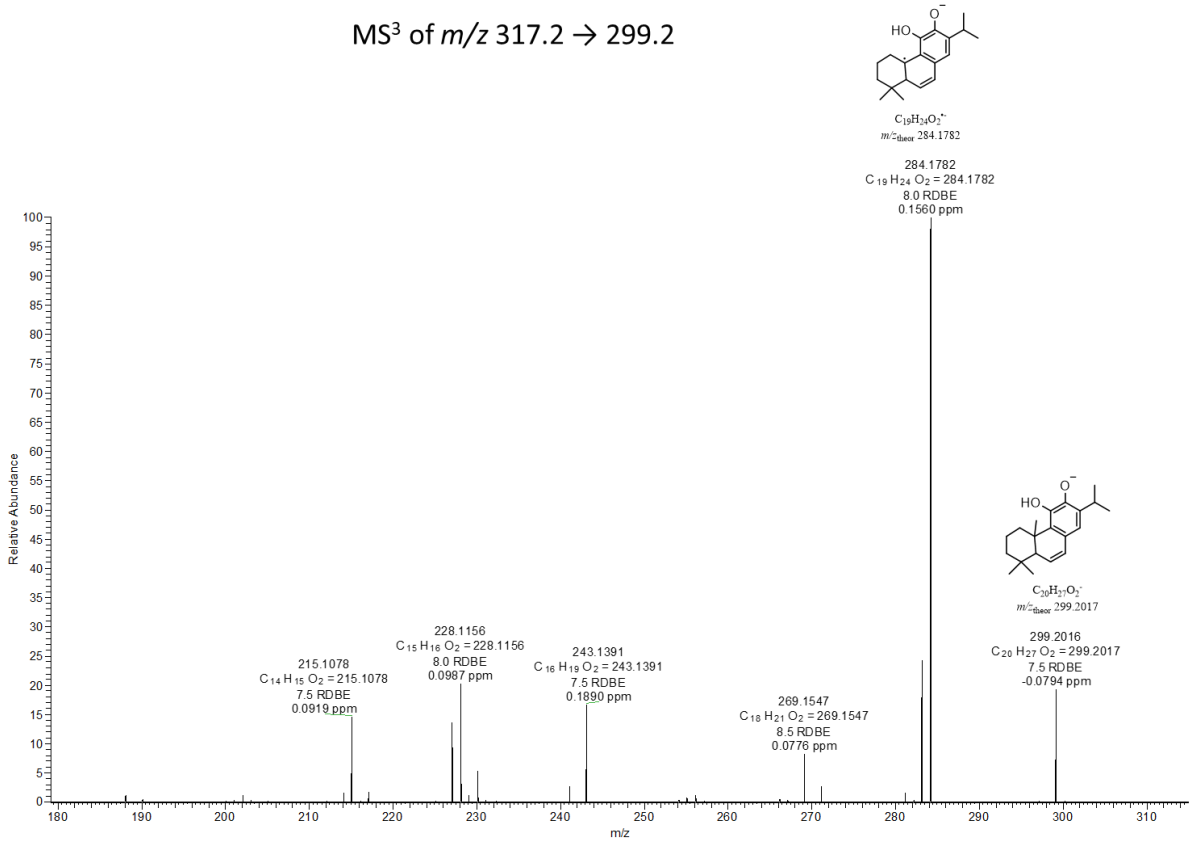

7,11-dihydroxy ferruginol (**5**)

MS^4 of *m/z* 317.2 → 299.2 → 284.2

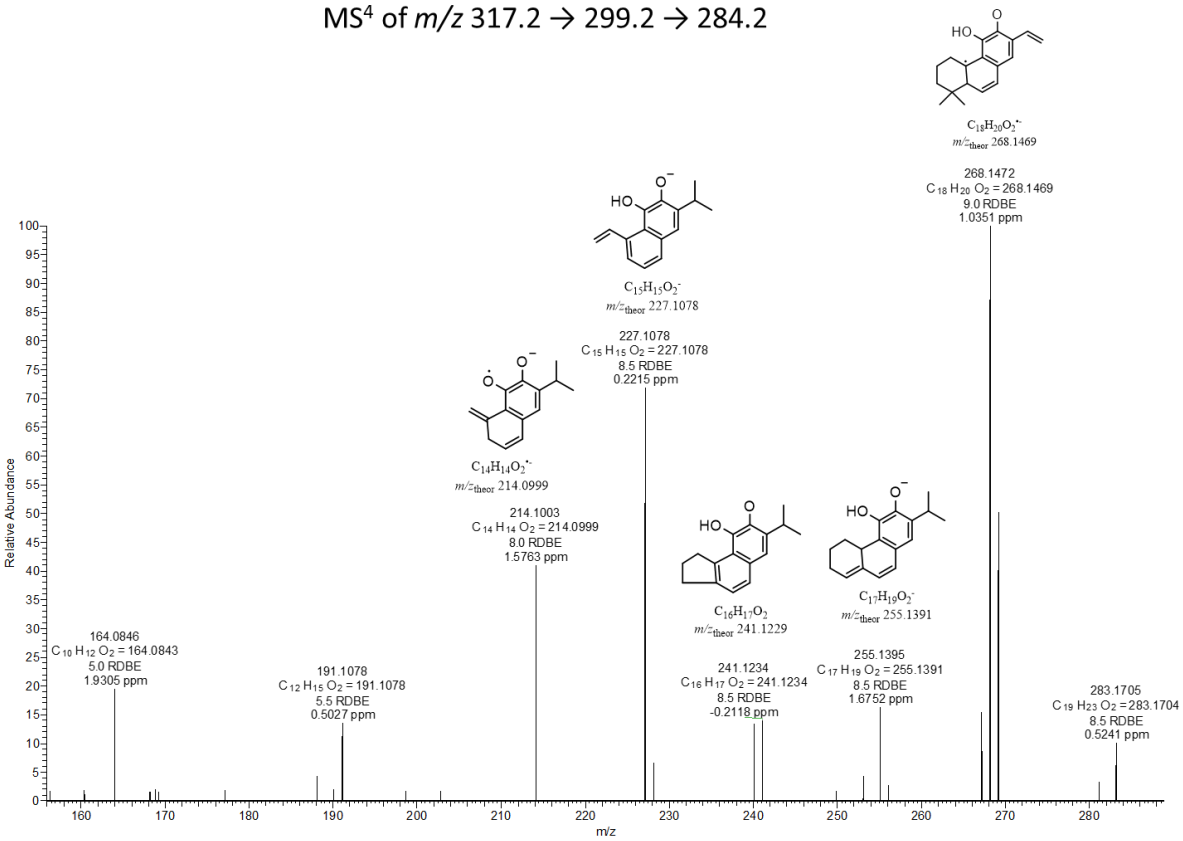

11-hydroxy sugiol (**6**)

MS^2 of *m/z* 315.2

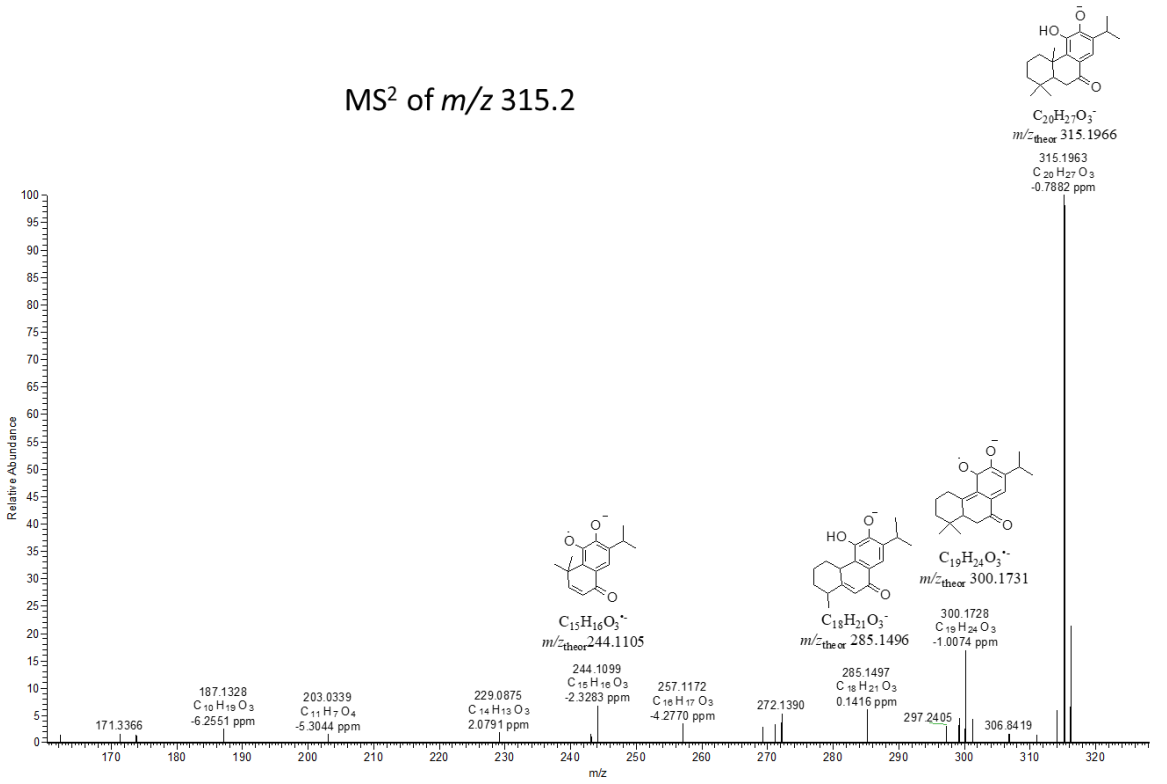

11-hydroxy sugiol (**6**)

MS^3 of *m/z* 315.2 → 285.2

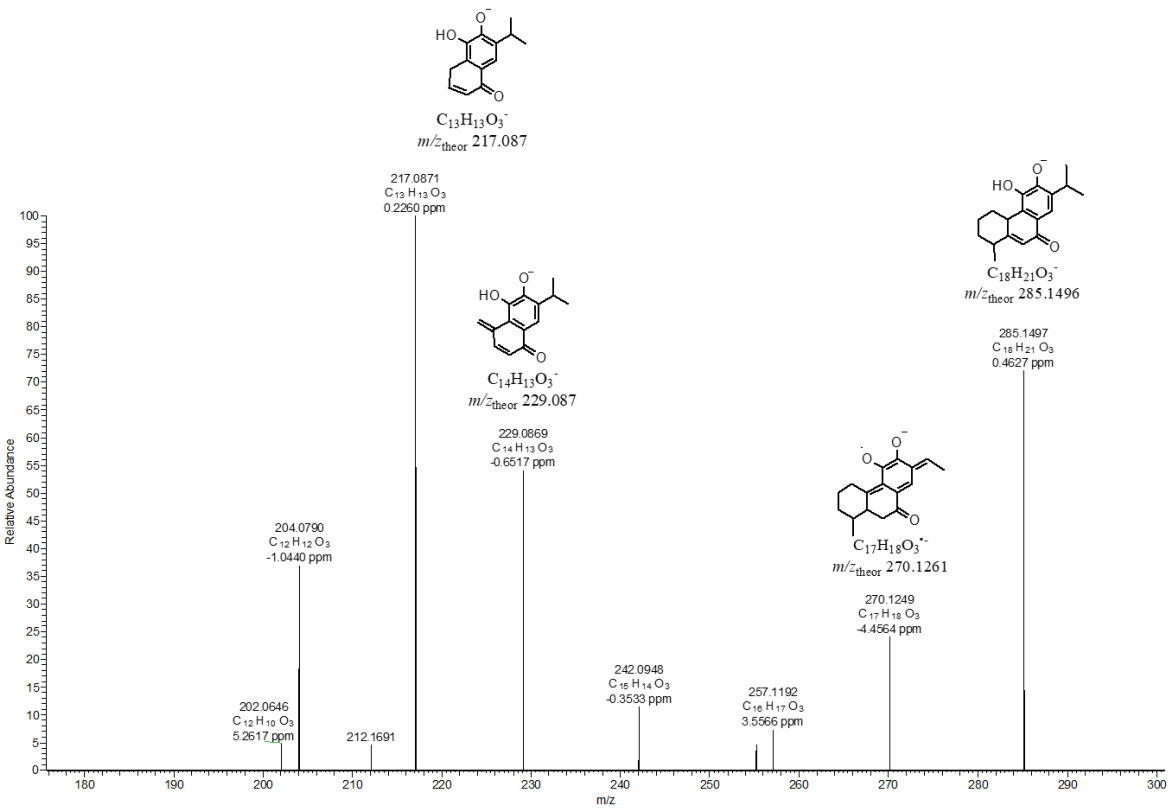

11,20-dihydroxy ferruginol (**8**)

MS^2 of *m/z* 317.2

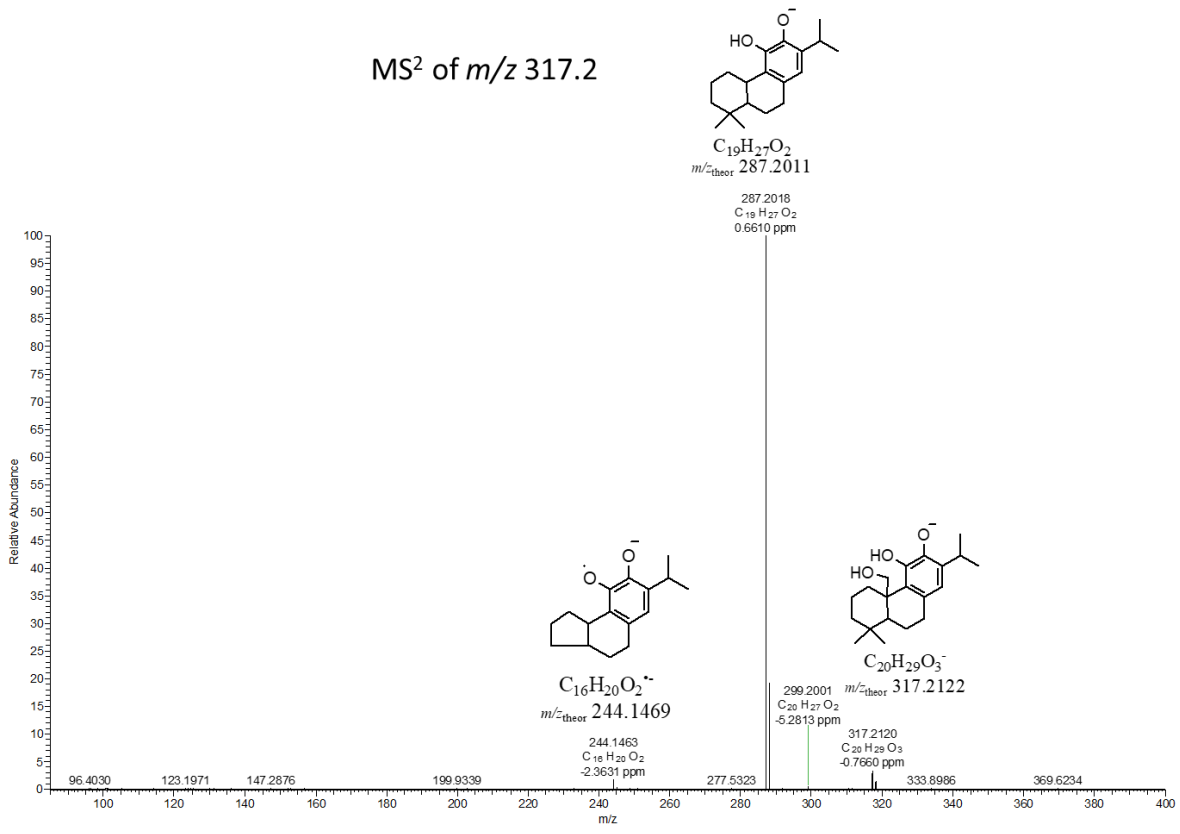

11,20-dihydroxy ferruginol (**8**)

MS^3 of *m/z* 317.2 → 287.2

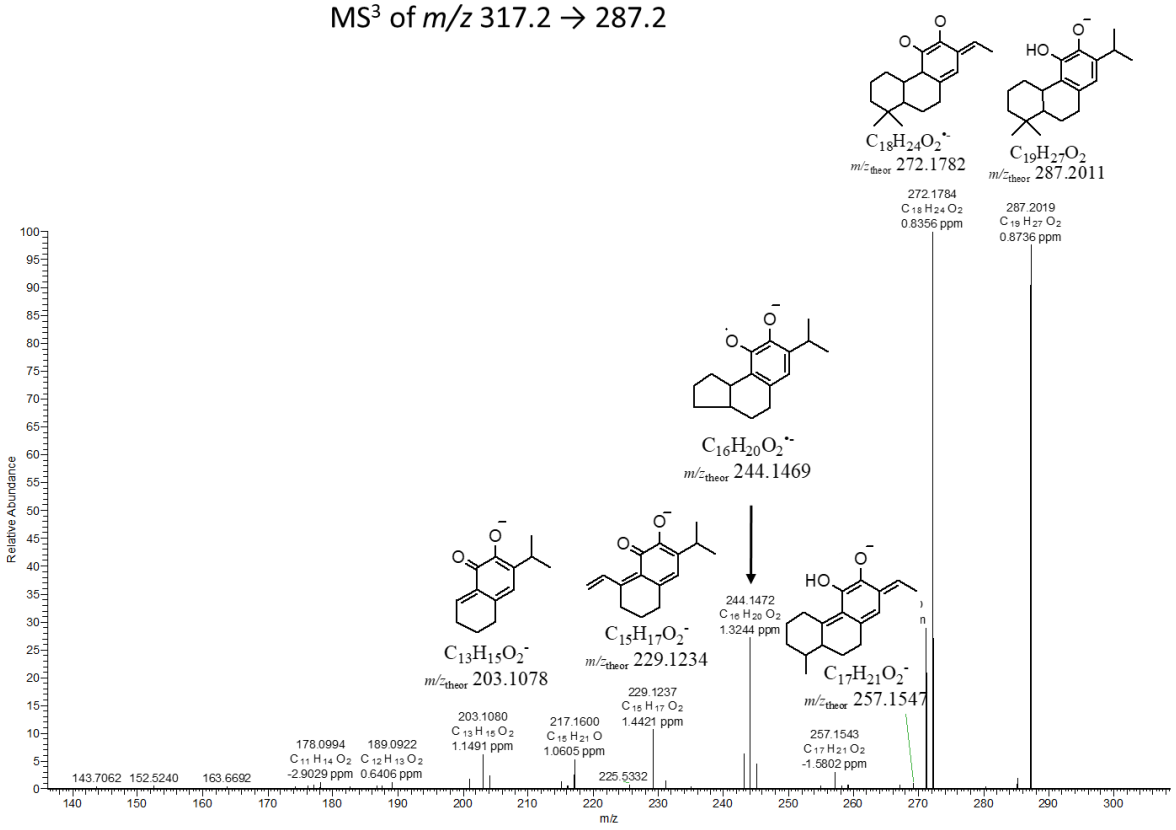

7,11,20-trihydroxy ferruginol (**9**)

MS^2 of *m/z* 333.2

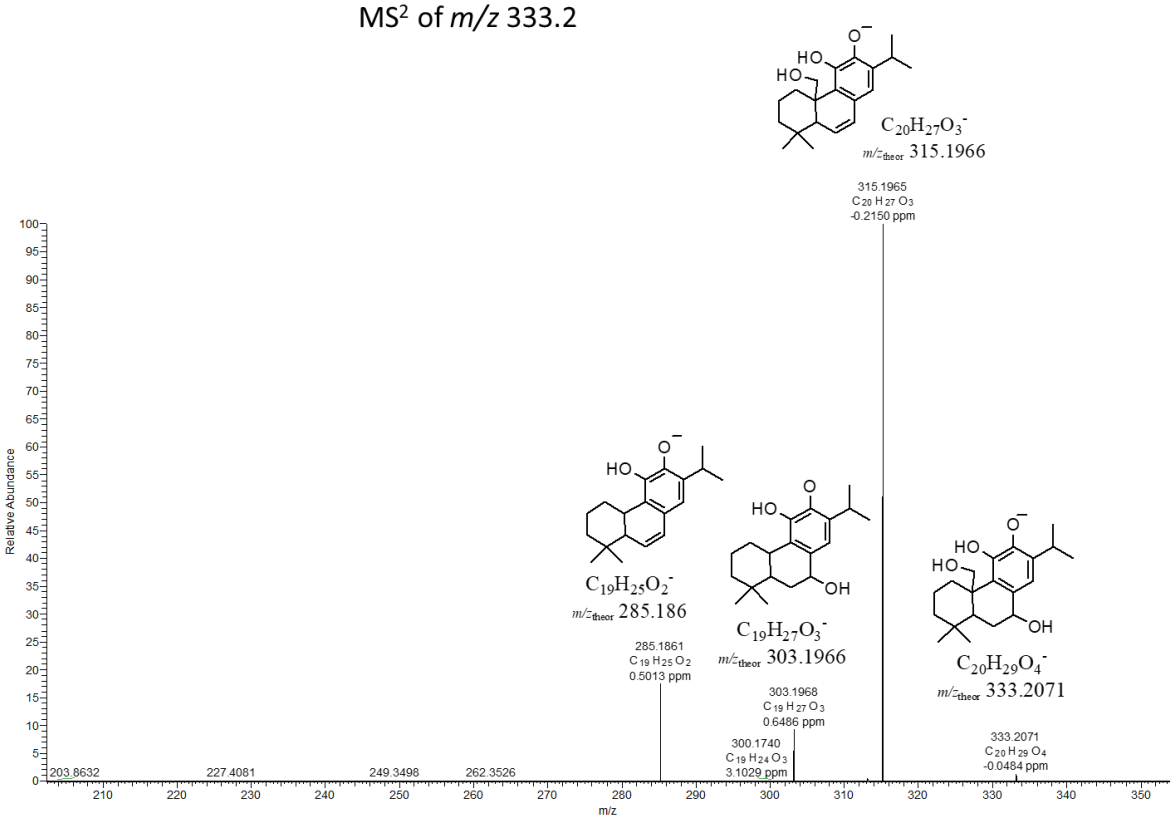

7,11,20-trihydroxy ferruginol (**9**)

MS^3 of *m/z* 333.2 → 303.2

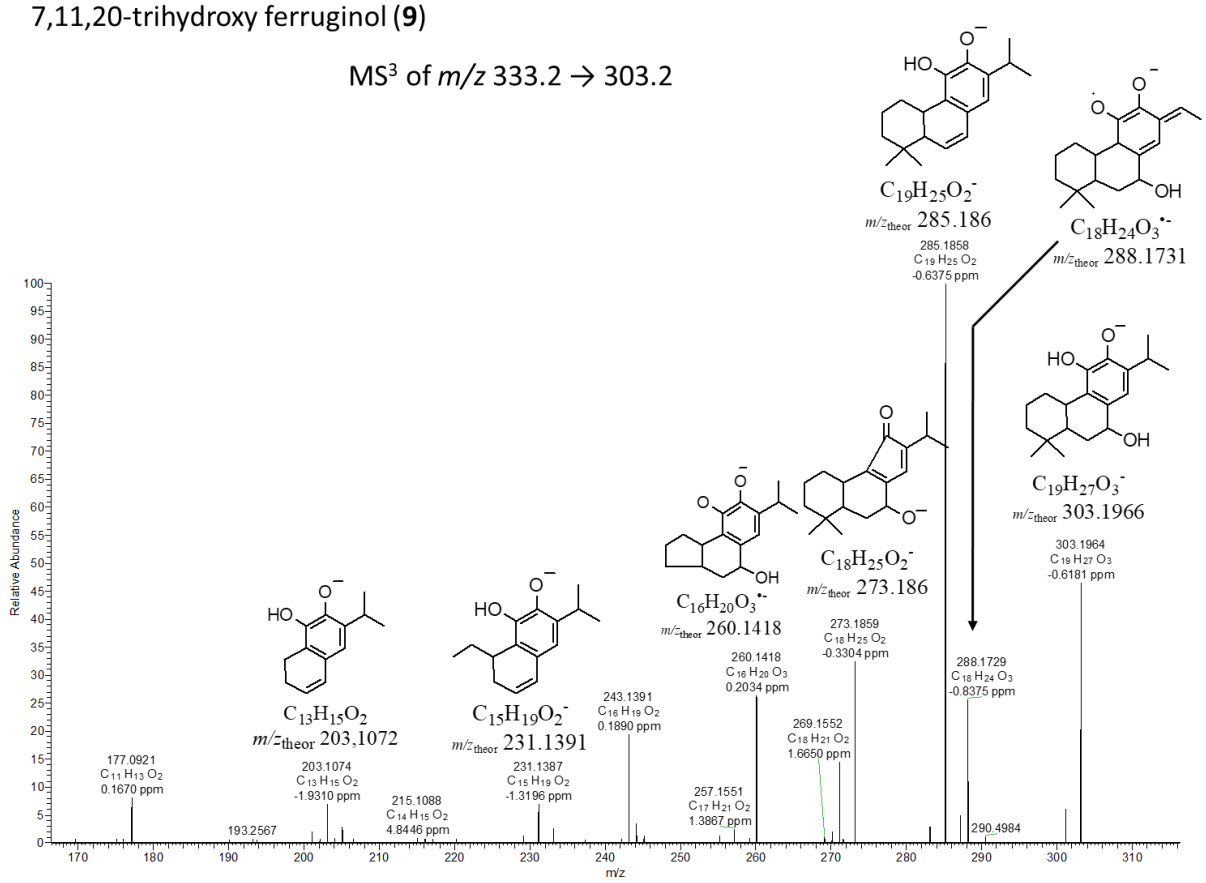

11,20-dihydroxy sugiol (**10**)

MS^2 of *m/z* 331.2

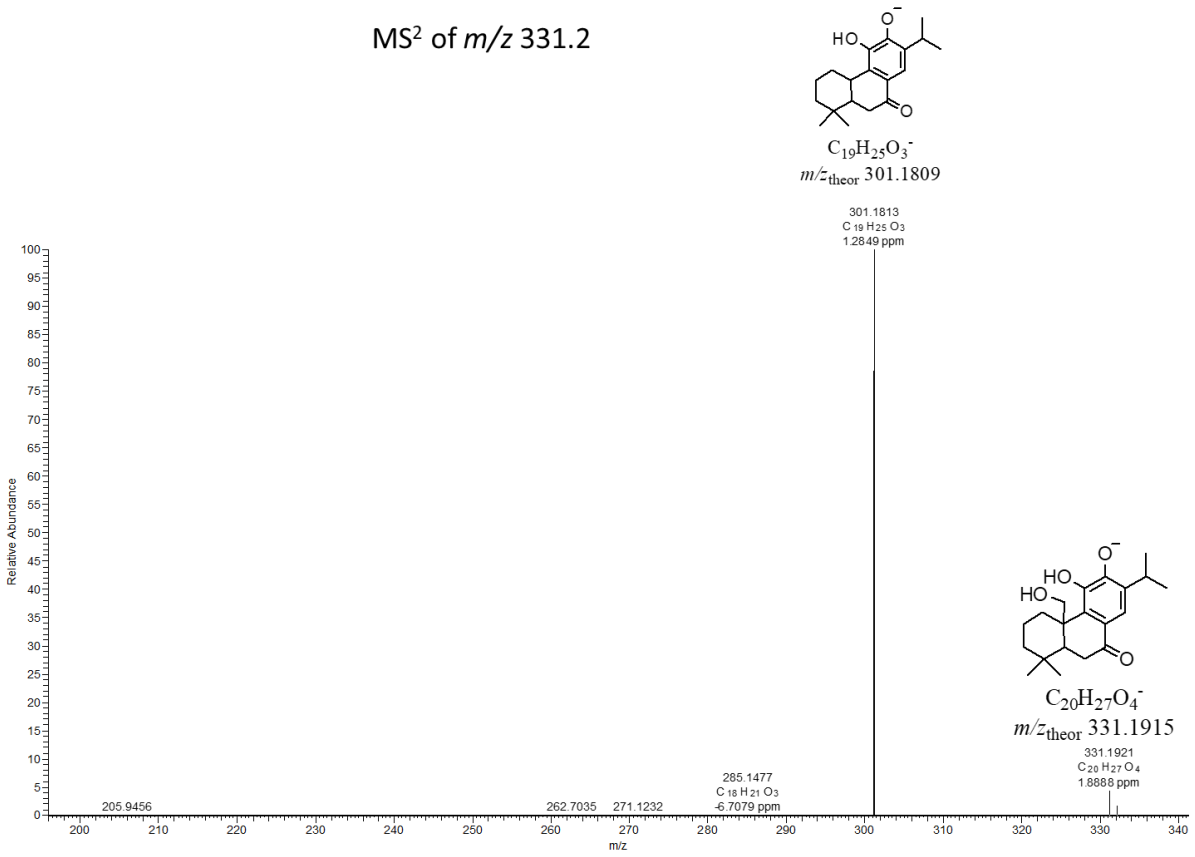

11,20-dihydroxy sugiol (**10**)

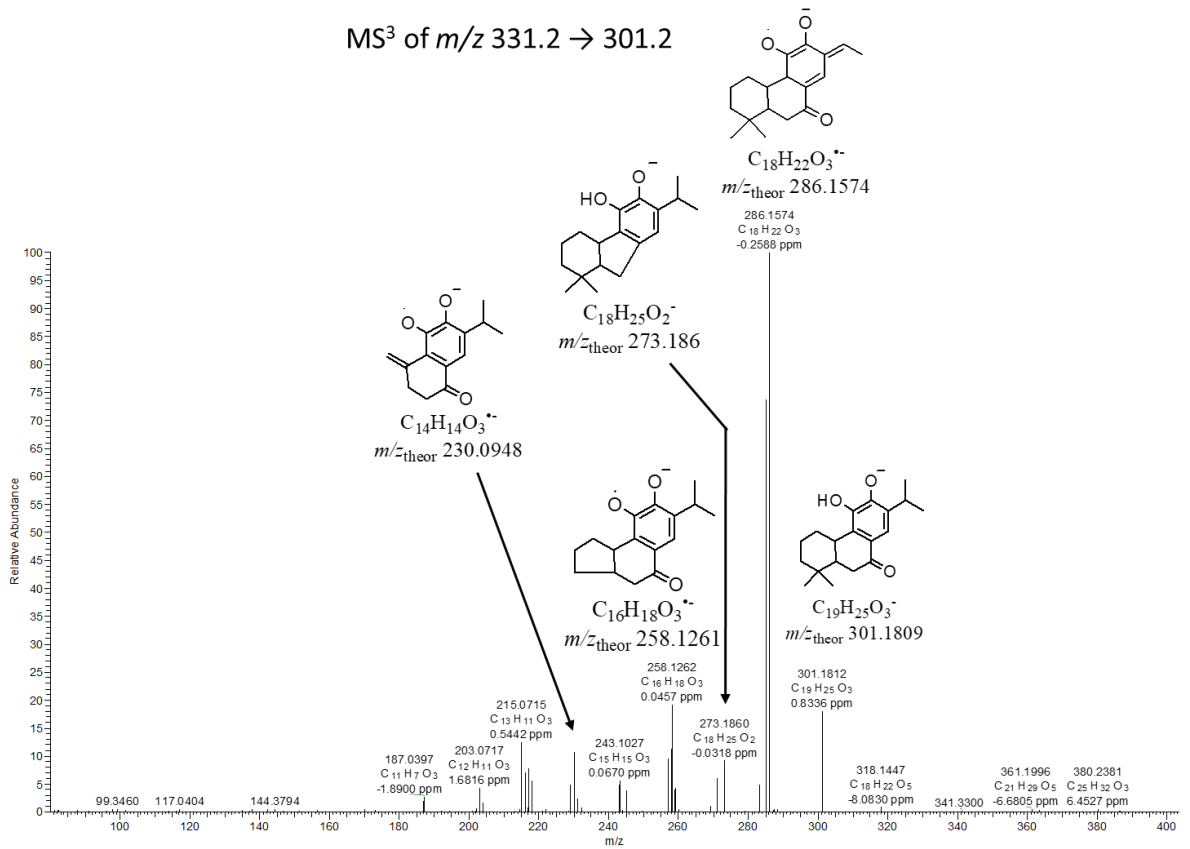

7-keto abietaquinone (**12**)

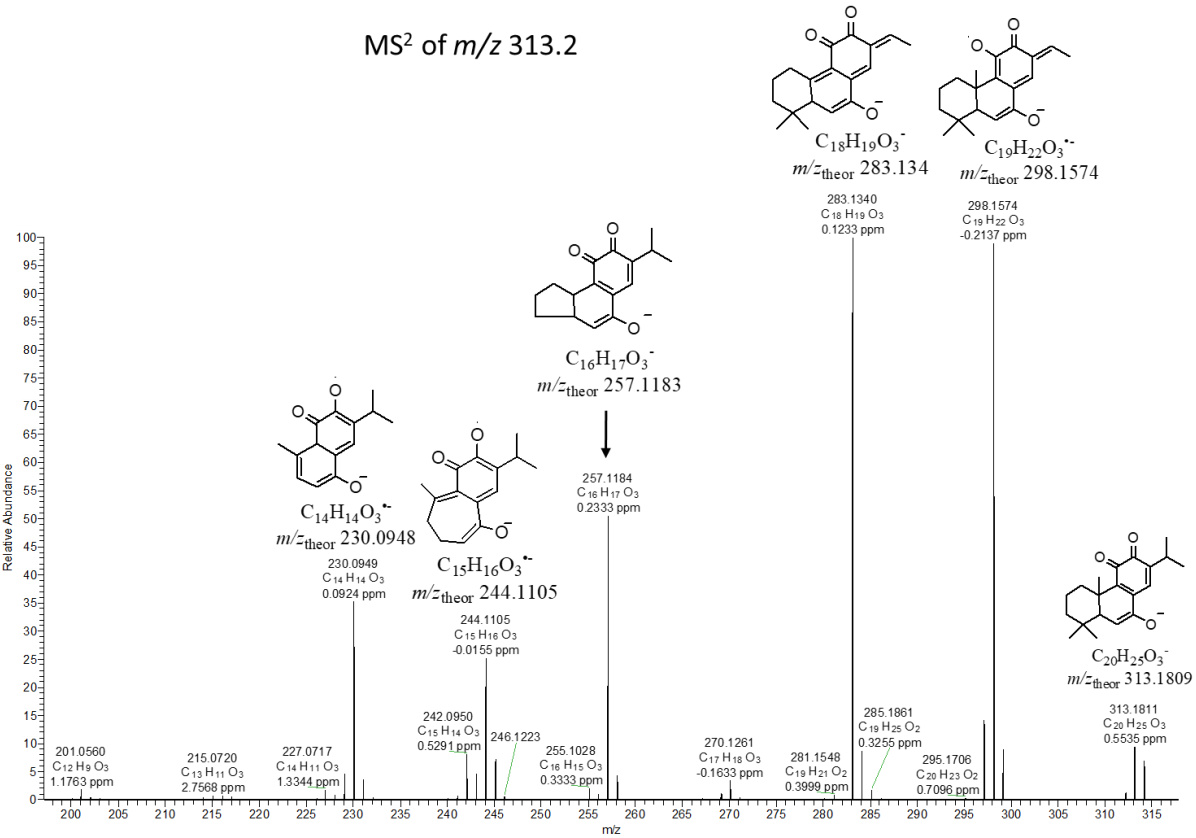

20-hydroxy abietaquinone (**13**)

MS^2 of *m/z* 315.2

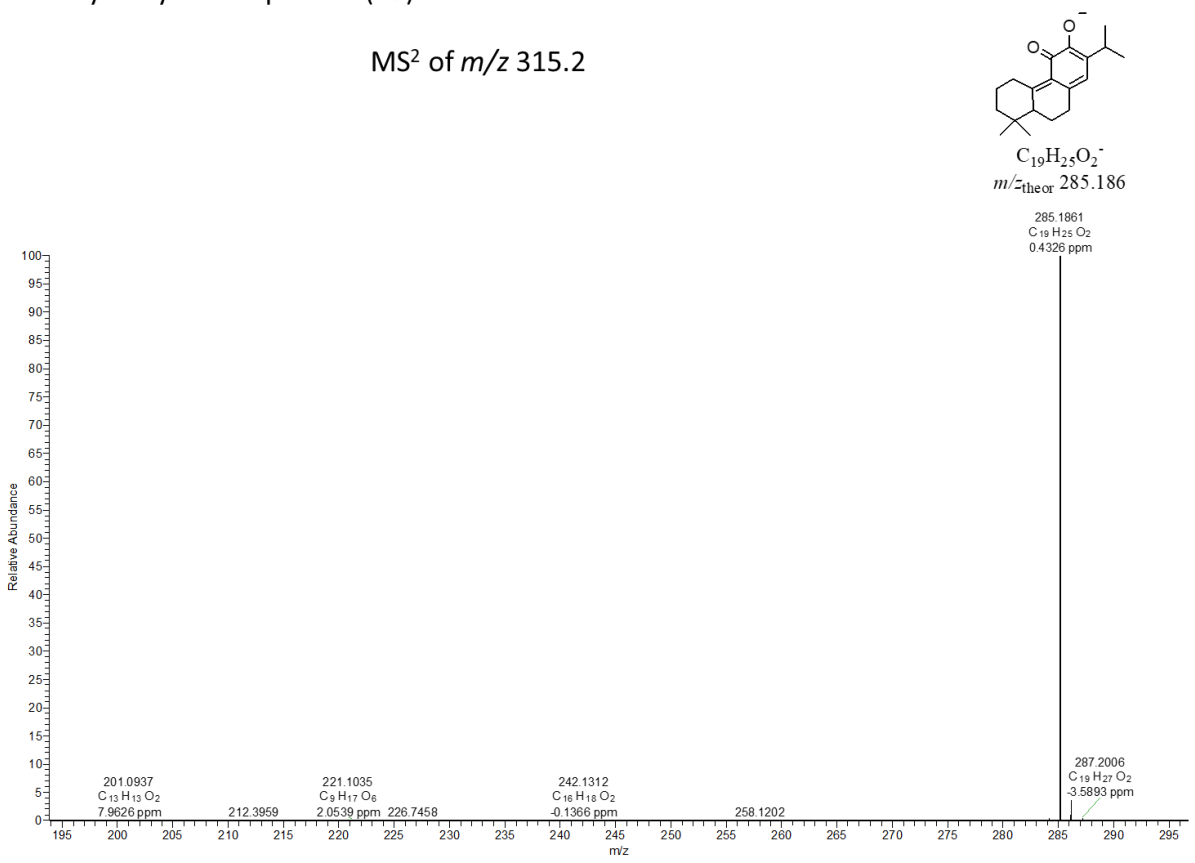

20-hydroxy abietaquinone (**13**)

MS^3 of *m/z* 315.2 → 285.2

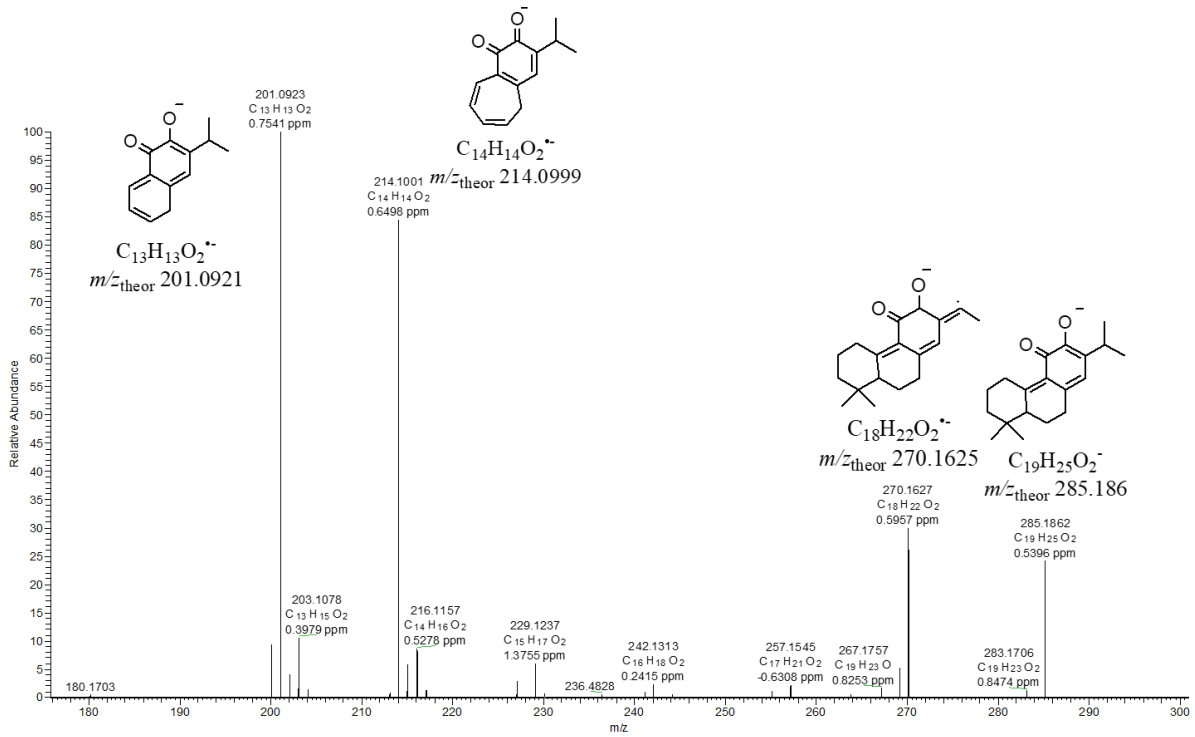

7,20-dihydroxy abietaquinone (**14**)

MS^2 of *m/z* 331.2

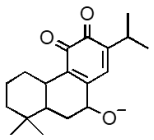

$C_{19}H_{25}O_3^-$
m/z_{theor} 301.1809

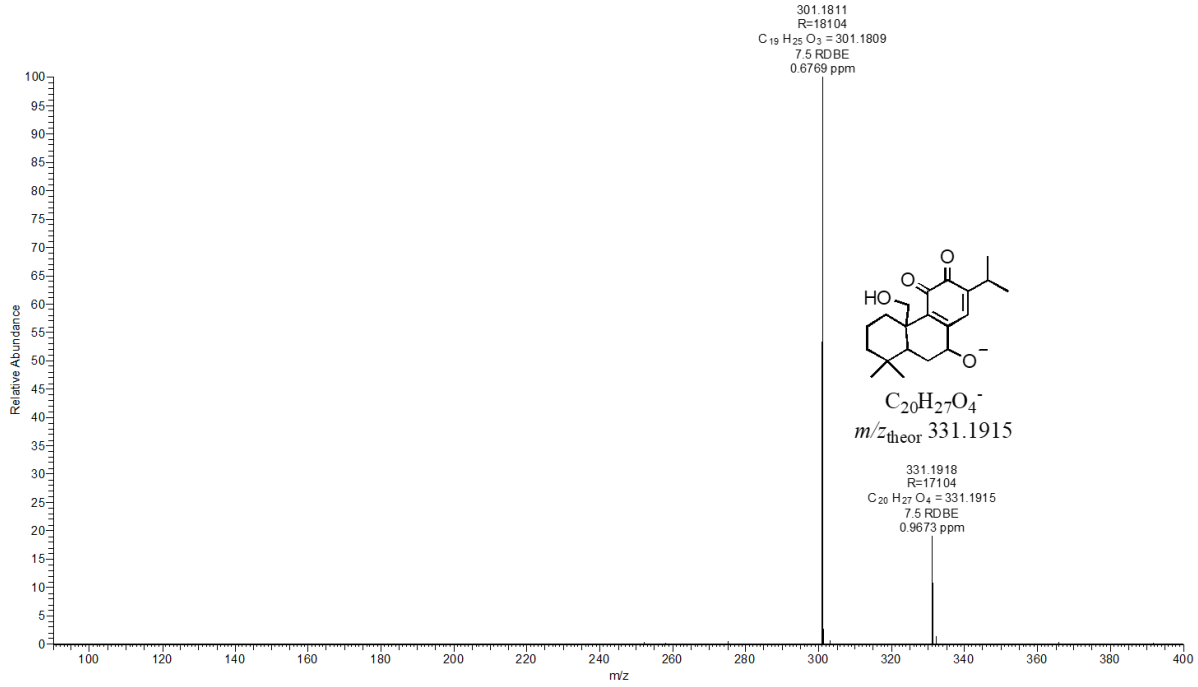

$C_{20}H_{27}O_4^-$
m/z_{theor} 331.1915

7,20-dihydroxy abietaquinone (**14**)

MS^3 of *m/z* 331.2 → 301.2

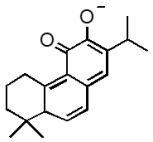

$C_{19}H_{23}O_2^-$
m/z_{theor} 283.1704

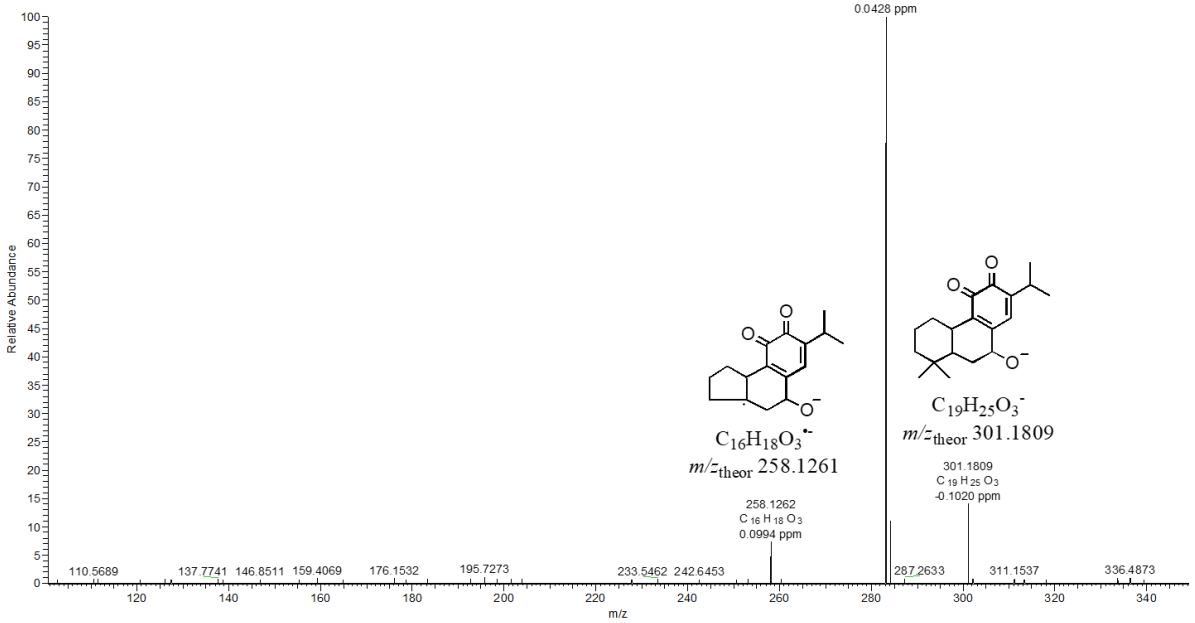

$C_{16}H_{18}O_3^{\bullet-}$
m/z_{theor} 258.1261

$C_{19}H_{25}O_3^-$
m/z_{theor} 301.1809

7-methoxy-11-hydroxy ferruginol (**15**)

MS^2 of *m/z* 331.2

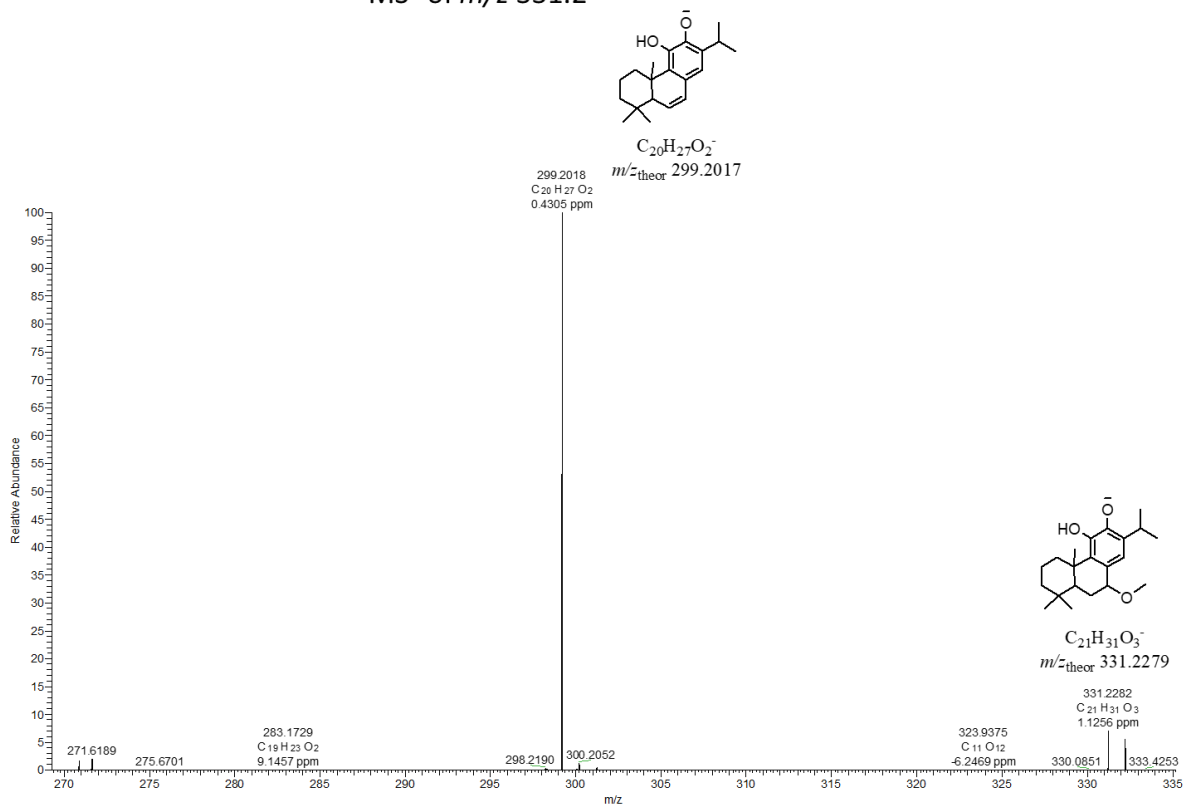

7-methoxy-11-hydroxy ferruginol (**15**)

MS^2 of *m/z* 331.2

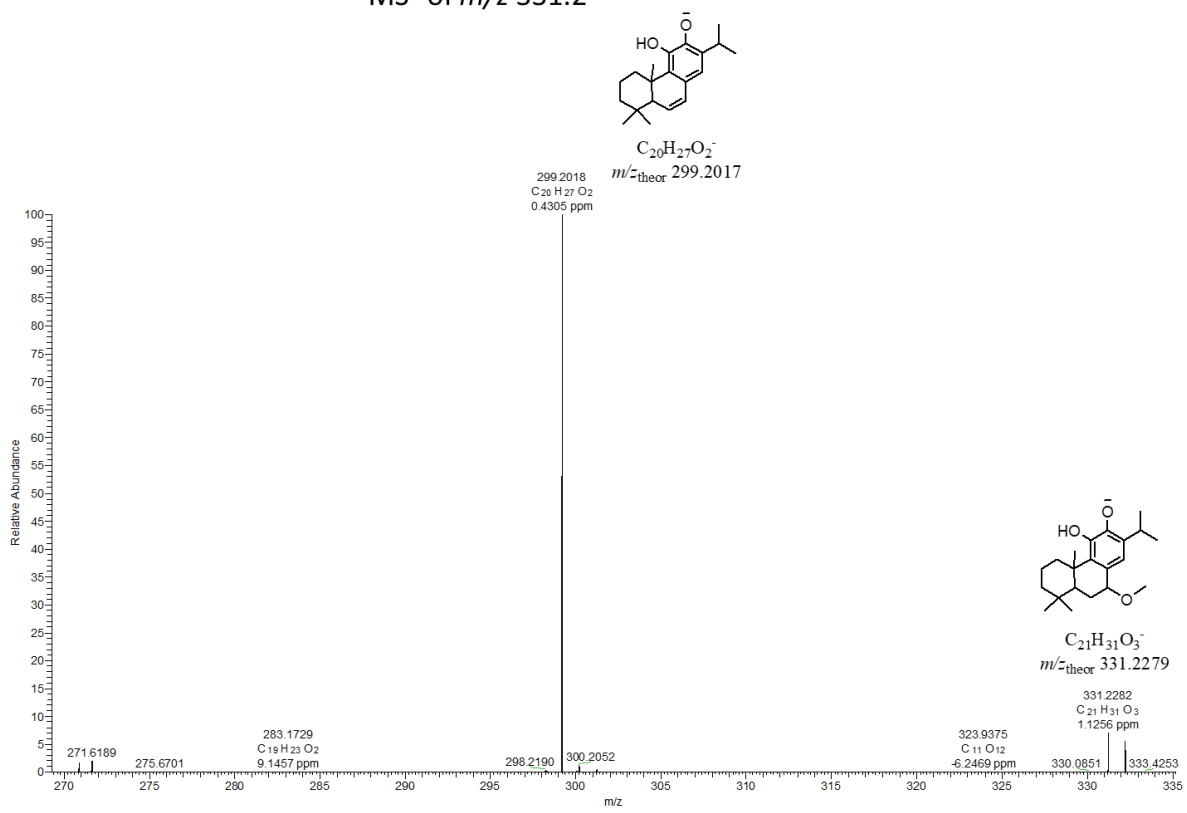

7-methoxy-11-hydroxy ferruginol (**15**)

MS^4 of *m/z* 331.2 → 299.2 → 284.2

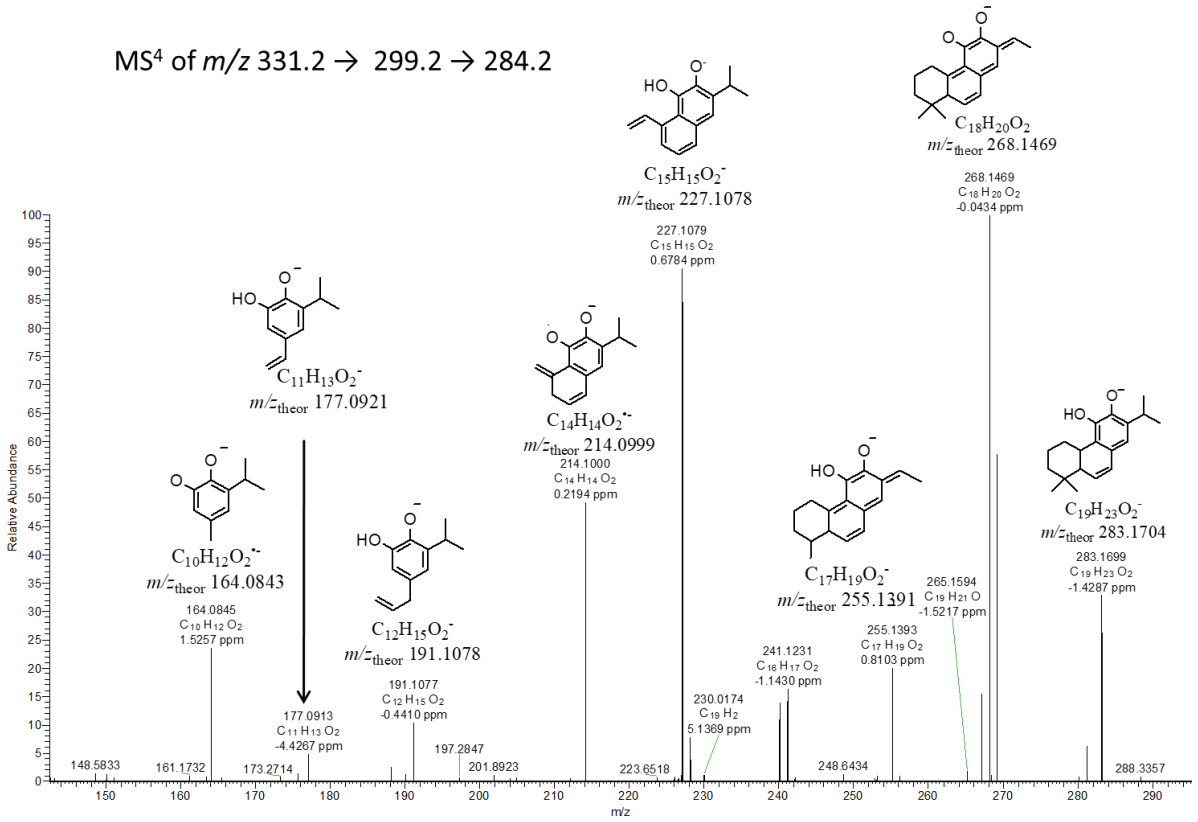

7-methoxy-11,20-dihydroxy ferruginol (**16**)

MS^2 of *m/z* 347.2

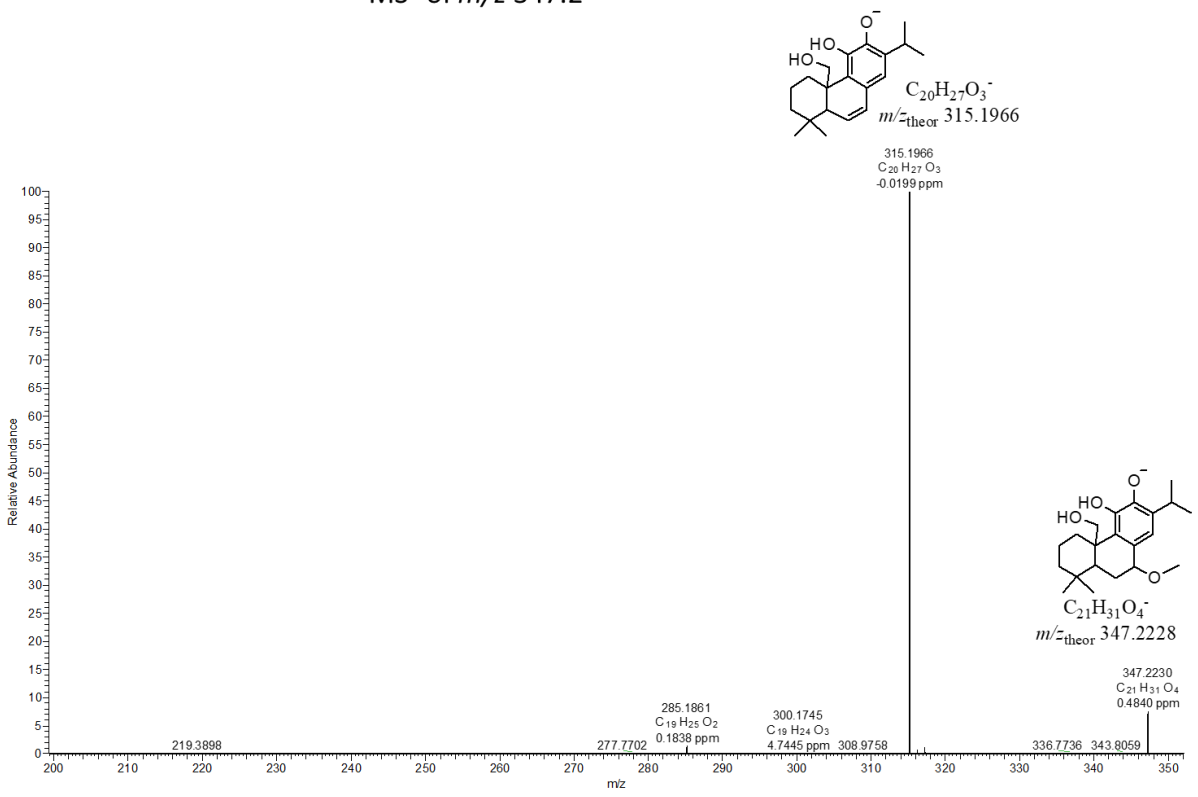

7-methoxy-11,20-dihydroxy ferruginol (**16**)

MS^3 of *m/z* 347.2 → 315.2

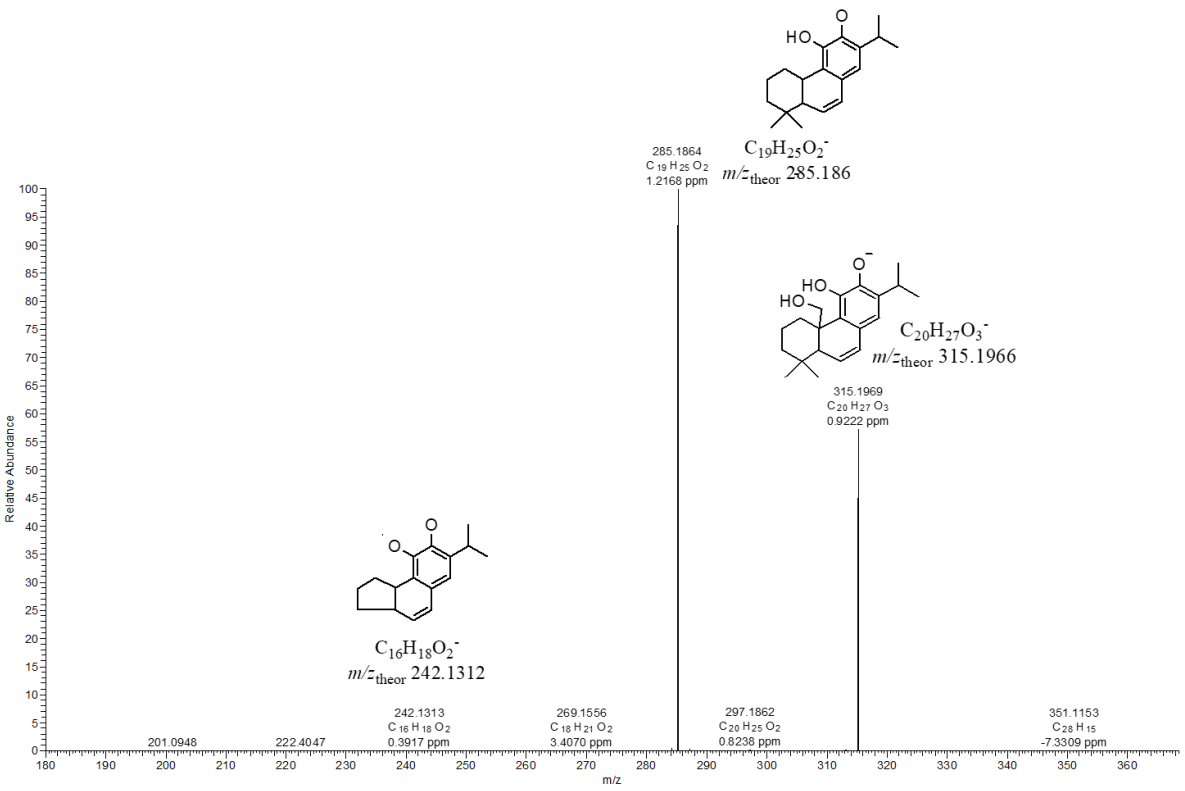

7-methoxy-11,20-dihydroxy ferruginol (**16**)

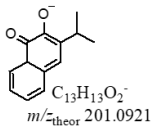

MS^4 of *m/z* 347.2 → 315.2 → 385.2

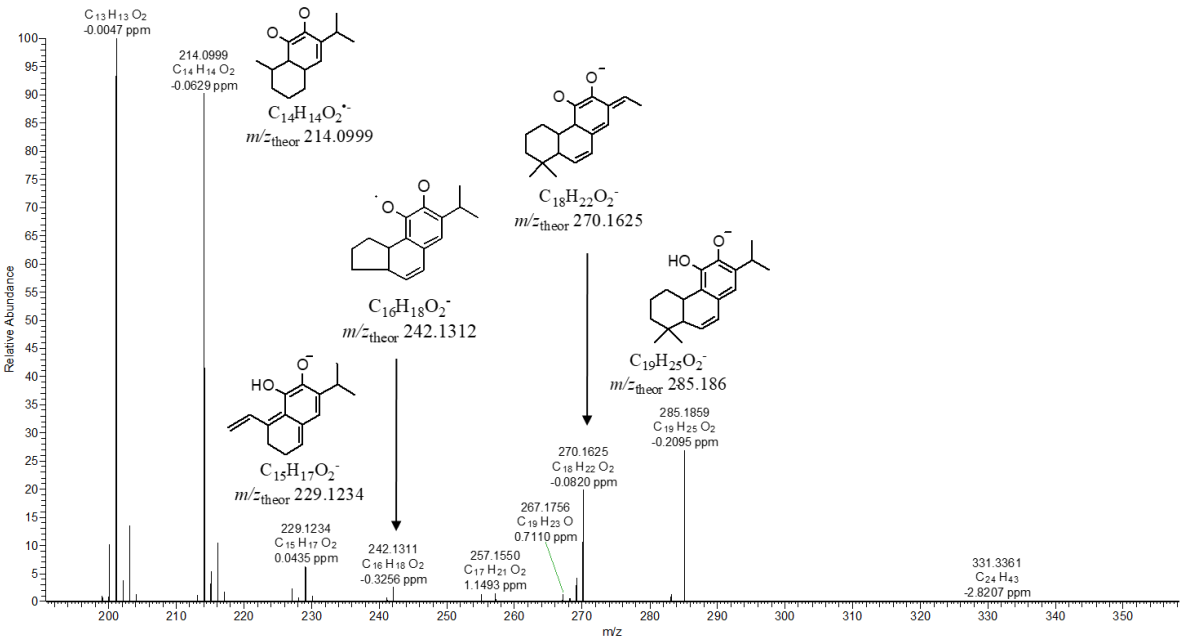

Figure S3: Tandem mass spectra (MS^2, MS^3 and MS^4) acquired for *m/z* 317.2 (**Figure S4** panels A and C), 315.2 (**Figure S4** panels B and G), 333.2 (**Figure S4** panel D), 331.2 (**Figure S4** panels E, H and I), 347.2 (**Figure S4** panel J), corresponding to the $[M-H]^-$ ions of 7,11-dihydroxy ferruginol (**5**, **Figure S4** panel A), 11-hydroxy sugiol (**6**, **Figure S4** panel B), 11,20-dihydroxy ferruginol (**8**, **Figure S4** panel C), 7,11,20-trihydroxy ferruginol (**9**, **Figure S4** panel D), 11,20-dihydroxy sugiol (**10**, **Figure S4** panel E), 7-keto abietaquinone (**12**, **Figure S4** panel F), 20-hydroxy abietaquinone (**13**, **Figure S4** panel G), 7,20-dihydroxy abietaquinone (**14**, **Figure S4** panel H), 7-methoxy-11-hydroxy ferruginol (**15**, **Figure S4** panel I) and 7-methoxy-11,20-dihydroxy ferruginol (**16**, **Figure S4** panel J). The spectra were acquired with an Orbitrap Elite hybrid linear ion trap-orbital trap (LIT-Orbitrap) mass spectrometer, operating in the negative ion FT-MS mode.

A 7,11-dihydroxy ferruginol (**5**)

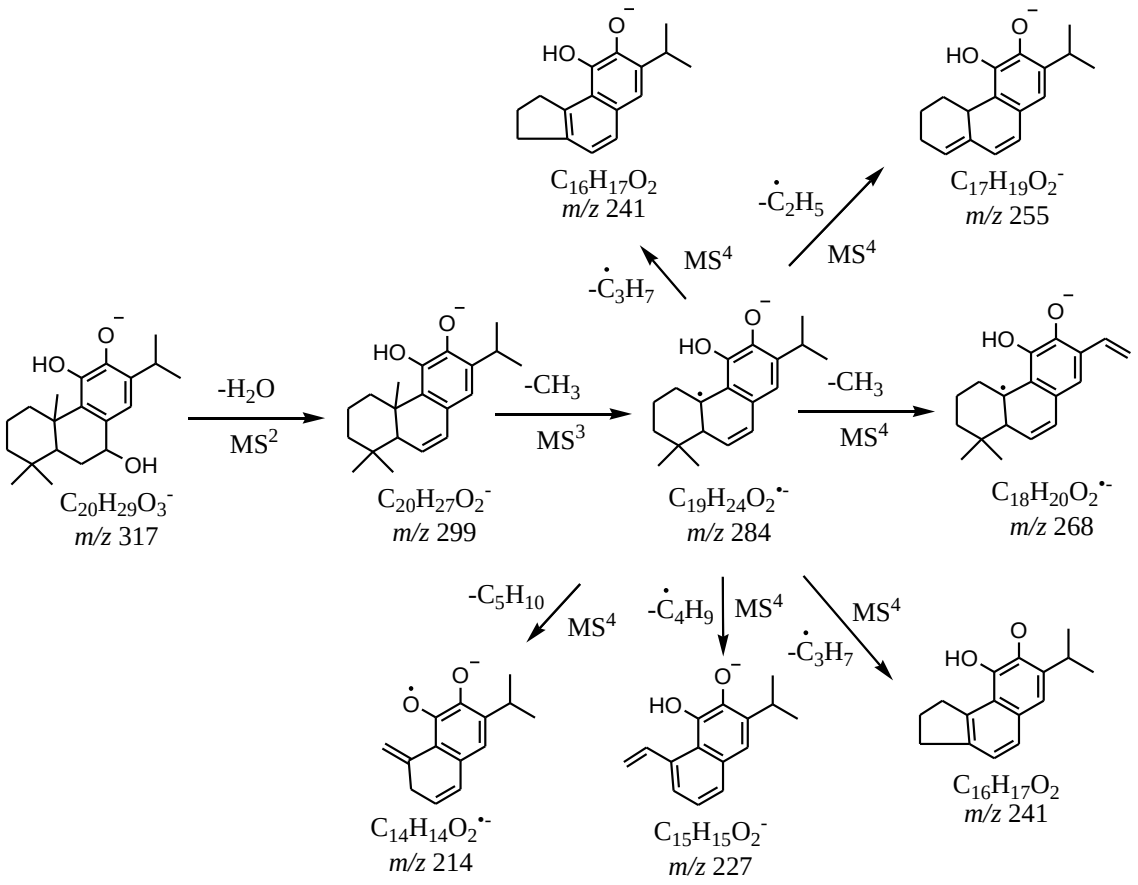

B 11-hydroxy sugiol (**6**)

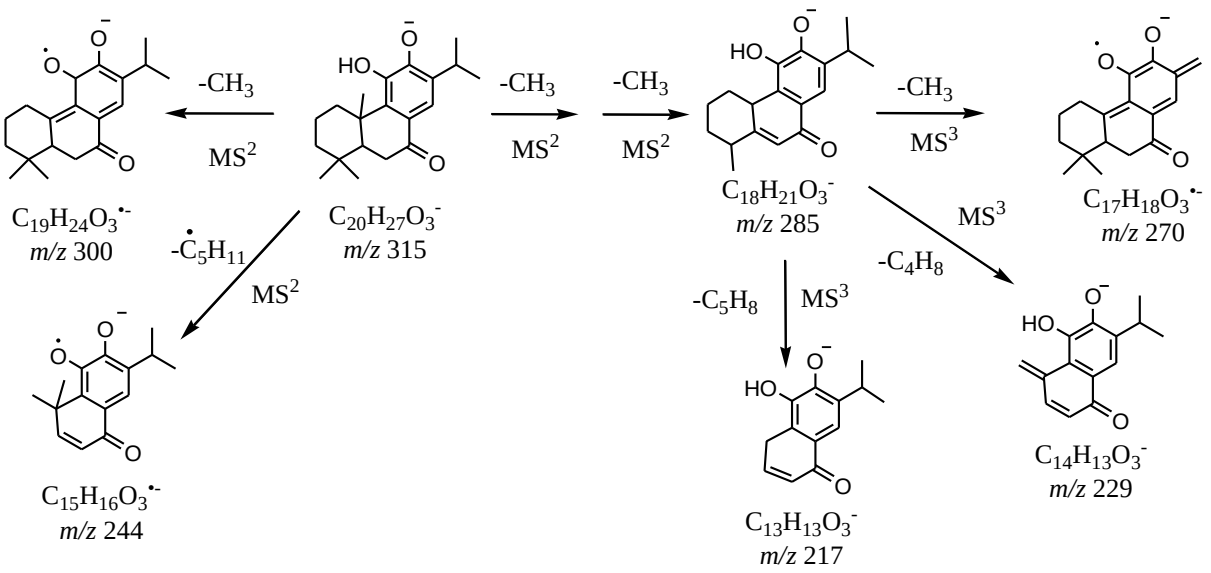

C 11,20-dihydroxy ferruginol (**8**)

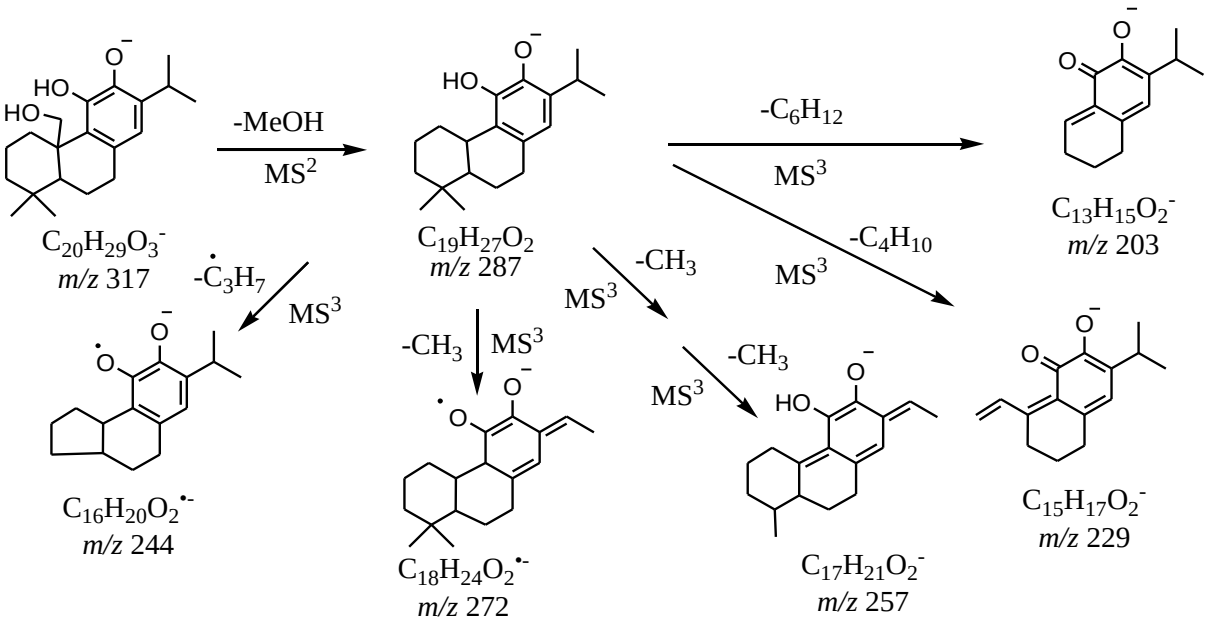

D 7,11,20-trihydroxy ferruginol (**9**)

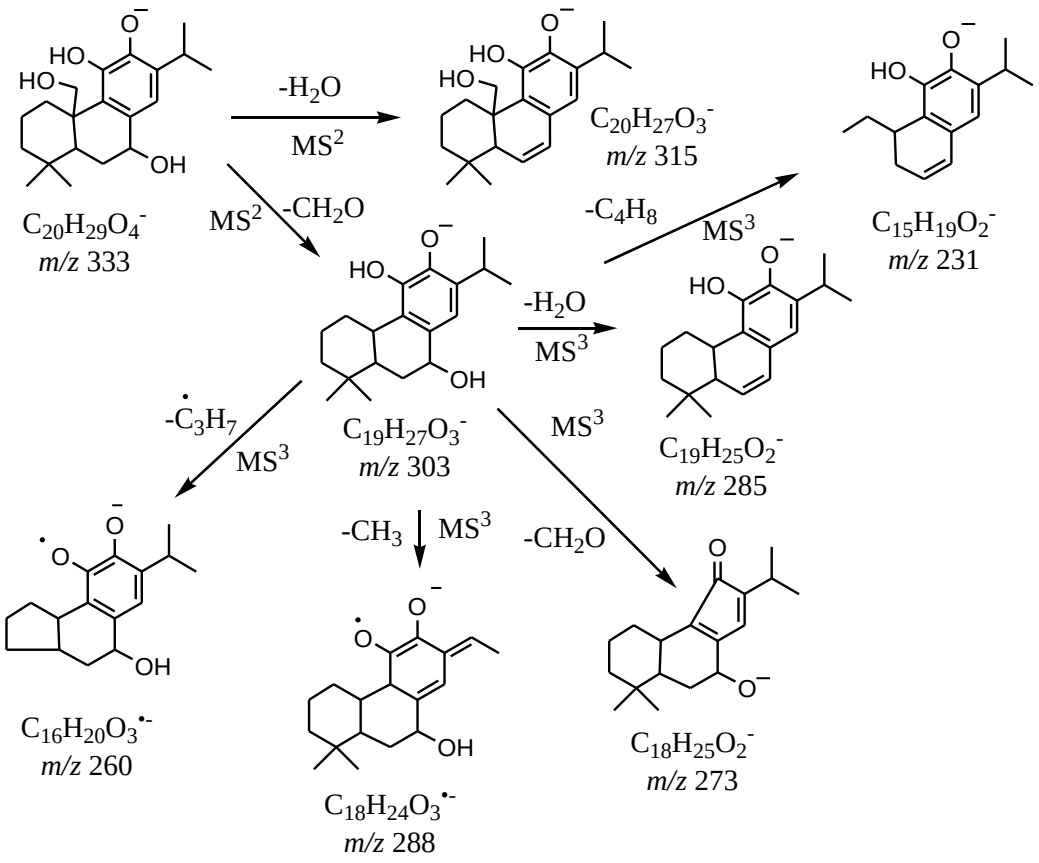

E 11,20-dihydroxy sugiol (**10**)

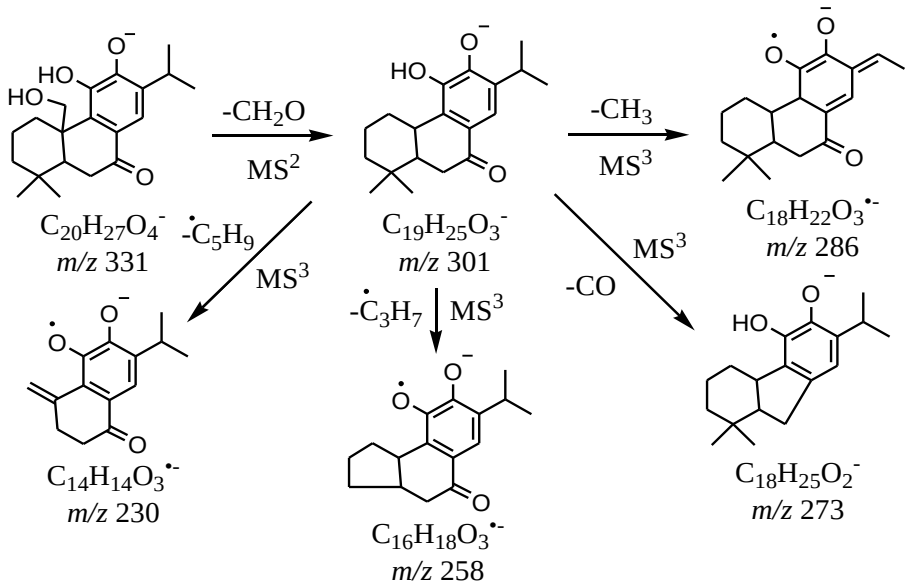

F 7-keto abietaquinone (**12**)

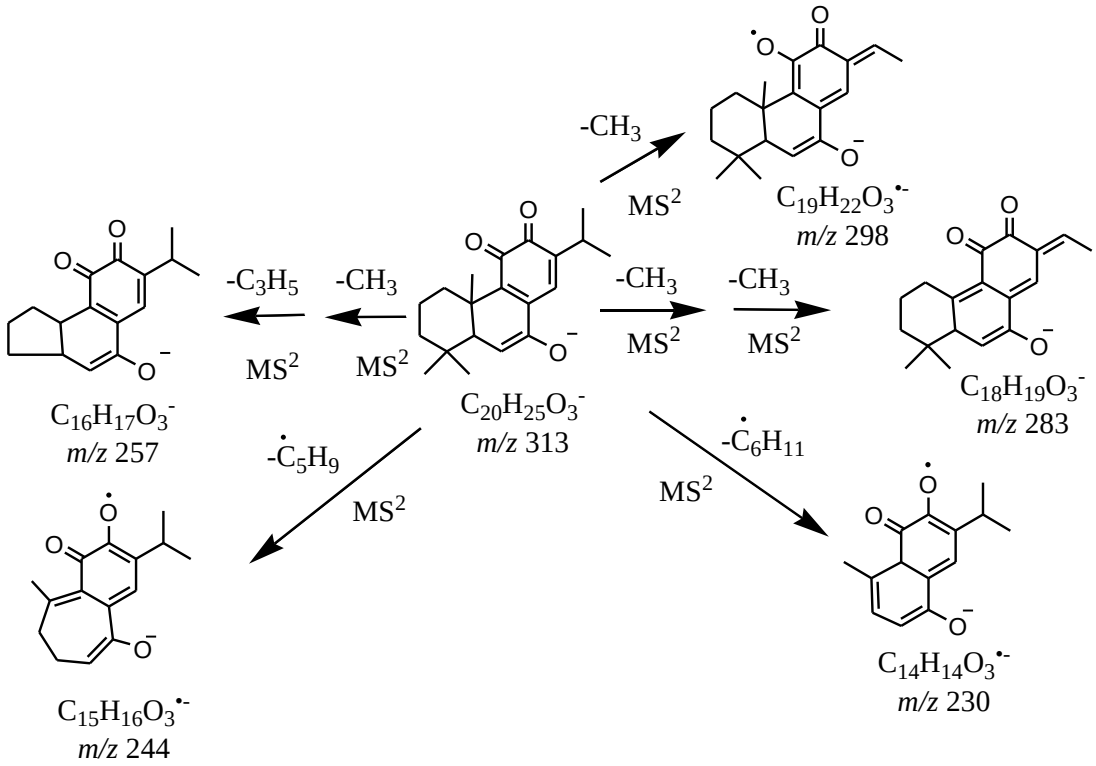

G 20-hydroxy abietaquinone (**13**)

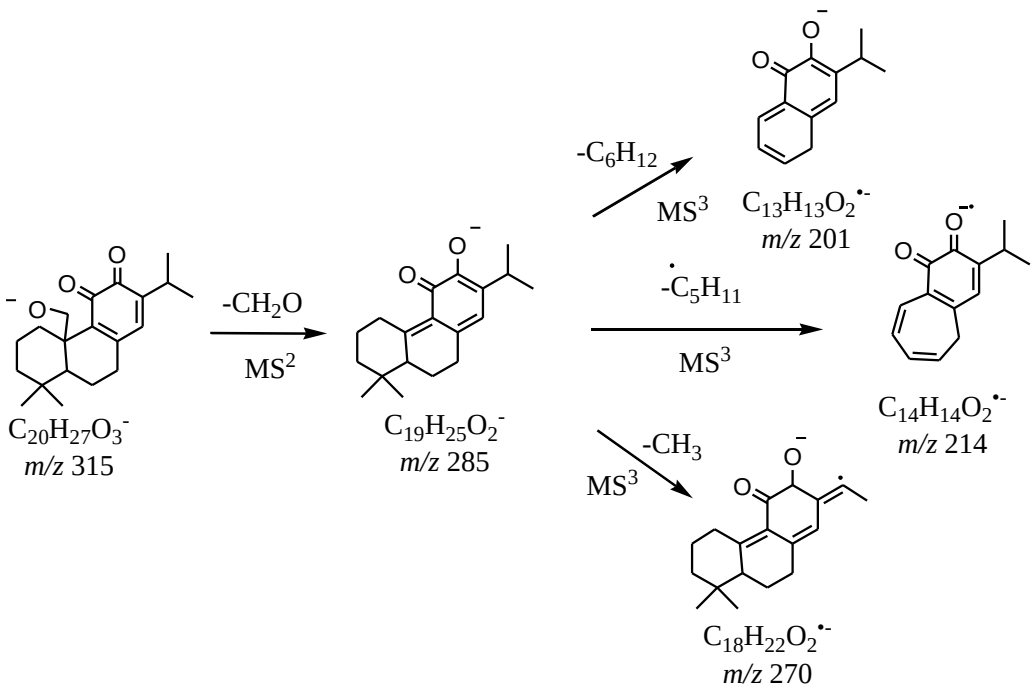

H 7,20-dihydroxy abietaquinone (**14**)

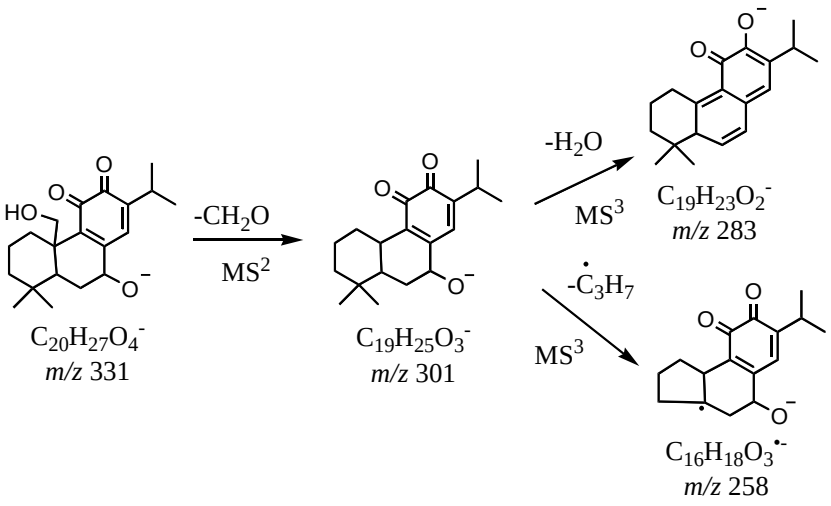

I 7-methoxy-11-hydroxy ferruginol (**15**)

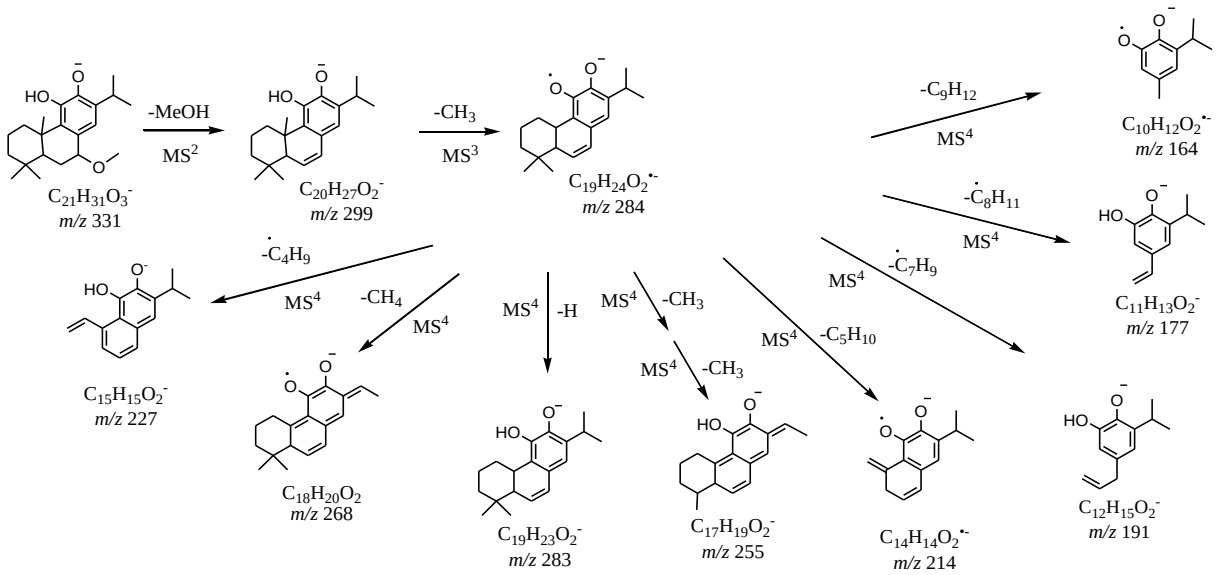

J 7-methoxy-11,20-dihydroxy ferruginol (**16**)

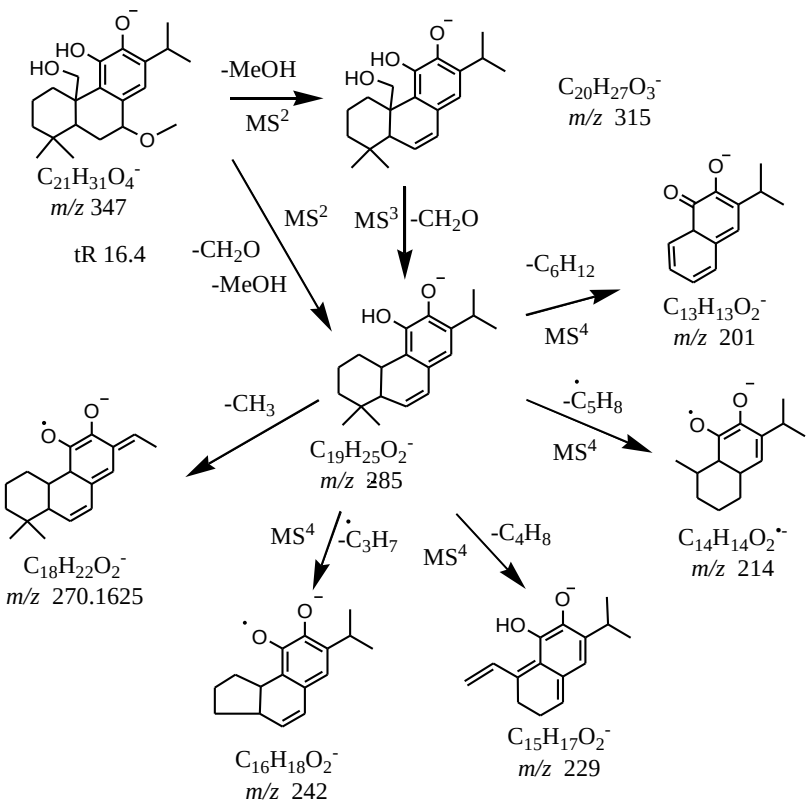

Figure S4: Tandem mass spectrometric (MS^n) fragmentation patterns obtained with the collision-induced dissociation (CID) capability of a hybrid linear ion trap-orbital trap (LIT-Orbitrap) mass spectrometer (LTQ-Orbitrap Elite) for *m/z* 317.2 (panels A and C), 315.2 (panels B and G), 333.2 (panel D), 331.2 (panels E, H and I), 347.2 (panel J), corresponding to the $[M-H]^-$ ions of 7,11-dihydroxy ferruginol (**5**, panel A), 11-hydroxy sugiol (**6**, panel B), 11,20-dihydroxy ferruginol (**8**, panel C), 7,11,20-trihydroxy ferruginol (**9**, panel D), 11,20-dihydroxy sugiol (**10**, panel E), 7-keto abietaquinone (**12**, panel F), 20-hydroxy abietaquinone (**13**, panel G), 7,20-dihydroxy abietaquinone (**14**, panel H), 7-methoxy-11-hydroxy ferruginol (**15**, panel I) and 7-methoxy-11,20-dihydroxy ferruginol (**16**, panel J).

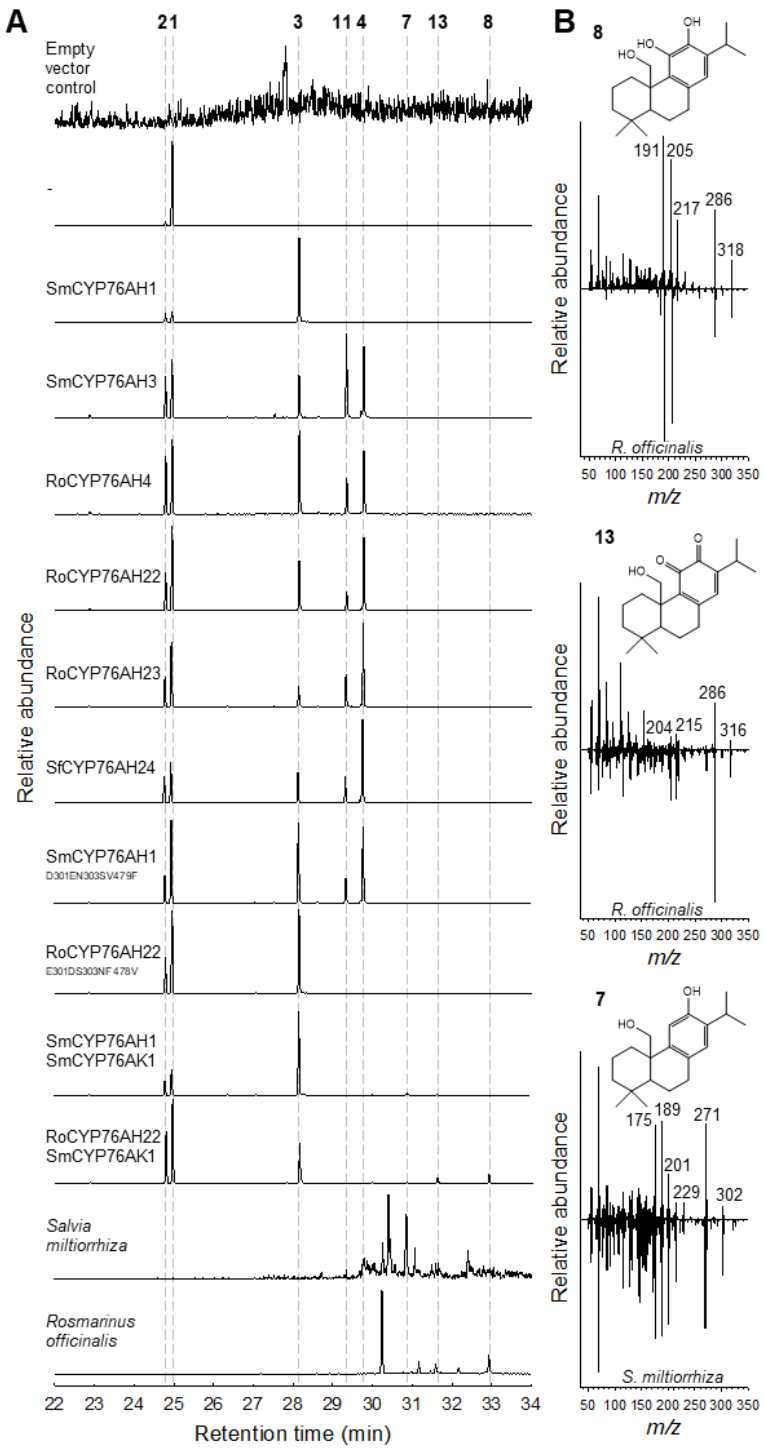

Figure S5: Chromatographic analysis of rosemary leaf surface extracts, sage root extracts or hexane extracts from yeast strains expressing the CM (core module) and the given CYPs. A, Results of GC-MS analysis (selected *m/z* signals: 270, 272, 286, 300, 302, 316 and 318). The labeled peaks correspond to miltiradiene (**1**), abietatriene (**2**), ferruginol (**3**), 11-hydroxy ferruginol (**4**), pisiferol (**7**), 11,20-dihydroxy ferruginol (**8**), abietaquinone (**11**) and 20-hydroxy abietaquinone (**13**). B, Electron impact mass spectra of ADs isolated from yeast (upper panel), which express the required enzymes for the biosynthesis, compared to ADs isolated from rosemary leaves or sage roots (lower panel).

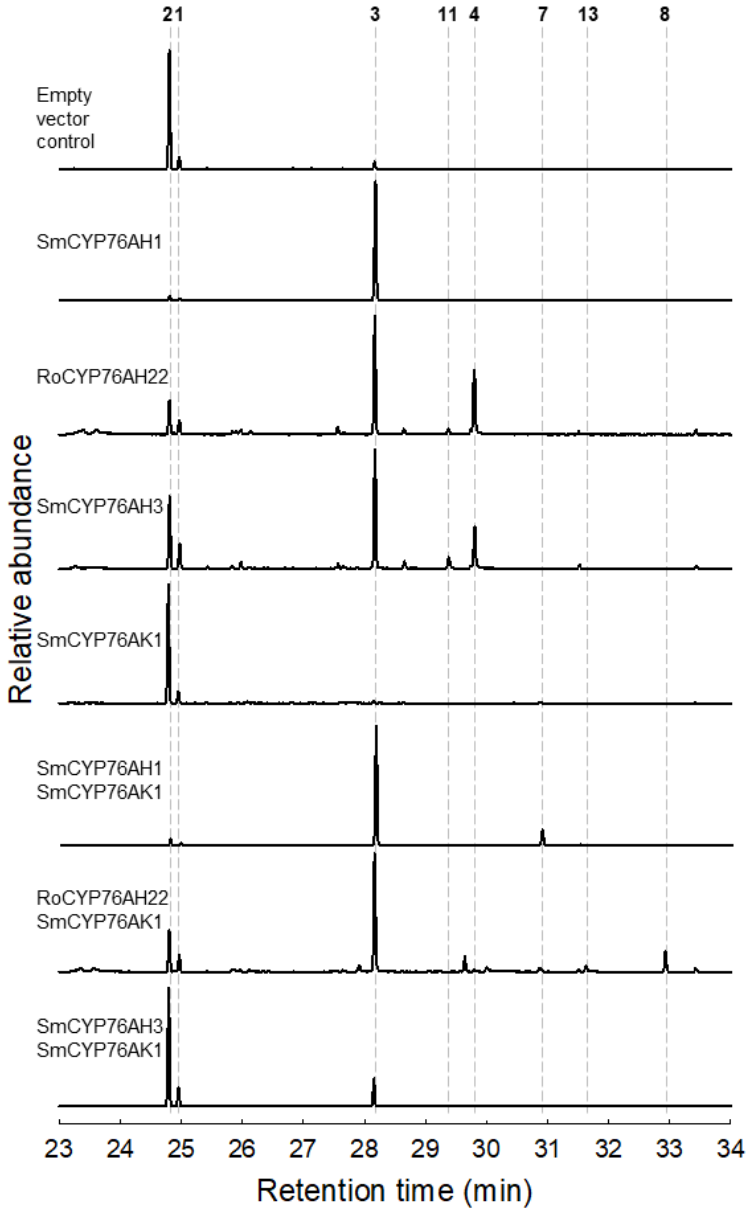

Figure S6: GC-MS analysis (selected *m/z* signals: 270, 272, 286, 300, 302, 316 and 318) of *in vitro* enzyme assays from microsomal preparations. ATR1 and the indicated enzymes were incubated with miltiradiene/abietatriene as substrate. Unfortunately, the substrate is not completely free of ferruginol (see empty vector control). However, all samples were treated and measured the same way, whereby the peak abundance of ferruginol (**3**) compared to miltiradiene (**1**)/abietatriene (**2**) can be compared. Ferruginol formation is therefore clearly shown for CYP76AH1, CYP76AH3 and CYP76AH22 by appearance of strong peak 3 in comparison to **1** and **2**. The labeled peaks are miltiradiene (**1**), abietatriene (**2**), ferruginol (**3**), 11-hydroxy ferruginol (**4**), pisiferol (**7**), 11,20-dihydroxy ferruginol (**8**), abietaquinone (**11**) and 20-hydroxy abietaquinone (**13**).

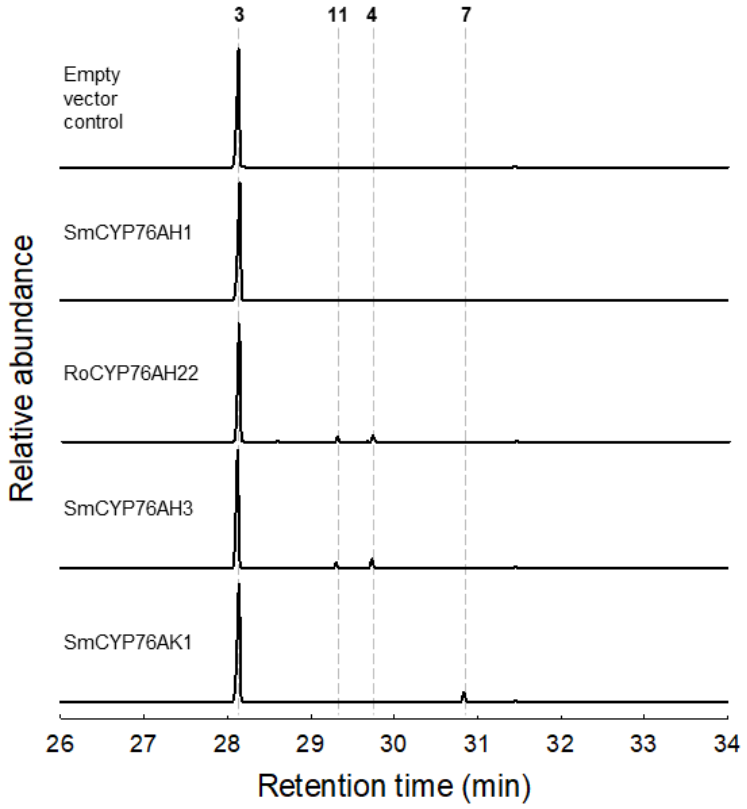

Figure S7: Results of GC-MS analysis (selected *m/z* signals: 286, 300, and 302) of *in vitro* enzyme assays from microsomal preparations. Microsomes containing the indicated enzymes and ATR1 were incubated with ferruginol. Ferruginol (**3**), 11-hydroxy ferruginol (**4**), abietaquinone (**11**) and pisiferol (**7**).

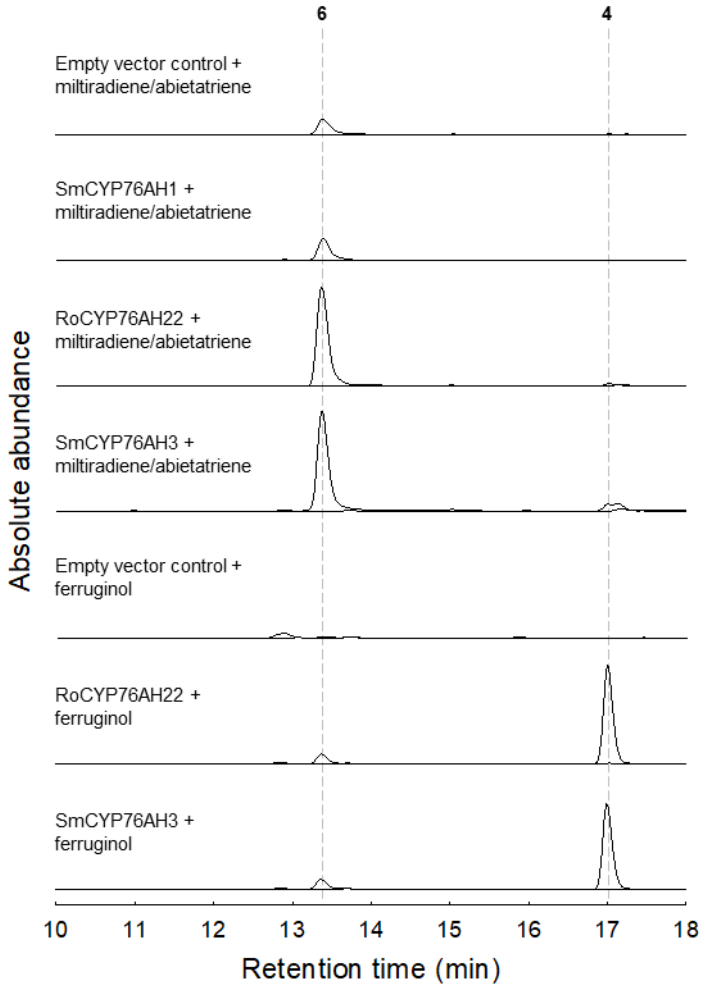

Figure S8: LC-MS analysis (selected *m/z* signals in the negative ion mode: 301.2017, and 315.196) of *in vitro* enzyme assays from microsomal preparations. Empty vector controls or (H)FS were incubated with the given substrates. 11-hydroxy ferruginol (**4**) and 11-hydroxy sugiol (**6**).

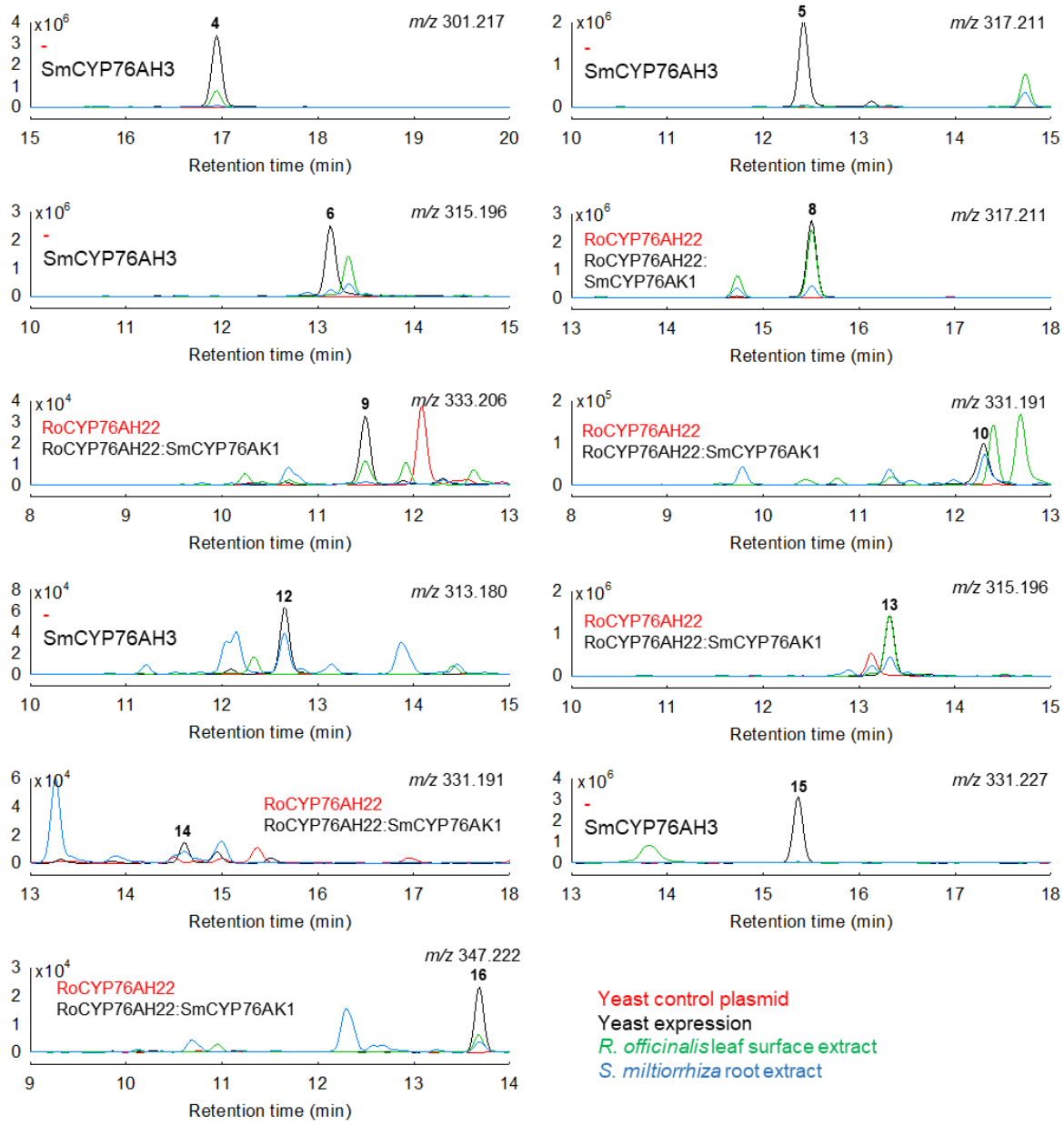

Figure S9: LC-MS analysis of rosemary leaf surface extracts (green trace), sage root extracts (blue trace) or hexane extracts from yeast strains expressing the CM and the given CYPs (red or black trace). The results are presented in absolute abundances with the given selected *m/z* signals in the negative ion mode. Labeled peaks are as follows: 11-hydroxy ferruginol (**4**), 7,11-dihydroxy ferruginol (**5**), 11-hydroxy sugiol (**6**), pisiferol (**7**), 11,20-dihydroxy ferruginol (**8**), 7,11,20-trihydroxy ferruginol (**9**), 11,20-dihydroxy sugiol (**10**), abietaquinone (**11**), 7-keto abietaquinone (**12**), 20-hydroxy abietaquinone (**13**), 7,20-dihydroxy abietaquinone (**14**), 7-methoxy-11-hydroxy ferruginol (**15**) and 7-methoxy-11,20-dihydroxy ferruginol (**16**).

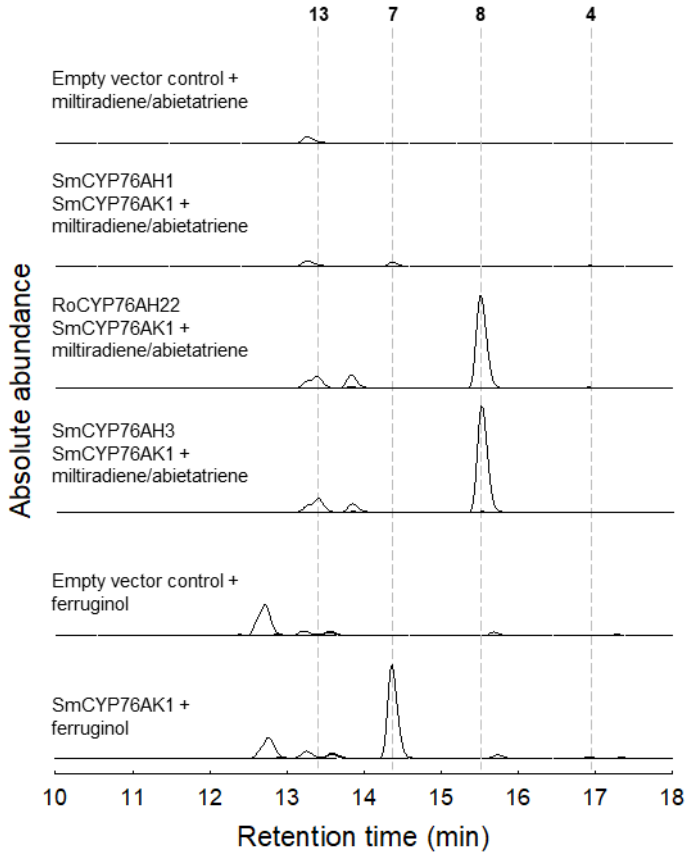

Figure S10: LC-MS analysis (selected *m/z* signals in the negative ion mode: 301.2017, 315.196 and 317.211) of *in vitro* enzyme assays from microsomal preparations. The microsomes containing the empty vector control or the given CYPs were incubated with the indicated substrates. The peaks correspond to 11-hydroxy ferruginol (**4**), pisiferol (**7**), 11,20-dihydroxy ferruginol (**8**) and 20-hydroxy abietaquinone (**13**).

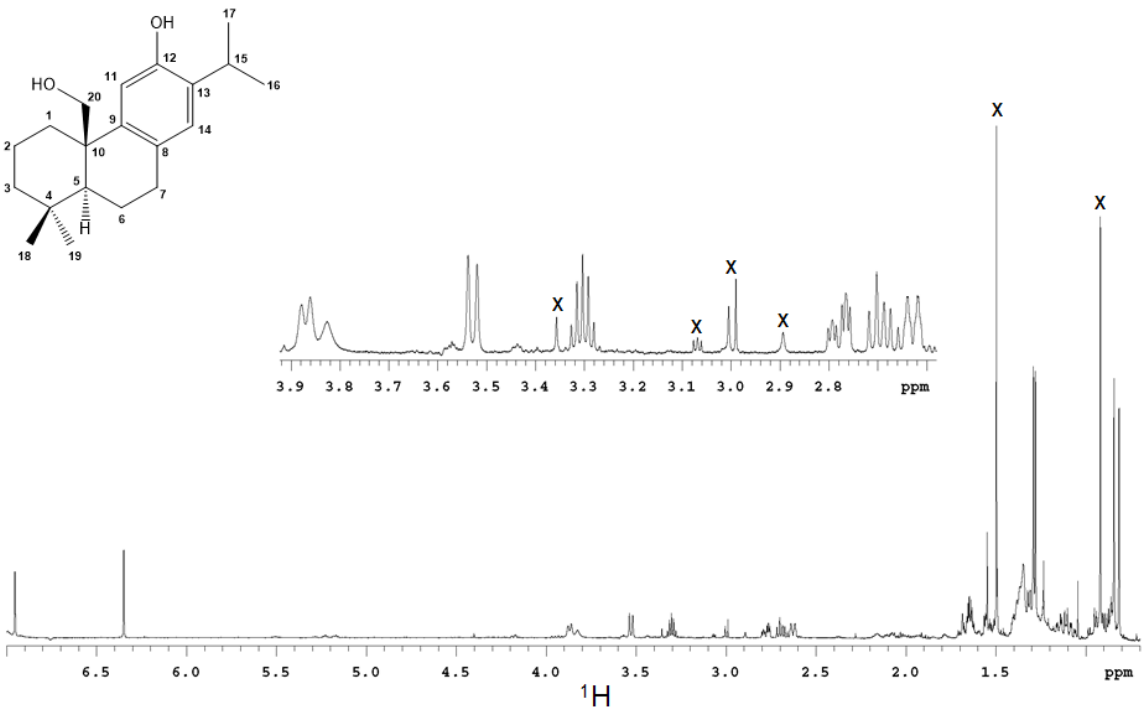

Figure S11: ^{1}H NMR spectrum (solvent C_6D_6) of pisiferol (7) (x: impurity).

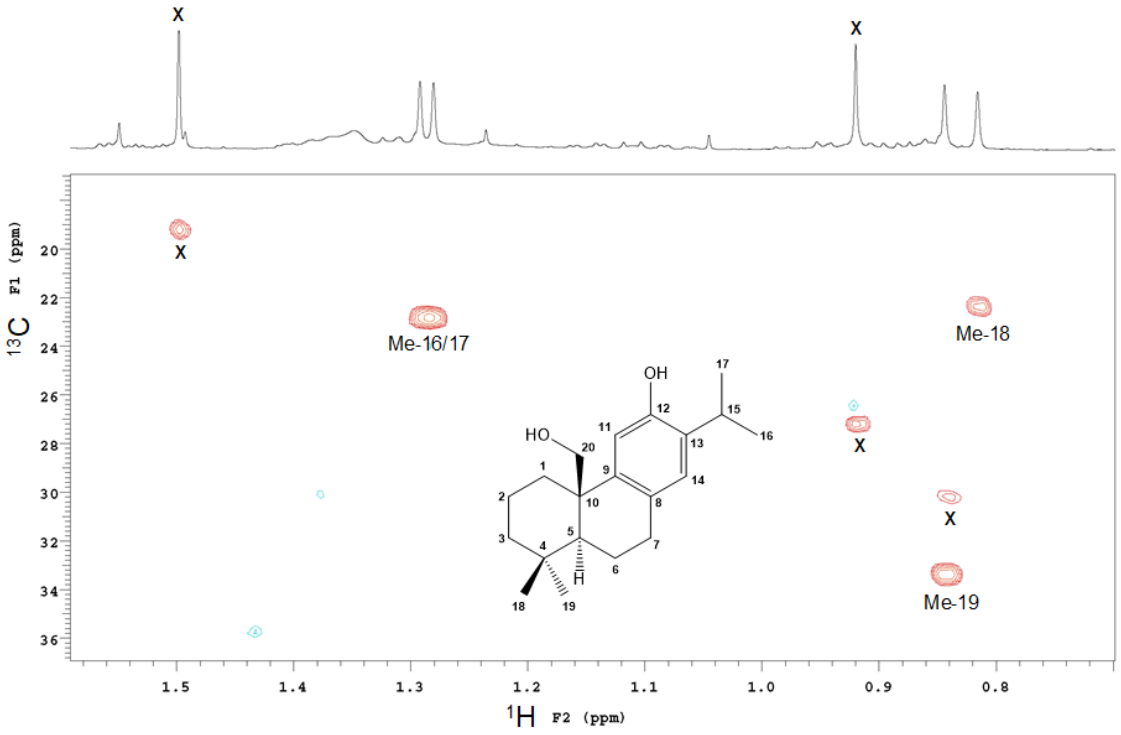

Figure S12: Methyl group region of the ^{1}H,^{13}C HSQC spectrum (solvent C_6D_6) of pisiferol (7) (x: impurity).

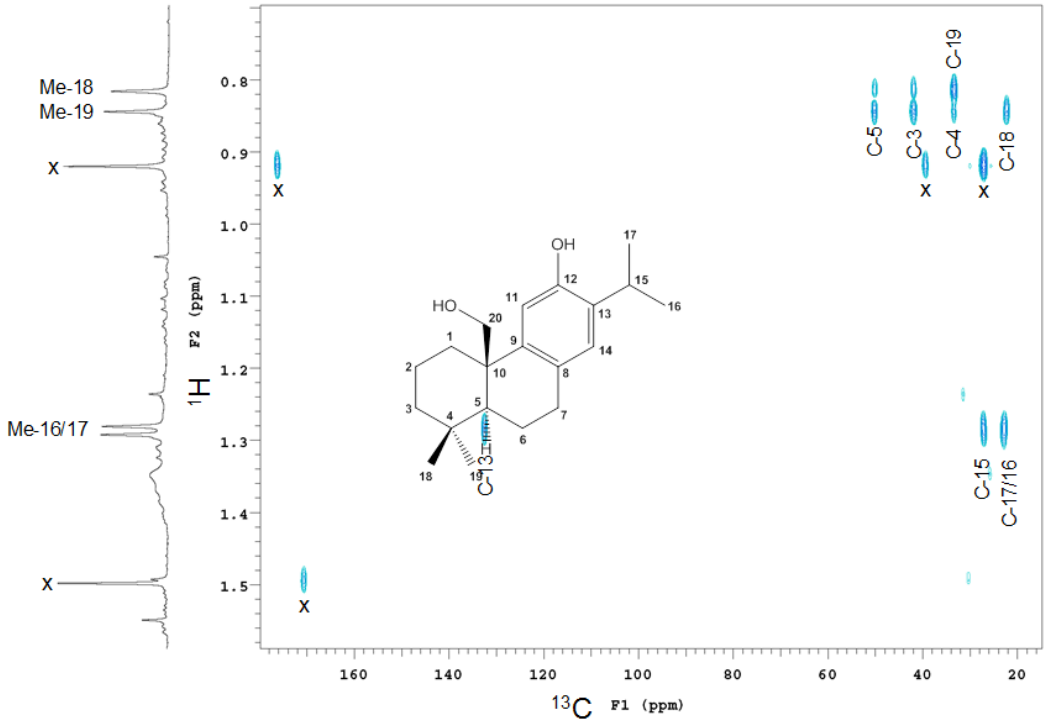

Figure S13: Methyl group region of the ^{1}H,^{13}C HMBC spectrum (solvent C_6D_6) of pisiferol (7) (x: impurity).

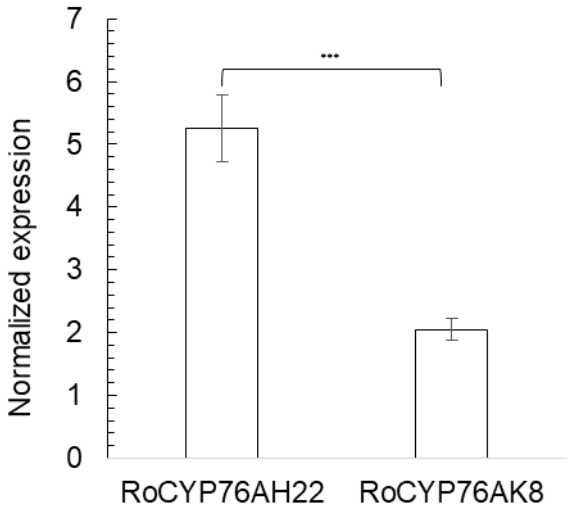

Figure S14: Transcript levels of RoCYP76AH22 and RoCYP76AK8 in young rosemary (variety Majorca Pink) leaves. The real-time quantitative PCR data were obtained from three biological replicates using BioMark™ (Fluidigm) according to the manufacturer's instructions with a cDNA concentration of 6 ng/µl and gene specific primers (CYP76AH22: GTGTGTTGTTTGGCTTTGCG and GTGACGAATACATATATGGGCGTAG; CYP76AK8: TGGATAGCGAGATTGATTTTGGAG and TCTGGAGTTGTTTGGATTCTGCC). Gene expression levels were normalized to the eukaryotic elongation factor 4a as reference gene.

Supplementary Tables

Table S1: Constructs and corresponding yeast strains.

Purpose	Strain	Transformed gene combination	Source
In vivo	INVScI	*GGPPS:CPS:MiS* (control)	[46]
		GGPPS:CPS:MiS:ATR1:CYP76AH1	[46, 103, 243]
		GGPPS:CPS:MiS:ATR1:CYP76AH3	[46, 186, 243]
		GGPPS:CPS:MiS:ATR1:CYP76AH22	[46, 47, 243]
		GGPPS:CPS:MiS:ATR1:CYP76AH23	[46, 47, 243]
		GGPPS:CPS:MiS:ATR1:CYP76AH4	[46, 102, 243]
		GGPPS:CPS:MiS:ATR1:CYP76AH24	[46, 47, 243]
		GGPPS:CPS:MiS:ATR1:CYP76AH22$_{E301DS303NF478V}$	[46, 187, 243]
		GGPPS:CPS:MiS:ATR1:CYP76AH22$_{D301EN303SV479F}$	[46, 187, 243]
		GGPPS:CPS:MiS:ATR1:CYP76AH1:CYP76AK1	[46, 103, 186, 243]
		GGPPS:CPS:MiS:ATR1:CYP76AH3:CYP76AK1	[46, 186, 243]
		GGPPS:CPS:MiS:ATR1:CYP76AH22:CYP76AK1	[46, 47, 186, 243]
		GGPPS:CPSMiS:ATR1:CYP76AK1	[46, 186, 243]
In vitro		*ATR1:CYP76AH1*	[103, 243]
		ATR1:CYP76AH3	[186, 243]
		ATR1:CYP76AH22	[47, 243]
		ATR1:CYP76AK1	[186, 243]
		ATR1:CYP76AH1:CYP76AK1	[103, 186, 243]
		ATR1:CYP76AH3:CYP76AK1	[186, 243]
		ATR1:CYP76AH22:CYP76AK1	[47, 186, 243]

Table S2: NMR data of pisiferol (7). (^{13}C: δ [ppm], ^{1}H: δ [ppm] m (J [Hz])) Spectra obtained from an Agilent VNMRS 600 instrument, ^{1}H @ 599.829 MHz, solvent C_6D_6, conc.: ca. 0.06 mmol/L (abs. amount ca. 15 µg), internal reference: ^{1}H/^{13}C: TMS = 0 ppm.

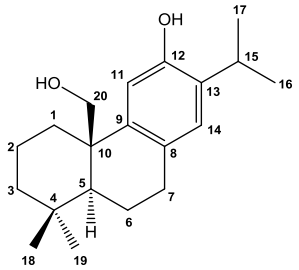

Pos.	^{13}C[a]	^{1}H	HMBC (H to C)
1	n.d.	2.629[b] br d (12.9); 1.08[b,c]	
2	n.d.	1.67 [b,c]; 1.53 [b,c]	
3	41.9	1.42 [b,c]; 1.13 [b,c]	
4	33.4	---	
5	50.2	1.33 [b,c]	
6	n.d.	1.65 [b,c] ,1,65 [b,c]	
7	29.0	2.779[b] ddd (16.9/5.7/4.3); 2.689[b] ddd (16.9/9.4/9.4)	
8	128.2	---	
9	142.3	---	
10	n.d.	---	
11	n.d.	6.349 s	8, 13
12	n.d.	---	
13	132.6	---	
14	n.d.	6.955 s	7, 9
15	27.2	3.304 sp (7.0)	
16	22.8	1.28.6 d (6.3)	13, 15, 17
17	22.8	1.28.6 d (6.3)	13, 15, 16
18	22.4	0.816 s	3, 4, 5, 19
19	33.4	0.844s	3, 4, 5, 18
20	n.d.	3.870 br d (11.0) / 3.529 d (11.0)	
12-OH	---	n.d.	
20-OH	---	3.826 br s	

[a] chemical shifts of HSQC or HMBC correlation peaks; [b] assignment tentatively; [c] chemical shift of DQFCOSY correlation peak; n.d. not detected; br broad; s singlet; d doublet; t triplet; sp septet.

5.3. Supporting information to 2.4.2.

Supplementary Tables

Suppl. Tab. 1 Protein sequences that were used for phylogenetic analysis.

Accession no.	Name	Host	Function
AB014459	AtCYP51A2	*Arabidopsis thaliana*	
Q93Z79	AtCYP714A1	*Arabidopsis thaliana*	
Q6NKZ8	AtCYP714A2	*Arabidopsis thaliana*	
AF318500	AtKAO1 (AtCYP88A3)	*Arabidopsis thaliana*	Kaurenoic acid oxidase (KAO)
AF318501	AtKAO2 (AtCYP88A4)	*Arabidopsis thaliana*	Kaurenoic acid oxidase (KAO)
AF047719	AtKO (AtCYP701A)	*Arabidopsis thaliana*	Kaurene oxidase (KO)
ACQ99375	CaKO (CaCYP701A)	*Coffea arabica*	Kaurene oxidase (KO)
HQ658173	CamKAO (CamCYP88A)	*Castanea mollissima*	
KT382342	CfCYP71D381	*Coleus forskohlii*	Forskolin biosynthesis
KT382346	CfCYP76AH10	*Coleus forskohlii*	Forskolin biosynthesis
KT382349	CfCYP76AH11	*Coleus forskohlii*	Forskolin biosynthesis
KT382358	CfCYP76AH15	*Coleus forskohlii*	Forskolin biosynthesis
KT382359	CfCYP76AH16	*Coleus forskohlii*	Forskolin biosynthesis
KT382360	CfCYP76AH17	*Coleus forskohlii*	Forskolin biosynthesis
KT382348	CfCYP76AH8	*Coleus forskohlii*	Forskolin biosynthesis
KT382347	CfCYP76AH9	*Coleus forskohlii*	Forskolin biosynthesis
NP_001267703	CsKO (CsCYP701A)	*Cucumis sativus*	Kaurene oxidase (KO)
AF212991	CumKAO (CumCYP88A2)	*Cucurbita maxima*	Kaurenoic acid oxidase (KAO)
AF212990	CumKO (CumCYP701A1)	*Cucurbita maxima*	Kaurene oxidase (KO)
KR350668	ElCYP71D445	*Euphorbia lathyris*	Casbene oxidase
KR350669	ElCYP726A27	*Euphorbia lathyris*	Casbene oxidase
KX428471	EpCYP71D365	*Euphorbia peplus*	Casbene oxidase
KJ026362	EpCYP726A19	*Euphorbia peplus*	Casbene synthase

KF986823.1	EpCYP726A4	*Euphorbia peplus*	Casbene oxidase
KF773141	GbCYP716B	*Ginkgo biloba*	taxoid-9α-hydroxylase
KHN31869	GsKO (GsCYP701A)	*Glycine soja*	Kaurene oxidase (KO)
FR666915	HaKAO1 (HaCYP88A)	*Helianthus annuus*	Kaurenoic acid oxidase (KAO)
FR666916	HaKAO2 (HaCYP88A)	*Helianthus annuus*	Kaurenoic acid oxidase (KAO)
AF326277	HvKAO1 (HvCYP88A)	*Hordeum vulgare*	Kaurenoic acid oxidase (KAO)
KX060559	JcCYP71D495	*Jatropha curcas*	Casbene oxidase
KF986815	JcCYP726A20	*Jatropha curcas*	Casbene oxidase
KF986816	JcCYP726A21	*Jatropha curcas*	
KF986818	JcCYP726A23	*Jatropha curcas*	
KF986819	JcCYP726A24	*Jatropha curcas*	
KX060558	JcCYP726A35	*Jatropha curcas*	Casbene oxidase
JF929910	JcKO (JcCYP701A)	*Jatropha curcas*	Kaurene oxidase (KO)
AB370238	LsKAO (LsCYP88A)	*Lactuca sativa*	Kaurenoic acid oxidase (KAO)
ADE06669	McKO (McCYP701A)	*Momordica charantia*	Kaurene oxidase (KO)
KF437682	MdKAO (MdCYP88A)	*Malus domestica*	Kaurenoic acid oxidase (KAO)
AY563549	MdKO (MdCYP701A)	*Malus domestica*	Kaurene oxidase (KO)
XP_010089925	MnKO (MnCYP701A)	*Morus notabilis*	Kaurene oxidase (KO)
XM_013607618	MtKAO (MtCYP88A)	*Medicago truncatula*	Kaurenoic acid oxidase (KAO)
AF116915	NtCYP51	*Nicotiana tabacum*	obtusifoliol 14-α demethylase
AF166332	NtCYP71D16	*Nicotiana tabacum*	CBT-ol oxidase
Q7XHW5	OsCYP714B1	*Oryza sativa*	
Q0DS59	OsCYP714B2	*Oryza sativa*	
AK109526	OsCYP714D1	*Oryza sativa*	
AK107418	OsCYP71Z6	*Oryza sativa*	
AK070167	OsCYP71Z7	*Oryza sativa*	Cassadiene oxidase
AK059010	OsCYP76M5	*Oryza sativa*	
AK101003	OsCYP76M6	*Oryza sativa*	Oryzalexin synthase
AK105913	OsCYP76M7	*Oryza sativa*	

AK069701	OsCYP76M8	*Oryza sativa*	Oryzalexin synthase
AK071864	OsCYP99A2	*Oryza sativa*	Pimaradiene oxidase
AK071546	OsCYP99A3	*Oryza sativa*	Pimaradiene oxidase
Q5VRM7	OsKAO (OsCYP88A5)	*Oryza sativa*	Kaurenoic acid oxidase (KAO)
Q5Z5R4	OsKO2 (OsCYP701A6)	*Oryza sativa*	Kaurene oxidase (KO)
AY579214	OsKOL4 (OsCYP701A8)	*Oryza sativa*	Kaurene oxidase (KO)
AY660664	OsKOL5 (OsCYP701A9)	*Oryza sativa*	Kaurene oxidase (KO)
KJ845667	PbCYP720B2	*Pinus banksiana*	Hydroxyl abietene oxidase
KJ845671	PcCYP720B1	*Pinus contorta*	Abietadienol/abietadienal oxidase
KJ845675	PcCYP720B11	*Pinus contorta*	
KJ845676	PcCYP720B12	*Pinus contorta*	Hydroxyl abietene oxidase
KJ845672	PcCYP720B2	*Pinus contorta*	Hydroxyl abietene oxidase
AEK01241	PcKO (PcCYP701A)	*Pyrus communis*	Kaurene oxidase (KO)
BAK19917	PhpKO (PhpCYP701B1)	*Physcomitrella patens*	Kaurene oxidase (KO)
AF537321	PsaKAO1 (PsaCYP88A6)	*Pisum sativum*	Kaurenoic acid oxidase (KAO)
AF537322	PsaKAO2 (PsaCYP88A7)	*Pisum sativum*	Kaurenoic acid oxidase (KAO)
AAP69988	PsaKO (PsaCYP701A)	*Pisum sativum*	Kaurene oxidase (KO)
HM245408	PsiCYP720B10	*Picea sitchensis*	
HM245397	PsiCYP720B12	*Picea sitchensis*	Hydroxyl abietene oxidase
HM245398	PsiCYP720B15	*Picea sitchensis*	
HM245399	PsiCYP720B16	*Picea sitchensis*	
HM245402	PsiCYP720B2	*Picea sitchensis*	Hydroxyl abietene oxidase
HM245403	PsiCYP720B4	*Picea sitchensis*	Diterpene C-18 oxidase
HM245406	PsiCYP720B7	*Picea sitchensis*	
HM245407	PsiCYP720B8	*Picea sitchensis*	
HM245410	PsiCYP720B9	*Picea sitchensis*	
AY779541	PtaCYP720B1	*Pinus taeda*	Abietadienol/abietadienal oxidase
XP_006386514	PtrKO (PtrCYP701A)	*Populus trichocarpa*	Kaurene oxidase (KO)
HM003112	PypKO (PypCYP701A)	*Pyrus pyrifolia*	Kaurene oxidase (KO)

KF986809	RcCYP726A13	*Ricinus communis*	
KF986810	RcCYP726A14	*Ricinus communis*	Casbene oxidase
KF986811	RcCYP726A15	*Ricinus communis*	Neocembrene oxidase
KF986812	RcCYP726A16	*Ricinus communis*	Casbene oxidase
KF986813	RcCYP726A17	*Ricinus communis*	Casbene oxidase
KF986814	RcCYP726A18	*Ricinus communis*	Casbene oxidase
KP091843	RoCYP76AH22	*Rosmarinus officinalis*	Hydroxyferruginol synthase
KP091844	RoCYP76AH23	*Rosmarinus officinalis*	Hydroxyferruginol synthase
	RoCYP76AH4	*Rosmarinus officinalis*	Hydroxyferruginol synthase
KX431219	RoCYP76AK7	*Rosmarinus officinalis*	C20 oxidase
KX431220	RoCYP76AK8	*Rosmarinus officinalis*	C20 oxidase
U74319	SbCYP51	*Sorghum bicolor*	obtusifoliol 14-α demethylase
KP091842	SfCYP76AH24	*Salvia fruticosa*	Hydroxyferruginol synthase
KX431218	SfCYP76AK6	*Salvia fruticosa*	C20 oxidase
Solyc08g005650.2.1	SlCYP71BN1	*Solanum lycopersisum*	
JX422213	SmCYP76AH1	*Salvia miltiorrhiza*	Ferruginol synthase
KR140168	SmCYP76AH3	*Salvia miltiorrhiza*	Hydroxyferruginol synthase
KR140169	SmCYP76AK1	*Salvia miltiorrhiza*	C20 oxidase
KP337688	SmCYP76AK2	*Salvia miltiorrhiza*	
KP337689	SmCYP76AK3	*Salvia miltiorrhiza*	
KJ606394	SmKO (SmCYP701A)	*Salvia miltiorrhiza*	Kaurene oxidase (KO)
KT157042	SpCYP71BE52	*Salvia pomifera*	C2 oxidase
KT157044	SpCYP76AH24	*Salvia pomifera*	Hydroxyferruginol synthase
KT157045	SpCYP76AK6	*Salvia pomifera*	C20 oxidase
AY364317	SrKO1 (SrCYP701A5)	*Stevia rebaudiana*	Kaurene oxidase (KO)
AY995178	SrKO2 (SrCYP701A)	*Stevia rebaudiana*	Kaurene oxidase (KO)
ADZ55286	TaKO (TaCYP701A)	*Triticum aestivum*	Kaurene oxidase (KO)
AY518383	TcaCYP725A6, T2OH	*Taxus canadensis*	taxoid-2α-hydroxylase
AF318211	TcuCYP725A1, T10OH	*Taxus cuspidata*	taxoid-10β-hydroxylase
AY056019	TcuCYP725A2, T13OH	*Taxus cuspidata*	taxoid-13α-hydroxylase

AY188177	TcuCYP725A3, T14OH	*Taxus cuspidata*	taxoid-14β-hydroxylase
AY289209	TcuCYP725A4, T5OH	*Taxus cuspidata*	
AY307951	TcuCYP725A5, T7OH	*Taxus cuspidata*	taxoid-7β-hydroxylase
MG696754.1	VacCYP76BK1	*Vitex agnus-castus*	
JQ086553	VvKO (VvCYP701A)	*Vitis vinifera*	Kaurene oxidase (KO)
ACG38493	ZmKO (ZmCYP701A)	*Zea mays*	Kaurene oxidase (KO)

Suppl. Tab. 2 CYPs that were reported to be involved in the biosynthesis of plant diterpenoids. Yellow: gibberellin biosynthesis, orange: specialized metabolism.

CYP subfamily	Enzyme	Sub-total	Grand total	Product	Number of products	Total number of products
88A	AtKAO1	12	**38**		3	**11**
	AtKAO2					
	CumKAO					
	HaKAO1					
	HaKAO2			kaurenol		
	HvKAO1			kaurenal		
	LsKAO			kaurenoic acid		
	MdKAO					
	MtKAO					
	OsKAO					
	PsaKAO1					
	PsaKAO2					
701A	AtKO	21			3	
	CaKO					
	CsKO					
	CumKO					
	GsKO					
	JcKO					
	McKO					
	MdKO					
	MnKO					
	OsKO2			hydroxy-kaurenoic acid		
	PcKO			GA_{12}-aldehyde		
	PhpKO			GA_{12}		
	PsaKO					
	PtrKO					
	PypKO					
	SmKO					
	SrKO1					
	SrKO2					

	TaKO					
	VvKO					
	ZmKO					
714A	AtCYP714A1	2		16-carboxy-16β,17-dihydro GA_{12}	3	
	AtCYP714A2			GA_{111}		
				GA_{53}		
714B	OsCYP714B1	2		GA_{53}	-	
	OsCYP714B2					
714D	OsCYP714D1	1		16α,17-epoxy GA_{12}	2	
				16α,17-epoxy GA_9		
714A	AtCYP714A1	2		steviol	1	
	AtCYP714A2					
701A	OsKOL4	1		3α-hydroxy-*ent*-kaurene	3	
				3α-hydroxy-*ent*-sandaracopimaradiene		
				3α-hydroxy-*ent*-cassadiene		
71BE	SpCYP71BE52	1		salviol	1	
71BN	SlCYP71BN1	1		epoxy-lycosantalene	2	
				lycosantalonol		
71D + 726A	NtCYP71D16	15	**61**	α-cembratrien-diol	16	**98**
				β-cembratrien-diol		
	CfCYP71D381			2-hydroxy-13*R*-manoyl oxide		
				19-hydroxy-13*R*-manoyl oxide		
	JcCYP71D495			5-keto-7,8-epoxy-casbene		
	ElCYP71D445			5-hydroxy casbene		
	EpCYP71D365			9-hydroxy casbene		
	RcCYP726A15			5-keto casbene		
	RcCYP726A14			9-keto casbene		
	RcCYP726A17			9-hydroxy-5-keto-casbene		
	RcCYP726A18			6-hydroxy-5-keto-		

				casbene		
	EpCYP726A19			6-hydroxy-5,9-diketo-casbene		
	JcCYP726A20			5-keto-6,9-casbene diol		
	ElCYP726A27			6-keto-5,9-casbene diol		
	JcCYP726A35			5-hydroxy-9-ketocasbene		
	EpCYP726A4			6-keto casbene		
	RcCYP726A16					
71Z	OsCYP71Z6	2		*ent*-isokauren-2-ol	5	
				ent-isokauren-2,3-diol		
	OsCYP71Z7			*ent*-cassadien-2-ol		
				ent-cassa-3-keto-diene		
				ent-cassadien-3-keto-2-ol		
76AH		12		ferruginol	16	
				sugiol		
	SmCYP76AH1			11-hydroxy ferruginol		
	SmCYP76AH3			hydroxy sugiol		
	RoCYP76AH4			11-keto miltiradiene		
	RoCYP76AH22			unknown		
	RoCYP76AH23			trihydroxy-abietatriene		
	SfCYP76AH24			11-oxo-13*R*-manoyl oxide		
	SpCYP76AH24			9-hydroxy-13R-manoyl oxide		
	CfCYP76AH11			1,11-dihydroxy-13*R*-manoyl oxide		
	CfCYP76AH15			9-deoxydeacetylforskolin		
	CfCYP76AH16			$C_{20}H_{32}O_3$		
	CfCYP76AH17			$C_{20}H_{30}O_4$		
	CfCYP76AH8			$C_{20}H_{32}O_4$		
				$C_{20}H_{34}O_4$		
				$C_{20}H_{30}O_5$		
CYP76AK		5		carnosaldehyde	7	
	CYP76AK1			carnosic acid		

	SfCYP76AK6			pisiferic acid		
	SpCYP76AK6			pisiferol		
	RoCYP76AK7			pisiferal		
	RoCYP76AK8			dihydroxy ferruginol		
				dihydroxy sugiol		
CYP76BK	CYP76BK1	1		labd-13*Z*-ene-9,15,16-triol	1	
76M	OsCYP76M5	4		*ent*-sandaracopimaradiene-7β-ol	5	
	OsCYP76M6			oryzalexin D		
	OsCYP76M7			oryzalexin E		
	OsCYP76M8			*ent*-cassadiene-11α-ol		
				syn-pimaradiene-7β-ol		
99A		2		*syn*-pimaradiene-ol	6	
				syn-pimaradiene-al		
	OsCYP99A2			*syn*-pimaradienoic acid		
	OsCYP99A3			*syn*-stemodene-ol		
				syn-stemodene-al		
				syn-stemodenoic acid		
716	GbCYP716B	1		9α-OH sinenxan A	1	
720B		8		abietadienal	24	
				abietadienol		
				abietic acid		
				dehydroabietadienal		
				dehydroabietadienol		
				dehydroabietic acid		
				isopimaradienal		
				isopimaradienol		
	PbCYP720B2			isopimaric acid		
	PcCYP720B1			levopimaradienal		
	PcCYP720B12			levopimaradienol		
	PcCYP720B2			levopimaric acid		
	PsiCYP720B12			neoabietanal		
	PsiCYP720B2			neoabietanol		
	PsiCYP720B4			neoabietic acid		

	PtaCYP720B1			palustradienal		
				palustradienol		
				palustric acid		
				pimaradienal		
				pimaradienol		
				Pimaric acid		
				sandaracopimaradienal		
				sandaracopimaradienol		
				sandaracopimaric acid		
725A		6		taxa-4(20),11(12)-dien-5α-ol	10	
				taxadien-5α-acetoxy-10β-ol		
	TcaCYP725A6			taxadien-5α,13α-diol		
	TcuCYP725A1			taxadien-5α, 10β-diol		
	TcuCYP725A2			taxadien-5α-acetoxy-13α-ol		
	TcuCYP725A3			taxadien-5α-acetate-14β-ol		
	TcuCYP725A4			taxadien-5α-acetate-10β,14β-diol		
	TcuCYP725A5			7β-hydroxytaxusin		
				2α-hydroxytaxusin		
				2α,7β-dihydroxytaxusin		

5.4. List of publications

K. Brückner, D. Božić, D. Manzano, D. Papaefthimiou, I. Pateraki, U. Scheler, A. Ferrer, R. C. de Vos, A. K. Kanellis, and A. Tissier (2014), Characterization of two genes for the biosynthesis of abietane-type diterpenes in rosemary (*Rosmarinus officinalis*) glandular trichomes. *Phytochemistry*, **101**: p. 52-64.

D. Božić, D. Papaefthimiou, K. Brückner, R. C. de Vos, C. A. Tsoleridis, D. Katsarou, A. Papanikolaou, I. Pateraki, F. M. Chatzopoulou, E. Dimitriadou, S. Kostas, D. Manzano, U. Scheler, A. Ferrer, A. Tissier, A. M. Makris, S. C. Kampranis, and A. K. Kanellis (2015), Towards elucidating carnosic acid biosynthesis in Lamiaceae: functional characterization of the three first steps of the pathway in *Salvia fruticosa* and *Rosmarinus officinalis*. *PLoS One*, **10**(5): p. e0124106.

U. Scheler, W. Brandt, A. Porzel, K. Rothe, D. Manzano, D. Božić, D. Papaefthimiou, G. U. Balcke, A. Henning, S. Lohse, S. Marillonnet, A. K. Kanellis, A. Ferrer, and A. Tissier (2016), Elucidation of the biosynthesis of carnosic acid and its reconstitution in yeast. *Nat Commun*, **7**: p. 12942.

U. Bathe & A. Tissier (2019) Cytochrome P450 enzymes: A driving force of plant diterpene diversity. *Phytochemistry*, **161**: p. 149

U. Bathe, A. Frolov, A. Porzel & A. Tissier (2019) CYP76 oxidation network of abietane diterpenes in Lamiaceae reconstituted in yeast. *Journal of Agricultural and Food Chemistry*, In Press

Acknowledgements

Choose to focus your time, energy and conversation around people who inspire you, support you and help you to grow you into your happiest, strongest, wisest self. (Karen Salmansohn)
With that in mind, I would like to thank the people who pushed me forward, inspired me and helped me to become the scientist I have ever wanted to be.

I especially thank…
…Alain Tissier for supervision, creative discussions and for the possibility to always enter his office whenever I had a question.
…Gerd U. Balcke for great advices and technical support concerning LC-MS analysis and for his never-ending scientific enthusiasm.
…Andrea Porzel for her support on NMR analysis and her friendly mind.
…Andrej Frolov and Jürgen Schmidt for MS^n experiments and for tolerating my pushing.
…Kathleen Rothe who always acts with patience and calm, for supervising my Master thesis and for introducing me into the field of abietane diterpenes.
…Petra Schäfer for listening and all the funny lunch breaks.
…Sylvestre Marillonnet for his unique ideas on Golden Gate modular cloning.
... Thomas Vogt for proofreading.
…the TERPMED consortium which represented a great collaborating team.
…the department "Cell and Metabolic Biology" at the Leibniz Institute of Plant Biochemistry, with specially thanks to the research group "Glandular Trichomes and Isoprenoid Biosynthesis" for the great lab atmosphere, helping each other and the good mood.
…the students and co-workers for their hard work and passion: Arianne Schnabel, Jacqueline Mathy, Sarah Vorndran, Lisa Tranelis, Oleh Mytakhir, Anna-Maria Treutler and Felix Pirwitz.

A special thanks full of love goes to my beloved husband Tim Bathe who always supports me whatever I do, and to my lovingly grandmother Ingrid Scheler who always worries about me.

Eidesstattliche Erklärung

Hiermit erkläre ich, dass ich die vorliegende wissenschaftliche Arbeit selbstständig und ohne fremde Hilfe angefertigt habe. Ich erkläre weiterhin, dass ich keine anderen als die von mir angegebenen Quellen und Hilfsmittel benutzt habe und die den Werken wörtlich und inhaltlich entnommenen Stellen als solche kenntlich gemacht habe. Mit dieser Arbeit bewerbe ich mich erstmals um die Erlangung des Doktorgrades. Diese Arbeit wurde an keiner anderen Fakultät oder Universität zur Begutachtung eingereicht.

Halle (Saale), den 15. Juli 2019

Ulschan Bathe

Curriculum vitae

PERSONAL INFORMATION

Birth date	01.02.1989
Maiden name	Ulschan Scheler
Civil status	married, 2 children (July 2018)
Address	Gräfestraße 13, 06110 Halle (Saale), Germany
Email	ulschan.bathe@ipb-halle.de

EDUCATION

PhD | 2019 (in completion)
Leibniz Institute of Plant Biochemistry, Halle (Saale), Germany
Thesis: The role of cytochrome P450 enzymes in the biosynthesis of abietane diterpenes from rosemary and sage
Supervisor: Prof. Dr. Alain Tissier

Master of Science | Nov 2013
Biochemistry, Martin Luther University Halle-Wittenberg, Germany
Thesis: Investigations on the role of P450 enzymes in the carnosic acid pathway of *Rosmarinus officinalis*
Supervisor: Prof. Dr. Alain Tissier

Bachelor of Science | Sep 2011
Biochemistry, Martin Luther University Halle-Wittenberg, Germany
Thesis: Untersuchung Herbivorie-induzierter Promotoren
Supervisor: Prof. Dr. Jörg Degenhardt

Abitur | June 2008
Carl-Friedrich-Gauß-Gymnasium, Frankfurt/Oder

RESEARCH EXPERIENCE

Postdoc. Researcher | Mar 2019 – present
Maternity leave | *July 2018 – Feb 2019*
Doc. Researcher | Jan 2014 – June 2018
Research Assistant | Oct 2013 – Dec 2013
Leibniz Institute of Plant Biochemistry, Halle (Saale), Germany

Visiting M.Sc. Student | Feb 2013 – Apr 2013
Department Plant Metabolism and Metabolic Engineering, Centre for Research in Agricultural Genomics, Barcelona, Spain

Student Assistant | Sep 2011 – Jan 2012, Jun 2012 – Aug 2012
Research group Pharmaceutical Biotechnology, Martin Luther University Halle-Wittenberg, Germany